Development of Amine Functional Hydrogels for Corneal Regeneration

Enas Dinah Hassan

Submitted for the degree of Doctor of Philosophy
Department of Materials Science and Engineering
September 2014

ACKNOWLEDGEMENTS

This thesis is dedicated to Dr Jaffer Hassan & Dr Jahid Hasan

ABBREVIATIONS

1,2 DAE	1,2-diaminoethane
1,3 DAP	1,3-diaminopropane
1,4 DAB	1,4- diaminobutane
1,6 DAH	1,6-diaminohexane
HMPP	2-Hydroxy-2-methylpropiophenone
MTT	3-(4,5-Dimethylthiazol-2-yl)-2,5-diphenyltetrazolium bromide
α	Alpha
ANOVA	Analysis of variance
ACAID	Anterior chamber-associated immune deviation
ABCG2	ATP-binding cassette, sub-family G, member 2
ATR	Attenuated total reflectance
CO_2	Carbon dioxide
cm	Centimetres
CLAU	Conjunctival limbal autograft
Cyt 3	Cytokeratin 3
dm	Decimetre
°C	Degrees centigrade
δ	delta (change in phase)
DA	Diacrylate
Dd	Diameter dehydrated
Dh	Diameter hydrated
DCM	Dichloromethane
DMSO	Dimetyhyl sulfoxide
DMEM	Dulbecco's Modified Eagle's Medium
eV	Electro volts
ET-1	Endothelin-1
EGF	Epidermal growth factor
EWC	Equilibrium water content
Eth	Ethanol
EGDMA	Ethylene glycol dimethacrylate
EDTA	Ethylenediaminetetraacetic acid
ECM	Extra cellular matrix
FCS	Foetal calf serum
FGF	Fibroblast growth factor
FITC	Fluorescein isothiocyanate
$\gamma0$	Gamma (strain)
GABA	Gamma-Aminobutyric acid
GME	Glycerol methacrylate
GMMA	Glycerol monomethacrylate
g	Grams
HSC	Haematopoietic stem cells
Hd	Height dehydrated
Hh	Height hydrated
HSA	Hemispherical analyser

HSK	Herpes simplex keratitis
hrs	Hours
hAM	Human amniotic membrane
HDF	Human dermal fibroblasts
HLA	Human leukocyte antigen
IMS	Industrial methylated spirit
IGF	Insulin-like growth factor
IPA	Iso propanol
KGF	Keratinocyte growth factor
KLAL	Keratolimbal allograft
LMA	Lauryl methacrylate
LESC	Limbal epithelial stem cell
LSCD	Limbal stem cell deficiency
lr-CLAL	Living related conjunctival limbal allografts
MHC	Major histocompatibility complex
MSC	Mesenchymal stem cell
μl	Micro litres
μm	Micrometres
mg	Milligrams
ml	Millilitres
mm	Millimetres
MW	Molecular weight
mol	Moles
nm	Nano meters
N	Newton's
ω	Omega (frequency)
P0	Passage 0
P1	Passage 1
PKP	Penetrating keratoplasty
%	Per cent
PBS	Phosphate buffer solution
PDMS	Poly (dimethylsiloxane)
PHEMA	Poly hydroxyethyl methacrylate
PLA	Poly lactic acid
PLGA	Poly lactide-co-glycolide
PMMA	Poly methyl methacrylate
PNVP	Poly N-vinyl-2- pyrrolidone
PEG/PAA	Poly (ethylene glycol)/poly (acrylic acid)
PCL	Polycaprolactone
PEG	Polyethylene glycol
PET	Polyethylene terephthalate
PTFE	Polytetrafluoroethylene
PVDF	Polyvinylidene difluoride
rCECs	Rabbit corneal epithelial cells
rLF	Rabbit limbal fibroblasts
rLECs	Rabbit limbal epithelial cells

rLFs	Rabbit limbal fibroblasts
rad	Radians
RPE	Retinal pigment epithelium
$\sigma 0$	Sigma (stress)
Shh	Sonic hedgehog
SEM	Standard error of the mean
G'	Storage modulus
$\theta°$	Theta
TM	Trade mark
TGF	Transforming growth factor
TAC	Transient amplifying cells
UV	Ultra violet
W	Watts
wt	Weight
Wd	Width dehydrated
Wh	Width hydrated
Wnt	Wingless
XPS	X-ray photoelectron spectroscopy

ABSTRACT

The aim of this thesis was to develop a synthetic polymethacrylate based hydrogel capable of regenerating a corneal epithelium for the purposes of treating blindness caused by limbal stem cell deficiency. Deficiency of limbal epithelial cells (LECs) causes conjunctival epithelial cells to move over the cornea, resulting in painful scaring, vascularisation and corneal opacity. Unilateral defects can be treated using LEC cultured from the unaffected eye, transplanting them to the affected cornea after scar tissue is removed. The underlying wound bed is often damaged, however, hence the need to develop a corneal inlay to aid in corneal re-epithelialisation, while replacing damaged stromal tissue. Transparent epoxy-functional polymethacrylate networks were synthesised using a combination of glycerol monomethacrylate, ethylene glycol dimethacrylate, lauryl methacrylate and glycidyl methacrylate that produced different bulk hydrogel compositions or "Bases" with different equilibrium water contents (EWC) (Base 0, 1 and 2) and different quantities of epoxy functionality (Bases 1.B, 1.15, 1.20 and 1.30). Sets of amine-functional hydrogels were produced following reaction of the epoxide groups with excesses of ammonia, 1,2-diamino ethane, 1,3-diamino propane, 1,4-diamino butane or 1,6-diamino hexane. The gels were assessed for their capacity to support the growth and proliferation for both rabbit limbal fibroblasts (rLFs) and rabbit limbal epithelial cells (rLECs). Overall no series of hydrogels supported the proliferation of rLFs irrespective of amine functionalisation, however gels functionalised with longer alkyl amines supported the adhesion and proliferation of rLECs, particularly when functionalised with 1,4-diamino butane. With Base 1 hydrogels (less so with Bases 0 and 2) a vigorous epithelial outgrowth was seen from small limbal explants and a confluent epithelial layer was achieved in vitro within 6 days. The data in this thesis support the development of hydrogels capable of selectively regenerating corneal epithelium with minimal stromal cell contamination.

TABLE OF CONTENTS

LIST OF FIGURES

LIST OF TABLES

CHAPTER 1

INTRODUCTION

TISSUE ENGINEERING CORNEA

CHAPTER 1: TISSUE ENGINEERING CORNEA

1.1   INTRODUCTION

The number of tissue engineering approaches has grown rapidly over the past 20 years with the ultimate goal, to produce cell and biomaterial constructs to repair or replace damaged tissues. This thesis focuses on corneal regeneration.

In any tissue engineering challenge there are several routes to take. Some approaches have utilized synthetic materials while others have manipulated extra cellular matrix proteins or even whole de-cellularised tissues. Getting closer to nature, by using naturally sourced materials, has its drawbacks and risks associated with disease transmission from donor tissues means their use is highly regulated. Thus, the supply of, for example decellularised tissues, can be a bottleneck in research or clinical applications. The same can be the case with manipulating ECM proteins, which even if reproduced by recombinant methods can be extremely expensive, making it impossible to even consider scaling up such therapies. Despite these issues, corneal transplants have been the gold standard treatment for most corneal pathologies for over 100 years (Arenas et al., 2012) and have had a high rate of success. In cases where a corneal transplant is not suitable other strategies must be considered. When designing a tissue engineering approach it is important to understand the natural healing and tissue regeneration process and before we have to know how normal functioning tissue is structured

1.1.1   THE EYE

Light waves first pass through the cornea, a transparent membrane at the front of the eye, then through the aqueous humour, which is a crystalline lens behind the pupil, and finally through the vitreous humour in the middle of the eye before finally reaching the retina and stopping at the retinal pigment epithelium. Here nerve impulses are triggered and sent towards the optic nerve, through the optic pathways and eventually to the visual processing centre, the occipital lobe, where the image is generated.

Light passing through the cornea converges before reaching the crystalline lens, to a nodal point immediately behind the back surface of the lens. This is where the image becomes inverted and reversed. Before this point the cornea refracts the light and is responsible for approximately 2/3 of the eyes optical power. The amount of light reaching the lens is also determined by the size of the pupil controlled by the iris. The iris is embedded with two kinds of tiny muscles, the sphincter and dilator muscles, which control the size of the pupil. The sphincter muscles are arranged around the pupil and contract in bright light to make the pupil smaller. The dilator muscles are arranged radially to pull the pupil more open when contracted.

The light continues through the vitreous humour, which makes up approximately 80% of the volume of the eye. It is a clear, transparent, heterogeneous gel mainly consisting of water, approximately 99% (Ratner, 1997) along with type II collagen and large Hyaluronic acid molecules which contributes to its gelatinous consistency making it 2 to 4 times more viscous than pure water. It is essentially acellular however isolated cells known as hyalocytes exist close to the retinal vessels. Their role is undetermined but studies have shown production of hyaluronate in vitro (Forrester et al., 2002). As well as its contribution to clear focus this part of the eye acts as a support to the curvature of the retina, it also serves as a diffusion barrier between the anterior and posterior segments of the eye. Finally the light hits the retina which is responsible for transforming it into nerve impulses, via photochemical inductions, which are then sent to the brain (Forrester et al., 2002). The retina is composed of two main layers: the neurosensory retina and the retinal pigment epithelium (RPE). The neurosensory layer can be separated into two major constituents: photoreceptors, i.e. rods and cones, which are responsible for vision in dim and bright light, respectively; and nerve cells, i.e. ganglion, bipolar, horizontal and amacrine cells, which are activated by the rods and cones and responsible for transmitting impulses to the optic nerve. The RPE consists of a continuous layer of epithelial cells that play a critical role in the normal visual process. Functions include phagocytosis of rod and cone segments, reduction of light scatter, and transport of metabolites and nutrients (Snell and Lemp, 1998).
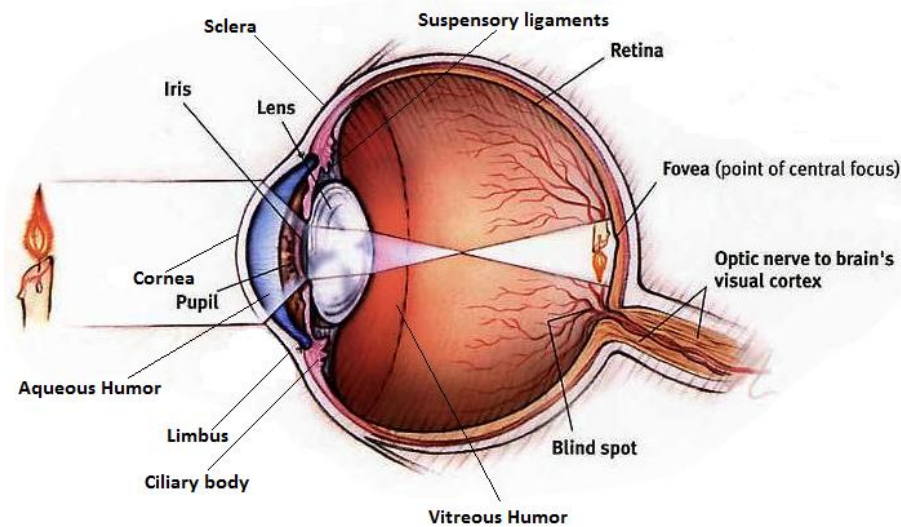
FIGURE 1.1: *Anatomy of the eye*

1.1.2 THE CORNEA

The Human cornea is a transparent avascular tissue and despite its strength it will be the first part of the eye susceptible to damage. So from a tissue engineering perspective regenerating a cornea after injury seems like a problem worth solving. Understanding the structure and function of the cornea is the first step in mimicking natural corneal wound healing.

1.1.3 INNERVATION

The Cornea is highly innervated; it contains a dense network of nerve bundles sourced from the Trigeminal nerve, the primarily sensory nerve that supplies the face. This branches into the ophthalmic nerve, which supplies the Cornea, cilliary body and iris as well as the conjunctiva and the skin of the eyelids, forehead, nose and eyebrows (Levin et al., 2011; Noback et al., 2005). From here there is a series of further branching until reaching the stroma. Soon after the nerves penetrate the stoma approximately 20% lose their myelin sheath and the distal ends reconnect to form the anterior stromal nerve plexus. Eventually a portion of the nerves from the dense complex stromal nerve plexus either turn 90° to run

parallel to the stromal collagen fibres or cross the bowman's layer to form a terminal intraepithelial plexus (Levin et al., 2011). These nerve terminals are concentrated more at the centre of the cornea and decrease gradually towards the limbus. The rich supply of nerve endings makes the cornea highly sensitive, and in comparison to our fingertips or teeth has a nerve density 300-400 times greater (Rozsa and Beuerman, 1982). Therefore, any injury to the superficial epithelium will expose these nerve endings and result in serious ocular pain (Krachmer et al., 2005a).

1.1.4 Vascular system

The cornea has to be avascular in order to maintain its transparency; however factors and nutrients are transported through the ophthalmic artery and anterior cilliary artery, which eventually terminates at the limbus. The remainder of the nutrients are delivered via the aqueous humour and the tear film (William M. Hart, 1992).

1.1.5 Tear fluid

The tear film is the first refractive surface of the eye and contributes to the smoothness of the epithelial surface. It protects the cornea from dehydration and due to the corneas absence of vasculature also serves as a diffusion medium for oxygen from the air to be supplied to the corneal epithelium (Korb et al., 2002). The tear film also behaves as a lubricant to reduce friction caused by blinking or eye rubbing. Despite its composition being around 98% water it contains vital biomolecules, which are secreted from many sources, mainly the Lacrimal, meibomian and accessory lacrimal glands as well as conjunctival goblet cells. The components of the tear film are arranged into 3 main layers (table 1) and approximately total 7μm in thickness. A good quality tear film is also important for clear vision, comfort and overall corneal health.

TABLE 1.1: modified from Cornea: Fundamentals, Diagnosis and Management (Krachmer et al., 2005a) and Adler's physiology of the eye (Levin et al., 2011)

Tear layer	Origin	Components	Physiological functions
Lipid layer	Meibomian gland Accessory lacrimal gland	Wax, cholesterol, fatty acid ester	Lubrication, prevention of evaporation, stabilisation
Aqueous layer	Lacrimal gland Accessory lacrimal gland	Water, Glucose, Vitamins, Electrolytes: Na^+, K^+, Cl^-, HCO_3^-, Mg^{2+} Proteins: albumin, lysozyme, lactoferrin, transferrin, ceruloplasmin, imunoglobulins: IgG, IgA, IgE, IgM Cytokines, Growth factors: EGF, TGF-α, TGF-β2, bFGF, HGF,	Lubrication, antimicrobial, bacteriostasis, oxygen and nutrient supply, mechanical clearance, regulation of cellular functions
Mucous layer	Conjunctival goblet cells, conjunctival epithelial cells, corneal epithelial cells	Sulfomucin, Cyalomucin, MUC1, MUC4, MUC5AC	Lowered surface tension, stabilization of aqueous layer
Glycocalyx (Hodges and Dartt, 2003)	Stratified squamous cell of the cornea and conjunctiva	A system of polysaccharides	Protects the epithelial surface, hygroscopicity

1.1.6 CORNEAL EPITHELIUM

The outermost surface of the cornea is the epithelium; approximately 50μm in thickness it is made up of 4-6 layers of cells, which are organised into 3 main levels

– Superficial squamous cells
– Central suprabasal cells
– Inner columnar basal cells

The superficial squamous cells are differentiated and non-keratinised with microvilli extending into the tear film for increased surface area for gaseous exchange. These cells are held together tightly by numerous intercellular junctions such as gap junctions, tight junctions (zonulae occludens), adherens and desmosomes to help resist shear (Klyce, 1972). The constant renewal of the corneal epithelium is maintained by the inner columnar basal cells which undergo mitosis to produce daughter cells which later become central suprabasal cells, these cells have an elongated convex morphology and are sometimes referred to as wing cells (Hanna and Obrien, 1960; Hanna et al., 1961). They divide less frequently than basal cells but migrate vertically and differentiate into squamous cells. As well as generating new suprabasal cells the inner basal cells deposit matrix proteins important for basement membrane maintenance (Friedenwald and Buschke, 1944).

This vertical proliferation or shedding is stimulated by friction from voluntary or involuntary eye blinking; it is thought that the signalling for proliferation occurs via gap junctions, in particular where there is expression of the gap junction protein connexion 43 (Williams and Watsky, 2002). The whole renewal of the corneal epithelium takes place approximately every 7 days.

1.1.7 BOWMANS LAYER

The Bowmans layer is a random arrangement of collagen fibres, mainly collagen types I and III. The individual fibres measure 20-30nm in diameter which is slightly smaller than the more regularly aligned collagen of the Stroma (Wilson

and Hong, 2000). In total Bowman's layer is approximately 10µm thick, the components of which are thought to be synthesised by both keratocytes and epithelial cells and serve as a barrier between the layers preventing the activation of quiescent Keratocytes (Krachmer et al., 2005a). The role of the Bowman's layer is still unclear as it appears in some species and not others (Merindano et al., 2003), even humans with congenital absences of Bowman's layer can still have a clear cornea and normal vision (Gordon et al., 1994). It has been speculated that Bowman's layer acts as a corneal frame to maintain corneal structure. Others have also suggested that it may act as a barrier to the posterior extension of herpes simplex and other viruses that infect the corneal epithelium (Wilson and Hong, 2000).

1.1.8 Stroma

The corneal stroma constitutes 90% of the total corneal thickness and is mainly composed of water, approximately 77%. The remainder of the stroma, responsible for the corneas shape and strength, is made from a complex network of regularly arranged collagen. The collagen, mainly type I, forms thick flattened fibril reinforced lamellae (Dodson and Hay, 1974), orientated parallel to the corneal surface. Between the lamellae are a sparse amount of keratocytes occupying approximately 2-3% of the stromal volume (Otori, 1967). It is these cells that are responsible for producing the majority of the extracellular matrix (ECM). Apart from a large amount of collagen the remainder of the stroma contains proteoglycans and salts which also help to retain the high volume of water in the cornea. The transparency of the cornea relies on the stromal interfibrillary distance (Maurice, 1957), which is controlled by the presence of glycosaminoglycans (Freund et al., 2008).

1.1.9 Dua's Layer

Recently the corneal anatomy was redefined by Dua *et al* who isolated a strong, acellular region between 6- 15 µm thick located at the interface between the posterior stroma and the Descemet's membrane. This defined layer is composed of five to eight lamellae of collagen I bundles which are shown to be arranged in transverse, longitudinal and oblique directions. Bundle spacing is similar to that

in stromal tissue, but Dua's layer is completely void of keratocytes and differs in architecture to the Descemet's membrane, which consists of finer, closer spaced, parallel collagen fibres arranged in banded and non- banded layers with endothelial cells (Dua et al., 2014).

1.1.10   DESCEMET'S MEMBRANE

Descemet's membrane is a thin homogeneous layer of type IV collagen fibrils arranged in a hexagonal pattern and embedded in matrix. It functions as the basement membrane of the corneal endothelium and is about 8-10μm thick. Its structure is composed of two distinct zones, a banded anterior third and a homogeneous nonbanded posterior two thirds. Apart from collagen type IV the membrane also contains laminin (Fitch et al., 1990), fibronectin and heparin sulphate (Levin et al., 2011). Collagen fibrils in the stroma are not continuous with Descemet's membrane unlike Bowman's Layer which leaves it vulnerable to shear stress however it adheres tightly to the posterior surface of the stroma via type V and VI collagen (Forrester et al., 2002). If Descemet's membrane is torn it cannot regenerate. When rupture occurs, aqueous humor can penetrate the stroma leading it to swell causing stromal edema; endothelial cells can migrate over the sight of injury allowing stromal edema to subside (Krachmer et al., 2005a).

1.1.11   ENDOTHELIUM

The Endothelium is primarily responsible for maintaining corneal transparency through the regulation of corneal hydration and nutrition. This is achieved by a process known as the pump-leak mechanism. A leaky barrier to the aqueous humour works in conjunction with metabolic pumps that move ions, drawing fluid from the stroma into the aqueous humour by osmosis (Bourne, 2003). A single layer of endothelial cells covers the posterior surface of Descemet's membrane forming an irregular polygonal mosaic pattern. These cells are mainly hexagonal in shape and approximately measure 5 μm thick by 20 μm wide. The posterior surface exhibits microvilli and marginal folds that extend into the aqueous humour, this increases surface area for nutrient uptake. The endothelial cells interdigitate and contain various junctional complexes including zonulae

occludens, macula occludens and macula adherens as well as gap junctions to allow the transfer of small molecules and electrolytes between endothelial cells. The corneal endothelium matures after birth and loses its proliferative capacity, as is the case with primates and cats. Human corneal endothelial cells have demonstrated the ability to proliferate in culture leading some to believe factors or other components in the aqueous humor inhibit proliferation. As a result the human endothelial cell density will decrease with age (Laule et al., 1978).

1.1.12   Limbus

The limbus was first acknowledged as simply a border between the cornea and the sclera. However it has since become recognised for its roles in corneal wound healing, hypersensitivity responses, nourishment of the peripheral cornea as well as guarding the ocular surface from infection (Forrester et al., 2002). The traditional role of the Limbus is the drainage of aqueous humour from the anterior chamber. Specialised tissues for filtering the aqueous humour include the trabecular meshwork, and an intricate group of aqueous vessels such as Schlemm's canal and aqueous veins which are responsible for transporting aqueous humour to the circulatory system (van der Merwe and Kidson, 2010). Regulation of aqueous humour outflow helps maintain the intraocular pressure (IOP) within the required physiological range (Llobet et al., 2003) preventing glaucoma. In order to carry out this function as well as the others mentioned the limbus has to be vascularised and hence unlike the cornea is not immunoprivileged.

Notara *et al.* (2011) identified two key limbal structures; focal stromal projections and limbal epithelial crypts, sometimes referred to as Palisades of Vogt (Vogt., 1921). They are visibly recognised as a localised undulation of epithelial cells, and can be seen as analogous to the rete pegs of the epidermis where the epithelium extends down into the stoma. Limbal crypts have however been better compared to the intestinal epithelial crypts, as they are shorter than rete pegs and are specifically orientated (Solanas and Batlle, 2011) to open towards the cornea rather than the conjunctiva (Shortt et al., 2007a). These

features have been characterised by many as a putative stem cell niche for corneal epithelial stem cells.
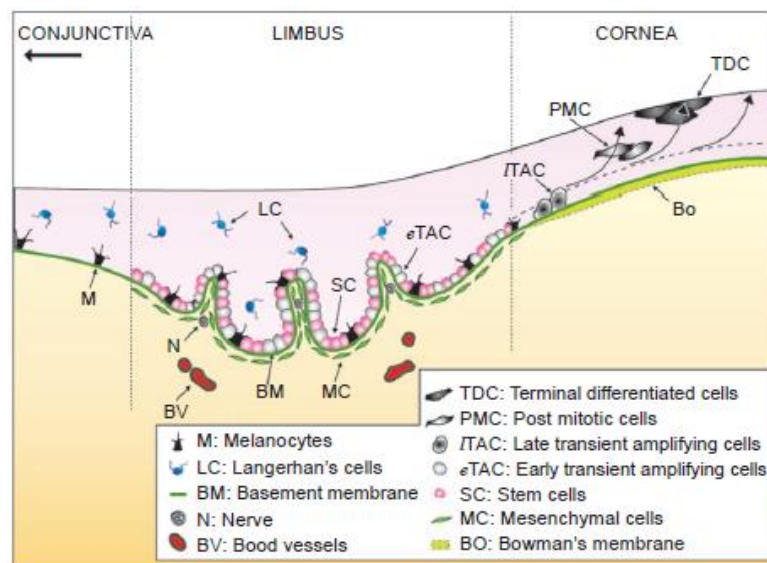
FIGURE 1.2: *The human limbus:*

In the basement membrane of the limbus, limbal epithelial stem cells maintain the corneal epithelium; they give rise to daughter transient amplifying cells. Support cells include melanocytes and fibroblasts (Secker and Daniels, 2009) *figure taken from* (Li et al., 2007)*.*

1.1.13   THE CONJUNCTIVA

The conjunctiva is a layer of tissue that covers the dense tough sclera; it consists of six to nine layers of epithelial cells. Unlike the cornea however, these cells are smaller, and are not as tightly arranged. This is due to fewer hemidesmosomal attachments from the basal epithelial cells to the underlying discontinuous basement membrane (Dua et al., 1994). In between these basal cells are a small population, 7%, of goblet cells that secrete mucin for lubrication (Dua et al., 2000). Conjunctival epithelium also contains lymphocytes, melanocytes, and Langerhans cells distributed randomly in the suprabasal layers. The conjunctival stroma has a much looser arrangement of collagen fibres than the cornea this is to allow lymphatics, blood vessels, and a variable number of lymphocytes, mast

cells, plasma cells (Weingeist, 1973), and neutrophils to be incorporated into its architecture (Dua et al., 1994; Kenyon, 1979).
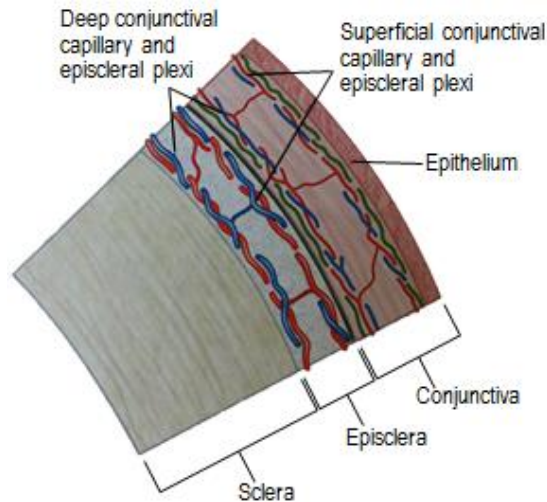
FIGURE 1.3: *Cross section of conjunctiva, episclera, and sclera. Showing green lymph vessels, red and blue blood vessels.*

1.2   NATURAL CORNEAL WOUND HEALING

Corneal reaction to injury is similar in some ways to any tissue; it depends on factors such as the nature, degree and location of the wound. Following injury, neighbouring undamaged tissue manage the condition by coordinating a series of responses. In general the events that follow are apoptosis and necrosis, inflammation, granulation, cell migration and tissue remodelling. Each layer of the cornea reacts differently to injury and contributes different aspects to healing.

1.2.1 EPITHELIAL RESPONSE

A steady state corneal epithelium is one of the most dynamic tissues in the body, and is continuously shedding its squamous epithelial cells into the tear film, at the same time cells are moving anteriorly from the basal layers and centripetally from the limbus. Thoft and Friend (1983) first modelled this process as an

equilibrium X + Y = Z. where X is the proliferation of basal cells, Y is centripetal migration of cells from the limbus and Z is the epithelial cell loss form the surface. Therefore disruption to the epithelium from injury would cause Z to increase forcing a reaction from the limbal and basal cells to compensate (Thoft and Friend, 1983). Usually when an epithelial cell is disrupted to an extent that junctional complexes are broken, it is lost to the tear film. Experimentally observed kinetics of corneal epithelial wound healing have characterised the process as having two distinct phases (Sheardown and Cheng, 1996), an initial latent phase followed by a linear healing phase (Crosson et al., 1986). During the initial stages of the latent phase the wound may appear larger as necrotic cells are shed. At the interface, extending peripherally from these dying cells, the intercellular junctions loosen but do not completely detach; this triggers the realignment of cell margins so that they slope towards the defect (Anderson, 1977; Shi et al., 2000). While intercellular junctions become looser, hemidesmosomal attachments between the basement membrane and the basal cells completely break down. The morphology of the superficial cells changes just before desquamation, they lose their microvilli and glycocalyx, the inner basal cells also look less columnar as the epithelium becomes thinner. At this point the epithelium is a single layer thick at the wound edge and 2-3 layers at the wound margin. The epithelial cells are now flattened and have started to form filopodia and broader lamelopodia which extend into the wounded region in preparation for cell migration. Apart from cellular changes the surrounding ECM becomes modified, fibronectin, fibrin and fibrinogen concentrations increase, as the cells are ready to begin the linear healing phase.

The linear healing phase is essentially the movement of cells to close the wound. For this to occur there is an increase in protein synthesis. Migration and healing depend on the synthesis of cytoskeletal proteins such as vinculin, actin, talin, and integrin as well as other cell surface receptors, e.g., CD44, the hyaluronan receptors (Soong, 1987; Stepp et al., 1996). Synthesis of cell surface glycoproteins and glycolipids also increase during wound healing (Gipson et al., 1984; Lu et al., 2001). The direction of migration is influenced by signals spilled out from the disrupted cells into solution, creating a chemotactic signal (Tuft et al., 1993) or

signals generated by exposure of epithelial basement membrane to either the circulation or the tear film through hapatotaxis (Krachmer et al., 2005a). In order for the cell mass to move towards the origin of the wound the amount of cohesion between the cells decreases and migrating epithelial cells dedifferentiate slightly. Orientation of cell migration is also dependent on the curvature of the leading edge of the epithelial cell mass. A concave leading edge acts as a relative stimulus to migration, so concave portions fill in first until the entire leading edge becomes concave. Tongues of epithelial cells then proliferate to fill in the remaining defect. If the leading edge is convex however, fewer cells at highest convexity will be prompted to migrate. Where there has been a delayed or abnormal reaction to injury the use of topical therapeutic agents has been investigated. Most of these agents are growth factors such as fibroblast growth factor (FGF), transforming growth factor (TGF), epidermal growth factor (EGF), keratinocyte growth factor (KGF), insulin-like growth factor (IGF), platelet-derived growth factor (PDGF) as well as interleukins-(IL) 1 and -6, TNF-α, endothelin-1 (ET-1) and fibronectin (Elliott, 1980; Imanishi et al., 2000; Kandarakis et al., 1984; Kawaba et al., 1984).

1.2.2   STROMAL RESPONSE

Cells that play a key role in tissue remodelling following injury are keratocytes. Ordinarily they are responsible for maintaining the shape and transparency of the cornea by producing stromal collagen while maintaining its correct orientation and alignment via the secretion of hygroscopic proteoglycans. Since the population of Keratocytes is small, reaction to injury is slow (Ohno et al., 2002) and even though they produce the correct extracellular matrix (ECM) components, it might not be the correct arrangement required for corneal transparency (Fini, 1999). The remodelling process continues by employment of a group of matrix metalloproteinases (Maguen et al., 2002) which are responsible for cleaving and degrading collagen and other ECM proteins, this is thought to free epithelial cells from their cell-ECM interactions to aid migration of cells to the site of injury (Krachmer et al., 2005a).

1.2.3 Limbal epithelial stem cells

One of the driving forces behind the corneas capacity for renewal is the population of limbal epithelial stem cells (LESC). Labelling these cells as stem cells is bold as there is still debate about the extent of their potency. However the general consensus is that a population of epithelial cells exists in the basal layer of the limbus, which appears to have a higher proliferative potential than corneal epithelial cells. These cells differ from central corneal cells in expression of certain proteins. Human limbal epithelial cells contain ABCG2, Keratin-19, vimentin, KGF-R, metallothionein, and integrin α9 (Schlötzer-Schrehardt and Kruse, 2005) and basal limbal epithelial cells in particular express higher levels of p63, α-enolase, Keratins 5 and 14, and HGF-R (Schlötzer-Schrehardt and Kruse, 2005). Basal cells from central corneal epithelium stain positively for Keratin 3 and 12, connexion 43, involucrin, integrins α2, α6, and β4 and P-cadherin. Aside from differences in expression profiles the behaviour and morphology of LESC can be characterised by a high colony forming efficiency (Pellegrini et al ., 1999) and high nuclear to cytoplasmic ratio. (Shortt, Secker, Munro, et al ., 2007).

1.3 Corneal pathology

1.3.1 Aniridia

Aniridia is a rare disorder that comes from an absence or incomplete formation of the Iris. This condition arises from a mutation of the PAX6 gene, sometimes called AN2, located on chromosome 11 (Zumkeller et al., 2003) which is either hereditary or sporadic. Sporadic Aniridia mutations affect the region adjacent to the AN2 Aniridia region, causing nephroblastoma (Wilms tumor) (Wright and Spiegel, 2002). These patients usually suffer from genitourinary abnormalities as well as significantly impaired cognitive function (WAGR syndrome). The severity of Aniridia depends on the type of mutation. In many cases Aniridia leads to impaired vision, glaucoma, cataracts and corneal vascularisation.

1.3.2 KERATACONUS

Kerataconus is a degenerative disorder, which results in a thinning and distortion of corneal curvature, making it more conical impairing vision and increasing photosensitivity. Diagnosis of kerataconus occurs during adolescence and in most cases progression will slow or cease during the patients twenties or thirties. Around 10-25% of cases will develop to a point where vision correction is no longer possible (Javadi et al., 2005; Schirmbeck et al., 2005), due to excessive corneal thinning, or scarring as a result of contact lens wear. A corneal transplant or penetrating keratoplasty may be necessary. Keratoconus accounts for approximately 25% of all penetrating keratoplasty procedures (Mamalis et al., 1992).

1.3.3 HERPES SIMPLEX KERATITIS (HSK)

HSK is the most common cause of corneal blindness in the western hemisphere with an incidence of 500,000 cases in the US alone. The main antigen-presenting cell in the cornea is the Langerhans cell. This is usually absent from the central cornea and resides in abundance in the limbus. A study by Miller *et al.* (1993) showed that these cells migrate to the central cornea when infected with Herpes Simplex Virus, with the number of Langerhans cells in the central cornea proportional to corneal damage (Miller et al., 1993). As is characteristic of infection, immune cells responding to the foreign presence release various cytokines. Cytokines direct cell migration and differentiation in development, homeostasis and defence. As HSK progresses different cytokines are released. During the early stages IL-1α, IFN-γ and IL-2 are released, with IL-4 present during the later stages (Heiligenhaus et al., 1999). IL-2 may have an important role to play in protecting against HSK as IL-2 knockout mice have been shown to be more prone to lethal infection whereas mice treated with recombinant therapy have improved chances of survival (Ghiasi et al., 1999).

1.4 CURRENT THERAPIES IN CORNEAL REGENERATION

The appropriate therapy will depend on the severity of the injury or disease and if the patient is bilaterally or unilaterally blind. These factors will dictate whether

the therapy will be allogeneic or autologous, careful assessment of each case would be required to confirm if the patient has partial or total limbal stem cell deficiency (LSCD) as the success of the procedure hinges on the ability of the patient to renew their epithelium.

1.4.1 KERATOPLASTY

This procedure involves the replacement of the abnormal host tissue by a healthy donor cornea. It is the most well established and most successful of all transplant procedures and has been performed for over 100 years. Two approaches may be adopted

- – A full thickness penetrating keratoplasty (PKP)
- – Partial thickness lamellar keratoplasty

Healthy donor corneal tissue is extracted within 24 hours of death. The diseased portion of the cornea is excised, while the donor corneal button is prepared (Mamalis et al., 1992; Panda et al., 2007). The donor cornea, the same size as the hosts is sutured with a continuous length of non-absorbable atraumatic suture material such as silk, since the healing time can take up to a year. Rejection may also not occur immediately and may take up to 6 months to see signs of graft rejection (Krachmer et al., 2005b).

1.4.2 LIMBAL STEM CELL DEFICIENCY

Limbal stem cell deficiency (LSCD) can be caused by many diseases and is usually characterised by conjunctival ingrowth, corneal inflammation, basement membrane damage and vascularisation (Chen and Tseng, 1991, 1990; Dua and Forrester, 1990; Huang and Tseng, 1991). In cases where there are little or no residual limbal stem cells, a standard keratoplasty is likely to fail, as the donor epithelium sheds naturally, host epithelial cells cannot repopulate the ocular surface (Holland and Schwartz, 1996; Tseng, 1996). The most common cause of LSCD is from chemical or thermal burns (Wagoner, 1997). Other causes include Stevens Johnson syndrome (SJS), aniridia and ocular cicatricial pemphigoid (OCP). The total prevalence of these conditions is 1 in 25,000 with approximately

10 % of these leading to LSCD, equating to 240 new cases each year in the UK (Daniels et al., 2001; Shortt et al., 2011).

In cases where patients suffer from unilateral LSCD, then the affected eye can be treated by transplanting autologous Limbal epithelial stem cells (LESC) from the patient's unaffected eye using a procedure called conjunctival limbal autograft (CLAU) (Jenkins et al., 1993; Moldovan et al., 1999; Morgan, 1996).

In cases of bilateral LSCD patients may require other forms of treatment such as a Keratolimbal allograft (KLAL), supplied by cadaveric donors, (Holland, 1996; Tan et al., 1996; Tsai and Tseng, 1994) or living related conjunctival limbal allografts (lr-CLAL) (Daya and Ilari, 2001). These treatment options require systemic immunosuppression and such procedures are considered to have a poor long term success rates (Tsubota et al., 1999, 1995). Alternatively, LESC transplants from ex-vivo expanded autologous (Pellegrini et al., 1997) or allogeneic (Vemuganti et al., 2004) limbal biopsies may be used. In severe cases of total LSCD this procedure may be used in conjunction with a penetrating or lamellar keratoplasy. This technique can offer advantages to the aforementioned surgeries such as smaller initial biopsies and reduced risk of allograft rejection (Shortt et al., 2007b). Since Pellegrini's pioneering work using ex-vivo expanded cells to treat LSCD, efforts have been made to maintain the stem cell phenotype of the cells transplanted into the eye so that the epithelium can be maintained for much longer. So far the best substrate for delivering LESC to the eye is human amniotic membrane (hAM) as it can act as a basement membrane substitute that aids adhesion and migration of basal epithelial cells (Boudreau et al., 1995; Grueterich et al., 2003). It also contains anti angiogenic and anti-inflammatory proteins, (Hao et al., 2000) which contributes to its efficacy and as a result has been demonstrated to treat partial LSCD alone (Anderson et al., 2001; Gomes et al., 2003). Despite this, long term success rates can be improved, as currently studies indicate a 68% (post 2 year) success rate (Sangwan et al., 2011). A synthetic alternative to amniotic membrane has also been explored to simplify this treatment process and overcome issues regarding donor variability and tissue banking (Deshpande et al., 2013). This study uses PLGA electrospun

scaffolds to create a synthetic AM substitute. This study also proposes eliminating ex-vivo expansion of LESC and use small limbal tissue explants to expand LESCs in situ in cases of unilateral damage.

1.5   IMMUNOLOGY

Corneal grafts are the most common form of allotransplantation in the western hemisphere with the number of grafts performed annually increasing from 45,000 to 60,000 in under 10 years (Dana et al., 2000; Panda et al., 2007). With transplantation of allogeneic tissue comes the associated risk of rejection and usually requires systemic immune suppression. Rejection is a complex immune sequence with initial recognition of a foreign antigens resulting in the release of inflammatory cytokines. These in turn attract host antigen presenting cells, which are stimulated by the pro-inflammatory cytokines to up-regulate major histocompatibility complex (MHC) antigen expression. The foreign MHC antigens are then recognised by the host immune cells leading to sensitisation and subsequently a specific response against the allograft, causing it to be rejected. In the cornea this can start from 10 days after the procedure and is characterised by an increase in the thickness of the graft, a visible rejection line separating the graft from the host tissue, and keratic precipitate. The cornea, however, has relatively much higher graft survival rates than other forms of allograft, even without routine human leukocyte antigen (HLA) matching, with >90% of allogeneic transplants surviving for two years in patients classed as low-risk, i.e. absence of vasculature and first graft, with no major histocompatibility complex matching and local immune suppression. Hence, the cornea is postulated to be an immunoprivileged site (Niederkorn, 2003). Many factors contribute to this privileged state and these include: (1) a lack of vascularity; (2) absence of lymphatics; (3) expression of immune modulatory factors and neuropeptides by corneal cells, inhibiting complement activation; (4) expression of FaS ligand to activate apoptosis of FaS+ cytotoxic T cells; and (5) anterior chamber-associated immune deviation (ACAID) (Streilein, 1995; Streilein et al., 2003; Stuart et al., 1997). When comparing this to a high-risk patient with extensive

neovascularisation of the corneal bed rejection rates jump to >50%, even with local and systemic immune suppression. Bed vascularisation is seen as a major indicator of rejection (Gottsch et al., 1992) and the level of vascularisation has been shown to be proportional to the rejection reaction (Khodadoust, 2008). There are many other factors that increase the risk of rejection. Risks associated with the patient include vascularisation, as previously mentioned, HLA and blood type matching, previous rejection of a graft resulting in sensitisation of the host (No Authors, 1992), inflammation due to keratitis (Koay et al., 2005), and active immune systems as found in young patients and those undergoing bilateral grafts (Inoue et al., 2001). Graft-related risks include storage and transportation, and the presence of donor-derived Langerhan's cells, the primary antigen presenting cell in the cornea, in the transplanted tissue (Niederkorn, 1995). Other risk factors may arise from surgical procedure, such as a penetrating graft, a >8 mm transplant size, and exposed suture knots which can cause irritation leading to inflammation resulting in the commencement of the immune cascade responsible for rejection of the graft.

The battle to prevent rejection of allogeneic corneal transplants is currently three-pronged. HLA and ABO matching have been shown to reduce the rejection rate by between 10-40% depending on the level of risk associated with the patient (Khaireddin et al., 2003). However, it has also been suggested that this strategy may only be successful in preventing rejection if used in conjunction with a nonvascularised bed (Streilein, 2003). Reducing the antigenic load also shows promise in reducing rejection rates. A central graft accomplishes this as it is likely to contain far fewer donor Langerhan's cells (Gillette et al., 1982). Ultraviolet light can also be used to deactivate donor cytotoxic T cells (Niederkorn et al., 1990).

1.6   STEM CELL NICHE

A stem cell niche is a habitat that sustains and allows stem cells to reproduce or self-renew. Adult stem cells have limited function without the stem cell niche, and nowhere is this more greatly exposed than with haematopoietic stem cells (HSC). These circulate freely in the body but appear to function when located within very specific locations (Scadden, 2006). The stem cell niche provides much more than a habitat for a stem cell as it modulates stem cell function to fulfil the physiological need. It has been shown that it is the interaction at the niche between stem cells and somatic cells that allows stem cells to retain their potency (Peerani and Zandstra, 2010). It has been postulated that the extracellular matrix may be sufficient in providing the cues required to maintain stem-cell features (Ohlstein and Spradling, 2006).

1.6.1 NICHE PROPERTIES

In order to develop a full understanding of the role played by stem cell niches in stem cell proliferation, differentiation and migration it is important to understand the influence of the surroundings on stem cell fate. As well as cell-cell interactions, the extracellular matrix, along with soluble factors, can provide the necessary cues for stem cell function. A niche has the capacity to reprogram cells, and this has been demonstrated in experimentally vacated ovarian germline stem cell niches in *Drosophila* where dedifferentiation of ectopic follicle progenitor cells and cell division of foreign somatic stem cells was induced (Kai and Spradling, 2003).

The ECM that interacts with limbal stem cells has different properties to the ECM that interacts with conjunctival or central corneal cells. It maybe this specific environment that enables LESC to maintain potency.

TABLE 1.2: Examples of the most highly expressed proteins in the basement membrane of the limbus, and cornea along with proteins expressed all over the ocular BM (Schlötzer-Schrehardt et al., 2007).

BM Limbus	Uniformly expressed in ocular BM	BM cornea
Collagen IV (α1 and α2 chains)	Collagen VII, XVII, XVIII, Collagen IV (α5 and α6 chains)	Collagen IV α3 chains
Laminin α5 β2 γ1 chains	Laminin 111 and 332	Collagen V
Nidogen 1 and 2	Laminin α3 β3 γ2 chains	Fibrilin 1 and 2
Thrombospondin 4	Matrilin 1 and 2	Thrombospondin 1
Versican (sub- BM)	Perlecan	Endostatin

We are now beginning to gain an insight into what a niche may look like for certain tissues, however with regards to corneal regeneration an understanding of the specific mechanisms that promote differentiation of LESC into transient amplifying cells (TAC) that then go on to become corneal cells is still under investigation.

1.6.2 CELL-CELL INTERACTIONS

Physical contact between stem cells and somatic cells present in the niche, via adherence or gap junctions, can be mediated by cadherins. These adhesion receptors also play a vital role in securing stem cells to their niche (Walker et al., 2009) and have been shown to direct self-renewal and maintenance of neural stem cells (Karpowicz et al., 2009). The Ephrin receptor-ligand system has been implicated in neural stem cell self-renewal and neurogenesis through cell-cell interactions between stem cells and niche constituents (Holmberg et al., 2005; Ricard et al., 2006). Stem cell and niche cell interactions, although not fully understood, are also responsible for stem cell migration, attraction, proliferation and differentiation in different stem cell niches. Vascular endothelial cells have been shown to attract HSC's out of the bone marrow into the blood stream at

specific sites, providing the specific microenvironment required to achieve this (Sipkins et al., 2005). In another example it has been shown that hippocampal neural stem cell proliferation and differentiation are regulated by contact with vascular cells (Palmer et al., 2000) and astrocytes (Song et al., 2002), respectively. To highlight the complexity and array of interactions taking place, it should be noted that as well as contacting other stem cells and astrocytes, neural stem cells in the subventricular zone of the adult brain also connect with blood vessel endothelial cells via long basal processes and ependymal cells present in the ventricular walls using short apical processes (Mirzadeh et al., 2008).

1.6.3 CELL-EXTRACELLULAR MATRIX INTERACTIONS

The extracellular matrix (ECM) present in a niche is comprised of various proteins such as different types of collagen, laminin, and fibronectin. These components provide a structural framework as well as signals that regulate stem cells (Vazin and Schaffer, 2010). ECM components can have different impacts depending on their location. Hyaluronic acid is highly expressed on bone marrow stromal cell and HSC surfaces, and has been associated with haematopoiesis in the HSC niche (Nilsson et al., 2002); whereas hyaluronic acid activity in the NSC niche is linked to NSC quiescence (Costa et al., 2007). Another example of ECM interaction is between neural stem cell surface integrins with ECM proteins. This has been demonstrated to shape neural stem cell behaviour (Shen et al., 2004), with integrins serving as key signalling molecules in regulating the neural stem cell environment (Mobley et al., 2009). The delicate combination of ECM, cell and systemic signalling imparts the necessary cues to determine whether a stem cell migrates out of the niche, self-renews, or remains in a quiescent state.

1.6.4 SOLUBLE AND IMMOBILIZED FACTORS

As well as taking cues from niche cells and ECM, stem cells are influenced by soluble small protein factors present within the niche (Watabe and Miyazono, 2009). Although these may be present in solution *in vivo*, studies have demonstrated their controllable use as immobilized proteins (Rider, 2006).

Immobilisation allows the modulation of the cues imparted on stem cells by these small protein factors through control of local concentration, bioavailability and stability (Vazin and Schaffer, 2010). Another method of control is the lipid modification of factors such as Sonic hedgehog (Shh) and Wingless (Wnt), which are involved in haematopoietic and neural stem cell niches (Lai et al., 2003; Lie et al., 2005), resulting in altered solubility and membrane association characteristics (Saha and Schaffer, 2006; Willert et al., 2003). These factors have also been shown to impact stem cells in a concentration dependent manner, with opposing gradients determining the specification of neural cell types during development of the central nervous system (Briscoe and Novitch, 2008). It has also been demonstrated that neurotransmitters play a role in regulating stem cells in their niche (Katayama et al., 2006). Gamma-Aminobutyric acid (GABA) was shown to influence HSC migration (Katayama et al., 2006) and regulate neurogenesis in adults (Ge et al., 2007).

As stem cells in their niche are influenced by an array of factors from cell-cell, cell-ECM and small protein interactions as well as systemic, spatial and possibly geometric cues, it is important to consider all these when attempting to mimic a stem cell niche *in vitro*.

1.7   MIMICKING A STEM CELL NICHE

It would seem logical when considering a tissue engineering approach to incorporate some of the features of the stem cell niche mentioned previously. Some of the key features that have been studied have exploited techniques such as the use of immobilised growth factors, binding ECM proteins to surfaces, surface topography, matrix stiffness and simulation of oxygen gradients. In some cases it may only require the manipulation of only one of these features to control stem cell fate. The rest of this chapter broadly explores some characteristics of substrates to influence cell adhesion and proliferation as well as influencing stem cell fate. These features maybe important in the optimisation of synthetic onlay materials.

1.7.1 MECHANICAL PROPERTIES

The mechanical properties of substrates have been shown to influence the behaviour of cell spreading, migration, growth and differentiation. Anchorage dependent cells will exert traction forces on the substrate by rearrangement of the cytoskeleton and increased lamellopodial activity (Brandl et al., 2007). In general cells will adhere and proliferate well on stiffer substrates (Wang et al., 2000) forming stable focal adhesions and organised F-actin (Discher et al., 2005) responding with up-regulation of $\alpha 5$ integrins (Yeung et al., 2005). Cells on softer surfaces will exhibit less resistance to cellular traction forces and have dynamic adhesions, this has been shown to correlate with increased cell motility (Pelham and Wang, 1997). Using this concept could be useful in tissue engineering strategies to direct specific cell populations to their target locations. Cell migration in response to mechanical properties or mechanotaxis was demonstrated by Lo *et al.* (2000). Fibroblasts were cultured on flexible polyacrylamide sheets coated with type I collagen. Extra rigidity was introduced in the central region of the sheet by localised concentration of the bis-acrylamide cross-linker. Cells migrated freely to stiffer regions (Lo et al., 2000). Micropatterning was exploited to produce similar results using fibronectin coated poly (dimethylsiloxane) (PDMS) of varied stiffness (Gray et al., 2003). Of course depending on the desired outcome hydrogels might not necessarily need to be stiffer to promote cell adhesion. The cell type and its native ECM can give clues as to what mechanical properties a synthetic substrate should have. One example from Deroanne *et al.* reduced tension between HUVECs and gelatin coated polyacrylamide gels to allow them to switch from a monolayer to a tube-like arrangement resembling the last stages of angiogenesis (Deroanne et al., 2001). Flanagan et al. (2002) also utilised softer gels to enhance neurite formation (Flanagan et al., 2002).

1.7.2 MATRIX STIFFNESS

One of the most apparent differences between adult tissues would be the mechanical properties of their ECM. They are highly specialised and rather than being the consequence of specific cell secretions, stem cell fate may be the

consequence of established matrix architecture and stiffness. Studies by Engler *et al.* demonstrated this mechanism by culturing MSCs on polyacrylamide substrates with varied compliances. Cells differentiated into a lineage that resembled the elastic modulus of its native ECM, i.e. bone like stiffness yielded osteoblasts, medium stiffness yielded muscle cells and compliant gels yielded neural cells (Engler et al., 2006). Pelham *et al.* (2010) had previously used the same substrate coated with collagen to show that cells on flexible substrates displayed reduced spreading and increased rates of migration or lamellipodial activity. Focal adhesions on stiffer substrates also appeared more stable and spread than that of flexible surfaces (Pelham and Wang, 1997). Studies by Opas (1989) also showed that retinal pigmented epithelial cells are fully maintained in their differentiated state only when the substratum is pliable enough to prevent cell spreading (Opas, 1989). Stiffness was also exploited by Jones *et al.* (Jones et al., 2012) to increase limbal epithelial cell adhesion and proliferation on stiffer compressed collagen gels (2.9 kPa). They also reported increased expression of Keratin 3, characteristic of differentiated corneal epithelial cells, on these gels than softer gels (3 Pa).

1.7.3 TOPOGRAPHY

Topography determines the orientation of the cells and influences the direction of migration. It also affects the intracellular cytoskeletal arrangements. The structure of basement membranes provides a complex landscape of fibrous ridges and pores (Flemming et al., 1999). In the cornea these components control the distribution of the cytoskeleton and in turn the integrin receptors, which modulate proliferation and migration (Grushkin-Lerner et al., 1997; X. Y. Wu et al., 1995). The influence of the topographical arrangement can be major as demonstrated by McMurray *et al.* (2011). They reported that by culturing MSCs on a PCL surface with 120nm pits arranged in an absolute square lattice symmetry there was prolonged retention of MSC markers and multipotency, while offsetting the pits to a non-square arrangement induced osteogenisis (McMurray et al., 2011). This approach exploits nanodisorder of substrates to promote lineage specific differentiation. Studies that exploit nanodisorder to

direct differentiation have suggested that the results depend on the ability of the cells to form mature fibrillar-like adhesions (Dalby et al., 2007) or the cytoskeletal reorganisation in response to the landscape of the substrate (Curtis and Wilkinson, 1997; McBeath et al., 2004; Wójciak-Stothard et al., 1996). It is also worth considering what priority the topography of the surface has over its chemistry when simulating niche environments. Work by Britland *et al.* (1997) explored this by culturing rat dorsal root ganglia on surfaces with strips of laminin cues and topographical cues arranged orthogonally to each other. Cells responded to the chemical cues when the grooves were 500nm or less. Once the grooves reached greater than 5 μm, 80% of the cells responded to the topographical cues and orientated themselves in the direction of the grooves (Britland et al., 1997). This principle of replacing the chemical cues with topographical ones has been widely implemented with the use of electrospun micro or nanofibers. Enhanced proliferation of murine ESCs as well as retention of Nanog expression and multipotency can be achieved by culturing on electrospun polyamide nanofibers that mimic basement membrane texture when compared to the smooth surface of a cover slip (Nur-E-Kamal et al., 2006). Electrospun scaffolds have also been investigated as an alternative to human amniotic membrane for delivering cultured epithelial cells to the cornea (Deshpande et al., 2010).

1.7.4 OXYGEN GRADIENTS

It is generally appreciated that stem cells retain greater pluripotency under slightly hypoxic conditions (Mohyeldin et al., 2010). Studies on mouse (Gibbons et al., 2006) and human (Forsyth et al., 2006) ESCs showed more rapid expansion under 2–5% compared to 20% O_2, and hESCs cultured under 3–5% retained expression of stem cell markers (SSEA-1, OCT-4 and SSEA-4) compared to 20% O_2 (Ezashi et al., 2005; Simon and Keith, 2008). A range of cell types and tissues were studied for their reaction to hypoxia, In particular studies have shown enhanced proliferation and reduced differentiation of limbal epithelial cells under hypoxic culture (2%) (Miyashita et al., 2007). Hypoxia has also been combined with air exposure to culture limbal epithelium (Li et al., 2011). One

reason that has been suggested for this effect is that low oxygen tension in niches may offer a selective advantage over fast cycling cells undergoing aerobic metabolism as they are more susceptible to oxidative stress (Cipolleschi et al., 1993). Evidence to support this comes from studies on mouse embryonic fibroblasts cultured in 20% O_2, an increased number of mutations were observed and senescence occurred faster in comparison to cultures in 3% O_2 (Busuttil et al., 2003). Since low oxygen tensions appear to be a requirement for preventing differentiation, designing a means of reducing oxygen in certain areas of a substrate could hold the key to engineering a successful niche. Electrolysis was a method exploited by Park *et al*. (2006) to achieve this. They fabricated a microscale device that regulates oxidative microgradients in culture using electrodes 3-40 μm apart to deliver precise doses of oxygen without bubbling (Park et al., 2006).

1.8   BIOMATERIALS

For a long time cells have been studied in 2D even though all tissues in the body are incorporated into complex 3D microenvironments. They are composed of an elaborate network of proteins organised specifically for the cells they are housing (Gelain et al., 2007). These microenvironments allow chemical gradients to be maintained so that cell communication and development can take place as well as more complex processes such as signal transduction and differentiation. To create an artificial 3D environment scaffold, fibres and pores should aim to have dimensions similar to that of ECM components so that each cell becomes surrounded by the appropriate conditions required for promoting the desired function. This concept has become the philosophy behind the creation of specialised niches for housing and supporting stem cell populations (Dellatore et al., 2008; Votteler et al., 2010).

The material properties of a scaffold can be considered a biological signal and hence much work has used biomaterials to support cell proliferation and migration and now even to maintain and control stem cell populations. Any material that can be used to support tissue regeneration or replace damaged tissue has to be biocompatible with the surrounding tissue and with the newly

formed tissue. Two main strategies for tissue engineering exist: using natural biological polymers such as collagen, fibrin, chitosan, gelatin, alginate and hyaluronic acid, or using synthetic polymers such as polyethylene glycol diacryltae (PEG-DA), poly hydroxyethyl methacrylate (PHEMA), poly N-vinyl-2-pyrrolidone (PNVP), poly lactide-co-glycolide (PLGA) poly lactic acid (PLA) and many more (Davis and Anseth, 2002; Peppas et al., 2000). Progress in development of corneal inlay materials has still required the use of proteins such as collagen (Myung et al., 2009; Zheng et al., 2011) or fibronectin to improve corneal epithelialisation.

1.9 SYNTHETIC POLYMERS

Synthetic polymers present numerous advantages over other materials for developing scaffolds in tissue engineering. The major advantages include the ability to modify mechanical properties, modulus of elasticity, stiffness, and degradation kinetics to suit specific applications. Also, synthetic polymer devices can be manufactured in sterile conditions in reproducible methods using good manufacturing processes. This level of control in manufacturing is often impossible for "natural" scaffolds. The major forms of synthetic polymers used in tissue engineering are fabrications into electrospun scaffolds, hydrogels and coatings. All three avenues have been explored for corneal tissue engineering (Deshpande et al., 2010, 2009; Nitschke et al., 2007; Rimmer et al., 2007). The resulting treatments from these avenues have created 3 classes of medical device (see figure 1.4).

– Entirely synthetic prosthetics (non epithelialised central optic)
– Biomimetic scaffolds encourage host cells to regenerate
– Degradable scaffolds as substrates for ex vivo expansion of limbal epithelial cells
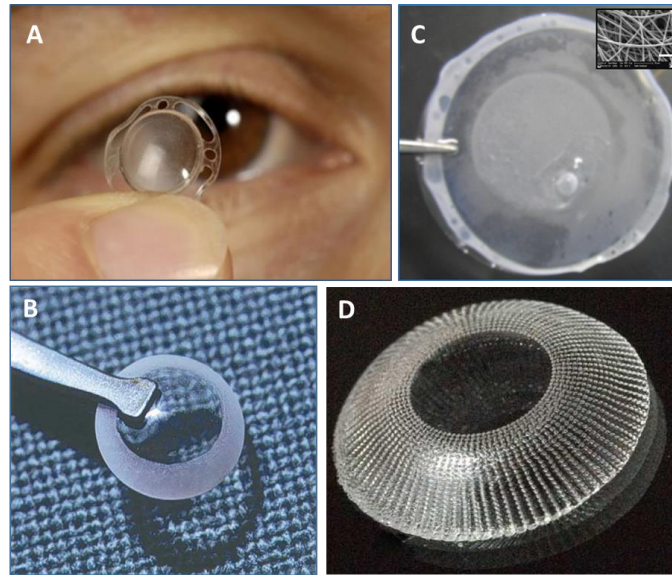
FIGURE 1.4: *Images of entirely synthetic keratoprosthetics, ArtCornea®* (Storsberg et al., 2012) *(A) and AlphaCor* (Hicks et al., 2003) *(B), degradable PLGA membranes* (Deshpande et al., 2013) *(C) and a surface colonisable biomimetic scaffold hydrogel Duoptix* (Myung et al., 2009) *(D)*

The AlphaCor artificial corneas are made entirely from the hydrophilic polymer poly(2-hydroxyethyl methacrylate), or P(HEMA), have a central optic region surrounded by a concentric skirt that is chemically identical yet higher in water content. The skirt is macroporous and allows stromal and scleral integration by tissue ingrowth up to the transparent edge of the device. It is inserted within a lamellar pocket after diseased tissue posterior to the device is removed. Once tissue has integrated into the porous skirt a secondary surgery removes damaged anterior tissue so the patient can obtain clear vision. Other keratoprosthestic polymeric devices that do not absorb water are the Boston K-pro made from poly methyl methacrylate (PMMA) (Bakhtiari et al.,2012) and ACTO TexKPRO made from polyvinylidene difluoride (PVDF) (Schrage et al., 2014) These materials do not support a corneal epithelium. Issues that have been reported from these synthetic keratoprosthetics are: tissue necrosis, leakages at the implant/ tissue interface, extrusion, (Chirila, 2001) and endophthalmitis (Jirásková et al., 2011).

Collagen-modified implants made from a poly(ethylene glycol)/poly (acrylic acid) (PEG/PAA) transparent central optic with a poly(hydroxyethyl acrylate)

(PHEA) hydrogel skirt, showed promising potential to replace non- epithelialised devices (Myung et al., 2009, 2008).

1.9.1 HYDROGELS

Non- hydrated polymers, while successful in some cases, can have limitations. Synthetic polymers are now being exploited to produce hydrogels for corneal regeneration. These specialised polymer networks are composed of hydrophilic polymer chains that are cross-linked with each other either chemically or physically. Chemical crosslinks are non-reversible covalently bonded junctions whereas physical cross-linking occurs via non-covalent interactions such as hydrogen bonding. To modulate the structural properties of the gel the degree of crosslinking can be adjusted. However, this is also related to the swelling capacity, which in turn influences the diffusion of key nutrients and soluble factors. The 3D water swollen gel has lower interfacial free energy improving the biocompatibility of the material (Jhon and Andrade, 1973). The option to tune the bulk properties of the hydrogel go hand in hand with the possibility of surface functionalisation which has the potential to turn a normally non-fouling, chemical releasing material into a cell adhesive tissue construct. Hydrogels tuned to influence cell behaviour could be an ideal material to serve as a corneal stromal mimic as they are usually non immunogenic and therefore biocompatible (Carraher Jr. et al., 2002; Lyndon, 1986; Nguyen and West, 2002). In addition most hydrogels can be transparent and they have high water contents to allow diffusion of glucose, this is important as some researches claim that bulk diffusion through the material is important for nutrition of the adherent epithelial cells(McCary and Schmidt, 1990; Thoft. et al., 1971; Myung et al ., 2008).

1.9.2 AMPHIPHILICITY

As well as adding functionality to polymers the bulk properties of the hydrogel should be carefully considered. One of the main features of the hydrogel is its ability to absorb large amounts of water. The extent of this feature can be determined by two factors, cross-linking density and degree of hydrophilicity: this property is routinely measured by surface contact angle.

Hydrogels of different chemical composition as well as entirely hydrophobic polymers are known as poor substrates for cell adhesion (Folkman and Tucker, 1980; Grinnell and Feld, 1982). However, studies have demonstrated the relationship between fibronectin on polymers and the adhesion and spreading of cells in vitro. Copolymers of hydrophobic EMA with hydrophilic HEMA in a 1:1 ratio support fibronectin adsorption and cell adhesion more than pure poly (HEMA) or poly (EMA) (Horbett and Schway, 1988; Horbett et al., 1988). Zhang *et al.* (2007) made polyurethane hydrogels using PEG/PCL of different ratios. In these studies higher PEG content, i.e. more hydrophilic, increased water absorbance and degradation rates. These gels were also less resistant to mechanical compression and showed lower chondrocyte cell attachment. Subsequent modification with a peptide sequence RGD was required to improve cell adhesion (Zhang et al., 2007). Other studies have also utilized amphiphilic material properties to enhance cell adhesion and proliferation (Deng et al., 2007; Haigh et al., 2002; Xiong and He, 2010) and it is generally acknowledged that highly hydrophilic synthetic materials will need modification with peptides or ECM proteins.

In some studies wettability was observed to be the overriding variable for optimal cell adhesion and stem cell maintenance. Mei *et al.* (2010) stated that the correlation between stiffness and colony-formation frequency of hESCs reflects the extent of polymer aphiphilicity since hydrophilic polymers swell to create compliant surfaces (indentation elastic modulus $E_i < 0:2$ GPa) that weekly support colony formation. They also demonstrate that through an array of hydrated polymers, colony formation is not strongly governed by polymer stiffness once the E_i exceeds 0.2 GPa but concluded that optimal colony formation frequency is governed by moderate wettability (contact angle~ 70°) (Mei et al., 2010).

Polymer network properties and swelling characteristics will further influence the mass transport kinetics of any biochemical in the aqueous environment (Drury and Mooney, 2003; Hoffman, 2002). This can be useful when designing materials that control the release of growth factors or drugs. These features are

usually incorporated by the use amphiphilic copolymers, which can form micelles at high concentrations encapsulating biomolecules of interest. (Kedar et al., 2010; Miyata et al ., 2011; Wei, Zhuo, & Zhang, 2013)

1.9.3 BIOLOGICAL PROPERTIES

Biochemical and physical properties are generally agreed to go hand in hand when related to cell behaviour and tissue regeneration. Cell migration involves the extension of a leading edge through rearrangement of actin filaments to form the lamellipodium, then, given the right cues these will attach to the substratum. One of the main ways cells respond to their surface is via a set of transmembrane receptors. They are heterodimers composing of an α and β subunit which connect the cells cytoskeleton to the ECM or substrate influencing cell behaviour (Clark and Brugge, 1995; Damsky and Werb, 1992; Huttenlocher et al., 1995). The roles of certain integrins in cell migration have been characterised in relation to certain proteins. For example, the α5β1 (Zhang et al., 1993) and α4β1 integrins have been shown to be responsible for migration on fibronectin (C. Y. Wu et al., 1995), whereas migration on collagen has been associated with integrin α2β1 (Schiro et al., 1991). Other cell surface receptors such as CD44 allow cells to bind to ECM components such as hyaluronate (HA), which is believed to be crucial in many cellular processes, including tissue remodelling (Sherman et al., 1994). Exploiting cell surface receptors to enhance cell adhesion and proliferation is usually achieved by covalently coupling short peptide sequences to the polymers. The most common peptide is RGD (arginine-glycine-aspartic acid) which is the key binding domain found in various ECM proteins. However more specific peptides that are derived from other proteins are summarised in the following table.

TABLE 1.3: Examples of peptide sequences used to replace the proteins they were derived from.

Peptide	Amino acid sequence	Protein from which its derived
RGD	arginine-glycine-aspartic acid	Fibronectin, Laminin, vitronectin, Collagen
REDV	Arginine-glutamic acid-aspartic acid-valine	Fibronectin
IKVAV	Isoleucine-lysine-valine-alanine-valine	Laminin
YIGSIR	Tyrosine-isoleucine-glycine-serine-arginine	Laminin

Synthesis of these peptides can be expensive and processes to incorporate them into hydrogels while preserving activity can become complicated. Therefore the ideal material for corneal regeneration maybe a hydrogel that can be tuned with properties discussed in this chapter such as stiffness, amphiphilicity, and water content. In addition, if the material can incorporate inexpensive and xeno-free cell receptive moieties it could have the potential to become a highly scalable, low risk alternative to biological substrates currently used to treat LESC.

1.10 SYNTHETIC HYDROGELS AS CORNEAL ONLAYS/INLAYS

A potential protein free, synthetic way to encourage corneal epithelialisation could be modification of hydrogels with alkyl amines. These hydrogels have been demonstrated to provide good substrata for corneal epithelial cells when co-cultured with bovine keratocytes (Rimmer et al., 2007; Sun et al., 2007). A similar study indicated that modifying hydrogels with 1,6-diamino hexane (1,6 DAH) can encourage A549 epithelial cells to grow up to and over their surface more effectively than unmodified gels (Zheng et al., 2011). The clinical efficacy of inlay materials will depend on the following criteria: they must be transparent, non-toxic, biostable and must have interfacial properties that permits sustained adhesion and proliferation of corneal epithelial cells (Evans et al., 2002; Khan et

al., 2001; Myung et al., 2008). A self-renewing healthy epithelium over a synthetic inlay is reputed to contribute to its survival (Du et al., 2012; Legeais and Renard, 1998; Myung et al., 2007) as the epithelium will help prevent entry of pathogens and fluid loss. However, non-colonisable inlays such as AlphaCor™ are still considered as treatments in exceptional cases (Hicks et al., 2006; Ngakeng et al., 2008).

To achieve epithelialisation, some of the strategies mentioned in this chapter may be used but, despite extensive studies in this field, there has been limited success with inlay devices. Some common yet complex issues have been highlighted. Collagen-modified surfaces have been shown to be prone to collagenase activity over time (Jacob et al., 2005), and methods used to increase protein adsorption, such as adding hydrophobicity or other proteins, may facilitate non-specific protein binding which has been thought to be the molecular event that triggers calcification (Myung et al., 2009; Vijayasekaran et al., 2000, 1997). Corneal inflammation may be a complication with implants coated in proteins such as fibronectin as it affects natural wound-healing processes such as fibroblast migration, (Sandeman et al., 2003) wound contraction and macrophage chemotaxis (Jester et al., 1999).

In general, most bulk hydrogel materials used for corneal regeneration have had moderate to high water contents to allow easy diffusion of nutrients and have used polymers such as poly(ethylene glycol)/poly(acrylic acid) (PEG/PAA) (Zheng et al., 2011), poly(hydroxyethyl acrylate) (PHEA) or poly(hydroxyethyl methacrylate) (PHEMA) (Oelker and Grinstaff, 2012). However, each of these systems requires proteins such as fibronectin, collagen or other peptides to facilitate cell adhesion (Myung et al., 2007) and proliferation. Also, modification with these matrix proteins inherently permits, to varying degrees, non-specific adhesion of cells.

Previous studies have shown that amine-modified polymethacrylate hydrogels can support epithelialisation both in mono-culture and co-culture with corneal stromal cells (Rimmer et al., 2007; Sun et al., 2007), or if coated with collagen IV (Ma et al., 2011) or VII (Evans et al., 2000). A small increase in epithelial cell

proliferation was observed in co-culture and some epithelialisation could also be achieved in mono-culture (Rimmer et al., 2009, 2007; Sun et al., 2007). It was evident from these earlier studies that alkyl amine functionality could transform hydrogels into effective substrates for epithelialisation. In contrast, aminated surfaces using plasma polymerization methods do not provide good substrates for general cell adhesion, while acid functionalization (Notara et al., 2007) can improve cell adhesion. Clearly, these studies suggest that both bulk and surface properties influence cell behaviour. These early studies indicate that optimisation of the alkyl-aminated hydrogels could provide a material that supports a stable epithelium.

Moreover, it is proposed that the selected material can be used to culture an epithelium with minimal stromal cell contamination directly from limbal explants. It is important to establish a corneal epithelial barrier quickly to minimize the risk of infections and further complications. This is an issue if the limbal epithelial stem cell (LESC) population responsible for corneal regeneration is destroyed due to injury or disease. The use of small limbal explants may contain the LESCs as well as the architectural microenvironments required for their survival. Regeneration of a corneal epithelium from limbal explants has recently been demonstrated in the clinic using small corneal explants fibrin-glued to a biological substrate, the amniotic membrane (Sangwan et al., 2012; Vemuganti et al., 2004). This concept has also recently been shown by our group to regenerate an epithelium on an ex vivo rabbit corneal model using a synthetic, rapidly degradable poly(D,L-lactide-*co*-glycolide) (PLGA) membrane developed as an alternative to the use of donor human amniotic membrane (Deshpande et al., 2013). The work in this thesis follows on from this concept and seeks to investigate whether synthetic hydrogels can be optimised to selectively promote epithelialisation. In looking at bulk hydrogel development and cell responses to these materials this study also examines the influence of bulk vs. surface properties of these materials on corneal epithelial and stromal cell adhesion, migration and proliferation.

AIMS AND OBJECTIVES

The aim of this thesis is to develop and investigate the potential use of various amine functionalised polymethacrylate hydrogels for use as a corneal inlay in the potential treatment of limbal stem cell deficiency (LSCD).

Deficiency of LESCs causes conjunctival epithelial cells to move over the cornea producing a thick scar pannus. Unilateral defects can be treated using LESC cultured from the unaffected eye then transplanting them to the affected cornea after scar tissue is removed. The underlying wound bed is often damaged however and conventional treatments may eventually fail, consequently there is a clinical need to develop a transparent corneal inlay to replace damaged stromal tissue and aid in corneal re-epithelialisation.

This study had three main objectives:

1. To produce a range of characterised hydrogels that can be functionalised with diamines.

   -To assess these materials for their suitability as cell culture substrates.

2. To assess the ability of the selected materials to support adhesion and proliferation of stromal cells, (limbal/dermal fibroblasts), in co-culture and with protein coating.

3. To assess the response of limbal epithelial cells on aminated hydrogels and various ECM proteins, and identify the most optimal material for future studies.

CHAPTER 2

HYDROGEL SYNTHESIS

TUNING AND ANALYSIS

CHAPTER 2: HYDROGEL SYNTHESIS TUNING AND ANALYSIS

2.1   INTRODUCTION

A typical corneal tissue engineering method begins with the development of a biocompatible substrate that supports the adhesion, proliferation and maintenance of a cell population. In many cases there is a temptation to approach a tissue engineering challenge by starting with a biological substrate known to contain the biological cues required for cell signalling, such as collagen obtained from either decellularised human or animal tissue or electrosupun bovine collagen (Torbet et al., 2007). Nevertheless synthetic polymer hydrogels can be useful for such purposes and unlike biological materials can be tuned to exhibit specific bulk and interfacial properties in order to support cells. Hydrogels in their swollen state allow diffusion of biomolecules through their networks and the low interfacial tension reduces immunogenicity (Carraher Jr. et al., 2002; Lyndon, 1986; Nguyen and West, 2002). This makes them an interesting option for use as a corneal inlay. However, hydrated networks are usually resistant to protein adsorption and hence are not cell-adhesive. As a result these types of hydrogel have previously been used as keratoprosthetics (Chirila, 2001; Legeais and Renard, 1998; Sandeman et al., 2003) or as cell delivery substrates after modification by methods such as plasma polymerization (Deshpande et al., 2009). For tissue engineering applications hydrogels can be modified to allow cell adhesion and proliferation while still exploiting the hydrogels' ability to allow diffusion of oxygen, water and glucose. Some common strategies employed to achieve this are: (i) modification with hydrophobic segments (Rimmer et al., 2005; Sun et al., 2007); (ii) modification with cell-adhesive peptides (Elbert and Hubbell, 2001; Hern and Hubbell, 1998; L Perlin et al., 2008; Lynne Perlin et al., 2008); (iii) modification with matrix proteins (Ma et al., 2011; Yanez-Soto et al., 2012) and (iv) surface modification with acid groups (Haddow et al., 2003; Notara et al., 2007) and other moieties. This study in particular focuses on the use of amine groups to modify hydrogels for corneal re-epithelialisation.

2.2   AIMS

The aim of this chapter is to produce a range of characterised polymethacrylate hydrogels that can be functionalised with amines and that will be suitable for use as cell culture substrates.

While optimising the production of these gels they are characterised for properties that are known to affect cell adhesion and proliferation.

1. Equilibrium water content (EWC) (Szycher, 1991)
2. Stiffness (Hopp et al., 2013; Yeung et al., 2005)
3. Wettability (Arima & Iwata, 2007; Lee et al, 1998; Tzoneva et al., 2007; Yanagisawa et al ., 1989)

Hydrogels were also qualitatively assessed for ease of handling and overall material integrity including assessment of cracks, faults, clarity and changes in appearance with solvent washes. . Finally, gels were screened for cytotoxicity effects before proceeding with cell and tissue culture studies.

2.3   MATERIALS AND METHODS

2.3.1   EQUIPMENT

Details of equipment used for the work carried out in this chapter are detailed in table 2.1

TABLE 2.1: Equipment used in production and characterisation of hydrogels.

Equipment	Brand	Supplier
12- well plates	Costar	SLS Scientific laboratory supplies
48 well plate	Griener	Griener- bio one
96 well plate	Costar	SLS Scientific laboratory supplies
Absorbance plate reader	Biotek	Bedfordshire, UK
Centrifuge	Rotafix	Hettich
Class II Laminar flow hood	Gelman Sciences	AS medical
Cork borer	--	SLS Scientific laboratory supplies
Cryovial	Simport	SLS Scientific laboratory supplies
Digital micrometer	Clarke	B&Q
Forceps	Prestige	Morton medical supplies

Fourier transform infra-red spectrometer	Perkin elmer	Perkin elmer
Goniometer	Rame-Hart	Rame-Hart Inc N.J USA
Incubator	Sanyo	Sanyo
Mr frosty ™	Thermo Scientific	Fisher Scientific
PET sheet	Hifi industrial film	Hifi, Hertfordshire UK
Pipette boy	Integra	SLS Scientific laboratory supplies
PTFE sheet (500 μm)	--	Direct plastics UK
Qurtz glass plates (2 mm)	UQG Optics	Cambridge UK
Raman Spectrometer	Thermo Scientific	Thermo Fisher Scientific, Inc
Rheometer (AR G2)	TA instruments	TA Instruments, Crawley England
Spray Mount adhesive	3M	Amazon
Spring clamps (50 mm)	Rolson	Amazon
T-25 Flask	Griener	Griener- bio one
T-75 Flask	Nunc	Thermo Fisher Scientific, Inc
ThinCert (0.4 μm) 12-well	Greiner	Greiner-bio-one
Ultra-pure water filter	Milli Q	Millipore UK
UV Curing Oven	Dymax	--
Wide neck laboratory glass bottle GLS 80 (250 ml)	Duran Group	SLS Scientific laboratory supplies
X- ray photoelectron spectrometer	Kratos	Kratos Analytical Ltd, Manchester UK

2.3.2   CHEMICALS

TABLE 2.2: Details of the chemicals used in the production and characterisation of hydrogels.

Chemical reagent	Supplier	
1,2 Diamino ethane (1,2 DAE)	Sigma-Aldrich Ltd	Dorset UK
1,3 Diamino propane (1,3 DAP)	Sigma-Aldrich Ltd	Dorset UK
1,4 Diamino butane (1,4 DAB)	Sigma-Aldrich Ltd	Dorset UK
1,6 Diamino hexane (1,6DAH)	Sigma-Aldrich Ltd	Dorset UK
Absolute ethanol	VWR international	
Ammonia in 0.2 M ethanol	Sigma-Aldrich Ltd	Dorset UK
Bake-o-glide	Falcon Products	Haslingden UK
Dichloromethane (DCM)	Sigma-Aldrich Ltd	Dorset UK
Dimethyl sulphoxide (DMSO)	Sigma-Aldrich Ltd	Dorset UK
Ethylene glycol dimethacrylate (EGDMA)	Sigma-Aldrich Ltd	Dorset UK
Glycerol monomethacrylate	Sigma-Aldrich Ltd	Dorset UK

(GMMA)		
Glycidyl methacrylate (GME)	Sigma-Aldrich Ltd	Dorset UK
2-Hydroxy-2-methylpropiophenone (HMPP)	Sigma-Aldrich Ltd	Dorset UK
Hydrochloric acid (HCL)	Sigma-Aldrich Ltd	Dorset UK
Lauryl methacrylate (LMA)	Sigma-Aldrich Ltd	Dorset UK
PEG- Diacrylate (PEG-DA)	Sigma-Aldrich Ltd	Dorset UK
Phosphate buffered saline (PBS)	Oxoid Ltd,	Basingstoke, Hampshire, UK
Propan-2-ol (IPA)	Sigma-Aldrich Ltd	Dorset UK
Rhodamine B	Sigma-Aldrich Ltd	Dorset UK
Trypan blue (Gibco®)	Gibco	Life technologies, Paisley UK
Videne	Ecolab	Ecolab UK
Cell culture and viability reagents		
Amphotericin B	Sigma-Aldrich Ltd	Dorset UK
Bleach (Presept disinfectant tablets)	Fisher Scientific	Loughborough UK
Dispase II	Roche	West Sussex UK
Dulbecco's modified eagles medium (DMEM)	Gibco	Life technologies, Paisley UK
Foetal calf Serum (FCS)	Biosera	East Sussex UK
Glutamine	Sigma-Aldrich Ltd	Dorset UK
MTT (3-(4,5-Dimethylthiazol-2-yl)-2,5-Diphenyltetrazolium Bromide)	Sigma-Aldrich Ltd	Dorset UK
Penicillin streptomycin (P/S)	Sigma-Aldrich Ltd	Dorset UK
Rabbit Eyes	Hooke Farm	Hooke UK

2.3.3 SYNTHESIS OF POLYMETHACRYLATE NETWORKS

The monomers, LMA, GMMA, EGDMA and GME in varying ratios (see table 2.3) (total 9 g) were dissolved in 4ml of isopropanol (IPA). The mixture was purged from oxygen, by bubbling nitrogen through the solution for 20 minutes. Just before curing, 90 mg, (1wt% monomers) of 2-hydroxy-2-methylpropiophenone (HMPP) was added and the total mixture degassed for a further 2 minutes. The solution was added to a polymerisation mould which stops oxygen entering the system and irradiated with 200 arc 400W mercury discharge lamp at a distance of 10 cm in a Dymax model Bondbox on a rotating table for 3 minutes, 90

seconds on each side. This initiated the conversion of monomer mixture to the polymer network shown in figure 2.1. The polymerisation mould consisted of two 2 mm thick quartz glass plates covered with 100 μm PET film attached by the minimum amount of 3M spray-mounts adhesive. The plates were separated with a rectangular 500 μm PTFE spacer and the whole assembly was held using spring clamps. The resultant polymer sheets were washed in IPA to remove any unreacted monomer and initiator (Haigh et al., 2002).
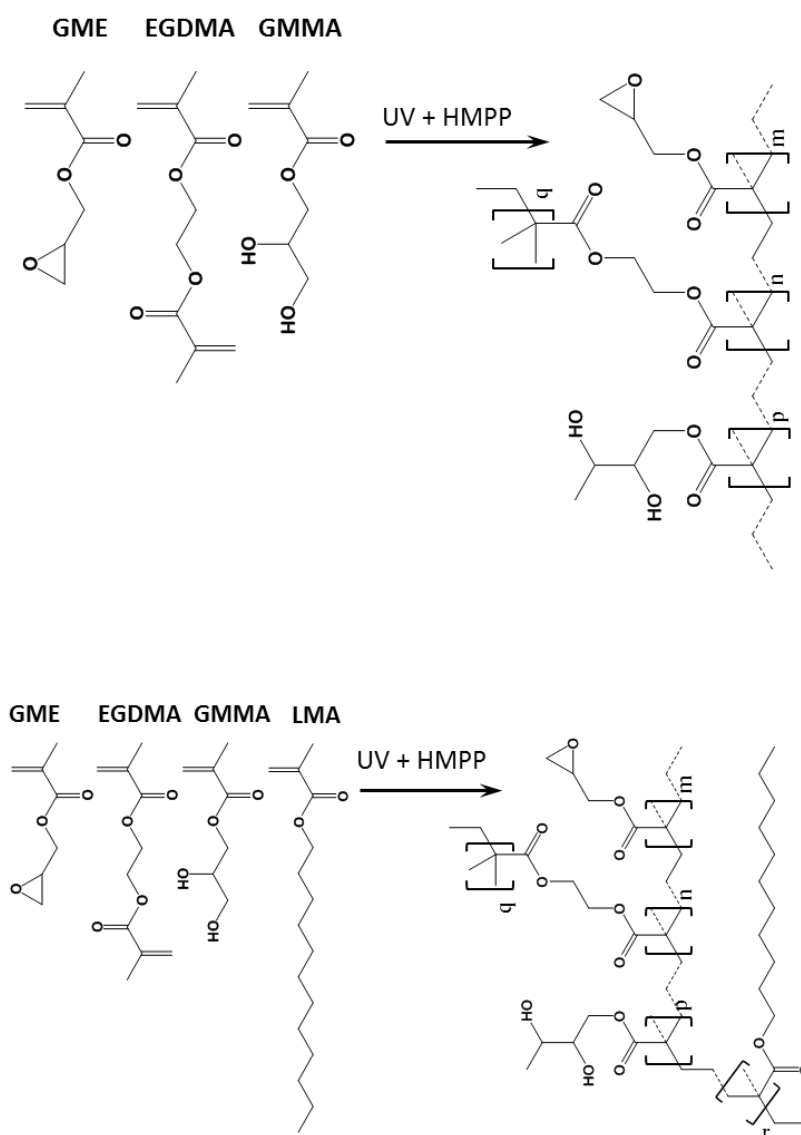
FIGURE 2.1: *Schematic representation of radical polymerization of the four monomers a) GME, EGDMA, GMMA and b) with LMA*

During the polymerisation process UV light causes two radicals to be formed from the HMPP via homolytic fission (figure 2.2). These highly reactive species then go on to react with methacrylate groups on the monomers initiating polymerisation. The polymer continues to propagate and crosslink, due to the difunctional EGDMA, forming a gel network.
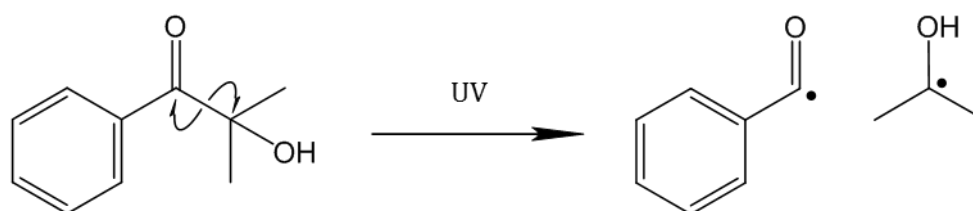
FIGURE 2.2: *Schematic representation of UV initiated radical production from HMPP.*

TABLE 2.3: Monomer percentage ratios made up to 9 g in 4 ml IPA, along with the hydrogel names used throughout this thesis.

Sort	Hydrogel	Glycerol monomethacrylate GMMA	Glycidyl methacrylate GME	Ethylene glycol dimethacrylate EGDMA	Lauryl methacrylate LMA
No LMA	Base A	85	5	10	-
	Base B	75	15	10	-
Increasing EGDMA	Base 0	82	5	1	12
	Base 1	80	5	3	12
	Base 2	75	5	8	12
Increasing GME	Base 1.B	75	10	3	12
	Base 1.15	70	15	3	12
	Base 1.20	65	20	3	12
	Base 1.30	60	30	3	12
	Base 1.40 **	55	40	3	12

2.3.4 SYNTHESIS OF ALKYL AMINE FUNCTIONALISED POLYMETHACRYLATE NETWORKS

Freshly prepared polymer sheets totalling 9 g were functionalized in 250 ml ethanol solutions containing the required amine (5 vol.%) to ensure >25 times excess (in terms of the epoxide groups) for 24 h at room temperature. The large excess minimises further crosslinking of the polymer by the free amine. The functional groups were provided by reaction with either ammonia, 1,2-diaminoethane (1,2 DAE) 1,3-diaminopropane (1,3 DAP) 1,4- diaminobutane (1,4 DAB) or 1,6-diaminohexane (1,6 DAH). For ammonia, functionalisation with a 0.1 mol.dm^{-3} ethanolic solution was used (Rimmer et al., 2007). The use of a large excess of the diamine ensures that all glycidyl ether groups are reacted through only one of the amine groups, allowing the other amine to be free to contribute to cell adhesion. This process (figure 2.3) was conducted in 500 ml laboratory glass bottles, which were sealed to minimize the amount of oxygen entering the system. Polymers were soaked five times overnight in absolute ethanol to remove excess diamine. Washing also removed any unreacted reagents.
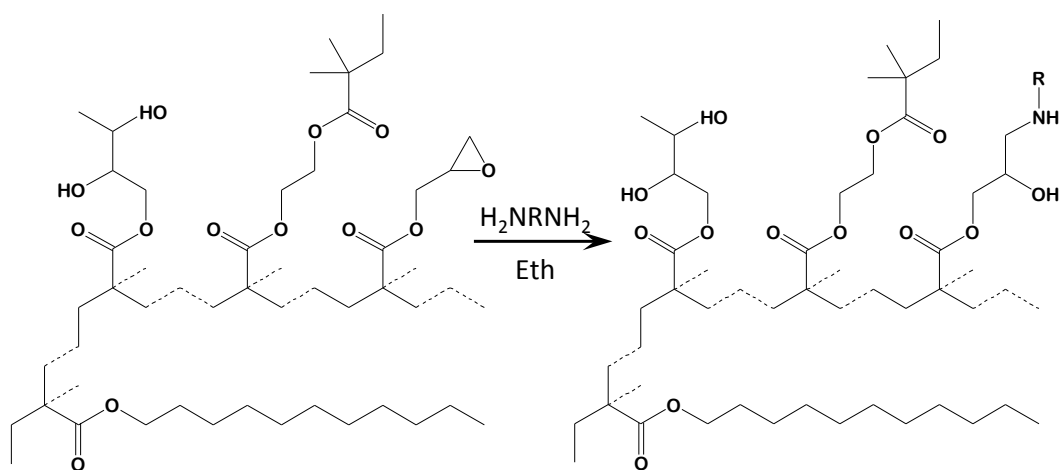
FIGURE 2.3: *Amination of hydrogels by post polymerisation with either ammonia or one of four diamines: 1,2 Diaminoethane, 1,3 Diaminopropane, 1,4 Diaminobutane.*

2.3.5 SYNTHESIS OF INERT PEG-DA 575 HYDROGELS

Inert surfaces known to be resistant to cell adhesion were made from Polyethylene glycol diacrylate (PEG-DA) (DeLong et al., 2005; Moon et al., 2009) to serve as negative controls in Chapter 3.

A PEG-DA solution was made by dissolving 9g of PEG-DA (MW 575) in 4 ml IPA and mixed thoroughly. Radical polymerization was initiated with HMPP as in 2.3.3 at 1% of the polymer weight. The solution was degassed for 2 minutes and injected into the polymer moulds as in 2.3.3. The resultant films were washed in IPA to remove any excess initiator and stored in ethanol until required.

2.3.6 EQUILIBRIUM WATER CONTENT MEASUREMENTS

The EWCs were determined by cutting sample discs from each polymer to be measured with a number 2 cork-borer (6 mm diameter) which were then dried in a dry incubator at 37 °C for 48 hours and then weighed. Samples were then hydrated over 24 hours in ultrapure water prepared by filtration (Milli-Q Systems). Wet and dry weights were noted and the EWCs were calculated using the following equation:

$$EWC = \frac{W_h - W_d}{W_h} \times 100$$ Equation (1)

Where W_h is the fully hydrated weight of the gel and W_d is the weight when fully dried. Directional swelling behaviour was also determined using the same method as above, however the percentage change in height and width were measured using a digital micrometer.

$$EWC = D_h\text{-}D_d/D_h \times 100$$ Equation (2)

$$EWC = H_h\text{-}H_d/D_h \times 100$$ Equation (3)

Where D_h is the fully hydrated diameter of the gel and D_d is the diameter when fully dried, H_h and H_d refer to the height of the hydrated and dry gel respectively.

2.3.7 CONTACT ANGLE MEASUREMENTS WITH CAPTIVE BUBBLE

A measure of hydrophilicity was obtained from hydrated samples using the captive bubble contact angle method. Contact angle measurements were carried out using a Rame-Hart goniometer with a quartz liquid bath attachment. This technique uses air rather than water to assess surface wettability, which reduces errors associated with water droplets receding into the bulk of the gel. Each sample was submerged in a quartz glass bath of ultra-pure water (MiliQ). A small bubble of air as close to 0.05 ml as possible was injected beneath the sample (see figure 2.4). The stability of the bubble depended on the surface, moving the chamber caused bubbles to roll off the sample and up to the surface. The angle made with the surface (θ) is the measure of the materials hydrophobicity as air is hydrophobic. To obtain hydrophilicity data, the value α is taken as $180° - \theta °$ (Figure 2.4). A large air contact angle (θ), or low water contact angle (α) indicates high surface wettability. A total of 8 contact angle measurements were taken from 4 samples of each gel type.
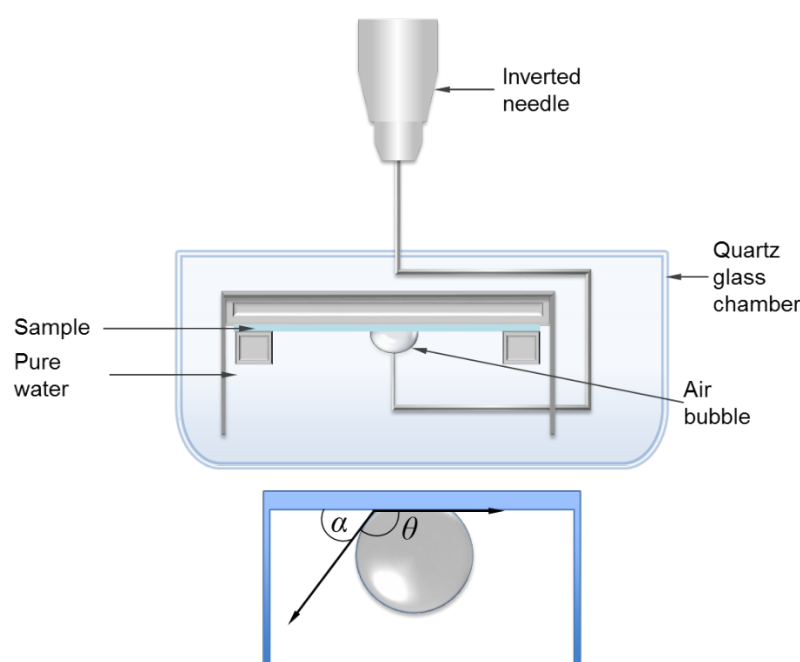
FIGURE 2.4: *Schematic representation of captive bubble measurement accessory to the goniometer used to determine contact angles.*

2.3.8 FOURIER TRANSFORM INFRA-RED SPECTROSCOPY

Information of the surface chemistry of the gels was obtained in the first instance from FTIR (Spectrum 100, Perkin Elmer, USA) using a universal ATR (attenuated total reflectance) accessory (figure 2.5). Gels were cut into 6 mm diameter discs and dried overnight in a dry incubator at 37 °C. The crystal sample area (figure 2.5) was cleaned using DCM (dichloromethane) and a background spectrum was collected. Gels were clamped between the sample area and the pressure arm and a pressure of approximately 80 % was applied. Spectra in the range of 4000 to 500 cm^{-1} were collected from an average of 275 scans at a resolution of 2 cm^{-1} using Spectrum ™ FTIR software.
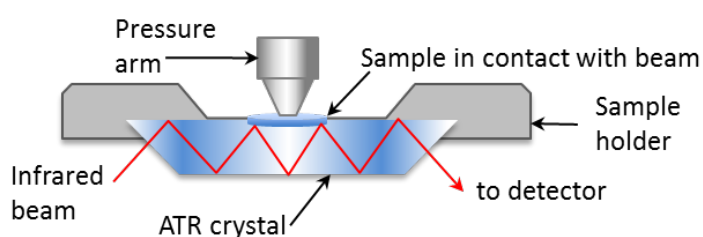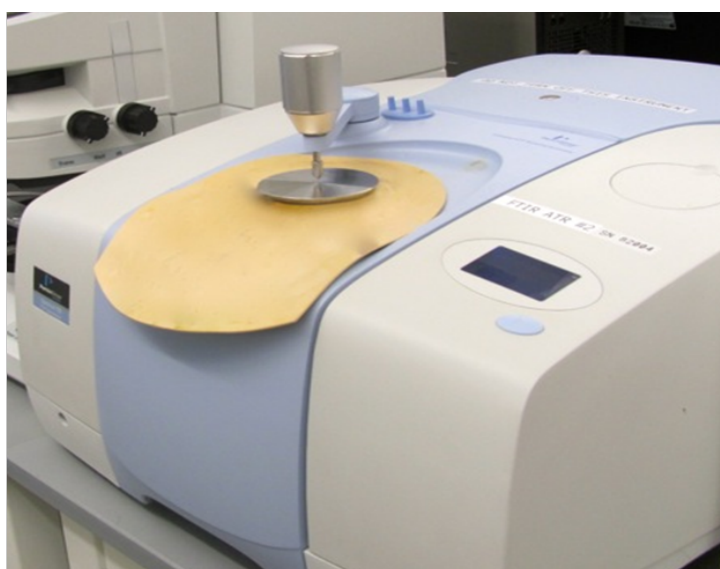
FIGURE 2.5: *Schematic representation of Fourier transform infrared spectroscopy (FTIR) unit with an Attenuated total reflectance (ATR) crystal accessory.*

2.3.9 XPS ANALYSIS

XPS (X-ray photoelectron spectroscopy) analyses the electron state and hence the atomic composition of a surface. Essentially it works by creating a localised photoelectric effect by bombarding the surface with photons. This leads to a discharge of electrons from the surface. The kinetic energies of discharged electrons are filtered through the hemispherical analyser (HSA), which allows the binding energy of the atom at the surface of a material to be determined. The intensity for a defined energy is recorded by a detector; this allows the concentration of a particular atom to be deduced (figure 2.6).
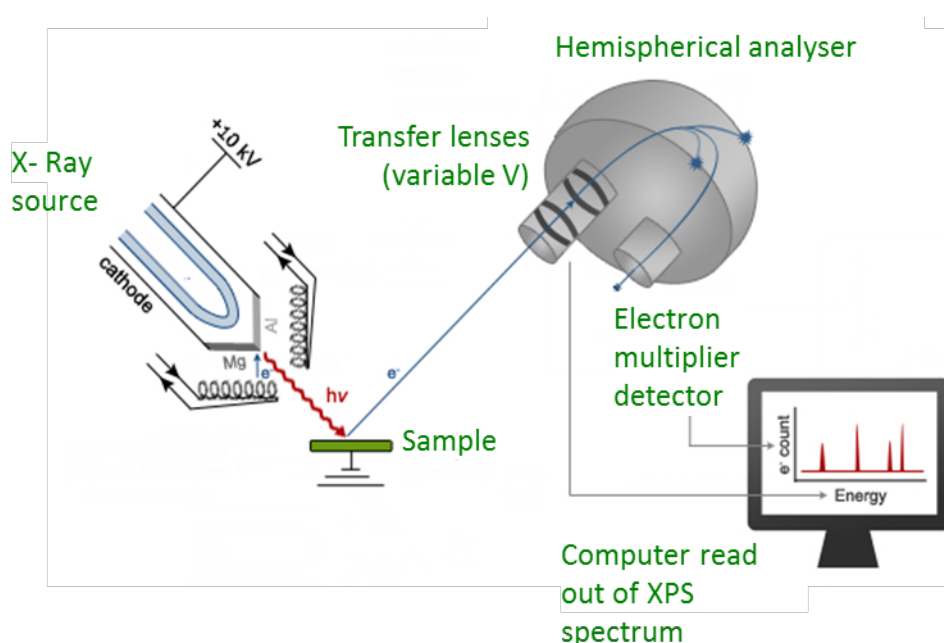
FIGURE 2.6: *Schematic representation of a typical X-ray photoelectron spectroscopy unit.*

In order to analyse the surfaces of the hydrogels using XPS the samples were cut using a number 2 cork-borer then immersed in absolute ethanol for 24 hours, washed in ethanol again and dried overnight in a dry incubator at 37 °C. Then each sample was placed in a well of a 48- well cell culture plate, (Greiner Bio-One, UK) each well contained a disc of a PTFE coated fabric (Bake-o-glide, Falcon Product Ltd, Haslingden, UK) to allow removal of gel discs without breaking from the plates. Gels were mounted onto a stainless steel grid before being sent for analysis *at the National EPSRC XPS User's Service (NEXUS) at*

Newcastle University, an EPSRC Mid-Range Facility. A Kratos Axis Ultra XPS instrument, with a monochromatic Al K_α X-ray source at energy of 1486.69 eV was used. In order to identify and quantify elements present on the surfaces, a survey of the binding energy at 1 eV and pass energy of 200 eV was obtained. A set of high-resolution scans (binding energy 0.1 eV and pass energy 50 eV) for carbon, nitrogen and oxygen was also obtained.

2.3.10 RAMAN SPECTROSCOPY

Raman spectroscopy was used to confirm the reaction of all the glycidyl ether groups, and compared against literature. Samples were prepared and dried in the same manner as in 2.3.9. Raman spectra were collected on a DXR™ Thermo Scientific Raman Microscope. A 10x Olympus objective was used with a 532 nm laser excitation and laser power 10 mW and a typical exposure time of 10s. A spot size of 2.1 μm and an aperture of 50 μm pinhole was set for collecting spectra.

2.3.11 RHEOLOGY MEASUREMENTS

All samples were cut into 15mm discs using a number 8 cork-borer and transferred from sterile ethanol storage solutions to PBS for a minimum of 24 hrs. An AR-G2 2000 rheometer (TA Instruments, Crawley England) was used to collect data. The fully hydrated samples were loaded between a heated Peltier plate, set at 37 °C, and 25 mm parallel plate geometry. Prior to the study, the criteria for valid modulus readings were set as: a) a normal compression force of 0.5 N and a gap of approximately 500 μm between the two parallel plates within which the discs were compressed, a couple of drops of PBS were pipetted in the gap in order to keep the gel swollen during measurements. Samples were then subjected to a standard oscillatory test (0.628 rad/s to 62.8 rad/s, 0.001 strain) (Figure 2.7). The upper plate oscillates at a fixed strain and records the stress response from the gels over a range of frequencies (ω) by measuring the torque on the drive motor. The digitally mapped bearing of this motor is used to record the absolute displacement, which is converted to strain. The resulting strain peak (γ0), stress peak (σ0) and difference in phase (δ) were measured for

each frequency. These values were used to calculate the elastic (storage) modulus (G′) (Figure 2.7). The mean storage modulus across all frequencies was used to describe the overall mechanical integrity of the gels while fully hydrated.

Where $G'_{\omega 1} = (\sigma_0 / \gamma_0) \cos \delta$
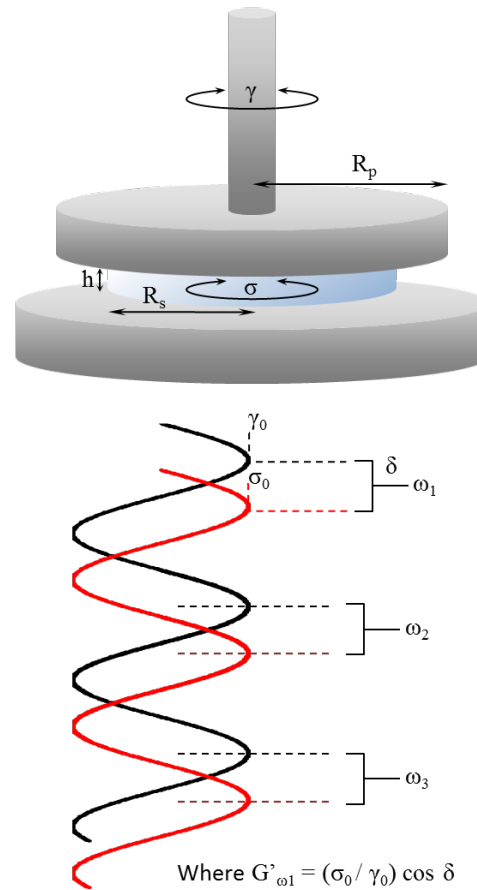
FIGURE 2.7: *Shows the dynamic sheer analysis operation on the Rheometer and the calculation of the storage modulus* (G′). *Samples are compressed between two parallel plates with a known force. The upper plate oscillates sinusoidally at a fixed strain and the resulting stress response is measured. G′ is calculated by measuring strain peak* (γ_0), *stress peak* (σ_0) *and the change in phase* (δ) *over a range of frequencies* (ω), *If there is no "deformation"* G′ *plotted over the frequency ranges should appear linear*

2.3.12 Primary rabbit limbal fibroblast isolation and maintenance

Rabbit eyes were obtained from Hook Farm, Hampshire, UK. They were received in chilled phosphate-buffered saline (PBS) within 24 hours of extraction. The eyes were first cleaned from excess tissue and then immediately disinfected using 3% Vidine for 2 minutes and washed in PBS. Eyes were then transferred to a class II tissue culture cabinet and immersed in 1.5% Videne for 1 minute before being washed in PBS.

The limbal regions were isolated and the remaining tissue discarded. The limbal explants were cut into 3–4 sections and placed in a solution of Dispase II (Roche) (2.5 mg.ml^{-1} in serum- free Dulbecco's Modified Eagle's Medium (DMEM) + Glutamax (Life Technologies, UK) and placed in an incubator for 1 hour at 37 °C and 5% CO_2. The tissue was de-epithelialised by transferring the explants to a dish of fresh DMEM + Glutamax media and scraping epithelial cells from the surface using a pair of blunt forceps (for retention of these epithelial cells see chapter 3) The remaining stromal tissue containing the fibroblasts was placed into T25 flasks and left in the incubator at 37 °C and 5% CO_2 to adhere before adding 10% DMEM (DMEM plus 10% FCS, 100 IU.ml^{-1} penicillin, 100 µg.ml^{-1} streptomycin, 2 x 10^{-3} mol.l^{-1} glutamine and 0.625 µg.ml^{-1} amphotericin B). Explants were cultured until rabbit limbal fibroblast (rLF) outgrowth reached 80% confluence, then passaged and used as required. For storage or passage of cells; culture media was removed and washed 3x with PBS. They were then detached from the flask using 2 ml of trypsin-EDTA (0.05% W/V trypsin -0.02% (w/v) EDTA), and incubated for 2 mins at 37 °C and 5% CO_2. The trypsin was deactivated by adding fresh 10% DMEM and the cell suspension was collected into centrifuge tubes and spun at 200 g for 5 minutes. For long term cell storage the cell pellet was resuspended in FCS containing 10% DMSO at a concentration of 400,000 cells.ml^{-1}, pipetted into cryo-vials and transferred into Mr frosty^{TM} freezing containers that provide cells with a cooling rate of -1 °C.min^{-1}. The containers were placed into a -80 °C freezer for 48 hrs before transferring into liquid nitrogen for storage at -196 °C. For passage of cells, pellets were resuspended in 12 ml DMEM with 10% FCS and the cell suspension

was transferred into a T 75 flask and cultured until 80% confluent. Cells were used up to passage 7. For retention of epithelial cells for experiments in subsequent chapters see chapter 3.
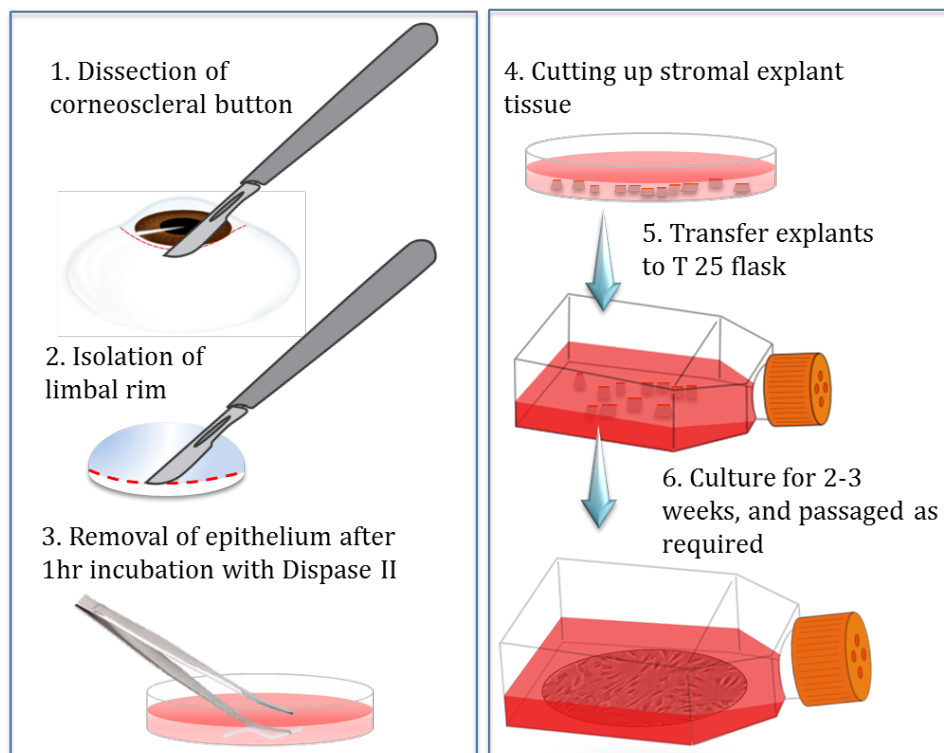
FIGURE 2.8: *Schematic representation of rabbit limbal fibroblast isolation from rabbit limbal rims.*

2.3.13 MTT

Hydrogels were evaluated for cytocompatibility by indirect culture with rabbit limbal fibroblasts (rLFs). Mitochondrial activity of the cells can be assessed using a colorimetric based assay such as an MTT (3-(4,5-Dimethylthiazol-2-yl)-2,5-diphenyltetrazolium bromide) assay. A colour change is observed as only metabolically active cells take up MTT by endocytosis. The tetrazolium ring of MTT is cleaved in active mitochondria by mitochondrial dehydrogenase forming formazan, a purple precipitate (Figure 2.9). Any formazan is solubilised using acidified isopropanol and used to obtain optical density readings that correlate to cell viability.

mitochondrial
reductase
enzymes

MTT - yellow tetrazolium

formazan dye - purple
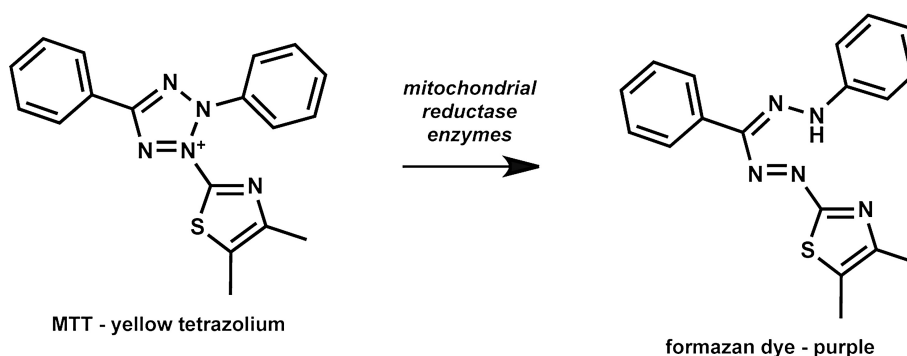
FIGURE 2.9 a): *Reduction of yellow tetrazolium to a purple formazan precipitate.*
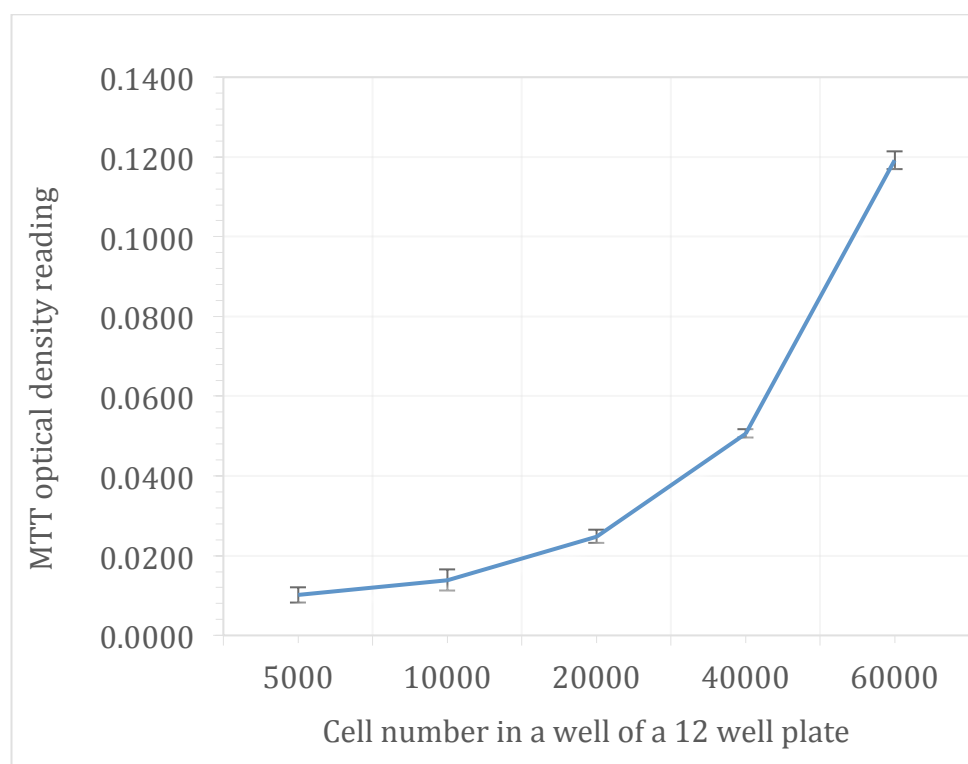
FIGURE 2.9 b): *A simple standard curve of optical densities obtained from an MTT assay of known rabbit limbal fibroblast cell numbers.*

2.3.14   INDIRECT CYTOTOXICITY TESTS

Gels with appropriate handleability were tested for leaching of any cytotoxic compounds from excess initiator, monomer, diamine or degradation products. Functionalised Base A, 1 and 2 polymer combinations were washed according to gel preparation method 2.3.3 and 2.3.4 then transferred to a sterile

environment and cut into discs using a number 10 cork-borer, (18mm). They were then washed in ethanol a further 2 times then in PBS 5 times including one overnight wash. Prior to seeding, the discs were saturated in DMEM with 10% FCS and incubated at 37 °C and 5% CO_2 for 2-3 hours to allow the gels to equilibrate swelling in the culture media.

Rabbit limbal fibroblasts were seeded at 30,000 cells per well of a 12-well plate (Costar, UK) and cultured in DMEM with 10% FCS at 37 °C and 5% CO_2 for 24 hours before introducing hydrogels. Hydrogels were placed into ThinCert ™ PET tissue culture inserts (Greiner, UK) of 0.4 μm pore size and suspended above the cells in the wells of a 12-well plate. An MTT- assay was carried out after 72 hours. Cells cultured in the presence and absence of the gels were washed 3x before adding 1 ml of MTT solution (0.5mg/ml MTT in PBS) and incubated for 40 minutes at 37 °C with 5% CO_2. Unreacted MTT was then removed and the resulting formazan salt was solubilised using 400 μl of acidified isopropanol (125 μl of 10M HCl in 100 ml isopropanol). For each sample 2 x 150 μl of the eluted formazan was transferred to wells of a 96 well plate. The optical density of the solution was measured at 540 nm with a reference at 630 nm, using an absorbance plate reader, see figure 2.9 b) standard curve for an approximate relationship between cell numbers and optical density.

2.4 STATISTICS

Statistical analysis using one-way ANOVA followed by a post Hoc Tukey test was performed using Origin Pro 8 and carried out either between functional groups of the same base or between bases of the same functional group. All data are expressed as mean ± standard error of the mean (SEM), with P < 0.05 considered significant. *Annotations are as follows *P < 0.05, **P < 0.005, ***P < 0.001.*

2.5 RESULTS

This study intended to define a set a materials that can be suitable for cell culture. To facilitate this an established recipe was modified. Each of the ingredients contributes certain properties. In this case the bulk of the gel is

made up of GMMA, this is hydrophilic and allows polymeric networks made with it to swell in water. The network is cross-linked together with EGDMA, controlling the amount of cross liker will control the amount of swelling the material will undergo when immersed in water. Amphiphilicity was introduced to the material by adding a hydrophobic monomer LMA. LMA also has a long hydrocarbon chain that creates spaces in the network that cannot be cross linked. These hydrophobic spaces within the network exclude water from the material reducing swelling while adding flexibility to the material. Finally, as mentioned earlier, hydrogels are intrinsically resistant to protein adsorption and hence cell adhesion. To overcome this, functional groups that may assist cell adhesion are added. This study investigates alkyl amines in particular which are added to the material by incorporating GME. GME allows amine coupling through ring opening of the epoxide group (figure 2.1 and 2.2). Changing the ratios of these monomers will produce materials with varying properties some of which may be more desirable. The following section demonstrates how changing monomer concentrations drastically affects the material properties especially when functionalised with amines of varied alkyl chain length.

2.5.1 PRODUCTION OF AMINE FUNCTIONAL HYDROGELS

Altering the ratio of the monomers GMMA, EGDMA, GME and LMA made 9 sets of gels. Table 2.3 classifies these types or "bases" of hydrogels into 3 groups. Bases A and B have no hydrophobic monomer, LMA, but differ in GME:GMMA ratio. Bases 0, 1 and 2 all have the same amount of GME and LMA but have increasing EGDMA:GMMA ratios. Finally 5 bases were made with increasing GME:GMMA ratios with a view to increase the concentration of alkyl amine on the surface of the gel. Modified GME containing gels could not be functionalised with longer alkyl chain amines as cracking issues were observed. Moreover functionalisation with ammonia and 1,2 DAE was not considered as preliminary studies suggested these groups were least conducive to cell adhesion. Therefore only 1,3 DAP and 1,4 DAB were used to assess the effect of surface amine concentration. Base 1.40 cracked even before reaction with amines so was discarded (see figure 2.10). With these exceptions bases were assessed as

unfunctionalised (plain) and when functionalised with ammonia, 1,2 DAE, 1,3 DAP, 1,4 DAB and 1,6 DAH giving a total of 42 different materials.
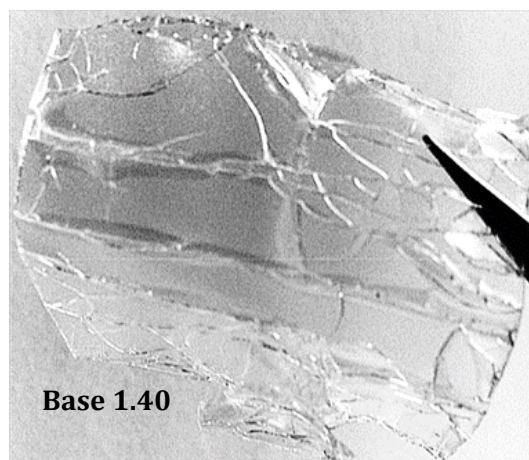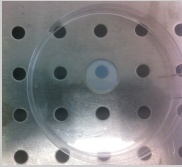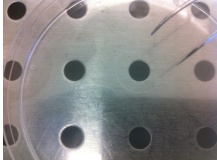
FIGURE 2.10: *Image of a sample of Base 1.40 after washing in IPA and before functionalisation.*

TABLE 2.4: Description of how each gel formula changes the appearance and handling of the material, when not functionalised (Plain) and when functionalised with each of the 4 diamines and ammonia.

Hydrogel	Plain	NH$_2$	1,2 DAE	1,3 DAP	1,4 DAB	1,6 DAH
Base A	No LMA resulted in all materials being stiff brittle, and difficult to cut					
Base B	stiff and brittle		small fractures imperfections in the material	larger cracks appearing material remains stiff and cracked	significant cracking material becoming more brittle	significant cracking material very brittle
Base 0	1% EGDMA results in high swelling and phase separation causes material to be cloudy			longer chain amine, seemed to increase swelling and opacity		
Base 1	This composition produced gels that did not change visually with functionality all were easy to process and transparent					
Base 2	gels were clear and slightly more brittle than base 1. Visually samples remained consistent after functionalisation.					

All bases in table 2.4 apart from Base B (15% GME) were successfully functionalised with all 5 amines and produced gels that may be evaluated as substrates for corneal tissue engineering. Base B showed progressive cracking and delamination, which can be visualised in figure 2.11. For ease of visualisation, gels were dyed bright pink by adding 100 mg rhodamine B per 100 ml of ethanolic storage solvent and allowed to soak for 2 hours before images were taken. First signs of fractures were observed 24 hours after functionalisation and drastically increased after the first solvent wash. All Base B gels were observed to be very brittle. Gels functionalised with 1,3 DAP, 1,4 DAB and 1,6 DAH cracked very easily when removed from their bottles or when handled with forceps with Base B/1,6 DAH being the most fractured and difficult to remove from its bottle.
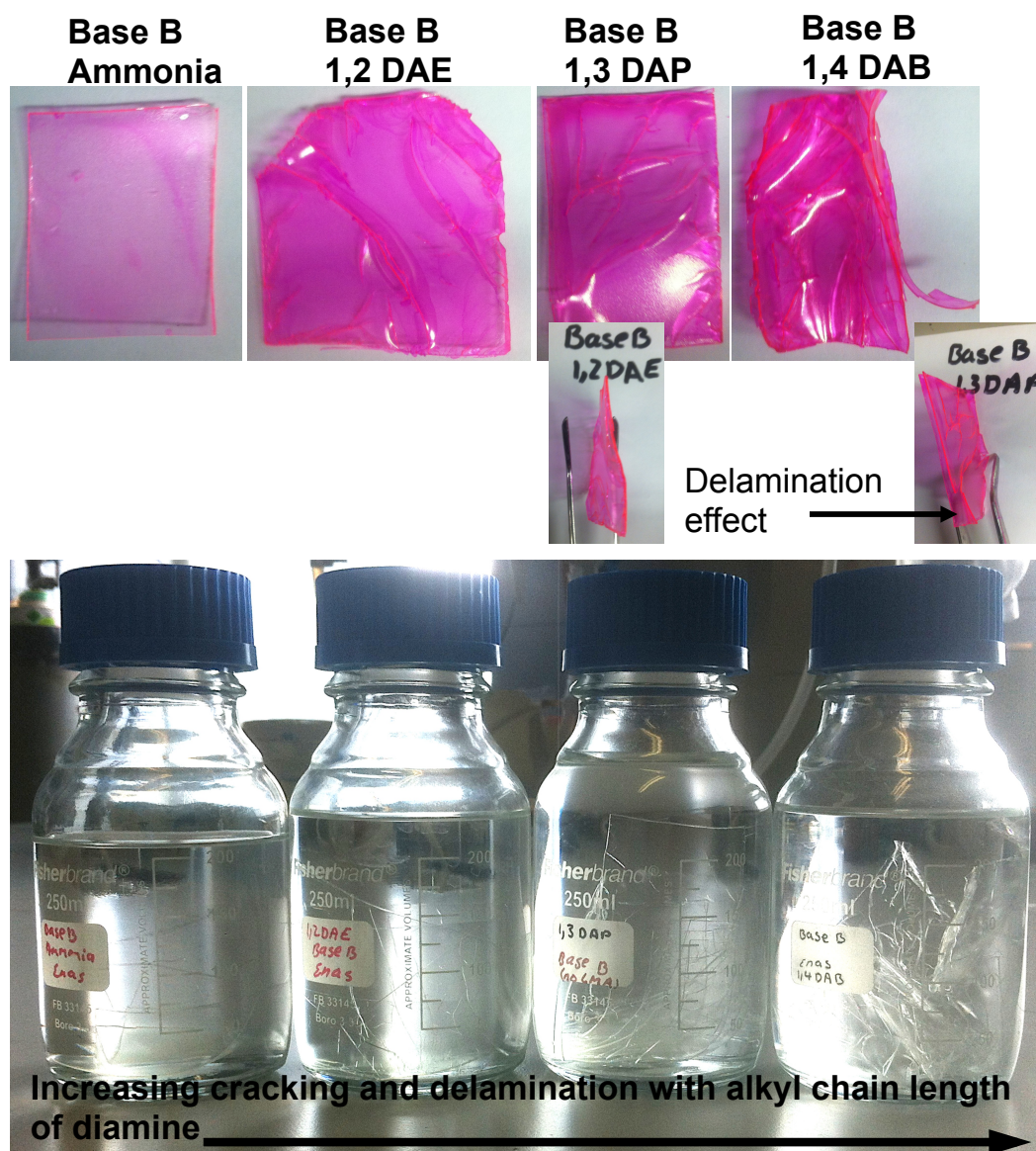
FIGURE 2.11: *Images of Base B shows the effect of excess GME when materials are functionalised with longer alkyl amines.*

Base A gels were not affected by the increasing carbon chain length of the functional groups, however all gels lacked flexibility and broke easily when removed from their bottles. Base 0 gels were very soft and easily pierced by forceps, these gels were also observed to become 'tacky' during the drying process. Sheets of these gels had a tendency to stick to each other especially when stored in IPA. All Base 0 gels were cloudy due to phase separation however when functionalised with 1,2 DAE gels were extra cloudy and were

observed to be slightly less prone to damage during handling. Bases 1 and 2 were clear, did not break during handling and were unaffected by the functionalisation process.

Bases 1.B. 1.15, 1.20 and 1.30 when unfunctionalised, functionalised with 1,3 DAP and with 1,4 DAB were evaluated after 4 washes in IPA, PBS and ethanol over 48 hrs. This evaluation was made in order to establish appropriate washing methods that do not lead to faults in the material.

Figure 2.12 shows how each material may stiffen, curl, crack and delaminate in each solvent. For ease of visualisation some samples were soaked in 10% trypan blue, which was much less intense than using rhodamine B, for 30 minutes. All unfunctionalised gels behaved normally and were unaffected by all three solvent washes.

Gels functionalised with 1,3 DAP became more faulty as the percentage GME increased, with ethanol causing more cracks and bubbles of delamination than PBS and IPA. These gels responded inconsistently to IPA, with some samples clear of faults however Base 1.30/1,3 DAP were consistently brittle and cracked. Moreover individual gel discs would bond to each other and break upon separation. Minimal defects were seen in gels washed with PBS apart from Base 1.30/1,3 DAP where some samples would curl and crack.

Gels functionalised with 1,4 DAB became defective after washing in ethanol and PBS, with extensive cracking and delamination when washed in PBS. There appeared to be least damage to 1,4 DAB gels after washing in IPA and faults that did occur were stiffening and curling which were found to be rectified if samples were functionalised in 250 ml wide top Duran jars that allowed sheets to remain flat during functionalisation. This way samples that may become cross-linked through both amines on 1,4 DAB do not take the shape of the curved bottles.
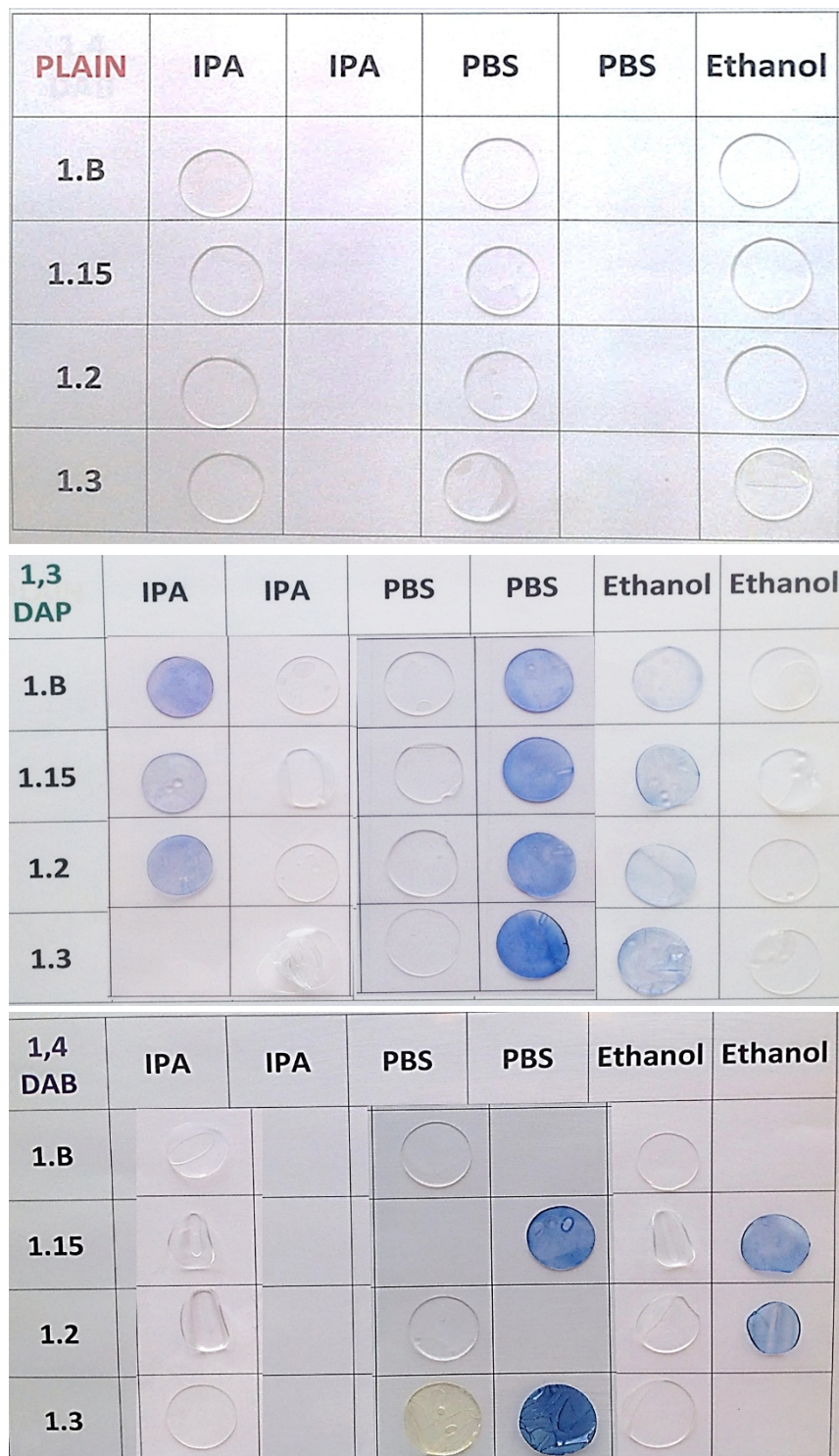
FIGURE 2.12: *Images of Base 1.B. 1.15, 1.20 and 1.30 when unfunctionalised, functionalised with 1,3 DAP and with 1,4 DAB in different washing solvents. For ease of visualisation some samples were soaked in Trypan Blue for 30 mins to high light any imperfections*.

TABLE 2.6: Summary of the behaviour of gels with increasing GME after they have been functionalised with 1,4 DAB and washed in IPA, PBS and ethanol.

1,4 DAB	IPA	PBS	Ethanol
Base 1.B	Normal hydrogel consistency	Normal hydrogel consistency	Normal hydrogel consistency
Base 1.15	Hydrogel starts curling and becomes stiffer	Normal hydrogel consistency with added bubbles of delaminated materials start to appear	Curling and stiffening of gel small bubbles forming where gel delaminates
Base 1.20	Hydrogel is stiff and curls easily	Small bubbles of delaminated material with added tiny fractures in the gel	Bubbles start to crack, gel prone to breaking, individual gel pieces stick together
Base 1.30	Normal appearance but brittle and stiff when handled	Severe delamination and cracking, brittle and stiff	Visible delamination, cracking and gel pieces bonding together
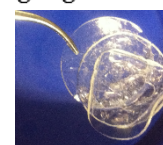
2.5.2 HYDROGEL SWELLING

By changing the monomer concentration as summarised in Table 2.3, it was possible to produce three bulk formulations with different swelling capacities by changing the ratio of GMMA to the cross-linker EGDMA. Base 0, 1 and 2 gels were made containing 1%, 3% and 8% EGDMA respectively, resulting in reduced swelling. The proportion of GME monomer units was not altered so that the amount of epoxide groups available for functionalisation would stay constant. The percentage of LMA was also kept constant in order to reduce any changes in the hydrophobicity of the hydrogel that may occur with increasing levels of cross-linker. Fig. 2.13 shows there were no significant differences between EWCs of Base 2 gels with different functional groups. Similarly, statistically significant differences were not seen in EWCs of Base 1 gels apart from when functionalised with 1,2 DAE, suggesting that the swelling behaviour is mainly due to the amount of EGDMA in these hydrogels.

Base 0 gels tend to increase in swelling with respect to alkyl chain length up to 1,4 DAB, beyond that, EWC of Base 0/1,6 DAH is not significantly higher than 1,3 DAP or 1,4 DAB functionalised gels.

In general there is an increase in swelling from Base 0 to 2 for all gels apart from those functionalised with ammonia and 1,2 DAE. For these functional groups, Bases 0 and 1 do not have a statistical difference in swelling.

Bases 1.B, 1.15, 1.20 and 1.30, which became prone to cracking when functionalised were also assessed for EWC. Figure 2.14 shows that swelling was lower with 1,4 DAB functionalised gels than with 1,3 DAP. There appears to be no correlation between the EWC and the percentage GME content. And in this case it appears to be the functional groups that influence EWC.
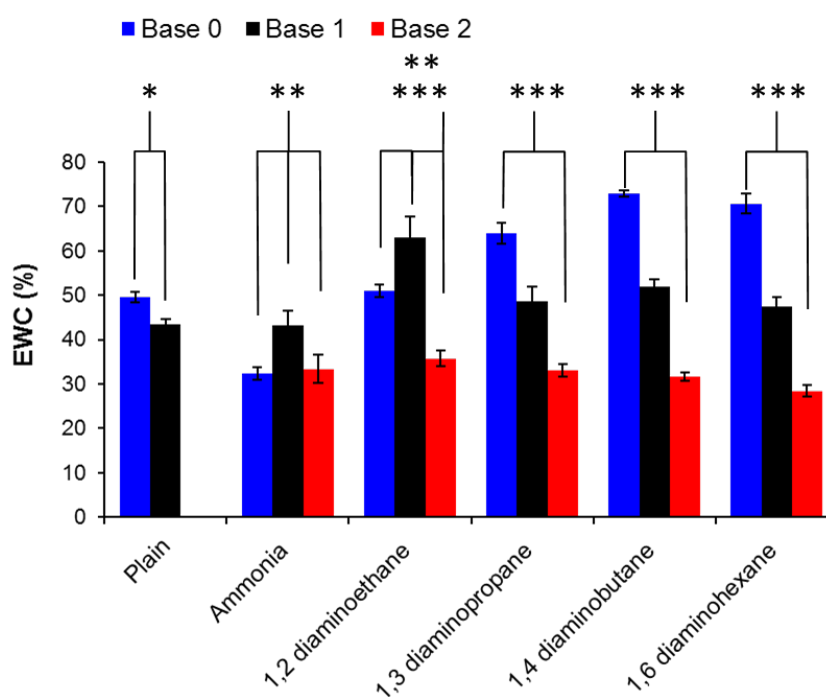
FIGURE 2.13: *Equilibrium water contents of Base 0, 1 and 2 after they have been functionalised with one of four diamines or ammonia. Results shown are means ± SEM of n=6. Statistically significant differences are marked as follows: Between bases of the same functional group,*
$*P < 0.05$, $**P < 0.005$, $***P < 0.001$.
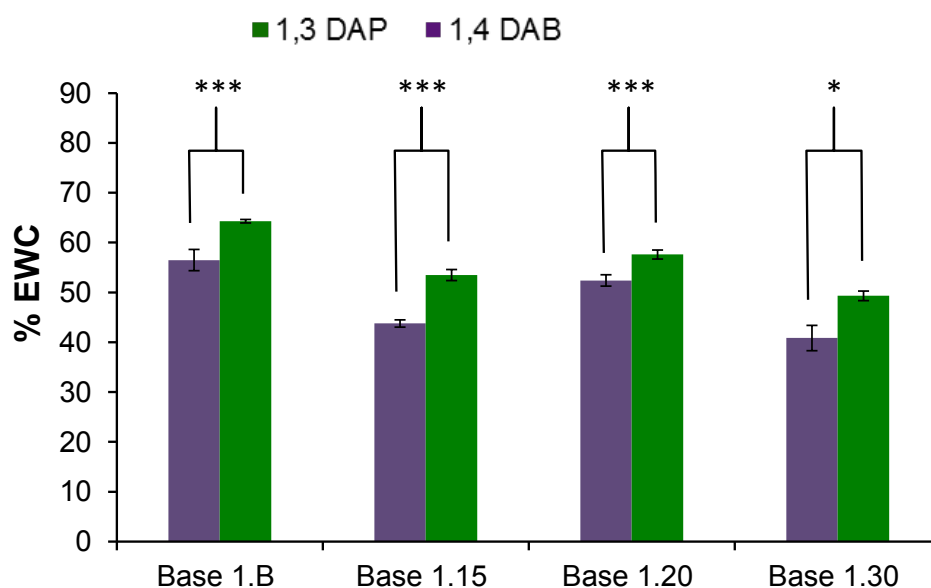
FIGURE 2.14: *Equilibrium water contents of Base 1.B, 1.15, 1.20 and 1.30 after they have been functionalised with 1,3 DAP or 1,4 DAB. Results shown are means ± SEM of n=6. Significance annotations are shown between functional groups of the same base. *P < 0.05, **P < 0.005, ***P < 0.001.*

2.5.3   BIAXIAL SWELLING BEHAVIOUR

Obtaining EWC measurements may not give a complete description of the materials. Often swelling behaviour is anisotropic which means expansion of the material is directional. If there is restriction in swelling at the surface of a material it may swell more in height, the consequences of this could be reduced diffusion of biomolecules to the surface where cells may adhere. One of the causes of anisotropy could be further cross linking of the surface from the free amine group on the diamine, this would result in a reduced concentration of free amine at the surface which may have further impact on cell adhesion and/or proliferation.

Base 0 gels do not exhibit statistically significant anisotropy when functionalised with 1,3 DAP, and 1,6 DAH however there is small but significant anisotropy with plain hydrogels, and hydrogels functionalised with ammonia, 1,2 DAE and 1,4 DAB. From these gels only 1,2 DAE functional gels would

display directional swelling in height. Plain gels and those functionalised with ammonia and 1,4 DAB display directional swelling in width (figure 2.15, A).

Unlike Base 0, Base 1 gels exhibit significant anisotropy when functionalised with 1,3 DAP, 1,4 DAB and 1,6 DAH. Plain Base 1 gels do not have a significant difference in swell height and width and may be categorised as isotropic. Base 1 gels that display anisotropy all swell directionally in height, with the Base1/1,4 DAB gels showing the highest degree of anisotropy (figure 2.15, B).

Excluding Base2/1,3 DAP, all other functionalised Base 2 gels demonstrated directional swelling in height, with the highest degree of anisotropy seen in 1,2 DAE functionalised gels (figure 2.15, C).

Biaxial swelling data was obtained from gels with increased GME content, both when functionalised with 1,3 DAP and when unfunctionalised. Data from 1,4 DAB functional gels could not be obtained due to deformation and cracking of samples after immersion in ultra-pure water. Figure 2.16, A) shows that all plain gels display significant directional swelling and each gel in this set swells more in height than width. In contrast, three of these gels display no significant anisotropic behaviour after functionalisation with 1,3 DAP. Only Base 1.15 retained its directional swelling behaviour after functionalisation (figure 2.16, B).
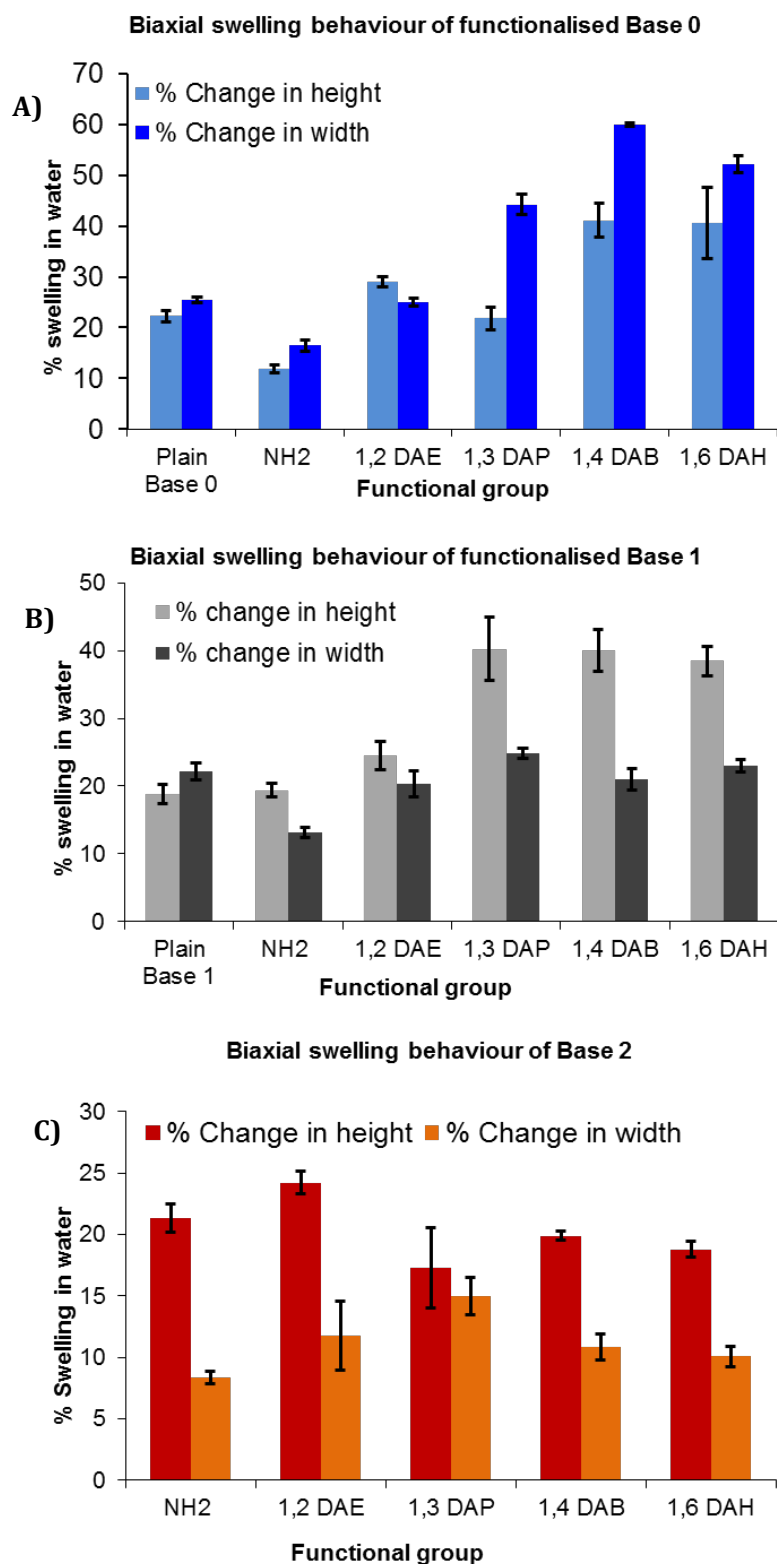
FIGURE 2.15: *Biaxial swelling behaviour of Base 0, 1 and 2 after functionalisation with four diamines or ammonia. Results shown are means ± SEM of n=6.*
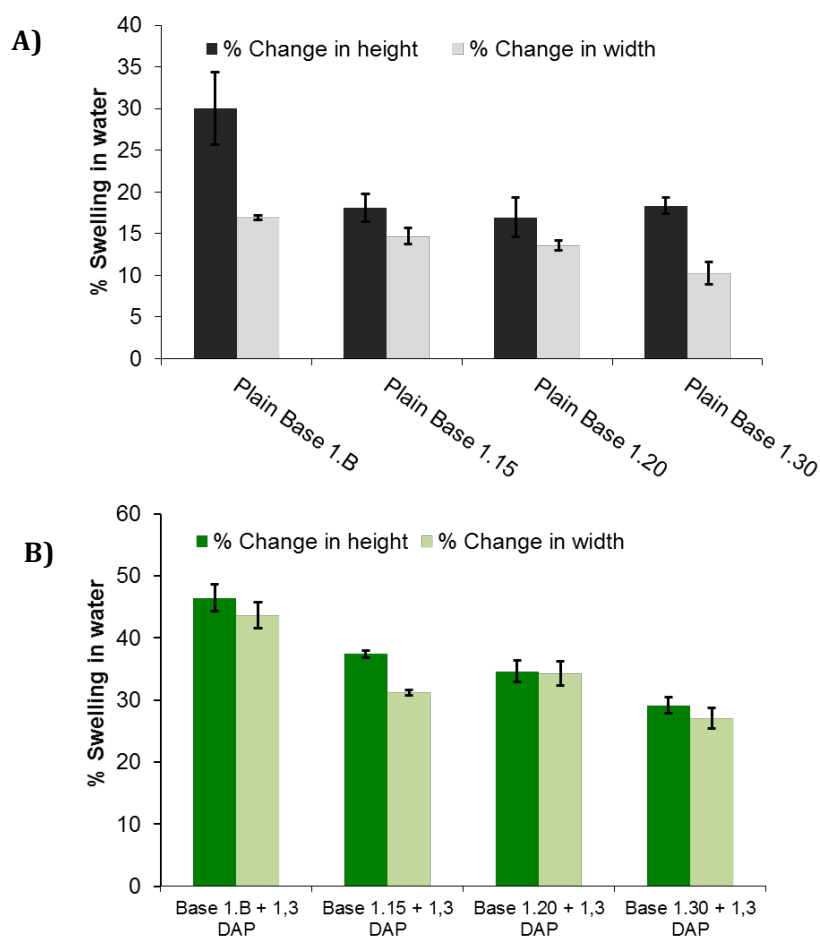
FIGURE 2.16: *Biaxial swelling behaviour of plain and 1,3 DAP functionalised Base 1.B, 1.15, 1.20 and 1.30. Results shown are means ± SEM of n=6.*

2.5.4 CONTACT ANGLES

Contact angle measurements were taken from gel sets (see table 2.3) that have increasing GME and increasing EGDMA. This was to understand how changing the chemical compositions alter the wettability of the materials. Since gels take up water quickly fully hydrated gels were measured using the captive bubble method (figure 2.4). Larger angle θ indicates more hydrophilicity and greater "wettability". Results are converted to a water contact angle $\alpha°$. Figure 2.17 A) shows there is no significant difference in plain gels with increasing EGDMA however there is a significant increase in wettability with increasing EGDMA when functionalised with ammonia and 1,2 DAE. Overall differences in surface wettability between Base 1 and 2 become insignificant when functionalised

with 1,4 DAB and 1,6 DAH. Moreover, Base 1 and 2 gels did not show significant changes in wettability after functionalisation with diamines but did when functionalised with ammonia. In general changes in wettability are due to cross linker rather than alkyl chain length.
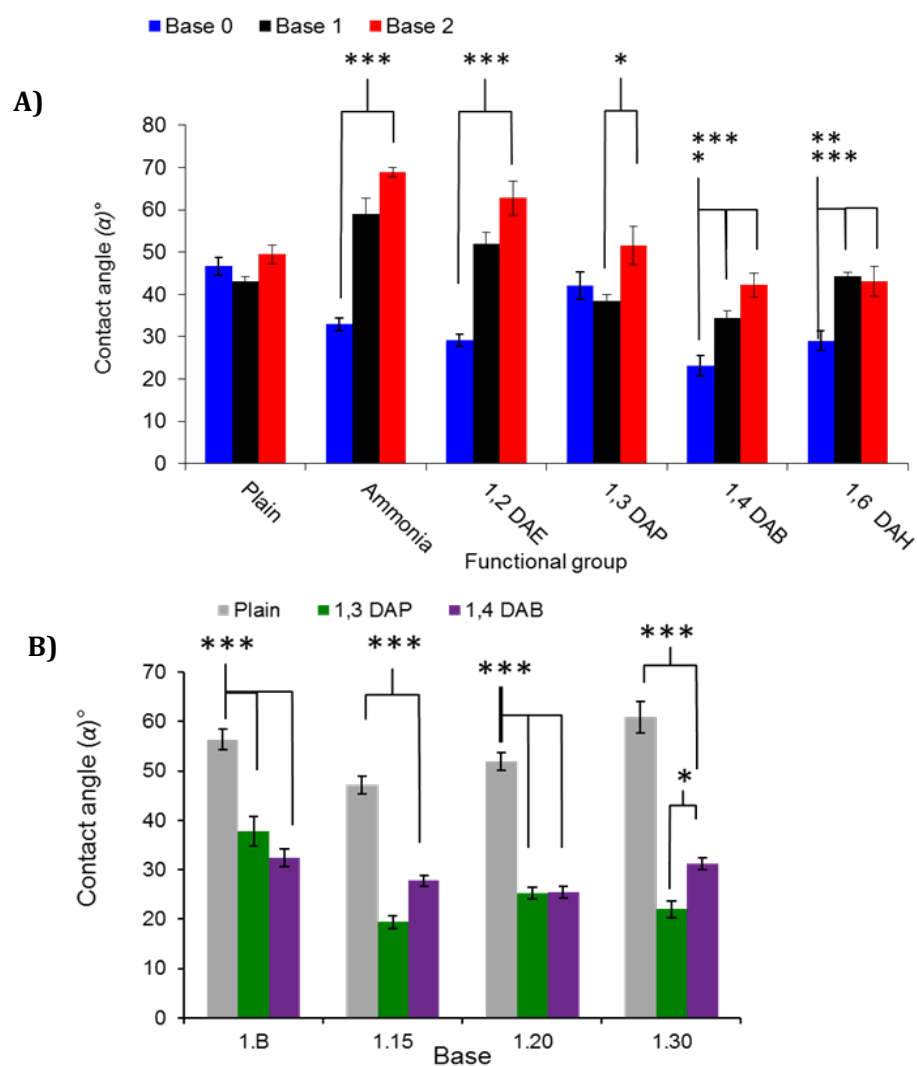
FIGURE 2.17: *Contact angle measurements for plain and functionalised Bases 0, 1 ,2 (A) and plain and 1,3 DAP or 1,4 DAB functionalised Base 1.B, 1.15, 1.20 and 1.30 (B). Significance annotations are shown between bases of the same functional group or between functional groups of the same base Results shown are means ± SEM of n=8.*

For gels with increasing GME, wettability was significantly higher after functionalisation with either 1,3 DAP or 1,4 DAB. Minimal changes were seen between these two functional groups and only Base 1.15 and Base 1.30 showed differences between 1,3 DAP and 1,4 DAB. For this group plain gels are more hydrophobic than functionalised gels, similarly Base 0 plain gels are more hydrophobic than all functional groups apart from 1,3 DAP. This correlates with the increase in swelling seen for Base 0 gels after functionalisation (figure 2.13).

2.5.5 FTIR

FTIR is a useful screening tool in the initial detection of amine functionality. Base 1 gels with amine functional groups 1,2 DAE and 1,6 DAH were compared against spectra from plain gels. The main ways to identify successful functionalisation is to determine peaks for primary and secondary alkyl amines or to determine epoxide groups on plain gels. It can be seen from figure 2.18 that there is a small peak in the region 1650-1590 cm^{-1}, characteristic of primary amines, which is not present in the plain gel sample. Epoxide groups typically have very week signals in the infrared, and are more apparent in the Raman spectrum (Coates and Ed, 2000).
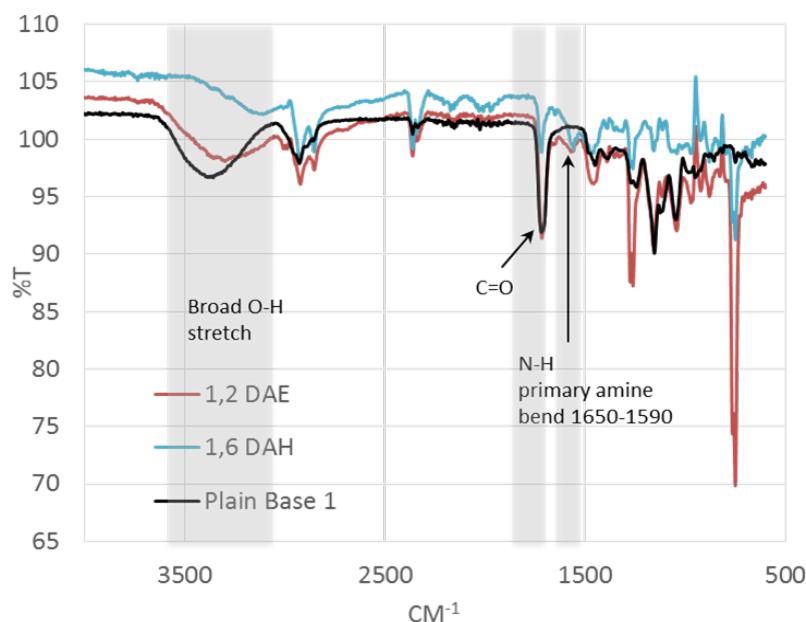
FIGURE 2.18: *FTIR spectra for plain Base 1 gel compared with spectra for Base 1/12DAE and Base 1/1,6 DAH.*

2.5.6 XPS ANALYSIS RESULTS

XPS was used to determine the extent of amine functionality and the coupling efficiency for those gels with increased GME content as well as Base 1 and 2 gels. Table 2.7 shows the theoretical and the actual percentage nitrogen content (averaged from 4 different spectra, 2 spots on 2 samples), highlighted in red is Base 1.20 /1,3 DAP that showed higher than theoretical values suspected to be due to either contamination, slight weighing errors of GME or trapped unreacted diamine within the gel. No nitrogen was detected for any unfunctionalised gels. A representative spectra of plain Base 1 shows a lack of nitrogen peak and no detected atomic nitrogen percentage (figure 2.19). Gels with increasing GME that were functionalised with 1,3 DAP showed a broad general increase in 1,3 DAP concentration with increasing GME from 10-30%. However as seen in figure 2.20 The average nitrogen content from these spectra showed some variability within the samples with no statistical differences in nitrogen content seen between 10-15% GME and 20-30%. Overall the same gels functionalised with 1,4 DAB showed much lower nitrogen contents than the theoretical values, potentially indicating further cross linking from free amine groups. Despite this nitrogen content for these gels were consistent and showed a statistically significant increase in nitrogen percentage.
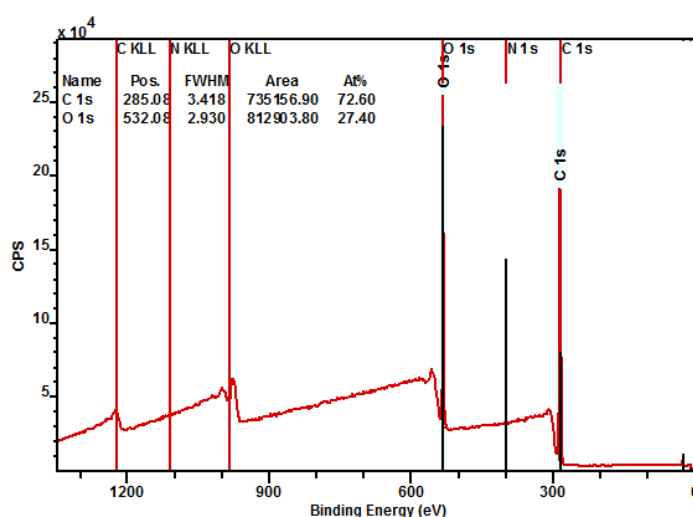
FIGURE 2.19: *An example of an XPS spectrum for a plain gel in this case Base 1*

TABLE 2.7: Theoretical percentage nitrogen concentration based on 100% coupling efficiency with GME compared with actual data extracted and averaged from four XPS spectra.

	Theoretical N%						Actual N%				
	NH2	1,2	1,3	1,4	1,6		NH2	1,2	1,3	1,4	1,6
Base 1	4.08	2.30	1.86	1.57	1.19	Base 1	1.57	0.74	0.95	1.81	1.04
Base 2	4.08	2.30	1.86	1.56	1.19	Base 2	0.82	1.07	1.14	1.36	1.29
1.B			3.56	2.99		1.B			3.53	1.96	
1.15			5.10	4.29		1.15			4.42	2.49	
1.2			6.52	5.47		1.2			**10.91**	3.08	
1.3			9.03	7.57		1.3			8.87	4.00	
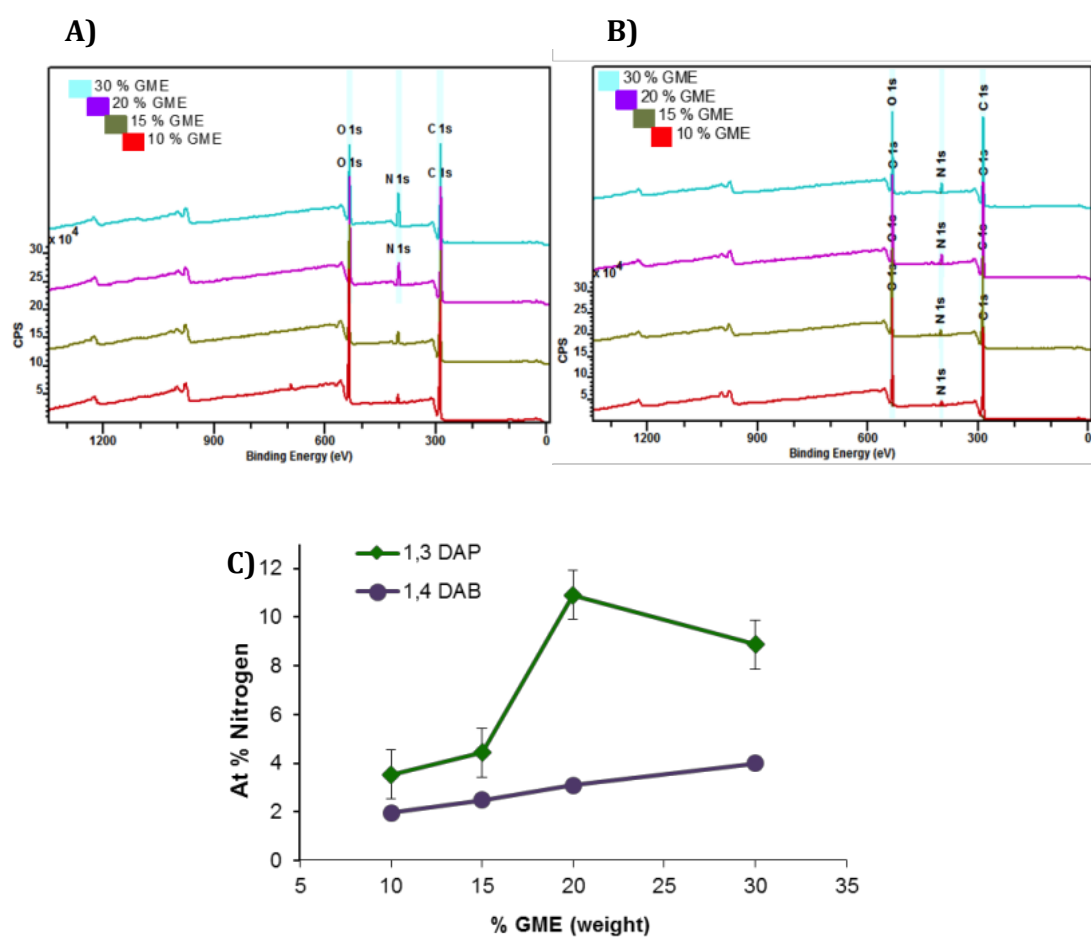
FIGURE 2.20: *XPS spectra showing nitrogen content for gels with increasing GME with 1,3 DAP (A) and 1,4 DAB (B) and a summary of atomic nitrogen (C)*

As well as the survey scans, a set of high resolution XPS scans were also obtained. Since little information was derived from the carbon and oxygen high resolution scans, the following data hones in on the nitrogen peaks, which relate directly to the extent of amine functionality. It is expected that diamines will produce 2 peaks, one from the amine covalently bound to the polymer and one from the terminal or "free" amine. If there is no extra cross linking of the diamines the 2 peaks should have an equal intensity. If cross linking occurs this means both amines are bound to the polymer, thus reducing the intensity of the free amine peak. By examining the high resolution scans for functionalised Base 1 gels, (figure 2.21) it can be seen that for 1,3 DAP, 1,4 DAB and 1,6 DAH functionality the peaks appear very similar, which is expected. In contrast the high-resolution nitrogen scans for gels with increased GME plus 1,4 DAB show a change in the free amine peak intensity. The difference in free amine peaks and bound amine peaks appear to increase as the percentage GME increases (figure 2.22) indicating an increased degree of surface cross linking by the 1,4 DAB.
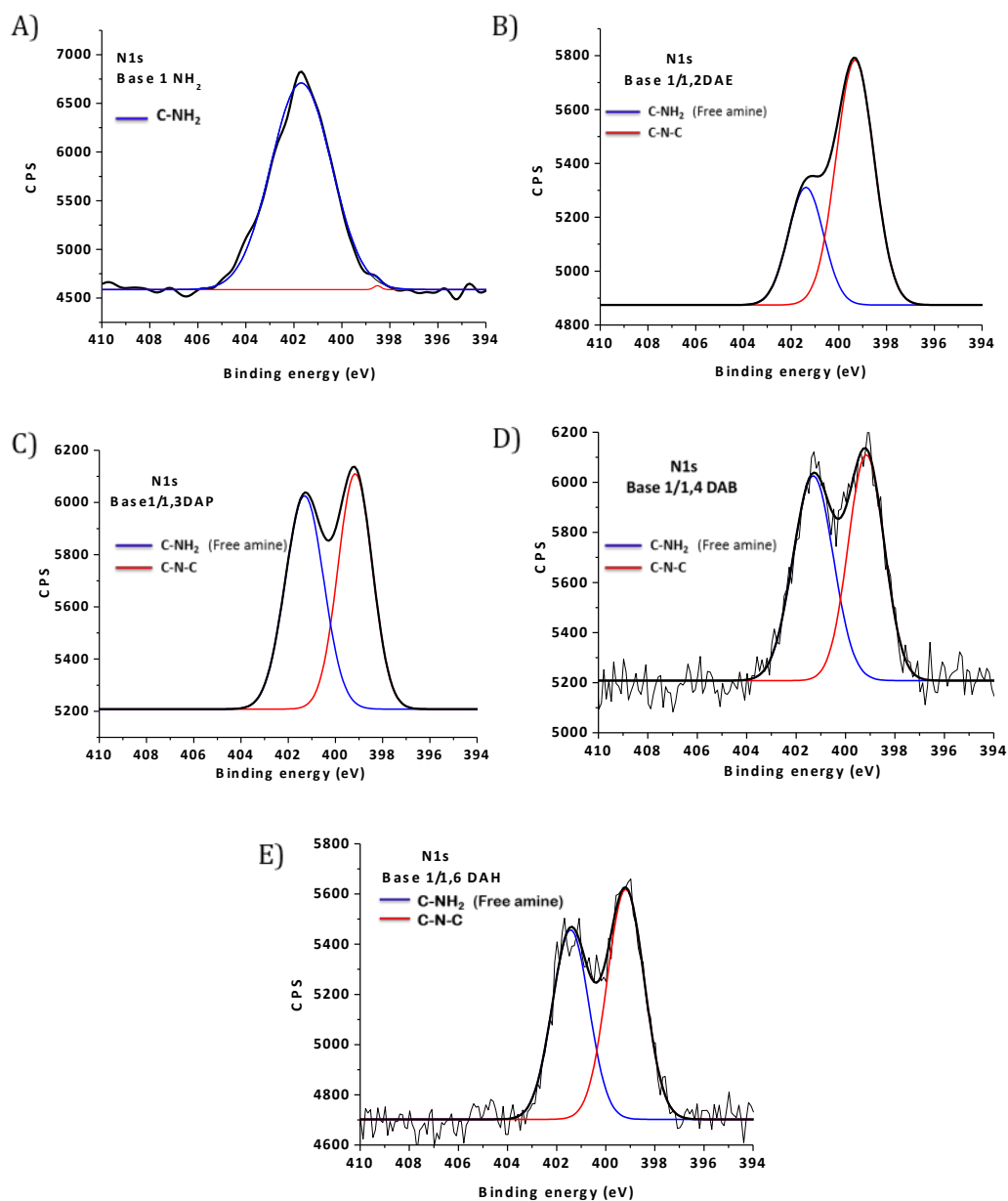
FIGURE 2.21: *Examples of XPS high resolution scans of the nitrogen peaks in Base 1 gels functionalised with A) ammonia, B) 1,2 DAE, C) 1,3 DAP, D) 1,4 DAB and E) 1,6 DAH. (Showing preliminary peak fittings)*
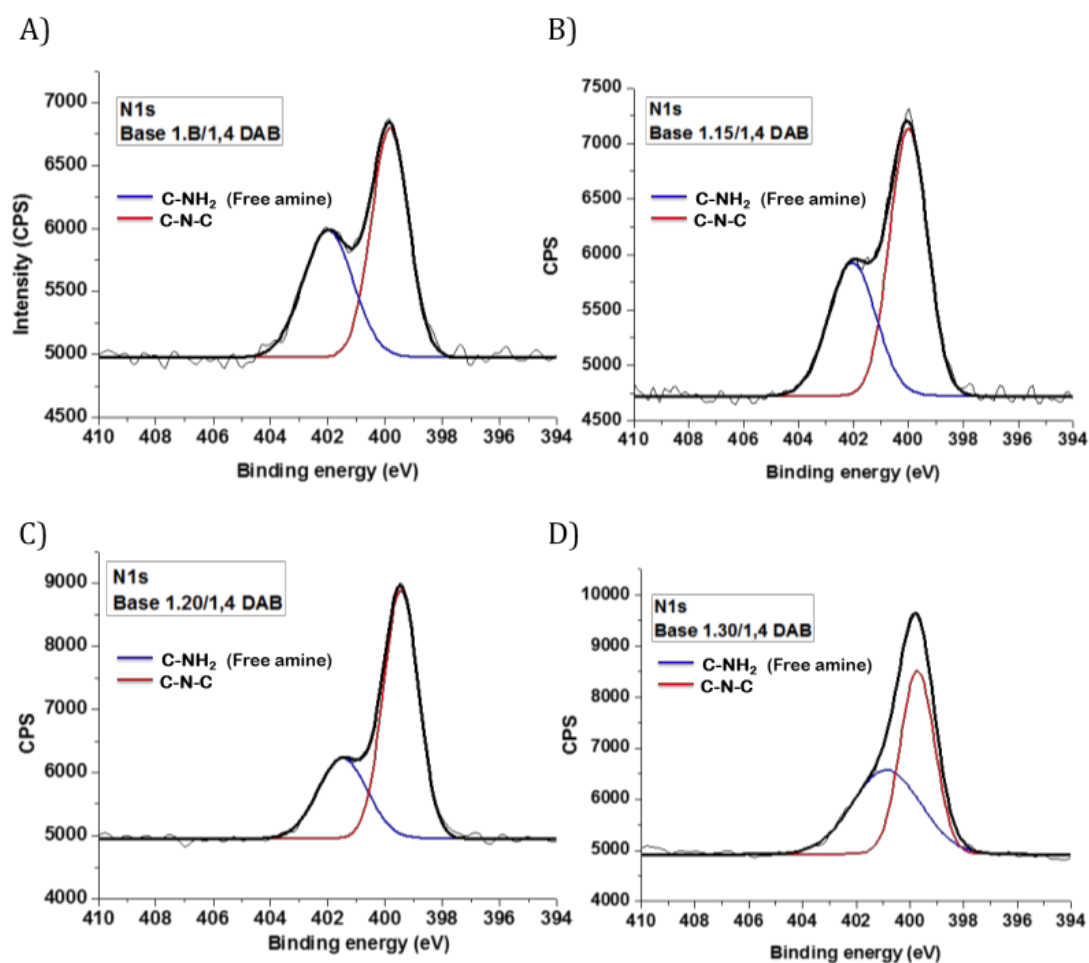
FIGURE 2.22: *XPS high resolution scans of the nitrogen peaks in 1,4 DAB functionalised A) Base 1.B, B) Base 1.15, C) Base 1.20 and D) Base 1.30. (Showing preliminary peak fittings)*

2.5.7 RAMAN

In order to obtain clues about why some of the 1,4 DAB functionalised gels may have very low coupling efficiencies a Raman spectra was taken from a sample of 3 gels with increasing GME. Base 1.15, 1.20 and 1.30 and compared with spectra from literature to check if those gels had any detectable unreacted epoxide groups. From figure 2.23 it can be seen that all 3 gels lacked the characteristic epoxide peak at ~809 where it has been seen in previous spectra obtained from Rimmer *et al.*
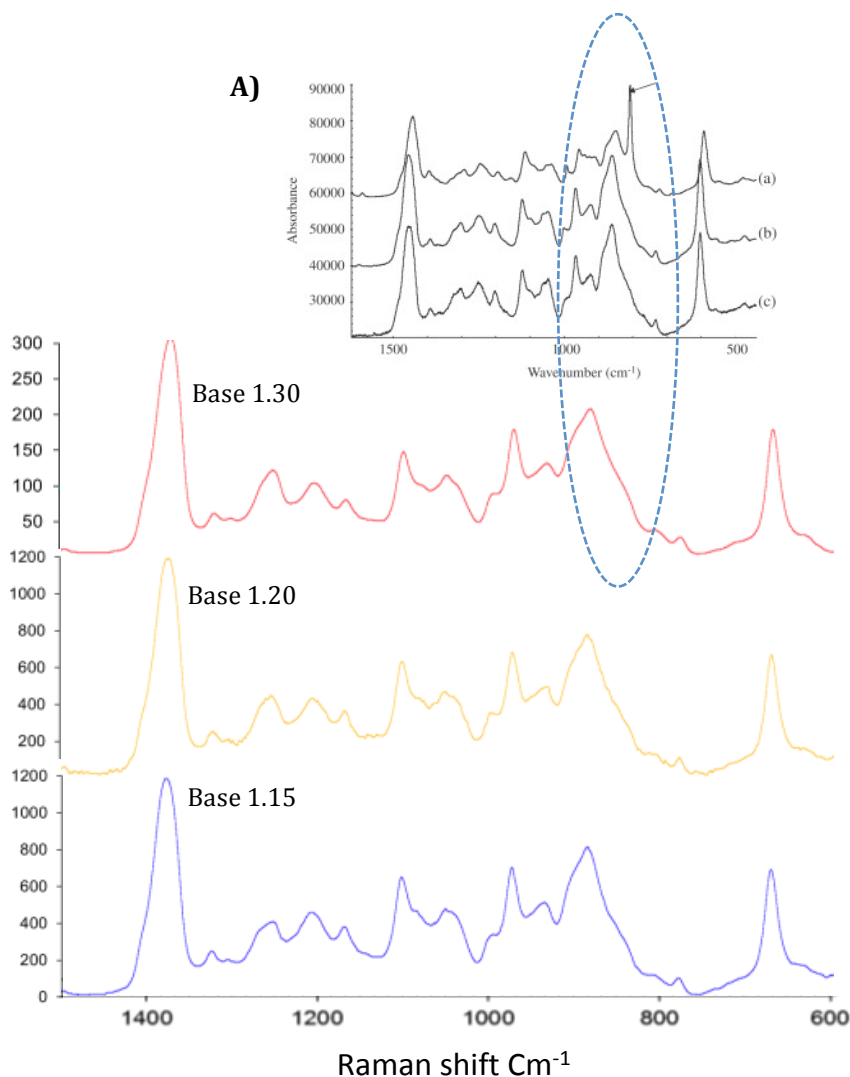
FIGURE 2.23: *Raman spectra of Base 1.15, 1.20 and 1.30 functionalised with 1,4 DAB and compared with A) Raman data from literature (Rimmer et al., 2007)*

2.5.8 DYNAMIC SHEAR ANALYSIS

Sample stiffness was measured for Base 0, 1 and 2 when plain and when functionalised with all 5 amines. The elastic storage modulus G' was obtained by averaging the G' values (see figure 2.24) across a range of frequencies from 0.628 rad/s to 62.8 rad/s. Figure 2.25 shows the overall stiffness of the gels increase with increasing cross linker. Base 0 gels display storage modulus values between 0.8 kPa and 9 kPa with plain gels exhibiting the least elasticity

and 1,2 DAE functional gels showing the most elasticity. In general Base 0 gels do not exhibit a correlation between amine alkyl chain length and storage modulus (figure 2.25 A).

Base 1 gels display storage moduli between ~ 6 kPa and 60 kPa and in stark contrast to Base 0 it is the plain gels that are the most elastic and 1,2 DAE which are least elastic within the group. Once again no correlation can be seen between storage modulus and alkyl chain length (figure 2.25 B).

Base 2 gels are overall much stiffer than the previous 2 groups with the highest stiffness exhibited by gels functionalised with 1,3 DAP at approximately 370 kPa and the most flexible gels being unfunctionalised with a storage modulus of approximately 11 kPa. (figure 2.25 C).

Storage moduli were obtained for plain, 1,3 DAP and 1,4 DAB functionalised gels with increasing GME content. Figure 2.26, A) shows that for plain gels there appears to be decreasing stiffness from gels with 15% GME to gels with 30% GME decreasing from approximately 40 kPa to 5 kPa. Base 1.B shows storage moduli that do not correlate with this trend and has a storage modulus of approximately 5 kPa.

In contrast gels with increasing GME content increase in stiffness after functionalisation with 1,3 DAP. Figure 2.26 B) shows how the storage modulus increases from 10 kPa with Base 1.B to 330 kPa with Base 1.30.

Gels functionalised with 1,4 DAB do not display any correlation between GME content and stiffness and all but Base 1.20 (the stiffest at 159 kPa) exhibit storage moduli of between 12 kPa and 20 KPa (figure 2.26 C). Data obtained from these samples may be affected by imperfections in the material caused by pre-swelling in PBS.
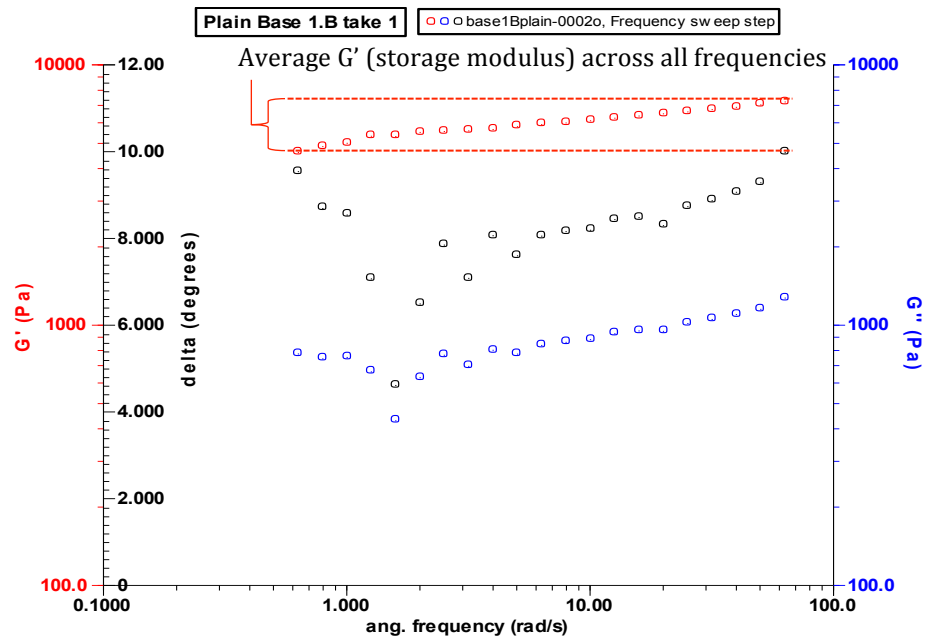
Figure 2.24: *A typical rheology plot for a sample undergoing dynamic shear analysis, storage (red) and loss (blue) moduli are plotted along with the phase difference delta (black) against frequency. Moduli for each material are calculated by averaging the storage moduli across all the frequencies.*
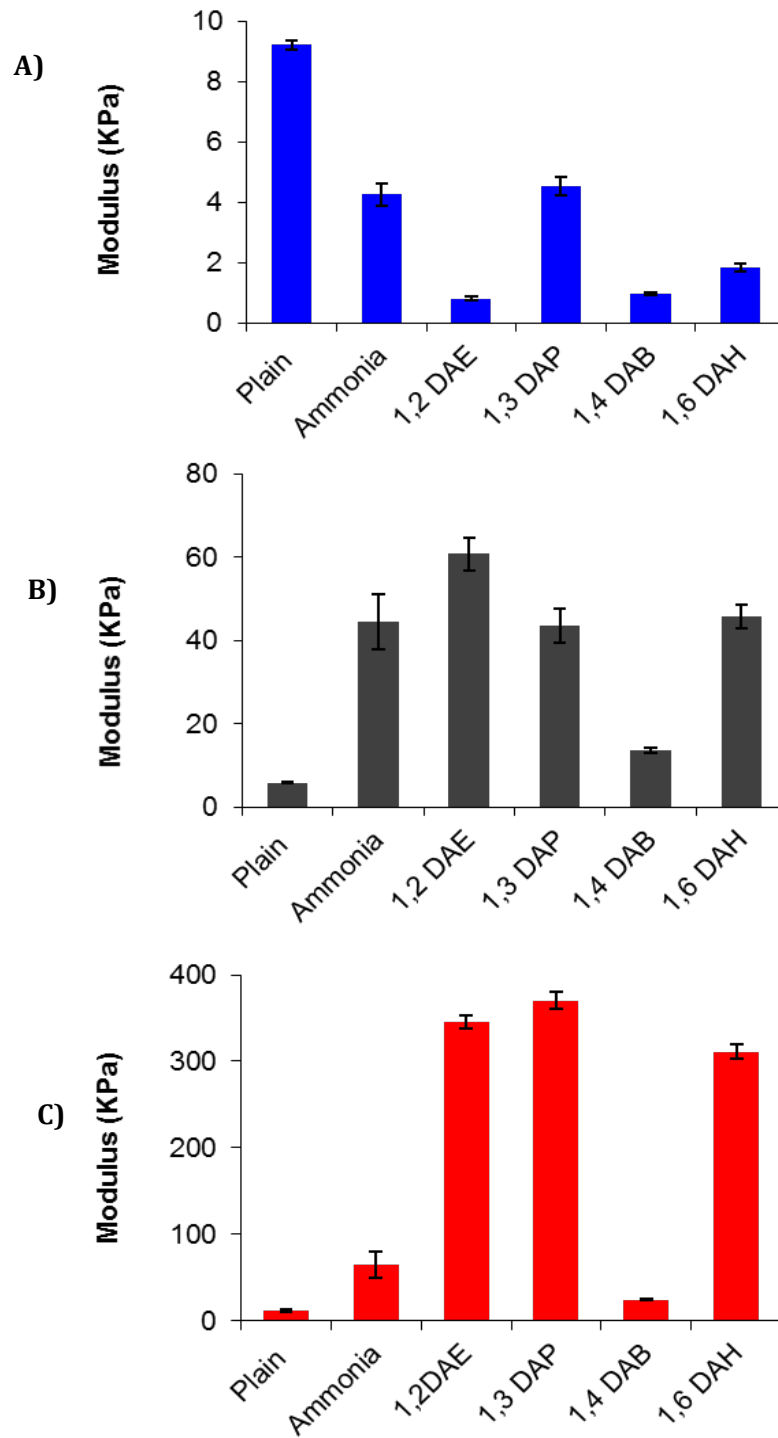
FIGURE 2.25: *Average storage moduli data of plain and functionalised Base 0 (A), 1 (B) and 2 (C). Each storage modulus was calculated as the average G' across all frequencies of three samples ± SEM.*
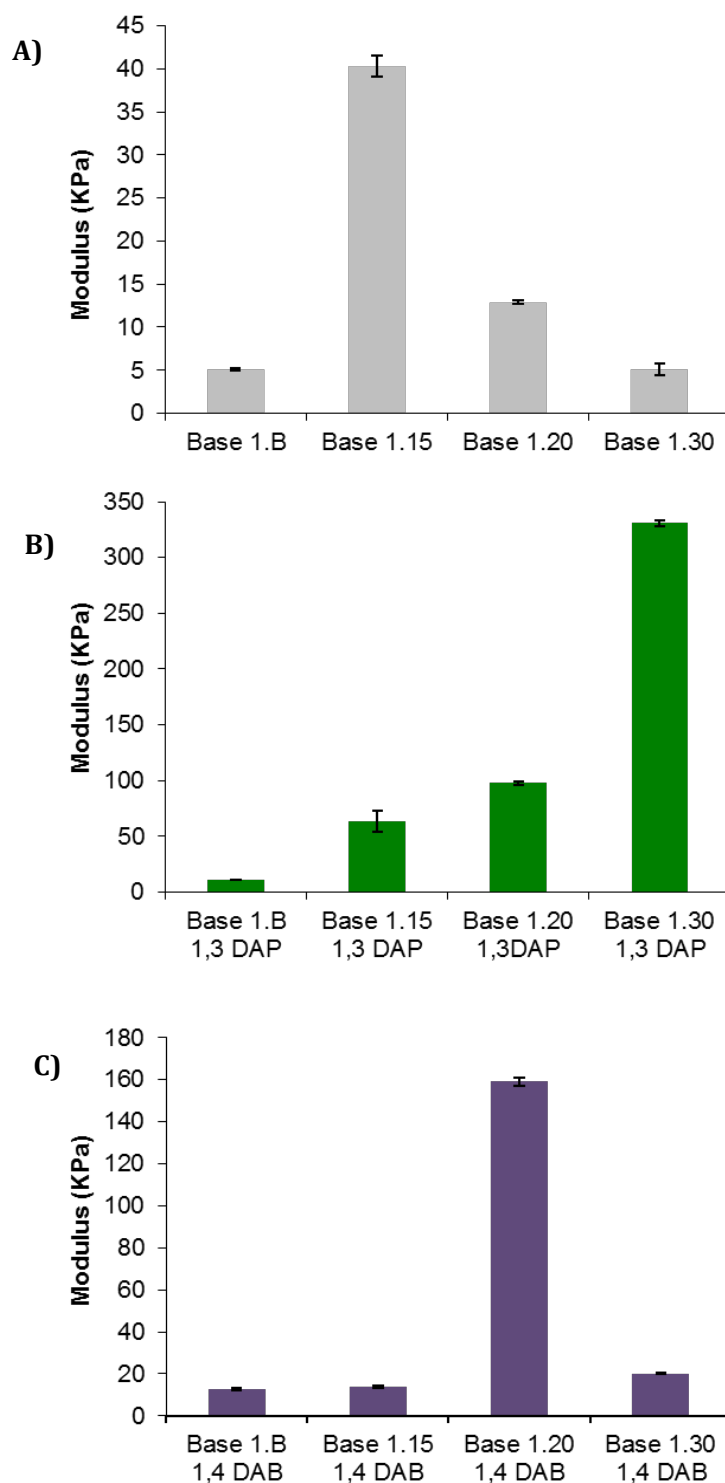
FIGURE 2.26: *Average storage moduli data of plain (A), 1,3DAP (B) and 1,4 DAB (C) functionalised Base 1.B, 1.15, 1.20 and 1.30. . Each storage modulus was calculated as the average G' across all frequencies of three samples ± SEM*

2.5.9 INDIRECT CYTOTOXICITY

A selection of gels were screened for indirect cytocompatibility to assess the impact (if any) of unreacted monomer or diamine leaching from the bulk of the gel.

Samples were suspended over rabbit limbal fibroblast cultures for 72 hrs as described in 2.3.14 and assayed for metabolic activity. It was seen that there was no significant decrease in metabolic activity of the cells when compared with the control (figure 2.27) apart from a small decrease in metabolic activity with 1,6 DAH functionalised Base A. All other gels did not appear to leach any toxic excess diamine or monomer. This indicates that these gels are suitable for the next stage of direct cell compatibility studies.
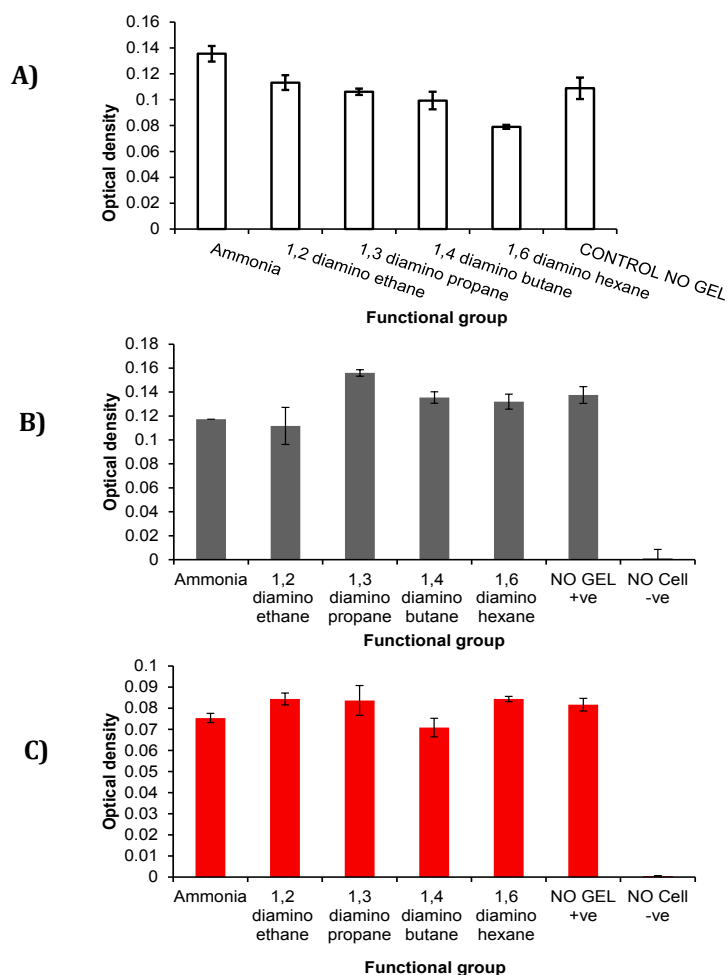
FIGURE 2.27: *Indirect cytotoxicity data, using MTT-assays with functionalised Base A (A), Base 1 (B) and Base 2 (C).*

2.6   DISCUSSION AND SUMMARY OF GEL PROPERTIES

2.6.1   LIMITATIONS OF HYDROGEL PRODUCTION

Each monomer chosen for this study was hypothesized to have predictable effects on the properties of the final hydrogel and so theoretically, it may be possible to create a desirable biomaterial simply by adjusting monomer compositions. However, tuning materials can be a challenge, as this chapter reveals, there is a very narrow range in which hydrogel tuning is possible without producing extreme faults in the material. The catch may also be that in narrowing the tunability range, less information can be derived from its effect on cells. Table 2.4 shows the how the chemical compositions of the hydrogels change the material properties just on appearance and handleability. Immediately it can be seen which materials can be rejected with regards to possible use as corneal inlay or onlay materials. Overall the most suitable gels appear to be Base 1 and Base 2, they are soft when hydrated, similar to native corneal tissue, but not too soft to handle. They are also clear, they do not crack after functionalisation and they can be sterilised with alcohol without affecting the gel structure. Base 0 gels are opaque and not seen as ideal materials for use as a corneal inlay, however later on in chapter 4 they will be tested for limbal epithelial adhesion and proliferation, and compared against clear hydrogels.

2.6.2   HYDROGEL SWELLING IN CORNEAL ONLAY MATERIALS

It was expected that reducing the proportion of cross linker EGDMA would naturally increase the water contents, however reducing the cross linker too much may reduce the mechanical integrity of the material. In this study the purpose was to produce gels with a range of water contents, with one set that approaches a water content seen in natural corneal tissue. Therefore the lowest amount of cross linker used was 1%, since it is seen as more desirable to aim for water contents resembling native cornea (78%) (Maurice., 1957) however, even with the low percentage cross linker the highest EWC obtained was 72%. The main purpose of aiming for high water contents is to maintain good biochemical diffusion rates to support epithelial overgrowth (Evans et al., 2002; Khan et al.,

2001). It has been widely accepted for some time that simply producing cell compatible substrates will not result in long term survival of corneal inlays. Knowles *et al* discovered that impermeable inlay materials lead to anterior stromal necrosis and deduced that corneal cells receive hydration and glucose from the aqueous humour rather than the tear film (Knowles, 1961). With this in mind polymers were optimised with diffusion capabilities for improved mass transport of glucose thus improving epithelial integrity. The range of EWCs produced from the gels in this study are below that of natural cornea, however some early studies using poly(HEMA) suggest that low EWC implants may still serve a purpose. Mester et al produced gels with EWCs of 38% and did not report any corneal necrosis (U. Mester, K. Roth, 1972). In selecting gels for cell culture it is also important to consider that swelling changes the final thickness of the material and has been shown to be a limiting factor in corneal integration despite exhibiting high water contents (Dohlman et al., 1967)

For Base 0 gels, those with the highest water content, it was not only the amount of EGDMA that influenced the water content, figure 2.13 shows an increase in EWC with some diamines. This unintentionally provides an additional variable for the Base 0 set making it difficult to derive conclusions from their effect on cell adhesion and proliferation and may provide justification for rejecting these gels for cell studies.

Since diffusion and permeability are desirable characteristics, information regarding the direction of swelling may be useful in understanding cell behaviour. If there is a directional restriction on swelling this will not only change the proportions/shape of the material but may limit diffusion of large biomolecules to the cell adhesion surface. In this study both Base 1 and Base 2 gels with higher alkyl chain diamine functionality exhibited noticeable anisotropy. This behaviour is similar for both, i.e both base 1 and 2 swell most in height, which makes these two gels easy to compare. This was originally hypothesised to be due to further surface crosslinking from free amine, however this does not account for anisotropy seen in Base1/ NH_2 or Base 2/NH_2 other causes of anisotropy could be due to the polymerisation process.

Preferential curing may occur on the top and bottom of the polymer sheets and hence less crosslinking within the bulk of the sheet. The data in 2.15 B) and C) suggests that there could be a combination of both happening as the difference in swelling generally increases with increasing alkyl chain length.

2.6.3 SURFACE WETTABILITY

Substrate wettability is known to influence cell behaviour (Yanagisawa I, Sakuma H, Shimura M, Wakamatsu Y, Yanagisawa S, 1989) and hydrogels with hydrophilic groups improve wettability which is thought to be vital for tear protein and mucin maintenance (Liu and Sheardown, 2005) many studies have concluded that moderate wettability improve cell spreading for a range of different cell types (Lee et al., 2000, 1998, 2003). Contact angles of around 55-60° have been cited as ideal for cell adhesion. This is promising as the range of gels produced in the chapter predominantly fall between or closely to this range with the Base 1 set fitting closest to this ideal.

2.6.4 EXTENT OF SURFACE FUNCTIONALITY

It was proposed that increasing the GME content of the hydrogels would increase the concentration of diamine on the surface of the hydrogel. This was achieved but not without limitations. Firstly a high GME will expose more epoxide groups on the gels surface generating more cross linking sites for the diamine. This can change the gels behaviour in many ways, apart from contributing to stiffness, "looping" of the longer chain diamines will decrease the proportion of expected amine on the surface. Evidence of this can be seen by increased cracking and delamination with 1,4 DAB functionalised gels (figure 2.12) as well as lower than expected actual nitrogen percentage (figure 2.20) which was earlier established, by Raman spectroscopy, not to be due to incomplete amination. The high resolution nitrogen scans also confirm reduced intensity of the free nitrogen peaks suggesting the remainder are bound to the surface. It is also worth observing that XPS data obtained from 1,3 DAP functional gels of increasing GME showed some variability in amine content of the same sample which could indicate there is heterogeneity on the surface.

This may also cause localised rigidity in the material contributing to a disordered surface.

Altering the extent of amine functionality also relies on changing the bulk hydrogel recipe. This bulk formulation may also contribute to changes in material properties such as wettability, EWC and stiffness. Even though the amine concentration appears to have increased with GME it will be worth noting for later studies that the conformation of these functional groups maybe more important than their concentration.

2.6.5 STIFFNESS OF MATERIALS

It is useful to characterise materials for stiffness as it is an additional material property that can influence cell behaviour such as cell adhesion, motility and differentiation (Discher et al., 2005; Pelham and Wang, 1997). However with this in mind this property may be overridden by ligand density (Engler et al., 2004) and hence should be evaluated alongside extent of surface functionality . In this study stiffness is intrinsically related to cross linking density and EWC even though some studies have aimed at maintaining rigidity while increasing water contents. Consequently this parameter may be determining factor in how different cell types respond. For example stiffer gels are better for fibroblasts (Hopp et al., 2013) while softer materials are better for epithelial cells (Levental et al., 2007; Paszek et al., 2005).

2.7 CONCLUSION

The aim of this chapter was to produce characterise and evaluate aminated hydrogels for use as cell substrates. Bases 1, 2 and A were seen as suitable substrates for further study. Base 0 is undesirable but reserved for further investigation with epithelial cells since high water contents approaching natural cornea is reputed to contribute to the formation of a stable epithelium (Myung et al., 2007). In addition, two sets of four gels with increased GME content were also made, with potential application for studying the impact of amine concentration on cell attachment and growth.

In summary the features of any material plays an important role in cell, adhesion, growth and differentiation. Each feature contributes important ingredients in healthy tissue maintenance. For instance, high EWC promotes diffusion of nutrients, stiffness and wettability promotes cell spreading, elasticity promotes migration, (both provide differentiation) and finally ligands or functional groups provide attachment.

CHAPTER 3

STROMAL CELL

RESPONSE TO

AMINATED HYDROGELS

CHAPTER 3: STROMAL CELL RESPONSE TO AMINATED HYDROGELS.

3.1   INTRODUCTION

It is established that fibroblasts show greater adherence and proliferation on stiffer rather than soft substrates (Hopp et al., 2013) so in order to investigate the impact of amine functional hydrogels on the growth and proliferation of fibroblasts, Base A, 1 and 2 were investigated since these were found in chapter 2 to be the stiffest gels that can be functionalised with all 4 diamines and ammonia. It has also been demonstrated that epithelialisation on many surfaces can be improved by co-culturing them with stromal cells (Bullock, Higham, & MacNeil, 2006; T. Sun et al., 2004). Accordingly it may be useful to understand the stromal cell response to the aminated hydrogels. In addition, fibroblasts are well known for being less selective with regards to the substrates they adhere to making these cells an ideal first stop for biocompatibility screening.

3.2   AIMS

The aim of this chapter is to test the stromal cell response to the aminated hydrogels selected from chapter 2 and compare their performance with co-cultures of cells which has previously been reported to improve cell adhesion and proliferation of total epithelial and stromal cell population.

3.3   MATERIALS AND METHODS

3.3.1 EQUIPMENT

Details of equipment and reagents used for the work carried out in this chapter are detailed in table 3.1 and table 3.2 In addition to those used for making and preparing hydrogels detailed in chapter 2.

TABLE 3.1: List of equipment used.

Equipment	Brand	Supplier
24- well plates	Costar	Corning USA
Cell crown		Scaffdex
Centrifuge	Roafix	Hettich
filter paper (240mm)	Whatman	Fisher scientific

Fluorescent microscope	Image Xpress	Molecular Devices USA
forceps	Prestige	Morton medical supplies
Incubator		Sanyo
medical grade stainless steel rings	Sheffield university materials workshop	
petri dish	Nunc	Scientific Laboratory Supplies Ltd
Pipette straw		Fisher scientific
Pipette	Gilson	
Pipette boy	Integra	
scalpel blades	Swann- Morton	
sterile filters	Sarstedt, Germany	
ThinCert	Greiner bio-one	
T- flask (T 25)	Greiner Bio one	
T- flask (T 75)	Nunc	

TABLE 3.2: List of reagents used.

Reagents	Supplier
3-(4,5-Dimethyl-2-thiazolyl)-2,5-diphenyl-2H-tetrazolium bromide	Sigma-Aldrich
4', 6-diamidino-2-phenylindole (DAPI)	Sigma-Aldrich
Acetic acid	Sigma-Aldrich
AlamarBlue® Cell Viability Reagent	Life technologies
Amphotericin B	Sigma-Aldrich
Anti cytokeratin 3 antibody	Merck Millipore
biotynilated goat anti-mouse IgG	Sigma-Aldrich
Calcium Chloride	Sigma-Aldrich
Collagen I	Sigma-Aldrich
Collagenase	Sigma-Aldrich
Dispase II	Roche
DMEM + glutamax	Gibco Life technologies
Epidermal growth factor EGF	Sigma-Aldrich
Foetal calf serum FCS	Sigma-Aldrich
Fibronectin (Human dermal fibroblasts)	Sigma-Aldrich
Fibronectin (Bovine Plasma)	Sigma-Aldrich
Formaldehyde	Sigma-Aldrich
Goats serum	AbD Serotec (Bio-Rad)
Hams F-12	Gibco Life technologies
Hanks Balanced Salt solution (HBSS)	Gibco Life technologies
Insulin	Sigma-Aldrich
L-GLutamine	Sigma-Aldrich
Monoclonal anti-fibronectin antibody	Sigma-Aldrich
Penicilin/streptomycin	Gibco Life technologies

Phalloidin Fluorescien Isothiocyante (FITC)	Sigma-Aldrich
Phosphate buffered saline tablets (PBS)	Oxoid microbiology (Thermo scientific INC)
Rabbit eyes	Woldsway foods Spilsby/ Hooke farm, Hooke
Streptavadin Texas red	Vector Laboratories
Streptavidin–FITC	Vector Laboratories
Transglutaminase	Sigma-Aldrich
Triton X	Polysciences Inc
Trypsin	Sigma-Aldrich
Tween20	Sigma-Aldrich
Videne	Ecolab UK

3.3.2 CELL ISOLATION AND CULTURE

Rabbit eyes were obtained from Hook farm, Hampshire UK and were received in chilled phosphate buffered saline within 24 hours of removal from New Zealand white rabbits (2.4-2.6 kg). The eyes were first cleaned from any extra tissue and fat to reduce risk of bacterial infection, then immediately disinfected using 3% Videne for 2 minutes and washed in PBS. The eyes were then transferred to a class II tissue culture cabinet and immersed in 1.5% Videne for 1 minute then washed in PBS. Cornea scleral buttons were cut out using a number 10 scalpel blade then transferred into a petri dish lid where limbal regions were isolated under a dissection microscope using a number 15 scalpel blade. The limbal explants were cut into 3-4 sections and placed in a solution of Dispase II (Roche) (2.5mg/ml in serum free Dulbecco's Modified Eagle's Medium + Glutamax) and placed in the incubator for 1hr at 37°C and 5% CO_2. Explants were subsequently transferred into a dish of fresh DMEM + glutamax media and cells were scraped from the epithelial surface into the media using a pair of blunt forceps, the resulting cell suspension was spun at 200 g for 5 minutes and resuspended in the epithelial culture medium and seeded into a T 25 flask containing murine growth-arrested 3T3 fibroblasts by gamma irradiation. The remaining explants were placed into T 25 flasks and left to adhere for 1 hr before adding 10% DMEM (DMEM plus 10% foetal calf serum (FCS), 1% penicillin/streptomycin, 1% L- Glutamine and 0.25% amphotericin B) as described in 2.3.12.

The rabbit limbal epithelial cells (rLECs) were cultured in rabbit limbal epithelial medium (RLE media) made with a 1:1 ratio of DMEM + Glutamax and Ham's F12 medium supplemented with 10% FCS, 0.05 µl/ml epidermal growth factor (EGF), 5 mg/ml insulin, 1% penicillin/streptomycin and 1% amphotericin B. The media was changed every 2-3 days and cells were passaged when they reached about 80% confluence. Trypsin was used to detach the cells after 3 washes with PBS, then collected with fresh media and centrifuged at 200 g for 5 minutes. The pellet was resuspended in more fresh media and seeded into new flasks containing irradiated 3T3s. Epithelial cells were used up to passage 1. All rabbit limbal fibroblasts (rLFs) in this chapter were isolated according to 2.3.12.

3.3.2.1 HUMAN DERMAL FIBROBLASTS

Human dermal fibroblasts (HDFs) were isolated from surplus skin obtained after breast reduction or abdominoplasty surgeries in Northern General Hospital, Sheffield, Department of Plastic Surgery, with full informed consent from the donor. All tissue was banked and anonymised according to the Human Tissue Authority Research Tissue Bank License number 12179. Primary dermal fibroblasts were isolated from dermis after mincing into small sections and 24 hr digestion with 15 ml of 0.05 % collagenase at 37°C with 5% CO_2. Collagenase solutions were prepared in DMEM and filter sterilized with 0.2 µm disposable sterile filters. The solution was supplemented with 10% FCS (v/v). After 24 hrs, the resultant cell suspension was centrifuged at 400 g for 10 min and resuspended in fresh 10 % DMEM. These cells were then seeded into T 25 flasks and incubated at 37 °C with 5% CO_2. Media was changed every 2 days and passaged as needed HDFs were used between P1 and P7.

3.3.3 CULTURE OF rLFs ON BASE 1 AND 2 AND BASE A (NO LMA)

After Bases A, 1 and 2 were functionalised, and washed according to 2.3.4 they were transferred to a sterile environment and cut into discs using a number 10 cork borer, (18 mm) They were then washed in ethanol a further 2 times then in PBS 5 times including one overnight wash. Prior to seeding, the discs were saturated in 10% DMEM and incubated at 37°C and 5% CO_2 for 2-3 hours to allow the gels to become saturated and swollen in the culture media. The hydrogel discs were transferred into standard 12-well Costar™ culture plates

and weighed down with medical grade steel rings, internal diameter 10 mm, in order to ensure direct seeding of cells onto the hydrogel. Each ring was seeded with a population of 5000 rLFs and allowed to attach for 24 hrs before the rings were removed and media was replenished. The cells were cultured on the discs and TCP control for 24, 48 and 72 hrs to assess initial adhesion and proliferation on all gels.

Tissue culture plastic (TCP) is used in this thesis as a positive control surface for all the cell culture studies. TCP is a modified polystyrene surface designed to facilitate cell attachment and spreading. Cells interact with the highly energetic oxygen ions grafted to the surface of the polystyrene that become hydrophilic and negatively charged when medium is added (Amstein et al., 1975; Andrade, 1985; Curtis et al., 1983; DuPont-Gillian et al., 2000; Shalaby et al 1984). This serves as a reasonable control surface as fibroblasts and epithelial cells readily attach and proliferate on TCP. All the hydrogels developed are amphiphilic and after amine functionalisation also present negatively charged groups at the material surface. (Rimmer et al., 2007)

3.3.4   MTT ASSAY OF CELLS CULTURED ON GELS

Media was removed from the wells and cells to be assayed were carefully immersed in PBS once, before removing and adding 1 ml of MTT solution (0.5 mg/ml in PBS) and incubated for 40 mins at 37°C and 5% CO_2. The MTT solution was carefully aspirated from each well ensuring no removal of cells. The purple formazan precipitate was dissolved in 400 µl of acidified isopropanol. Two 150 µL volumes of this was then transferred to wells of a 96-well plate and an optical density measurement was taken at wavelength 540 nm using a reference of 630 nm.

3.3.5   CULTURE OF HDFS ON BASE 1 AND 2

In order to validate the stromal interaction with gels, primary HDFs were cultured on functionalised Base 1 and 2. These gels were prepared and cultured in exactly the same way as in 3.3.3. MTT- assays were carried out at 24, 48 and 72 hrs.

3.3.6 STAINING WITH FLUORESCENT DYES DAPI AND PHALLOIDIN-FITC

Cells in both wells and on hydrogel were washed 3 times in PBS, fixed with 3.7% buffered formaldehyde after which they were rinsed 3 times again with PBS. Nuclei stain 4', 6-diamidino-2-phenylindole (DAPI) at a concentration of 0.5 µg/ml in PBS was added to cells (Just enough to cover sample) and incubated at room temperature for 10-15 minutes. DAPI was then aspirated and gels washed 3 times. DAPI is excited at 340 nm and has an emission at 488 nm. For staining the actin filaments in the cells, Phalloidin-FITC was used. After fixing cells, they were permeabilised using 1% Triton solution in PBS and incubated at 4°C for 5 mins. The Triton was removed and Phalloidin-FITC solution 2 µg/ml in PBS was added to cover the cells and incubated for 30 mins at room temperature, the solution was later aspirated and samples washed in PBS 3 times before imaging with an Image express fluorescent microscope.

3.3.7 CO-CULTURE WITH rLECS ON TCP AND COLLAGEN

Co-culture experiments were initially carried out on TCP or collagen coated TCP to gain a better understanding of the cells viability, morphology and arrangement when in co-culture. Cells were seeded at 10,000 cells per well whether for mono or co-culture. Before seeding, wells to be coated with collagen were prepared using collagen (0.2 µg/ml in 0.1 M acetic acid). 1 ml of collagen solution was pipetted into the wells and left to adsorb to the TCP for 3 hrs in an incubator at 37°C and 5% CO_2. Six culture conditions were set up, rLECs on collagen, rLFs on TCP, rLECs on TCP, rLECs on TCP with indirect co-culture of rLF using ThinCerts, Direct co-culture of both rLECs and rLFs in 3:1 ratio, and direct co-culture of rLECs and rLFs in 3:1 ratio with removal of fibroblasts using 5% EDTA for 5 mins (figure 3.1). Cells were cultured for 7 days and media was changed every 2 days. Any co-cultures and rLEC cultures were fed using RLE media and rLF cultures were fed using 10% DMEM.
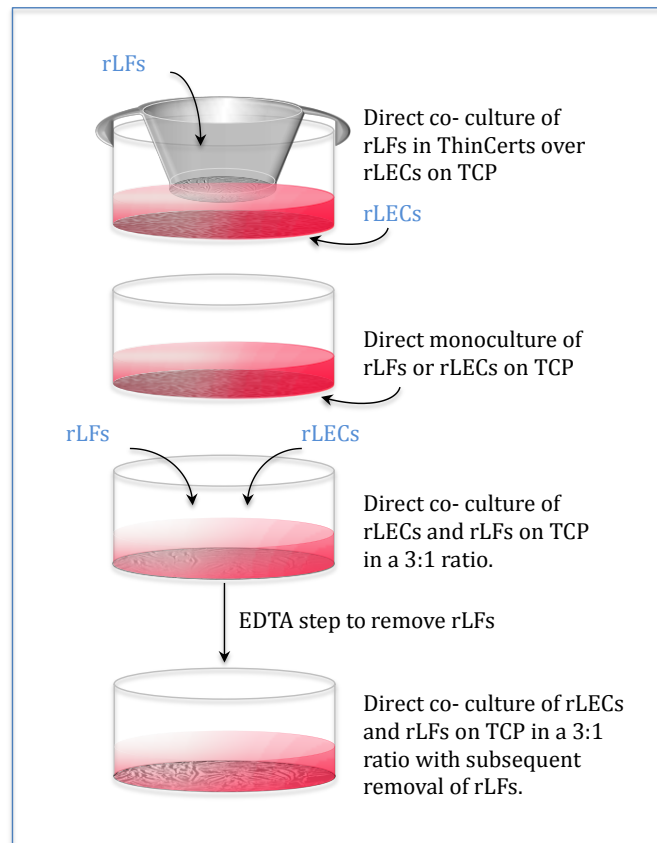
FIGURE 3.1: Schematic of culture conditions; Indirect co-culture, direct monoculture, direct co-culture (with removal of rLFs with EDTA)

3.3.8 STAINING rLECS FOR CYTOKERATIN 3 WITH DAPI AND PHALLOIDIN-FITC

Co-cultures of rLFs and rLECs were washed 3 times in PBS, fixed with 3.7% buffered formaldehyde after which they were rinsed 3 times again with PBS. Blocking of non-specific binding sites was carried out with a blocking buffer (10% goat's serum in PBS). Cells were then permeablised by treatment with 0.1% Triton X for 5 min. After removing and washing off excess Triton X, samples were incubated at 4°C overnight with the primary antibody, a mouse monoclonal antibody against cytokeratin 3 (Anti-Cytokeratin 3 antibody Abcam UK) diluted 1:50 in 1% blocking buffer. The following day samples were washed several times in PBS. Gels were then incubated at room temperature for 2 hrs with a biotynilated goat anti-mouse IgG (Vector labs, UK) diluted 1:1000, again in 1% blocking buffer. After 3 washes with PBS, the samples were incubated at room temperature in the dark for 1.5 hrs with Streptavadin Texas red (vector labs UK) diluted 1:1000 in a solution of DAPI (0.5 μg/ml in PBS) with Phalloidin-

FITC (2 μg/ml). Samples were finally washed 3 times before imaging using the Image Xpress fluorescent microscope.

3.3.9 Co-culture on Base 1 1,3 DAP and inert PEG-DA 575

To assess the influence of co-culture on overall cell viability and arrangement on hydrogels, Base 1 functionalised with 1,3 DAP and inert PEG-DA hydrogels were cut and washed as described in 3.3.3 and placed in wells of a 12 well plate. Medical grade stainless steel rings were used to weigh down the gels and ensure direct seeding onto each sample. Cells were initially seeded at 4000 cells per well and for co-cultures rLECs and rLFs were seeded in a 3:1 ratio. For the positive controls tissue culture plastic (TCP) was used for co-culture and rLFs, Collagen (0.2 μg/ml in 0.1 M acetic acid) was used to coat the wells before seeding rLEC controls. An MTT assay was carried out after 7 days in culture. All co-cultures and rLEC cultures were fed using RLE media and rLF cultures were fed using 10% DMEM every 2 days.

3.3.10 Coating gels with fibronectin

Unfunctionalised Base 1 and Base 1/1,3 DAP hydrogel discs, cut to size with a number 9 cork borer, were washed in absolute ethanol twice and PBS 5 times including one overnight wash under sterile conditions. Each gel to be coated with fibronectin was placed in a well of a 24 well plate and immersed in a 500 μl solution of 1.5 μg/ml bovine plasma fibronectin (Fn) (Sigma- Aldrich) diluted in PBS, and incubated for 2 hrs at 37°C, excess fibronectin solution was removed and replaced with 2 ml of 10 % DMEM and incubated at 37°C and 5% CO_2 for at least 3 hrs in order to allow the gels to reach saturation.

3.3.11 Culture of rLFs on fibronectin coated gels

Unfunctionalised Base 1 and Base 1/1,3 DAP hydrogel discs were cut using a number 10 cork borer and prepared as above (3.3.10). Coated and uncoated gels were placed in wells of a 12 well plate and weighed down using medical grade stainless steel rings. Gels and TCP were seeded with 2500 rLFs and incubated at 37°C and 5% CO_2. An MTT assay was carried out (as described in 3.3.4) after 1, 3 and 5 days in culture. Gels were also fixed at day 5 and stained with DAPI and Phalloidin-FITC for imaging with the Image Xpress fluorescent microscope. A second cell viability experiment on the same conditions as

mentioned above was carried out, this time using an Alamar blue Assay. This is another colorimetric assay but unlike MTT it is nontoxic to cells and can be used on cells multiple times during culture (figure 3.2) Before seeding with rLFs, gels were clamped to the bottom of a 24 well plate using an inverted cell crown (Scaffdex), then 2500 cells were seeded per well. After 24 hrs the media was changed to DMEM containing 10% Alamar-blue® solution (Invitrogen) and incubated for 4 hrs at 37°C and 5% CO_2. After 4 hrs, 150 µl from each well was pipetted into a well of a 96 well plate to be read using a Biotek Plate reader at 562 nm with a reference of 630 nm. The culture media was then replaced with fresh media again until the next time point where another Alamar blue reading would be taken; they were taken at days 1, 5 and 8.

Resazurin (blue weakly fluorescent salt) λ_{abs} =604 nm

Resorufin (red highly fluorescent salt) λ_{abs} =571/585 nm
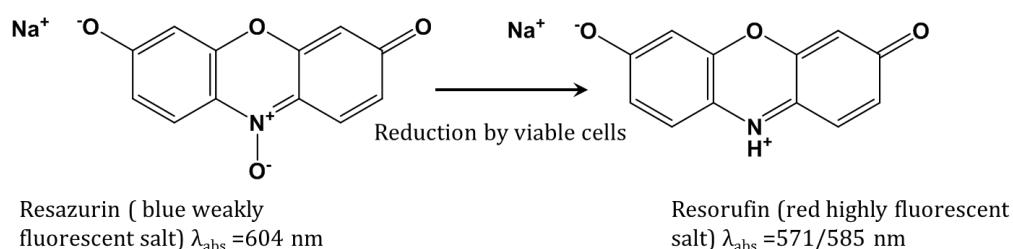
FIGURE 3.2: *AlamarBlue is a cell viability assay reagent which contains a resazurin salt that is a blue, cell permeable, non-toxic dye. Resazurin becomes reduced to red resorfurin by metabolically active cells. The fluorescence produced by resorfurin is proportional to the number of living cells*

3.3.12 CULTURE OF rLFs ON FIBRONECTIN COATED AND BOUND GELS

Unfunctionalised Base 1, Base 1/1,3 DAP and Base 1/1,6 DAH were prepared and coated with bovine fibronectin in the exact manner as 3.3.10, from now on referred to as the Fn A group. In parallel to this group, gels were bound with fibronectin using transglutaminase. Gels were incubated over night at 4°C with 500 µl of 1.5 µg/ml bovine plasma fibronectin and 25 µl of 1U/ml transglutaminase supplemented with 2.5mM $CaCl_2$. These gels were referred to as Fn B gels (figure 3.3). All Fn A and Fn B were washed 3 times in PBS, saturated in 10 % DMEM for 2 hrs and clamped to the bottom of the well using an inverted cell crown as in 3.3.11 before 2500 rLFs per sample were added.
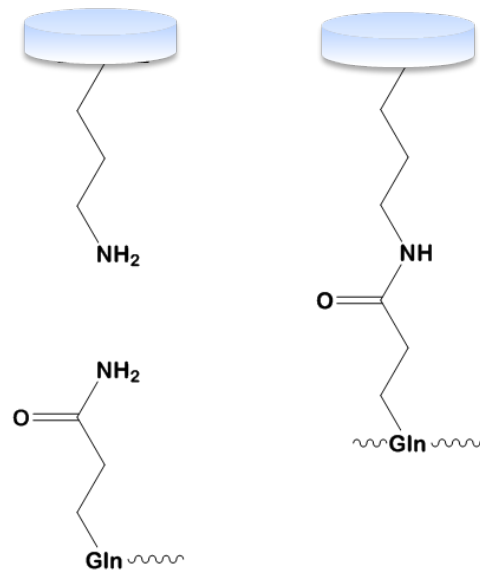
FIGURE 3.3: *Schematic representation of Transglutaminase catalysing the formation of a covalent bond between free amine groups, in this case from the free propylamine and the ᵞ-carboxamide group of proteins or peptide-bound glutamine residues found on fibronectin.*

3.3.13 TESTING THE EFFECTIVITY OF TRANSGLUTAMINASE MEDIATED FN BINDING

Verifying the effect of transglutaminase on protein binding is very challenging. Conventional colorimetric assays produce erratic results due to reagents becoming trapped in the gel which were difficult to reliably remove. One method could be used to qualitatively confirm presence of Fn by staining gels using immunohistochemistry with anti-fibronectin primary antibody. This method may produce a uniformly fluorescent gel, which is insufficient to verify Fn bound to the gel. So to tackle this, a method that aims to localise regions of bound Fn by "blotting" or "dropping" transglutaminase solution onto a Fn adsorbed gel was used. Base 1/1,3 DAP gels were washed and cut into discs using a number 6 cork borer (11.25 mm diameter) and placed into wells of a 24 well plate. Gels were then immersed in a 1 ml solution of 1.5 µg/ml fibronectin from human fibroblast culture (sigma-Aldrich) in HBSS (Hanks balanced salt solution) for 2 hrs at 37°C. Excess Fn solution was aspirated and gels were allowed to dry in a dry incubator at 37°C. Once all gels were dry, either a "blot" or drop of transglutaminase solution (1U/ml transglutaminase dissolved in PBS containing 2.5mM CaCl₂) was placed on the gel for 4 hrs at room temperature. These were then washed in a large excess of PBS to remove unbound Fn (see

figure 3.4). Gels were immersed in blocking buffer (10% goat's serum in PBS) for 2 hrs at room temperature. Blocking buffer was removed and gels washed in PBS with 0.05 % Tween20 (PBS-TW) 3 times. Primary antibody, monoclonal anti-fibronectin antibody produced in mouse, was diluted 1:200 in PBS-TW and incubated with the gels overnight at 4°C. Primary antibody was removed and gels were washed 3 times with PBS-TW. The secondary antibody, a biotynilated goat anti-mouse IgG diluted 1:1000 in PBS, was then added to the gels for 2 hrs at room temperature. Gels were washed again 3 times in PBS to remove excess secondary antibody and incubated with Streptavidin–FITC (1:1000 in PBS) for 1.5 hrs at room temperature. Gels were imaged at excitation wavelength 488 nm using florescent microscopy. The controls for this experiment were, a no transglutaminase drop (i.e drop contained only PBS) and a no primary anti fibronectin step.
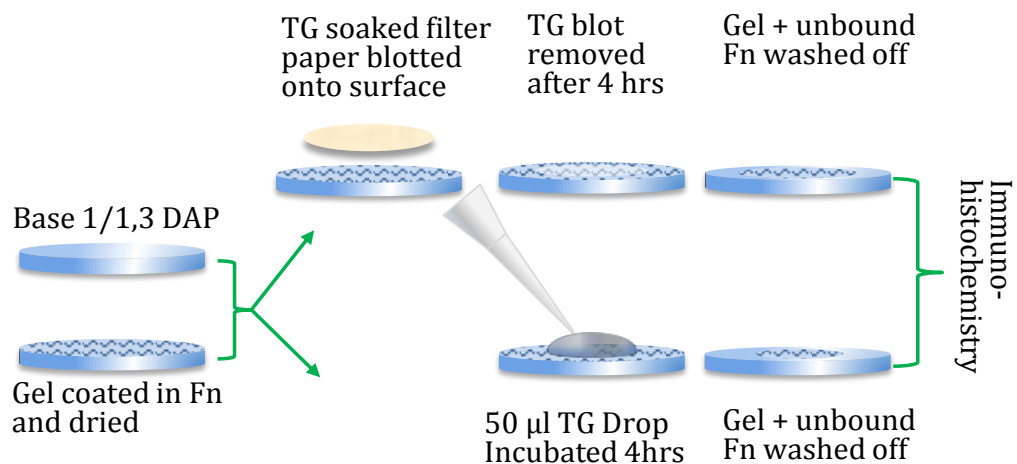
FIGURE 3.4: *Schematic representation of the localising fibronectin method using a transglutaminase drop or blot.*

3.3.14 STATISTICS

During the rest of this thesis statistical analysis using one-way ANOVA followed by a post hoc Tukey test was performed on the replicates within the same experiment and unless stated otherwise n values refer to the number of replicates within experiments. All results shown are the 2nd reproducible experiment (unless stated otherwise). All data are expressed as mean ± standard error of the mean (SEM), with $p < 0.05$ considered significant. Annotations are as follows *$p < 0.05$, **$p < 0.005$, ***$p < 0.001$3.4

3.4.1 CELL VIABILITY BASE A (NO LMA)

MTT assays were used to assess the viability of rLFs on functionalised Base A. In general rLFs did not grow well on any of the gels but with 1,2 DAE, 1,4 DAB and 1,6 DAH cells initially adhere in a manner similar to the TCP control.
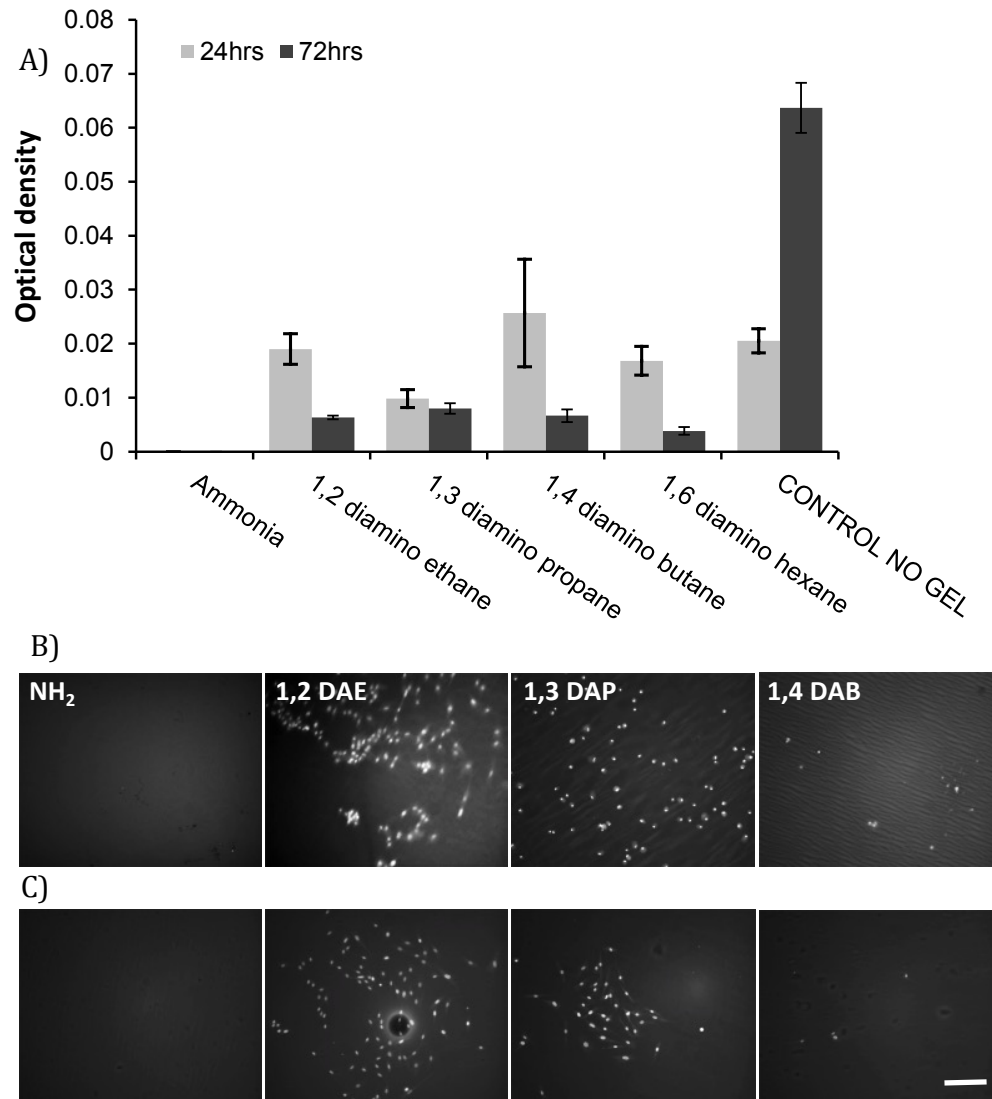
FIGURE 3.5: *(A) Metabolic activity of rLFs cultured on functionalized Base A (B) Images of rLFs taken after 24 h. C) Images of rLFs after 48hrs. Cells were stained with DAPI to visualise the low cell numbers and imaged using an Image Express fluorescent microscope. Results shown are means ± SEM of triplicate cultures. Scale bar represents 200 μm.*

There appears to be no relationship between the increases in carbon chain length of the diamines and cell adhesion or proliferation as was previously hypothesised (Rimmer et al., 2007). Despite the indirect cell culture studies (section 2.4.9) showing minimal effects on viability, all the surfaces show very little support for cell adhesion and from figure 3.5 A) shows poorer support for proliferation. Images of rLFs on the gels in figure 3.5 B) and C) show little to no cell adhesion on all of the aminated hydrogels.

3.4.2 VIABILITY OF rLFs ON BASE 1 AND BASE 2

The cell viability of rLFs cultured on functionalised Base 1 and Base 2 were also assessed. RLFs cultured on Base 1 functionalized with 1,2 DAE and 1,3 DAP attached well initially, but then detached rapidly over 72 hrs (figure 3.6 A). Cells cultured on Base 2 also failed to proliferate over 72 hrs regardless of the functional groups present (Figure 3.5 B). Images of rLFs presented in figure 3.7, show how cells have grown on the Base 1 networks after 48 hrs. However very few cells remained adhered to any of the gels in comparison to the TCP control.
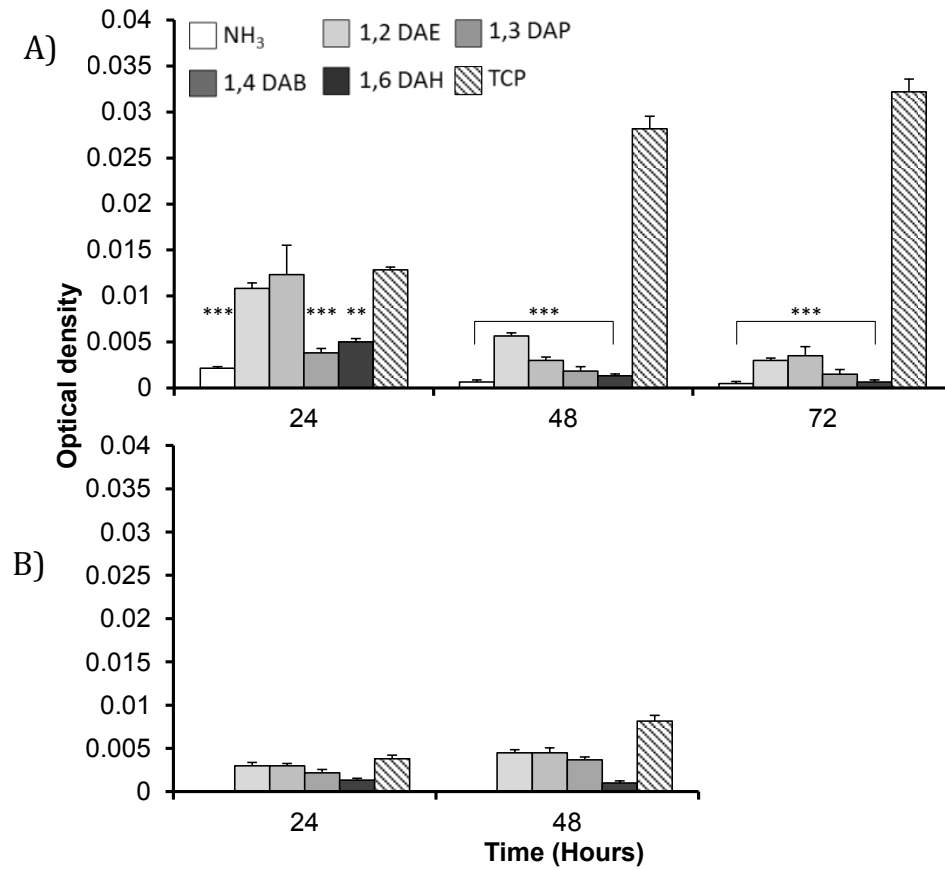
FIGURE 3.6: *Metabolic activity of rLFs cultured on functionalised Base 1 (A) and on functionalised Base 2 (B) over 2 or 3 days. However, optical density readings on functionalised base 2 were below the limit of detection after 72 hrs. Results shown are means ±SEM of triplicate cultures. Significance is relative to the tissue culture plastic positive control. *P<0.05, **P<0.005, ***P<0.001*
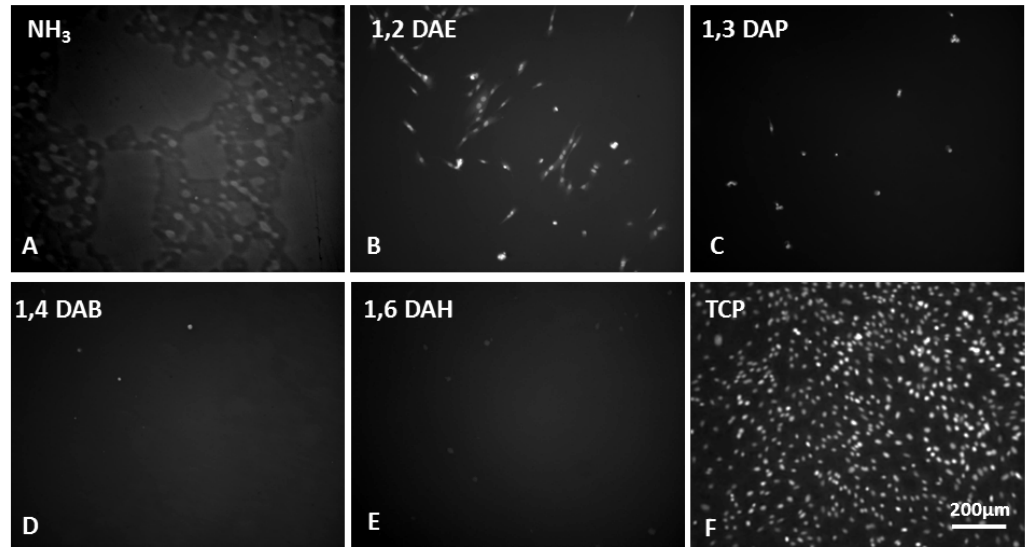
FIGURE 3.7: *Images taken of rLFs on functionalised Base 1 after 48 h, cells were stained with DAPI to visualize the low cell numbers and imaged using an Image Express fluorescent microscope.*

3.4.2.1 VIABILITY OF HDFS ON BASE 1 AND BASE 2

To verify this relationship, HDFs were also cultured on these surfaces as they grow quickly and easily. Figure 3.8 shows similar overall results to rLFs, in that there is a decrease in viability on both Base 1 and 2 over 72 hrs even though the HDFs appear to adhere initially. These cells do not detach as rapidly as rLFs did on these materials and remain adhered up to 48 hrs. In the 1,4 DAB and 1,6 DAH functional Base 1 gels, cell viability briefly increases before falling again. HDF viability on Base2/1,6 DAH gels also briefly increases before falling after 48 hrs Figure 3.9 shows the remaining cells adhered to the Base 1 gels after 72 hrs compared to a near confluent TCP control.
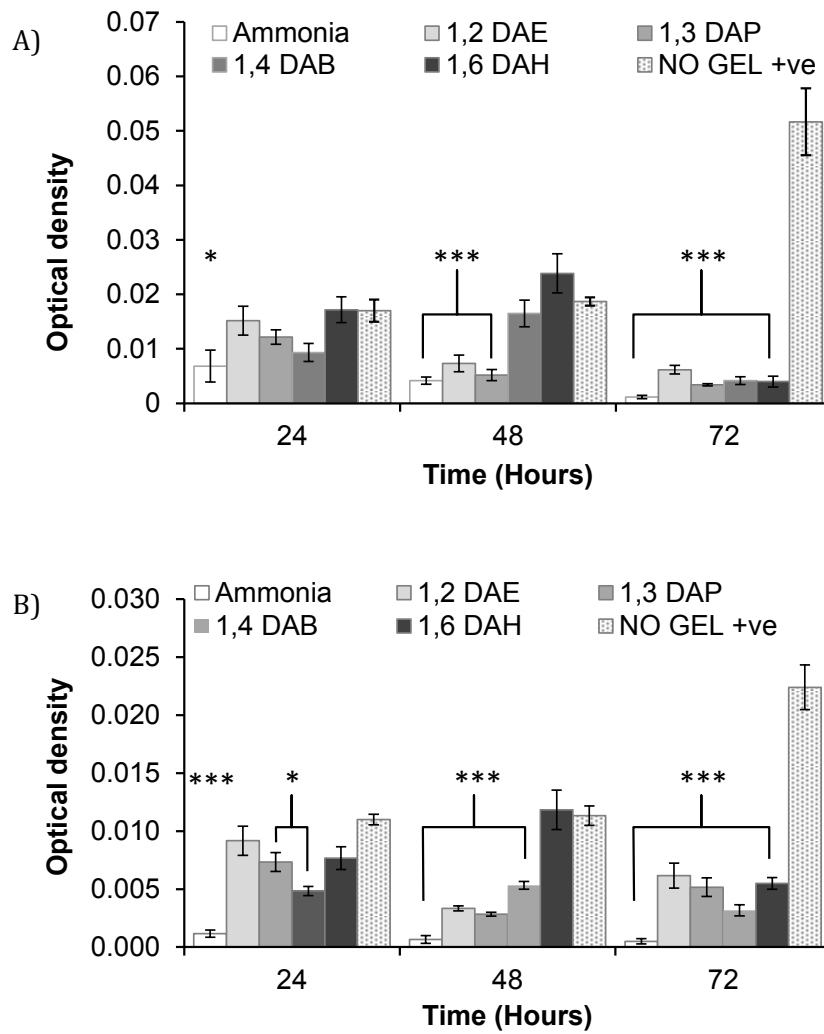
FIGURE 3.8: *Metabolic activity of Human dermal fibroblasts (HDFs) cultured on functionalised Base 1 (A) and on functionalised Base 2 (B) over 3 days. Results shown are means ± SEM of triplicate cultures. Significance is relative to the TCP positive control. *P < 0.05, **P < 0.005, ***P < 0.001*
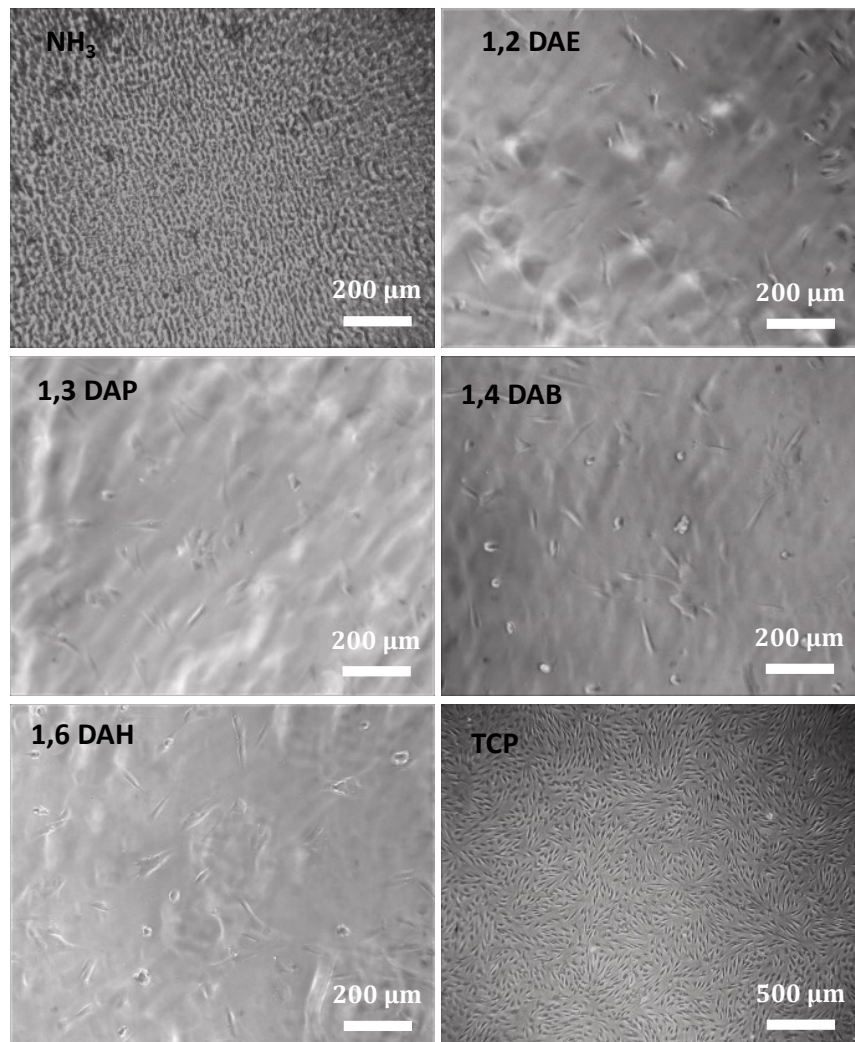
FIGURE 3.9: Light microscopy *Images of HDFs on functionalised Base 1 taken after 72 hrs.*

3.4.3 CO-CULTURE WITH rLECS ON TCP AND COLLAGEN

After studying the potential of these hydrogels for supporting fibroblast cell culture alone, it was postulated that the co-culture of stromal and epithelial cells would improve the gels ability to support cell attachment and proliferation. To determine the optimal cell culture conditions 6 combinations were set up,

1.   rLECs on TCP

2.   rLFs on TCP

3.   rLECs on collagen I coated TCP

4.   rLECs and rLFs on TCP in a 3:1 ratio

5.   rLECs and rLFs on TCP in a 3:1 ratio with removal of fibroblasts using EDTA.

6.   Indirect co-culture of rLECS on TCP with rLFs

Direct co-culture of both cell types appears to yield greater overall viability than if the same number of cells were seeded alone. Over 7 days there was no statistical difference between rLEC and rLF viability on TCP. There was also no significant improvement in rLEC viability with indirect co-culture of fibroblasts or with using collagen as a substrate (figure 3.10) It was observed that removal of fibroblasts after 7 days led to a final average ratio of 7:1 fibroblasts to epithelial cells. However this could be due to removal of epithelial cells with fibroblasts as some wells did produce final ratios of 5:1 which is more consistent with the literature (Ebato, Friend, & Thoft, 1988; Garfias, Nieves-Hernandez, Garcia-Mejia, Estrada-Reyes, & Carmen Jimenez-Martinez, 2012)
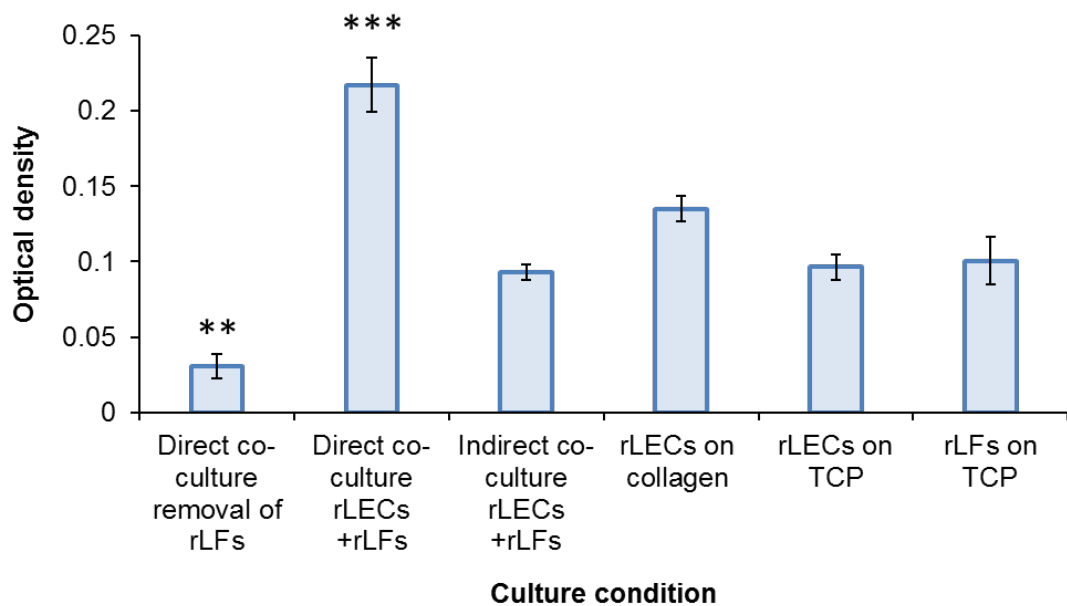
FIGURE 3.10: *Metabolic activity of Mono and co- cultures over 7 days. Results shown are means ± SEM with N= 6. Significance is relative each culture condition control. *P < 0.05, **P < 0.005, ***P < 0.001*

The cells were stained with DAPI and actin stain Phalloidin FITC and for the epithelial cell marker keratin 3 to visualise the proportion and arrangement of epithelial cells at confluence. Images were taken using the Image Xpress fluorescent microscope (figure 3.11). It was observed that the rLECs retained their characteristic cobblestone morphology much better when cultured on TCP or with fibroblasts than on collagen 1, it was also observed that epithelial cells grown in the presence of but not directly on fibroblasts, expressed high levels of the epithelial cell marker Keratin 3. The arrangement of the cells were mixed, and there did not appear to be any clear epithelial dominant regions or obvious layering of cell types as is seen in native cornea or 3D cultures (T. Sun et al., 2005). Figure 3.11 panel E shows that removal of fibroblasts with 5% EDTA also removed epithelial cells which also suggests no clear segregation between the cell types.
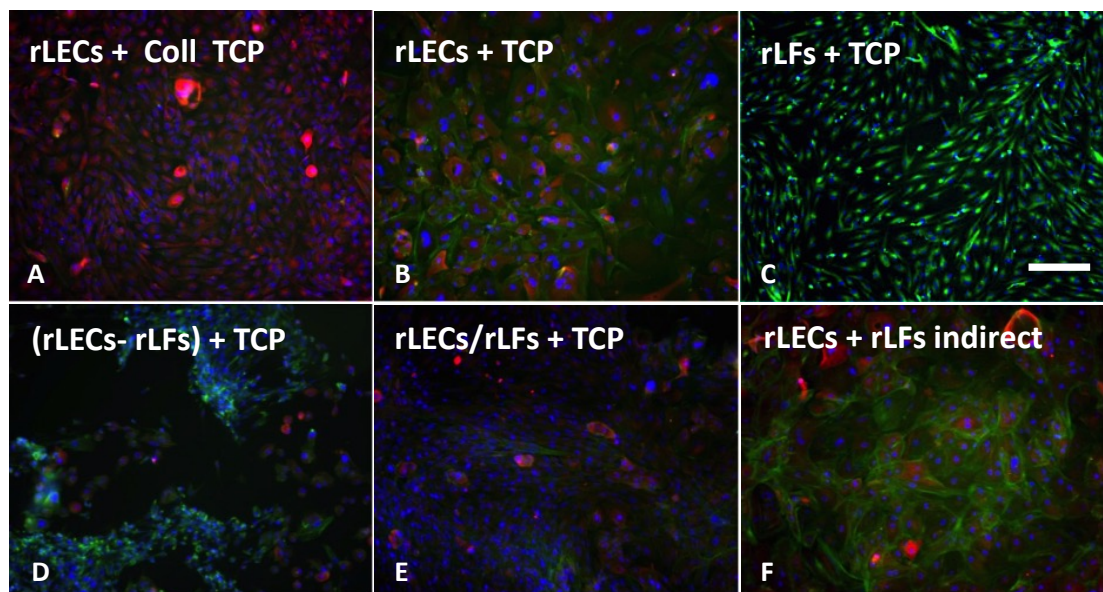
FIGURE 3.11: *DAPI (blue), Phalloidin FITC staining (green) of mono and co-cultures of rLECsand rLFs, with cytokeratin 3 immunohistochemistry staining (red) of differentiated rLECs. A) rLECs on collagen 1 coated TCP. B) rLECs cultured on TCP. C) rLFs on TCP. D) rLECs and rLFs on TCP with removal of rLFs with EDTA. E) Direct co-culture of rLFs with rLECs on TCP F) rLECs on TCP in the presence of rLFs suspended over cultures in ThinCerts. Scale bar represents 200 μm.*

In the direct co-culture conditions it was observed that confluence was reached at day 5, whereas other conditions did not reach confluence until day 7, shown in figure 3.11 as an over confluent layer of fibroblasts and epithelial cells indistinguishable from each other. The results of this experiment indicated that the synergistic relationship between fibroblasts and epithelial cells when cultured in direct contact with each other may be exploited to optimise cell viability on non-cell adhesive hydrogels.

3.4.4 CO-CULTURE ON BASE 1 1,3 DAP AND INERT PEG-DA 575

In this experiment 3 substrates were compared in co-culture

1.   Base 1 hydrogel functionalised with 1,3 diamino propane (1,3 DAP)

2.   PEG-DA (average MW 575) hydrogel

3.   TCP

PEG-DA hydrogels are inherently non cell adhesive and highly resistant to protein adsorption

The following culture conditions were used;

1.   rLECs alone

2.   rLFs alone

3.   rLECs and rLFs seeded in a 3:1 ratio

The total cell number on each sample was 20000. In the case of Base 1/1,3 DAP there was no significant difference in cell viability regardless of culture condition according to the MTT data (figure 3.12). However a previously inert hydrogel PEG-DA saw a brief increase in cell viability for the co-culture conditions at day 3, more cells were also seen at day 7 after staining with DAPI. For this experiment it appears that in 7 days cells on the TCP controls have become over confluent. Images of the gels showed the disparity between the amounts of cells adhered in each culture condition. Images also show that Base1/1,3 DAP gels shows some promise with regards to cell adhesion and viability with the rLFs exhibiting least preference for the gel. Very similar cell numbers were seen on these gels for both mono and co-culture of rLECs. It can also be clearly seen that the TCP control vastly out performs all other materials over the 7 day culture (figure 3.13).
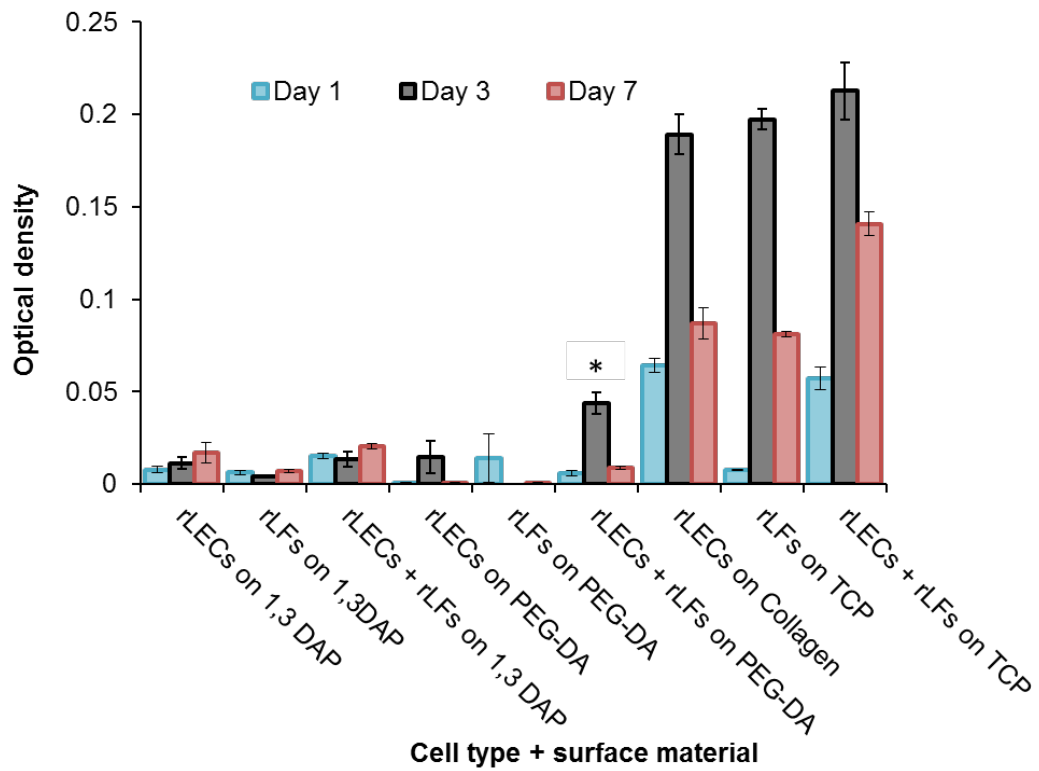
FIGURE 3.12: *Metabolic activity of mono and co-cultures on Base 1/1,3 DAP and PEG-DA over 1, 3 and 7 days. Results shown are means ± SEM of triplicate cultures. Significance is relative each material and culture condition. *P < 0.05, **P < 0.005, ***P < 0.001*
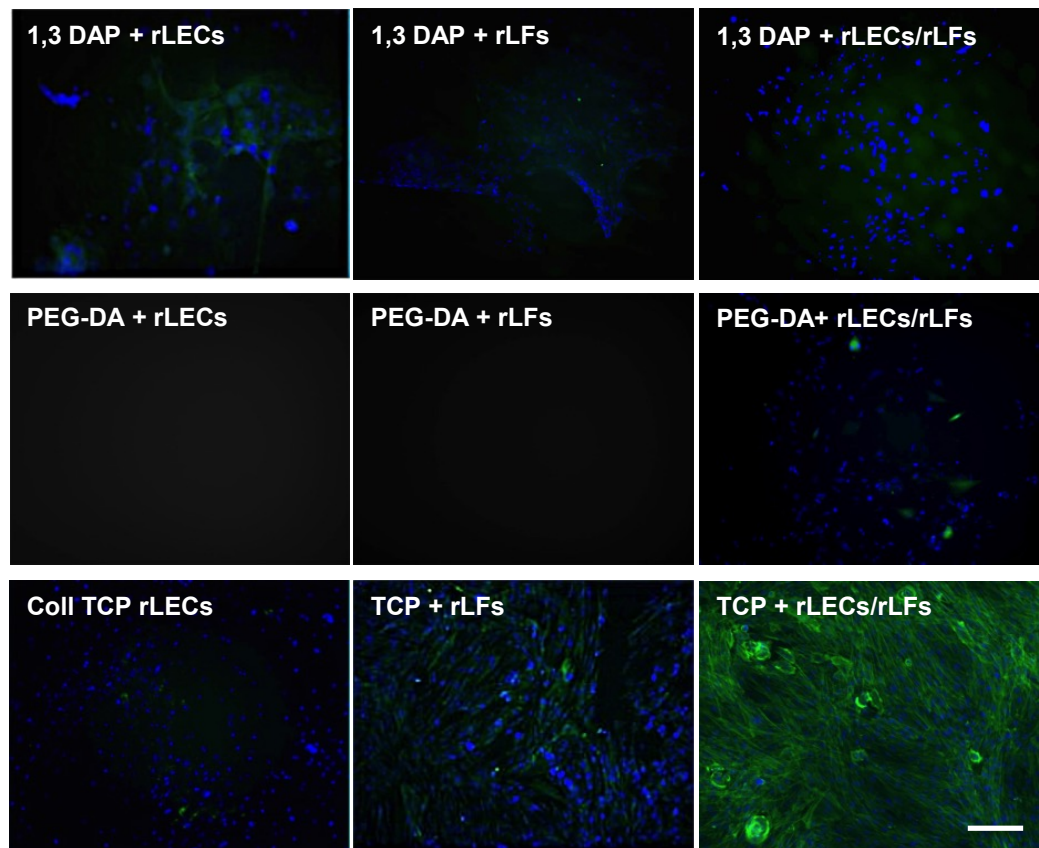
FIGURE 3.13: *DAPI (blue) and Phalloidin FITC (green) staining of mono and co-cultures on Base 1/1,3 DAP, PEG-DA and TCP after 7 days in culture. Scale bar represents 200 μm.*

3.4.5 CULTURE OF RLFS ON FIBRONECTIN COATED GELS

These polymethacrylate networks are minimally conducive to protein adsorption, which could be the reason cells do not adhere well to them. Plain and 1,3 DAP functionalised gels were coated with fibronectin (Fn) according to 3.3.10 and used as substrates to culture rLFs. These Fn coated gels were compared against the same gels without Fn. Only the plain Base 1 gels showed a significant difference in cell viability between Fn coated and non-coated gels. For TCP controls and 1,3 DAP functionalised gels Fn coating did not significantly improve the cell viability over 5 days (Figure 3.14)

The same experiment was also carried out using the Alamar- blue viability assay (figure 3.16) as this is more quantitative as all cells are assayed alive hence fewer cells may detach during the process. It was observed that during the MTT

assay, removal of MTT solution could have also removed cells that have detached during the MTT incubation period. Both assay methods show comparable data however and there was no significant improvement in cell viability with the addition of Fn to either plain or functionalised gels. Both sets of images (figure 3.15 and figure 3.17) also show an improvement in cell adhesion on plain Base 1 gels after coating with Fn. Overall it can be clearly seen that these gels are not conducive to protein adhesion and hence coating in protein is not sufficient to improve stromal cell adhesion.
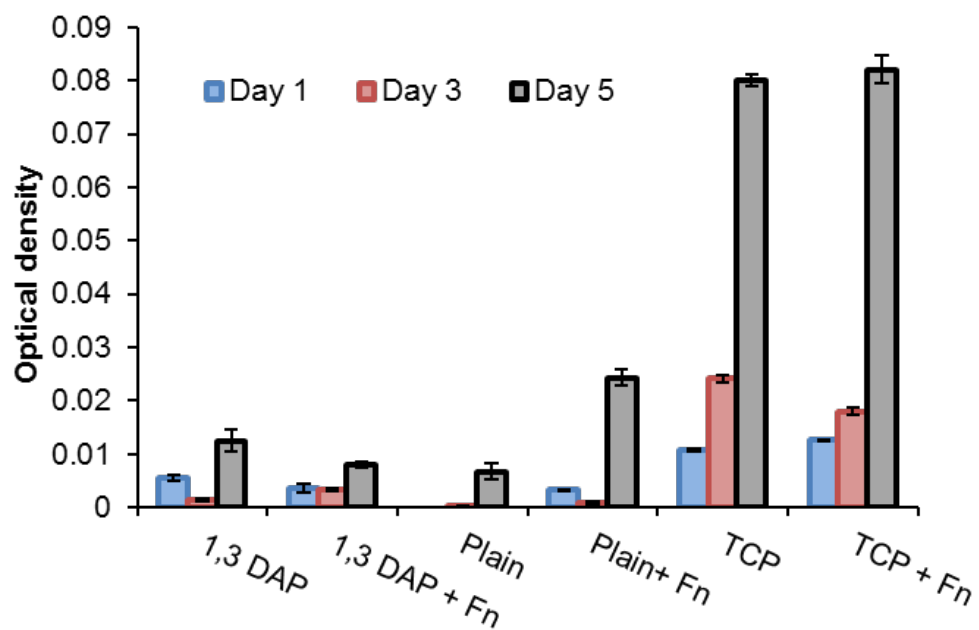
FIGURE 3.14: *Metabolic activity of rLFs on fibronectin coated and uncoated unfunctionalised (plain) and functionalised 1,3 DAP at day 1, 3 and 5. Results shown are means ± SEM where N=4.*
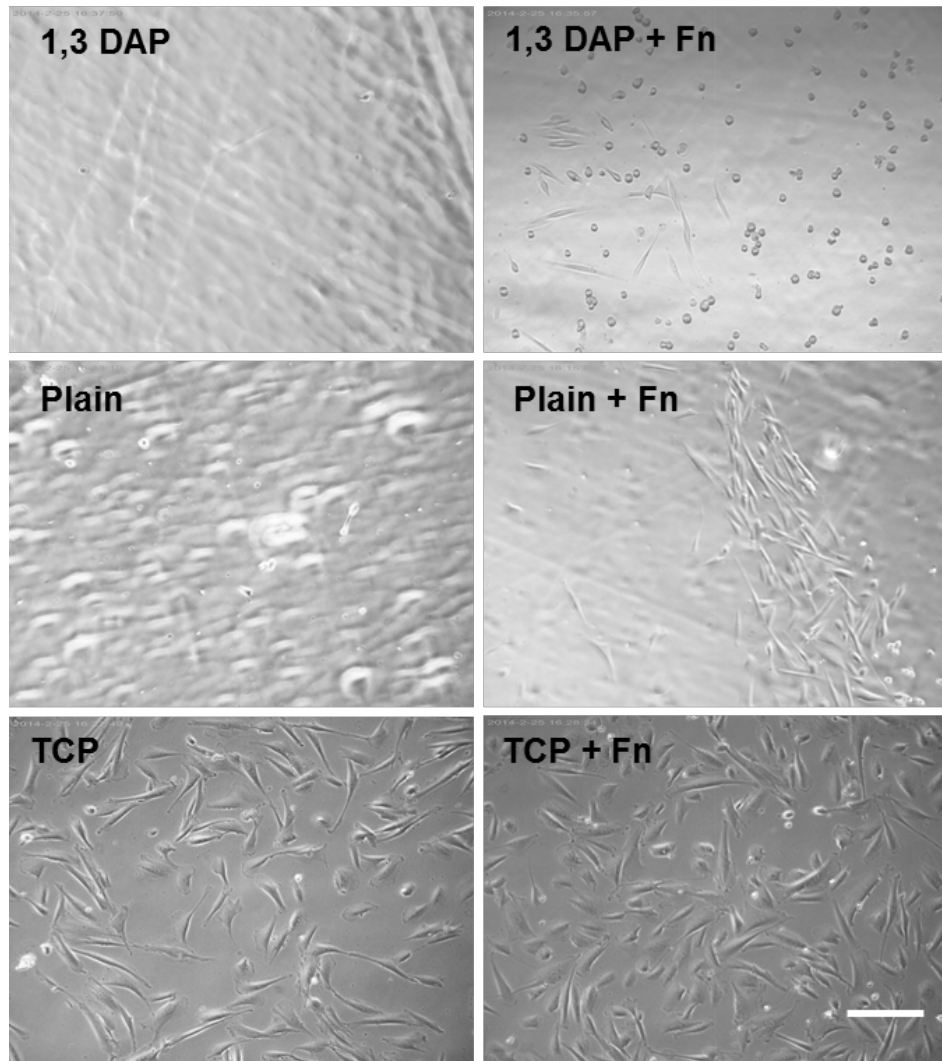
FIGURE 3.15: *Light microscopy images of rLFs on gels and TCP coated and uncoated with fibronectin. Scale bar represents 200µm.*
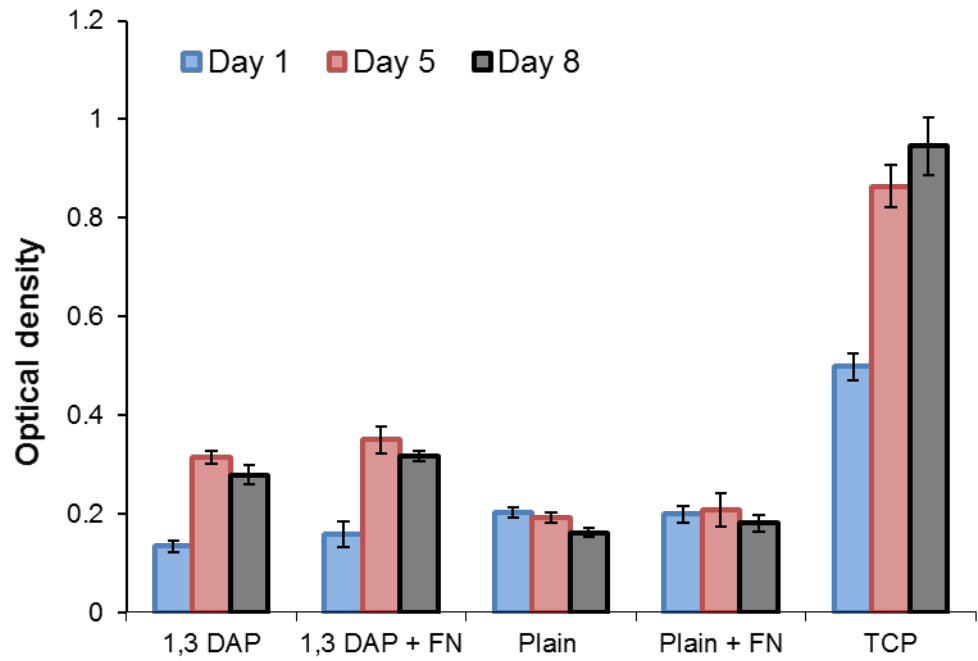
FIGURE 3.16: *Metabolic activity of rLFs on gels and TCP coated and uncoated with fibronectin, using the Alamar-blue assay. Results shown are means ± SEM of triplicate cultures.*
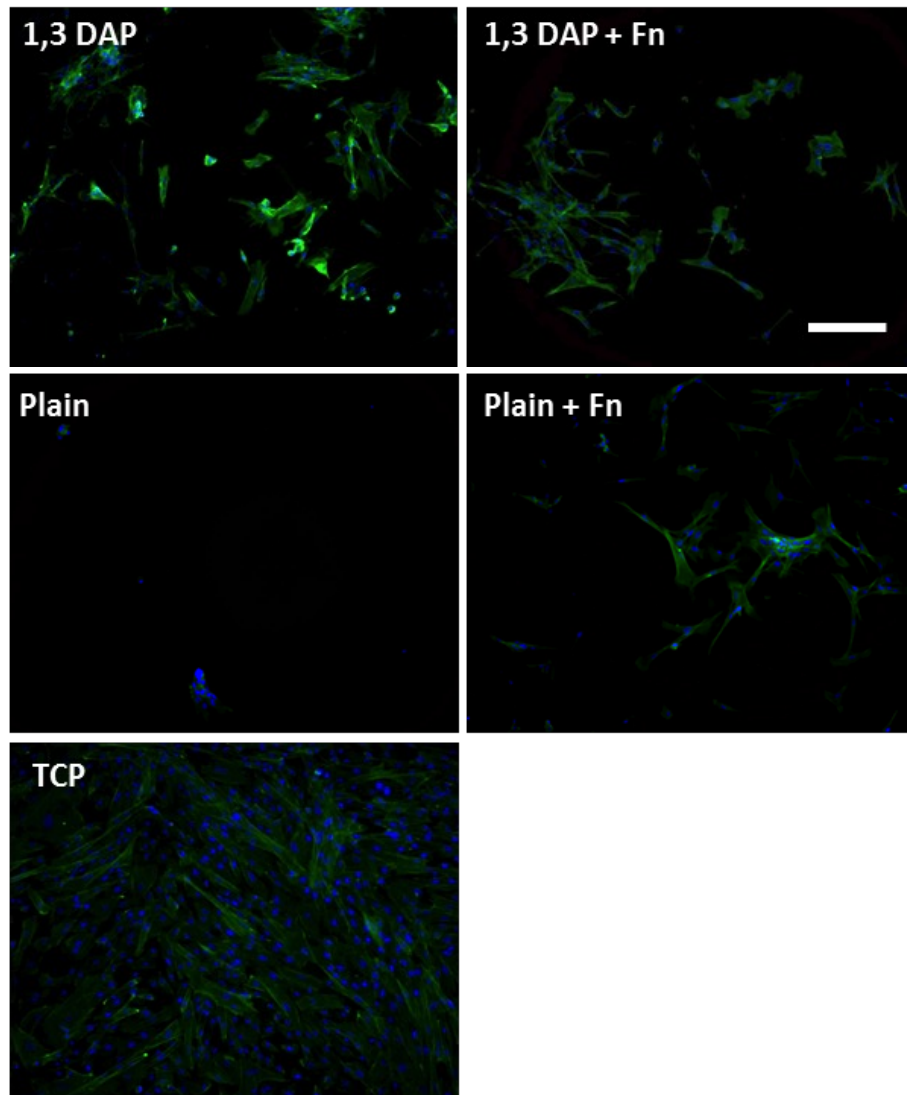
FIGURE 3.17: *DAPI and Phalloidin FITC staining of rLFs on gels with and without Fn. Scale bar represents 200 μm.*

3.4.6 CULTURE OF rLFs ON FIBRONECTIN COATED GELS BOUND WITH TRANSGLUTAMINASE

It was hypothesised that protein adsorption onto the hydrogel surface was not sufficient to effect cell adhesion and may suggest a link between poor protein adsorption and poor cell adhesion. To investigate this further, the next stage was to immobilise the fibronectin using transglutaminase (TGase), which is a Ca$_2^+$ dependent extracellular enzyme that forms protein cross links. It catalyses the isopeptide bond formation between the γ-carboxamide group of protein bound glutamine residues found on fibronectin and the ε-amino group of protein-bound lysine residues . Amines, diamines, and polyamines can also act

as amine donors (Folk and Finlayson 1977; Lorand and Conrad 1984). Using this principle it was hypothesised that fibronectin could be bound to the alkyl amines on the gels and in turn improve the adhesion and proliferation of rLFs on these surfaces.

Figure 3.18 shows that fibronectin coated or bound to the gels still does not improve the cell adhesion or proliferation of rLFs on any of the surfaces over the 5 day culture.
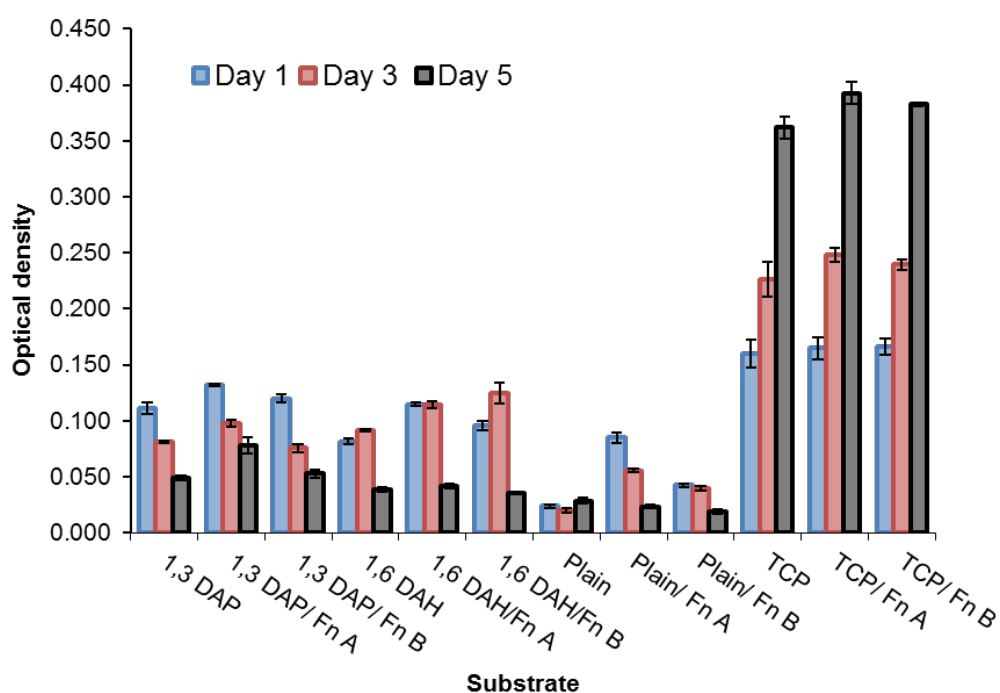
FIGURE 3.18: *Metabolic activity of rLFs on Plain, 1,3 DAP and 1,6 DAH functionalised Base 1, without Fn and with Fn coated and bound with TGase. Results shown are means ± SEM of triplicate cultures.*

3.4.7 TESTING THE EFFECTIVITY OF TGASE MEDIATED FN BINDING

The aim of this experiment was to localise the binding of Fn onto gels using TGase drops or blots so that a qualitative screen for the presence of bound Fn can be made. From figure 3.19 the blot and drop boundary can be seen (red arrow) close to the edge of the hydrogel (white arrow). In the blot method there

appears to be a more uniform distribution of bound Fn than in the drop method. The drop method shows a higher concentration of bound Fn at the edge of the drop, (panel B red arrow) there are also small regions of no Fn possibly due to air bubbles in the drop.
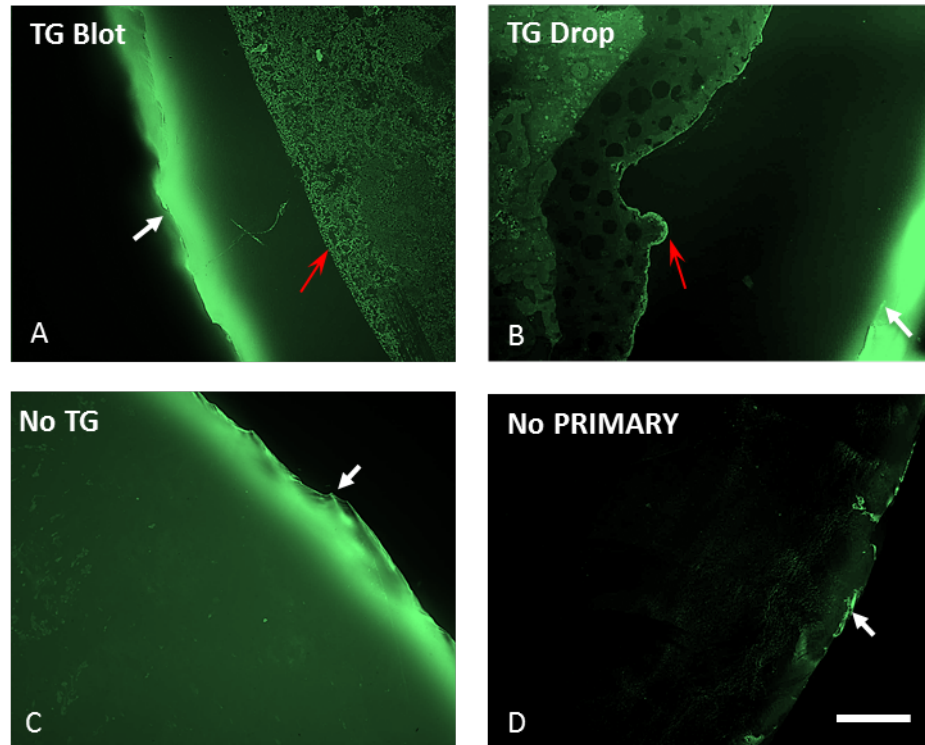
FIGURE 3.19: *Fluorescence images of Base 1/1,3 DAP coated with Fn then bound using TGase, (A) the blot and (B) drop method. C) Shows no TGase and D) a negative control of no primary. Scale bar represents 200 µm.*

3.5   DISCUSSION AND SUMMARY RLF RESPONSE

Following on from the aims in chapter 2, stromal cells, rabbit limbal fibroblasts in particular were chosen to initially assess the potential of these gels to be used as corneal onlays. The basis for using stromal cells were i) they are abundant, as they can be expanded and used up to passage 7, ii) they are easy to maintain in culture iii) they adhere and reach confluence more quickly than epithelial cells thus allowing a quick screen of the gels biocompatibility iv) they are robust adherent cells that have been shown to aid epithelialisation and finally they have been shown to grow well on hydrophilic less flexible substrates.

Previous work has suggested that poly(GMMA-co-EGDMA-co-GME-co-LMA) networks perform better than those without the hydrophobic monomer (Rimmer et al., 2007; Y. Sun, Collett, Fullwood, Mac Neil, & Rimmer, 2007). In this case there appears to be no increase in cell adhesion over prolonged cultures of over 5 days regardless of LMA content, swelling and amine carbon chain length. Moreover, the addition of fibronectin either by adsorption or by TGase mediated coupling did not improve cell adhesion or proliferation. One reason for this could be related to a tendency for hydrophilic substrates to generally adsorb lower quantities of protein (Lestelius, Liedberg, & Tengvall, 1997). Proteins are also prone to unfolding at the interface of hydrophobic surfaces (Baujard-Lamotte, Noinville, Goubard, Marque, & Pauthe, 2008; Iuliano, Saavedra, & Truskey, 1993). This implies that proteins would retain their active conformation on more hydrophilic surfaces provided they could adsorb readily. From figures 3.14-3.18 it can be seen that coating gels in Fn or binding Fn to gels using TGase did not improve the adhesion of rLFs to the gels. This could be due to low protein adsorption for coated gels and incorrect conformation of the Fn on the Fn bound gels.

The data presented in this chapter could highlight the importance of bulk vs interfacial chemistry, understanding how the balance of both these parameters influence stromal cell behaviour could shed light on why there is contrasting literature with regards to amination of non-fouling substrates. The principle behind adding amines, is to increase the net surface charge either by increasing the concentration of amines or in this case increasing the carbon chain of the diamines (Rimmer et al., 2007). Increasing surface charge density improves wettability and hence cell and protein adhesion (Lee, Jung, Kang, & Lee, 1994). However in some cases the tactics to achieve this have favoured acrylic acid or carboxylic acid negatively charged groups over positively charged amine functionality (Notara et al., 2007). Some studies have shown that ammonia or 1,2 DAE plasma treated poly(L-lactide/epsilon-caprolactone) (PLLA/ε-C) does not adequately enhance fibroblast cell attachment and growth despite performing better than non-treated PLLA/ε-C (Aydin, Türk, Calimli, & Pişkin, 2006). In contrast, ammonia and allyamine plasma modified

polyethylenterephtalat (PET) membranes improved fibroblast adhesion and growth when compared to unmodified PET, though allylamine modification had better cell adhesive properties than ammonia plasma treatment (Hamerli, Weigel, Groth, & Paul, 2003). Ammonia plasma treatment of other non-fouling substrates such as polytetrafluorethylene (PTFE) has been shown to improve adhesion and proliferation of human umbilical vein endothelial cells (HUVECs) better than ammonia treated PET (Pu, Williams, Markkula, & Hunt, 2002). These studies could suggest that bulk material properties may not be completely overridden by surface chemical modification. One study that successfully improved fibroblast adhesion to hydrogels, incorporated a series of amines to poly(hydroxy ethyl methacrylate) (p(HEMA)) based gels. This method increases the cationic concentration throughout the bulk and surface of the gel which may contribute to the improved cell adhesion.

Poor stromal cell adhesion seen in this chapter could be due to a conflict of bulk properties relating to high water contents (Haigh, Rimmer, & Fullwood, 2000) and stiffness, despite previous results suggesting HDFs adhere and proliferate well on similar gels. (Y. Sun, Maughan, et al., 2007). From figure 3.13 hints about the materials ability to support epithelial cells alone without the aid of a stromal monolayer can be seen, indicating the protein and stromal cell resistance could still be exploited to regenerate corneal epithelium without the need for protein modification or without a stromal cell interaction. This could be beneficial as figures 3.10 and 3.11 show that despite an initial seeding ratio of 3:1, rLECS to rLFs, there will an eventual overgrowth of rLFs if a material such as TCP that supports both cell types is used. A selective material that is resistant to protein adsorption but is capable of supporting an epithelium could also contribute to an onlay or inlay's optical clarity, resistance to inflammation and infection (Du, Chen, Yan, & Wu, 2012; Myung et al., 2007).

CHAPTER 4

EPITHELIAL CELL RESPONSE

TO AMINATED HYDROGELS

AND PROTEIN COATED

SURFACES

CHAPTER 4: EPITHELIAL CELL RESPONSE TO AMINATED HYDROGELS AND PROTEIN COATED SURFACES

4.1   INTRODUCTION

Epithelial cells isolated from soft tissues such as cornea tend to grow best on softer substrates (Levental et al., 2007). In particular the corneal epithelium is supported by an elastomeric hydrated stroma, these features enable the cornea to respond to intraocular pressure changes (Jacob et al., 2005) and allow diffusion of oxygen and glucose through the tissue, contributing to epithelial tissue survival. (Khan et al., 2001; McCarey and Schmidt, 1990; Thoft et al., 1971). In developing a stromal mimic to support an epithelium after disease or injury it is worth incorporating these features into a biomaterial, although some success has been seen in treatment of extreme cases with AlphaCor, a transparent device that functions without an epithelium. Efforts are now being made to improve such devices by promoting epithelialisation, which will prevent entry of pathogens and water loss. Thus, from chapter 2, softer, higher swelling gels such as Base 0 and 1 may be of particular interest. Ideally the optimal material will not require further modification with protein, however the addition of ECM proteins, should they be required, may contribute to the maintenance of the limbal epithelial stem cell phenotype. The "stemness" of the cells could also be preserved from the intact niche architecture transplanted to the materials from the limbal explants.

4.2   AIMS

The aim of this chapter is to evaluate the limbal epithelial cell response to selected aminated hydrogels and other protein substrates using cell suspensions and limbal explants. From this evaluation the final aim is to identify the most optimal material for potential use as a corneal inlay.

4.3   MATERIALS AND METHODS

Materials used in this chapter are the same supplier as in table 3.2 any reagents not included in chapter 3 are listed in the table below.

TABLE 4.1: Source of reagents used in this chapter, which is not already included in table 3.2.

Reagents	Supplier
ABCG2 antibody	Abcam
cell tracker green	Invitrogen life technologies
cell tracker red	Invitrogen Life technologies
DMEM/F-12 phenol free media	Gibco Life technologies
laminin	Sigma-Aldrich
P63 antibody	Abcam
vitronectin	Sigma-Aldrich

4.3.1 DYNAMIC SHEAR ANALYSIS OF NATIVE RABBIT CORNEA

Rabbit eyes were cleaned, and excess tissue removed in the same manner as for cell isolation, 3 rabbit corneal buttons were trephined using a 10 mm biopsy punch and transferred to fresh PBS for transport. An AR-G2 2000 rheometer (TA Instruments, Crawley England) was used to collect data. Hydrated corneas were loaded between a heated Peltier plate, set at 37 °C, and 25 mm parallel plate geometry. The criteria for valid modulus readings were set the same as for the hydrogel measurements in 2.3.11: a) a normal compression force of 0.5 N and a gap of approximately 500 μm between the two parallel plates within which the corneas were compressed, PBS was pipetted in the gap around the corneas to keep them from drying out during measurements. Samples were then subjected to a standard oscillatory test (0.628 rad/s to 62.8 rad/s, 0.001 strain) (Figure 2.7). The upper plate oscillates at a fixed strain and records the stress response from the corneas over a range of frequencies (ω) Storage moduli were calculated in the exact manner as described in 2.3.11.

4.3.2 PROTEIN COATING SURFACES

TCP was coated with different ECM proteins to assess the growth, proliferation, morphology and expression of ABCG2 and cytokeratin 3 of rLECs and rabbit corneal epithelial cells (rCECs). 12 –well plates were coated with 1ml per well of the proteins in table 4.2 according to the dilutions listed and allowed to adhere

to the TCP in the incubator at 37°C 5% CO_2. Once plates had been coated all wells were washed with PBS twice and immediately used for cell culture.

TABLE 4.2: Details of protein source, dilution and incubation times for coating culture plates.

Protein	Source	Dilution	Incubation
Laminin (LN)	Engelbreth-Holm-Swarm (EHS) murine sarcoma basement membrane	2 µg/ml	2 hrs 37°C
Fibronectin (FN)	Bovine plasma	1.5 µg/ml	2 hrs 37°C
Vitronectin (VN)	Recombinant, expressed in Human Embryonic Kidney 293 cells	2 µg/ml	2 hrs 37°C
Collagen 1 (COL I)	Rat tail	0.2 µg/ml	2 hrs 37°C

4.3.3 LIMBAL AND CORNEAL EPITHELIAL CELL CULTURE ON PROTEINS

Primary rCECs were isolated from rabbit eyes dissected and cleaned in the same manner as in 3.3.2 corneal buttons were cut out after limbal regions were isolated. Corneal buttons were placed in a petri dish and immersed in Dispase II solution (2.5mg/ml in serum free Dulbecco's Modified Eagle's Medium + Glutamax) and placed in the incubator for 1hr at 37°C and 5% CO_2. Corneas were subsequently transferred into a dish of fresh DMEM + glutamax media and cells were scraped from the epithelial surface into the media using a pair of blunt forceps, the resulting cell suspension was spun at 200 g for 5 minutes and resuspended in the epithelial culture medium and seeded directly into the coated wells that were prepared in 4.3.2. Freshly isolated rLECs, isolated in same manner as described previously (3.3.2) were also seeded onto separate protein coated plates. Additionally a set of uncoated wells and wells pre-seeded with irradiated 3T3s were seeded with freshly isolated rLECs or rCECs. Cells were cultured on these proteins for 7 days at 37°C and 5% CO_2.

4.3.4 IMMUNOHISTOCHEMISTRY WITH ABCG2 AND CYT3

Cultures from 4.3.3 were washed with PBS 3 times and then fixed using 3.7% buffered formaldehyde for 15 mins, cells were rinsed a further 3 times with PBS.

Blocking buffer (10% goat's serum in PBS) was then added and incubated for 1 hr at room temperature. Cells were then permeablised by treatment with 0.1% Triton X for 5 min. After removing and washing off excess Triton X, samples were incubated at 4°C overnight with the primary antibody, either a mouse monoclonal antibody against cytokeratin 3 (Anti-Cytokeratin 3 antibody Abcam UK) diluted 1:50 in 1% blocking buffer or for ABCG2 staining (mouse monoclonal antibody for ABCG2) also diluted 1:50 in 1% blocking buffer. Primary antibody was then removed and cells were washed 3 times with PBS. Cells were then incubated at room temperature for 2 hrs with a biotynilated goat anti-mouse IgG (Vector labs, UK) diluted 1:1000, again in 1% blocking buffer. After 3 washes with PBS, cultures were either incubated with Streptavadin Texas red (for cytokeratin 3 staining) or Streptavadin Fluorescein (for ABCG2 staining) diluted 1:1000 in a solution of DAPI (0.5 µg/ml in PBS) at room temperature in the dark for 1.5 hrs. Cells were given 3 final washes with PBS before imaging with the Image Xpress fluorescent microscope.

4.3.5 EFFECT OF CYT 3 EXPRESSION IN P0 AND P1 rLECs CULTURED ON TCP

It is useful to assess how quickly rLECs become differentiated into corneal epithelial cells. Primary rLECs were isolated as described in 3.3.2 and immediately seeded onto tissue culture plastic (12- well plate) with no i3T3 feeder layer and allowed to proliferate until 80% confluence, which in this case was 4 days. One quarter of the wells that were seeded were passaged and allowed to grow for another 4 days. The remaining p0 cells were fixed with 3.7% buffered formaldehyde for 15 mins, and stained for cytokeratin 3 as described in 4.3.4. Cells cultured at p1 were also fixed and stained in the same way 4 days later. Cells were then imaged with fluorescence microscopy.

4.3.6 LIMBAL EPITHELIAL CELL CULTURE AND VIABILITY ON GELS

For this study Bases 0, 1 and 2 were washed according to 2.3.4, transferred to a sterile environment, cut with a number 10 cork borer and washed twice with absolute ethanol and once with 70% IMS (industrial methylated spirit). Gel discs also went through 5 cycles of PBS washes including 1 overnight wash to

remove traces of alcohol. Due to p0 cell numbers being low, initial studies were carried out after expansion of rLECs on i3T3 cells for 7 days. Gels were saturated in RLE media for 2-3 hrs at 37°C and 5% CO_2. Gels were transferred to 12 –well plates and weighed down with medical grade stainless steel rings. Each ring was seeded with 5000 rLECs, which were allowed to adhere for 24 hrs before rings were removed and media was changed. Cells were cultured on the gels for 24, 48 and 96 hrs to assess initial adhesion and proliferation on all gels compared to a TCP control. Imaging with light microscopy and MTT assays were carried out at each time point.

4.3.7 LIMBAL EPITHELIAL CELL CULTURE AND VIABILITY ON INCREASED GME GELS

From chapter 2 there were issues regarding gels with increasing GME in particular their response to certain solvents. This made it slightly difficult to culture rLECs on these materials, however it was possible if the washing regime was modified. Bases 1.B, 1.15, 1.20 and 1.30 gels were functionalised with either 1,3 DAP or 1,4 DAB and cut into discs using a number 10 cork borer. Gels were washed several times with Isopropanol in a sterile environment and immersed immediately into RLE media without a PBS step as this was shown to cause cracking of the materials. The gels went through 5 cycles of 1 hr media washes including a final overnight wash with incubation at 37°C and 5% CO_2. Discs were transferred to a 12-well plate and weighed down with seeding rings as described previously, 5000 p1 rLECs were seeded onto each gel and cultured for 4 days with MTT assays carried out at 24, 48 and 96 hrs.

4.3.8 CELL PREFERENCE STUDY

In order to evaluate the affinity rLECs have for some of the materials a cell preference study was carried out, the best performing materials with regards to supporting rLEC growth appears to be Base 1/1,3 DAP and Base1/1,4 DAB. These discs were prepared as described previously (4.3.6) and placed in wells of a 12 well plate, these gels were not restricted by seeding rings and rLECs were seeded at 10000 cells per well and allowed to adhere randomly to either TCP or

gels. After culture for 4 days, hydrogels were removed and placed into fresh wells. MTT assays were carried out on the TCP and the gels.

4.3.9   EXPLANT CULTURE AND IMAGING ON BASE 1 AND BASE 2

After obtaining rLEC growth comparable to TCP on some of these gels it was then important to observe how p0 rLECs respond to these materials by using small limbal explants which has also been used in the clinic to successfully regenerate corneal epithelium on amniotic membrane (Sangwan et al., 2012). Base 1 and 2 hydrogels functionalised with 1,3 DAP, 1,4 DAB or 1,6 DAH were washed and prepared in the same manner described for cell viability studies. Gels were then saturated in media as described in the previous sections. Two or three discs of each hydrogel were placed in a dry well of a 12-well plate. Meanwhile, rabbit limbal tissue was finely diced to give limbal explants measuring approximately 500 mm × 300 mm. Between 5 and 8 of these small explants were placed on each disc and allowed to adhere in the incubator at 37°C 5% CO_2 for 3 hrs before RLE media was added. Three experiments were carried out using different batches of rabbit eyes; the first experiment was carried out in duplicate while subsequent experiments were in triplicate. Cultures were monitored by light microscopy with images taken at days 5, 6, 7 and 14. Explant adherence as well as outgrowths were recorded as a total of initial explants cultured.

4.3.10   IMMUNOHISTOCHEMISTRY OF EXPLANT OUTGROWTH P63 AND CYT 3

Explant out growths on the most effective hydrogels, Base 1/1,4 DAB, were characterised by immunohistochemistry using cytokeratin 3 and p63 staining after 6 days. Remaining explants and rLECs on the gels were washed three times in PBS and fixed with 3.7% buffered formaldehyde, after which they were rinsed three more times with PBS. Goat's serum blocking buffer (10% in PBS) was used to block non-specific binding sites for 1hr at room temperature. Cells were then permeablised by treatment with 0.1% Triton X for 5 min. After removing and washing off excess Triton X with PBS, samples were incubated at 4°C overnight with the primary antibody, a mouse monoclonal antibody against cytokeratin 3

(anti-cytokeratin 3 antibody, Abcam, UK) or anti-P63 antibody (Abcam), both diluted 1:50 in 1% blocking buffer. The following day samples were washed several times in PBS. Gels were then incubated at room temperature for 2 hrs with a biotinylated goat anti-mouse IgG (Vector Labs, UK) diluted 1:1000, again in 1% blocking buffer. After three rinses in PBS, the samples were incubated at room temperature in the dark for 1.5 hrs with Streptavadin Texas red (Vector Labs UK) diluted 1:100 in a solution of nuclei stain 4′,6-diamidino-2-phenylindole (DAPI) at a concentration of 0.5 µg ml–1 in PBS. Samples were finally washed three times before imaging using a Zeiss LSM 510 META confocal microscope with ×10 or ×40 objectives at laser wavelengths of 800 and 543 nm.

4.3.11   CO-CULTURE MODEL OF STROMAL EXCLUSION USING CELL TRACKER

A full set of Base 1 functionalised with all amines was prepared in the same manner as described previously in Sections 2.3.3 and 2.3.4. A near-confluent layer of rLFs were incubated at 37° C, 5% CO2 with 7 ml of serum-free DMEM containing CellTrace™ Oregon Green 488 (Invitrogen Molecular Probes, 50 µg in 7 µl DMSO) for 40 min. At the same time rLECs at 80% confluency were incubated with 7 ml DMEM containing CellTracker™ Red CMTPX (50 µg in 7 µl DMSO, C34552, Molecular Probes). Cells from each flask were detached and resuspended in epithelial media. 5000 of each cell type was seeded onto the gels and tissue culture plastic (TCP) in the same manner as described in Section 4.3.6. Images were taken using a Zeiss LSM 510 META confocal microscope at laser wavelengths of 488 nm and 543 nm at days 1, 3 and 6.

4.3.12   CULTURE OF rLECs ON FIBRONECTIN COATED AND BOUND GELS

To assess if adding protein could enhance the rLEC growth on some of these gels, the same fibronectin coating experiment as described in 3.3.10-11 was carried out. Unfunctionalised Base 1, Base 1/1,3 DAP and Base 1/1,6 DAH were prepared and coated with bovine fibronectin (Fn) in the exact manner as 3.3.10 or coupled with Fn using transglutaminase as described in 3.3.12. Fn coated and bound gels, referred to as Fn A and Fn B gels respectively, were washed 3 times in PBS, saturated in RLE media for 2 hrs and clamped to the bottom of the well

using an inverted cell crown as in 3.3.11 before 2500 rLECs per sample were seeded. And an Alamar blue assay was carried out on the gels on days 1, 3 and 5.

4.3.13   PHENOL FREE rLEC CULTURE ON BASE 1

During the course of cell compatibility studies with these hydrogels it was observed that the gels not only absorbed the media they were immersed in but appeared to absorb more phenol red from the media with longer alkyl chain length amines or with more amine, causing gels to appear darker in colour indicating a higher uptake of phenol red. Since most studies have indicated that the nature of the functional group directly influenced rLEC but not rLF adhesion and proliferation a comparison of phenol red and phenol free cultures was made to assess the effect of this phenomenon.

Two sets of 1,3 DAP, 1,4 DAB and 1,6 DAH functionalised Base 1 gels were prepared in the same manner as has been described throughout these studies. One set was saturated in standard RLE media and one set saturated in phenol free RLE media made from DMEM/F-12 (without phenol red) (Gibco Life technologies) supplemented with 10% FCS, 0.05 µl/ml epidermal growth factor (EGF), 5 mg/ml insulin, 1% penicillin/streptomycin and 1% amphotericin B.

Both sets of gels were transferred to 12 well plates and weighed down with stainless steel seeding rings before seeding 5000 p1 rLECs suspended in the corresponding media (with or without phenol red) onto each gel. MTT assays for each set were carried out at day 1, 2 and 4, with light microscopy images taken at days 1 and 4.

4.3.14   COMPARISON OF PHENOL RED ADSORPTION

Relative phenol red absorption profiles were assessed for Bases 0, 1 and 2 functionalised with ammonia and all diamines. Gels were cut out using a number 2 cork borer and saturated overnight in RLE media containing phenol red. Discs were then removed and washed once in PBS before being blotted dry and placed in wells of a 96 well plate an and absorption readings taken at 562

nm. An average of 4 absorbance readings from 4 samples were taken from each gel type.

4.4   RESULTS

4.4.1 STORAGE MODULUS OF NATIVE RABBIT CORNEA

It is well established that different cell types will respond according to the physiological elasticity or rigidity of a substrate, and as mentioned earlier in this chapter epithelial cells extracted from soft tissues grow well on softer substrates with a G'≈ 100Pa (Paszek et al., 2005) (Levental et al., 2007). With regards to this study it is important to acknowledge that the cornea as a whole is not homogeneous and different components of the cornea such as the basement membrane, epithelium, stroma and Descemet's membrane have been reported to have unique elastic moduli (Thomasy et al., 2013) and these local moduli influence cell behaviour. However, in terms of clinical application, broad rheological experiments on whole cornea can give clues to how a hydrogel may be developed. At least from a bio-integration perspective it can be assumed that bulk materials much stiffer or softer than the tissue they intend to replace may cause extrusion or failure, as they will be unable to deal with intra-ocular pressure changes. Therefore it was important to compare the stiffness of the hydrogels selected for optimisation to the stiffness of the natural cornea. The elastic storage moduli of 3 corneas were obtained from the mean G' values obtained across a range of frequencies (0.628-62.8 rad/s). Figure 4.1 shows that there are slight variations between samples however they all fall within a range of approximately 195-254 Pa, which is much lower than the range obtained from the hydrogels in chapter 2. The closest material made is Base 0 which has moduli falling between 800 and 9000 kPa. The age of the rabbits corneas were unknown and it is noted that this may contribute to the slight variations in corneal modulus.
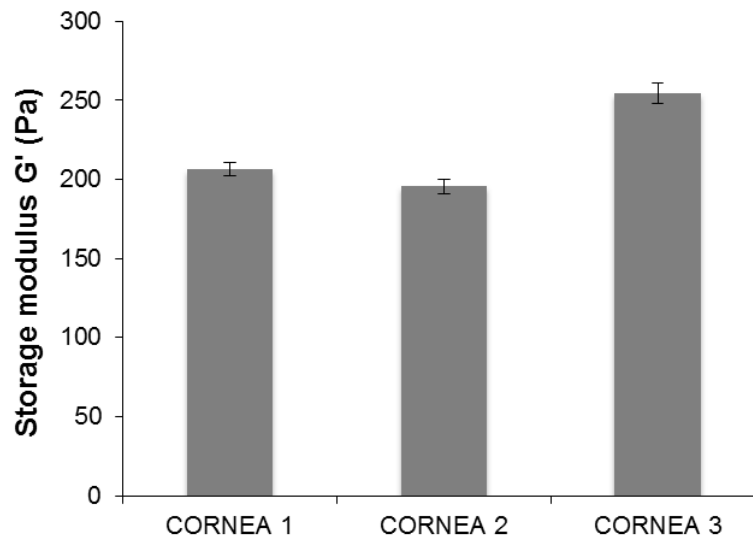
FIGURE 4.1: *Elastic storage moduli data of 3 fresh corneas. Results are calculated from the average of storage moduli across a range of frequencies.*

4.4.2 EFFECT OF SUBSTRATE PROTEIN ON ABCG2 AND CYT3 EXPRESSION

Conventionally, limbal epithelial cells are cultured on i3T3s as a feeder layer to provide support for their growth and proliferation. Feeder layers have also been shown to allow these cells to maintain an undifferentiated phenotype. This experiment aimed to assess other protein substrates for their ability to support rabbit limbal epithelial cells in this way. Cells from both the limbal region, which contain limbal epithelial stem cells (LESCs), and the central corneal region were qualitatively assessed for expression of putative stem cell marker ABCG2 and corneal cell differentiation marker cytokeratin 3. Results were used to compare protein substrates to the feeder layer gold standard, which may be later used on hydrogels to enhance performance. Aside from expression markers, the morphology of LESCs are much different from transient amplifying cells (TACs) or terminally differentiated corneal cells. They are usually smaller when undifferentiated (10.1 ± 0.8 compared to 17.1±0.8 μm) (Romano et al., 2003) and express a high nuclear to cytoplasmic ratio, another feature of immature cells (Chen et al., 2004). LESCs also have high colony forming capacity and

produce tightly packed homogeneous cell colonies called holoclones (Pellegrini et al., 1999)

In figure 4.2 a) it can be seen that there is some positive ABCG2 staining of rLECs on all substrates, with the highest expression appearing to be from cells on Fn, however these cells also appear to be larger than some of the cells on i3T3s and Vn, which is more typical of immature cells. Cells also grew well on TCP without a feeder layer, but they appeared to stain less strongly for ABCG2. Vibrant ABCG2 staining of rLECs on Ln was observed, there also appeared to be sparse non uniform cell growth, i.e. some cells remained small with high a nuclear to cytoplasmic ratio and some cells appeared larger and more elongated.

Figure 4.3 b) shows that central corneal cells did not express any ABCG2 unless cultured on i3T3s which is could be attributed to the corneal basal cells that are yet to differentiate at the corneal surface. There appears to be a very low but detectable concentration of ABCG2 from central corneal cells cultured on Vitronectin. As expected there is no positive expression of cytokeratin 3 of rLECs on any of the substrates which is seen with most of the corneal cells on all of the substrates, most strongly on collagen. Table 4.3 summarises the cells phenotype and growth.

Table 4.3: *Limbal and central corneal cell expression of ABCG2 and CYT3 on different proteins, TCP and i3T3 cells*

Substrate	Limbal			Central corneal		
	ABCG2	CYT 3	Proliferation	ABCG2	CYT 3	Proliferation
Collagen	++	--	+++	--	+++	+
i3T3s	++	--	+++	+	++	+++
Laminin	++	--	+	--	+	++
Vitronectin	++	--	++	-	++	++
Fibronectin	+++	--	+++	--	++	+
TCP	+	--	+++	--	++	+

a)

b)
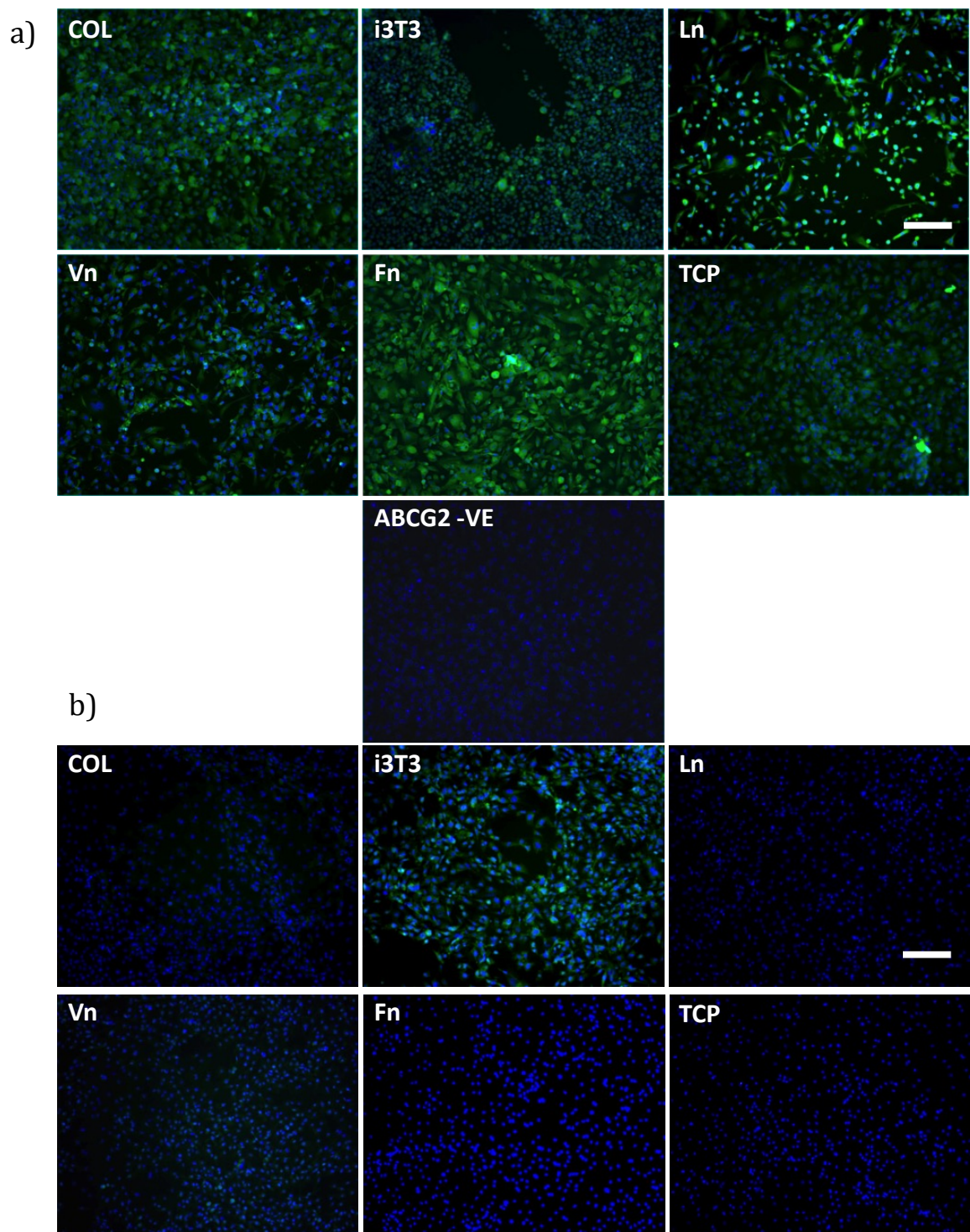
FIGURE 4.2: *Immunohistochemistry of rabbit limbal epithelial cells a) and rabbit central corneal cells b) after culture on collagen (col), irradiated 3T3 fibroblasts (i3T3), laminin (Ln), vitronectin (Vn), fibronectin (Fn) and TCP. Images show ABCG2 staining (green) and nuclei staining (blue). Scale bar represents 200 µm*
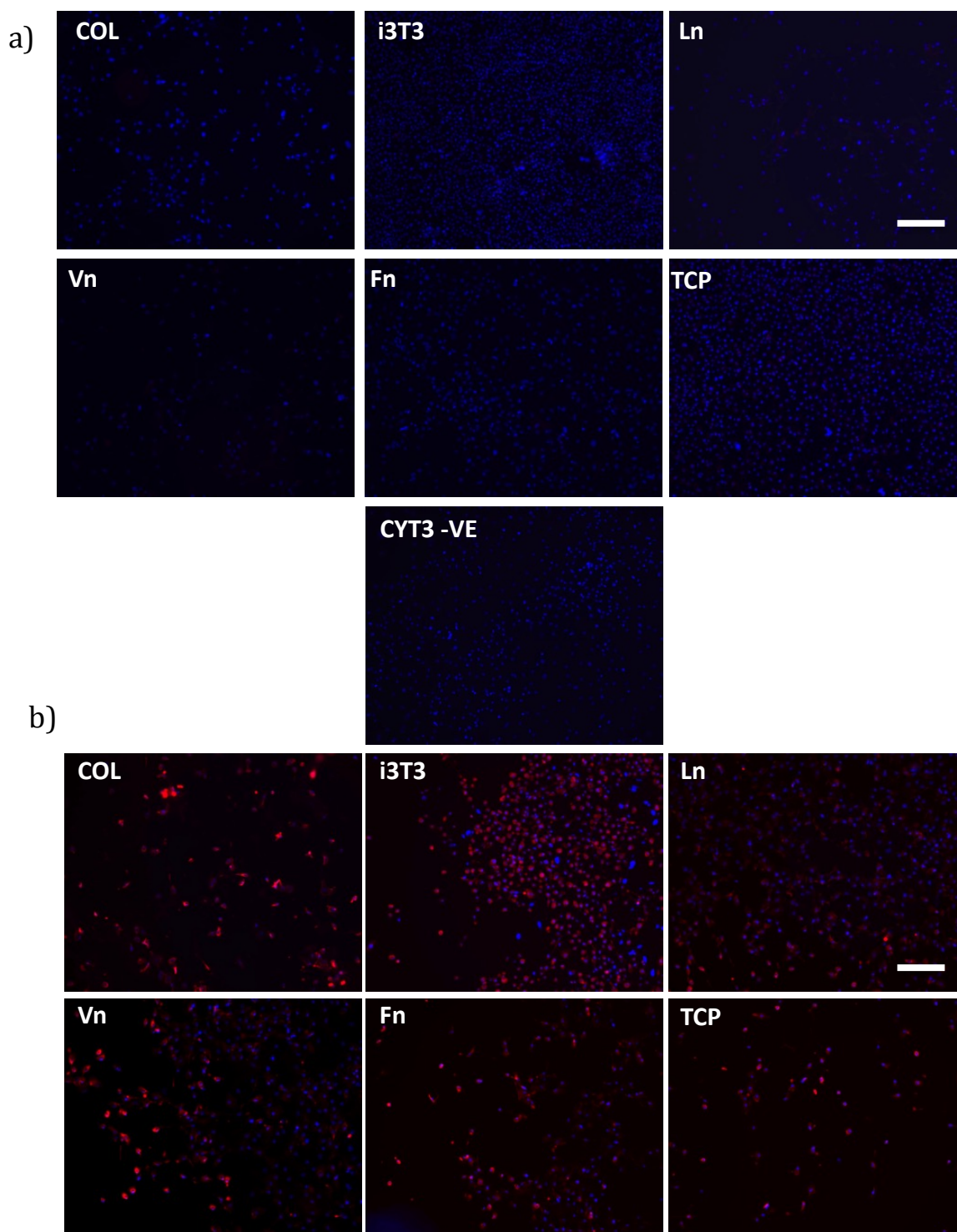
FIGURE 4.3**:** *Immunohistochemistry of rabbit limbal epithelial cells a) and rabbit central corneal cells b) after culture on collagen (col), irradiated 3T3 fibroblasts (i3T3), laminin (Ln), vitronectin (Vn), fibronectin (Fn) and TCP. Images show cytokeratin 3 (CYT3) staining (red) and nuclei staining (blue) Scale bar represents 200 μm.*

4.4.3   EFFECT OF CYT 3 EXPRESSION IN P0 AND P1 RLECS CULTURED ON TCP

Before assessing the response of rLECs on the selected hydrogels it is useful to determine the phenotype of rLECs after culture and passaging, cells were grown directly on TCP from freshly isolated limbal rims, after 4 days some cells were passaged and the remainder fixed and stained for cyt 3 and the same was done for p1 cells. Figure 4.4 shows p0 cells, as expected, did not stain positively for cyt 3 however after one passage rLECs quickly differentiated and stained positively for cyt 3.
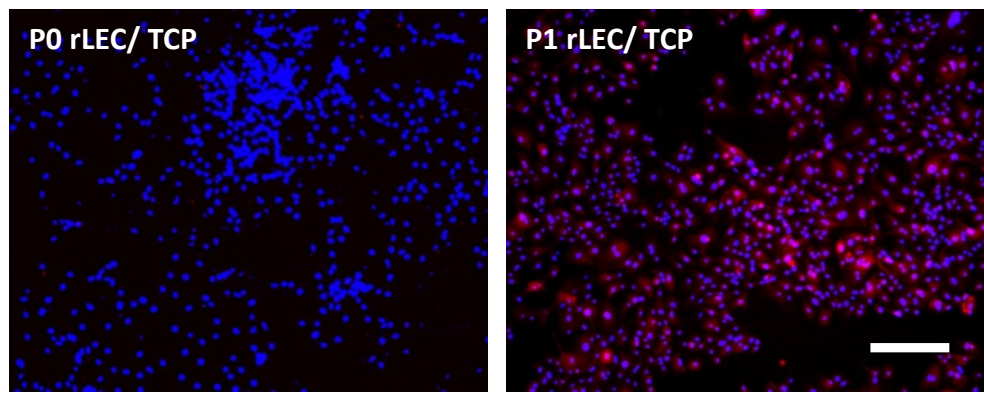
FIGURE 4.4: *Immunohistochemistry of rabbit limbal epithelial cells cultured on TCP at p0 and p1. Images show cytokeratin 3 (Cyt3) staining (red) and nuclei staining (blue) Scale bar represents 200 μm.*

4.4.4   VIABILITY OF RLECS ON BASE 0, 1 AND 2

Viability of rLECs on functionalised Base 0 gels decreases sharply after 48 hrs despite adhering and proliferating during this time. It was observed that although cells initially attached to the gels they were not adhered strongly and cells could have detached during the media change at day 2. Figure 4.5 a) shows that 1,4 DAB functionalised gels appeared to perform better than other functional groups. Nevertheless TCP out performs all gels with regards to cell adhesion and proliferation. Images of rLECs on Base 0 gels shows rounded and scattered cells on all but 1,4 DAB functionalised gels, these cells appeared well spread with visible lamellipodia (Figure 4.6 a)

131

Base 1 gels performed very differently: rLECs cultured on the TCP control attached well initially and for up to 48 h showed little increase in metabolic activity, but there was then a clear increase by 96 h. Hydrogel functionalisation with ammonia inhibited cell attachment, while increasing alkyl amine chain length improved cell adhesion and growth. In particular, gels functionalised with 1,4 DAB showed results comparable to cells cultured on TCP over 4 days. Cells attached poorly to 1,2 DAE functionalised gels and failed to proliferate. Functional groups 1,3 DAP and 1,6 DAH promoted cell proliferation after 96 h but to a lesser extent than 1,4 DAB (figure 4.5 b). Images of rLECs presented in figures 4.5 b, show how cells have adhered and grown on the Base 1 gels over 48 h. The morphology of the cells attached to 1,3 DAP, 1,4 DAB and 1,6 DAH had a normal appearance and showed a tendency to grow in colony-like clusters, typical of epithelial cells. This was not seen for cells cultured on 1,2 DAE gels, which appeared to be rounded and diffuse.

Cells cultured on Base 2 gels showed a similar trend to Base 1 gels in that increased alkyl amine chain length improved cell adhesion. The main difference was that Base 2 gels still did not outperform TCP over 4 days (figure 4.5 c). Images in figure 4.6 c) shows the most cell attachment on Base2/1,4 DAB and fewer cells attached to 1,3 DAP and 1,6 DAH functionalised gels. For all bases 1,4 DAB functionality appears to be the most successful moiety however the extent of its success clearly depends on the bulk hydrogel properties, with Base 1 yielding optimal overall results.
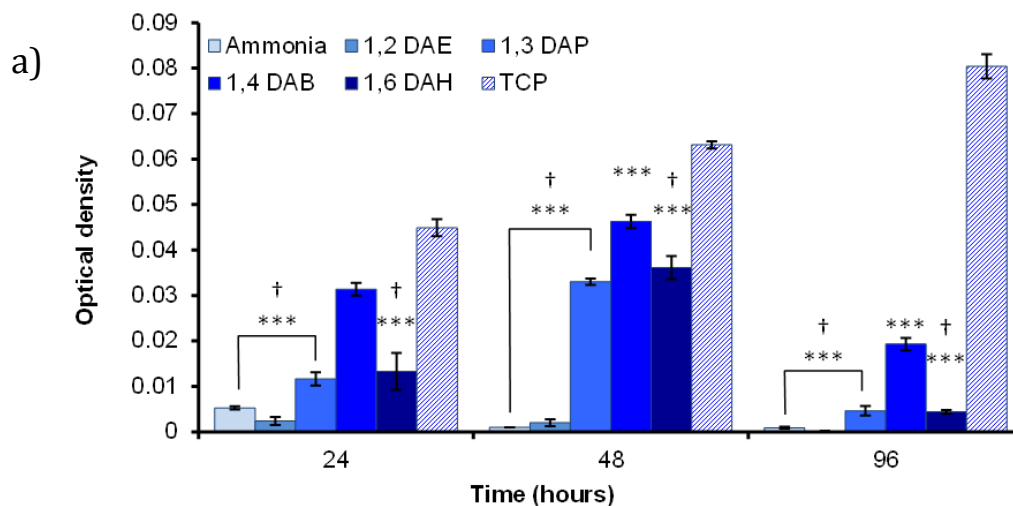
FIGURE 4.5 a): *Metabolic activity of rLECs cultured on functionalised Base 0 (a) over 4 days. Results shown are means ±SEM of triplicate cultures. Significance is relative to the tissue culture plastic positive control. *p<0.05, **p<0.005, ***p<0.001 and †p<0.05 relative to gels functionalised with 1,4 DAB.*
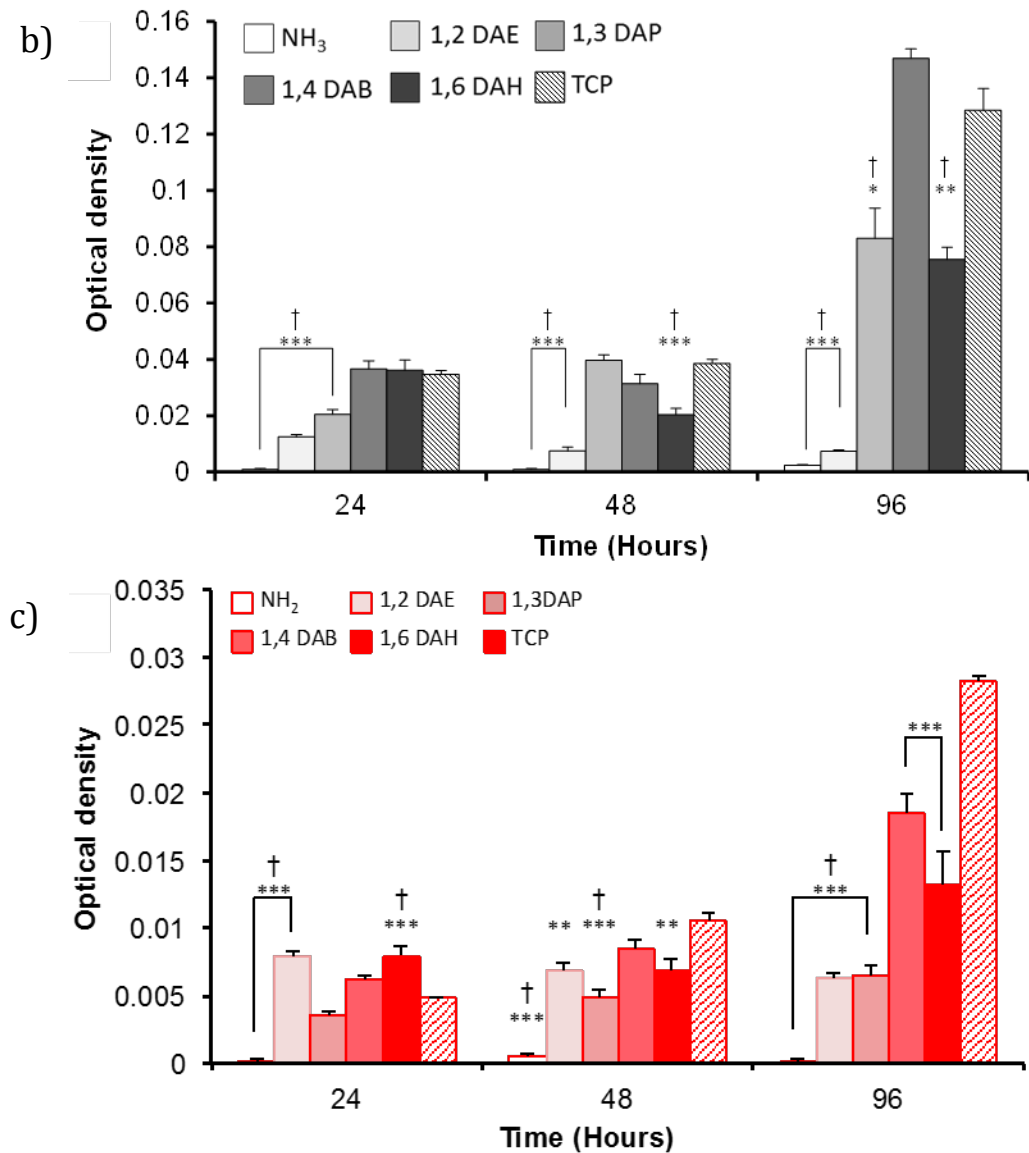
FIGURE 4.5 b) and c): *Metabolic activity of rLECs cultured on functionalised Base 1 (b) and on functionalised Base 2 (c) over 4 days. Results shown are means ±SEM of triplicate cultures. Significance is relative to the tissue culture plastic positive control. *p<0.05, **p<0.005, ***p<0.001 and †p<0.05 relative to gels functionalised with 1,4 DAB (Hassan et al., 2014)*
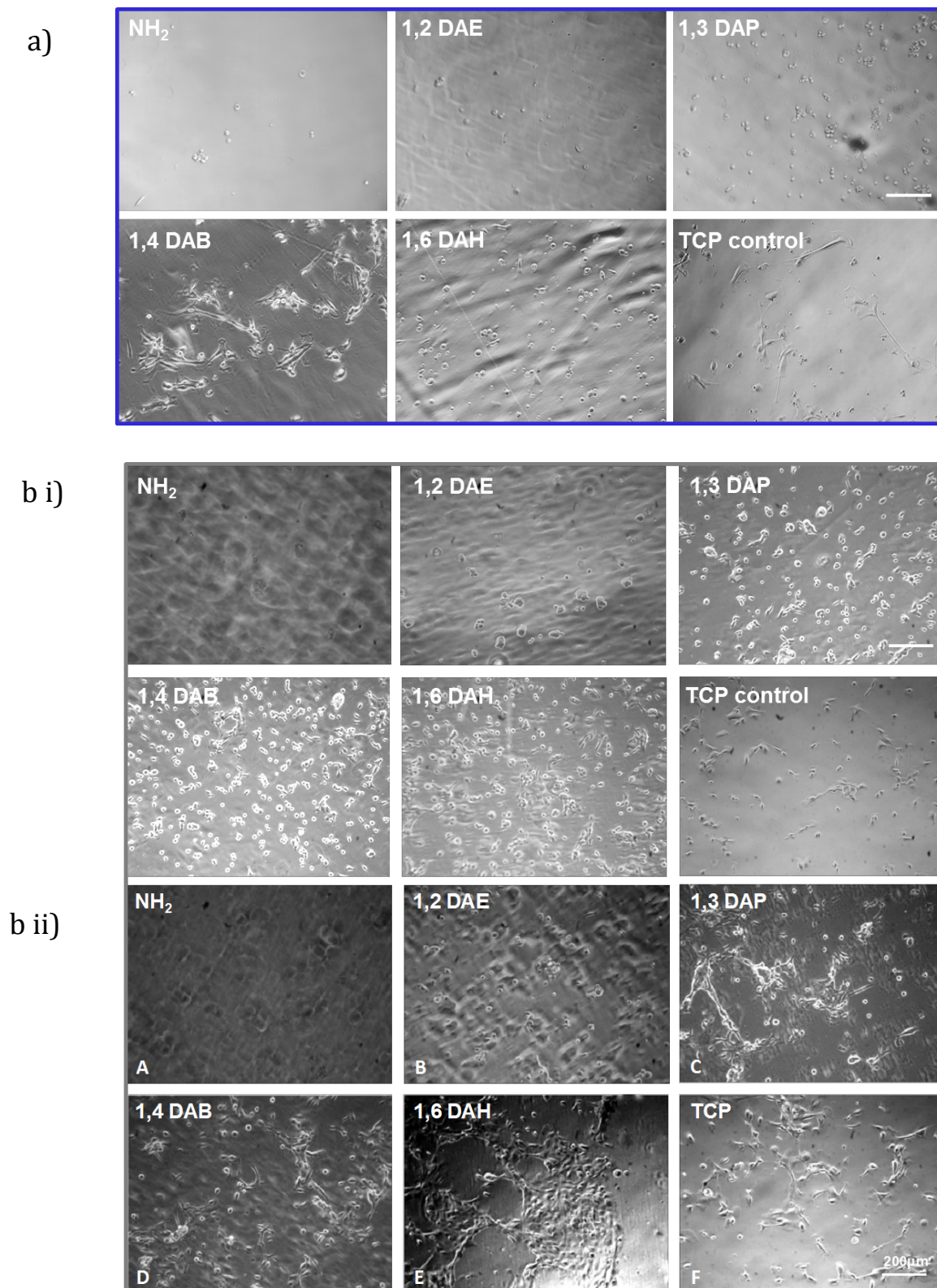
FIGURE 4.6: *Light microscopy images of rLECs on functionalised Base 0 after 48 hrs a), rLECs on functionalised Base 1 after 24 hrs b i) and after 48 hrs b ii) Scale bar represents 200 μm.*
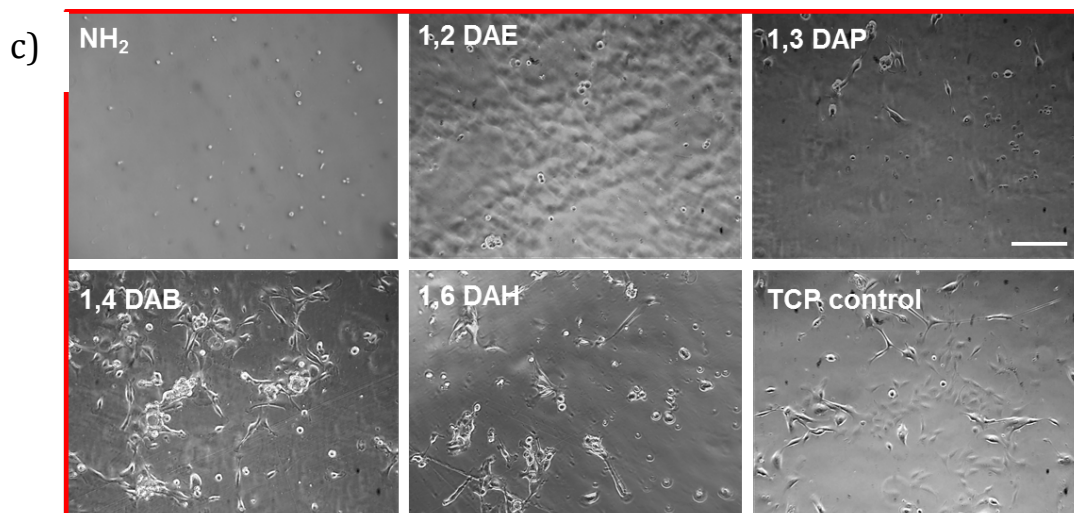
FIGURE 4.6 c): *Light microscopy images of rLECs on functionalised Base 2 after 48 hrs c) Scale bar represents 200 μm.*

4.4.5 CELL PREFERENCE

To confirm the preference of rLECs for Base1/1,4 DAB gels over TCP, and the extent of this preference, cells were randomly seeded in wells containing either Base1/1,4 DAB or Base1/1,3 DAP. Cell proliferation on the gels and TCP were measured with the MTT assay after 4 days in culture. Figure 4.7 and 4.8 show that rLECs will adhere preferentially to Base1/1,4 DAB gels, (by 20% ± 5%) rather than TCP. The reverse is true for Base1/1,3 DAP gels; rLECs would adhere preferentially to TCP by up to 36%. This indicates that rLEC affinity is greatest with Base1/1,4 DAB >TCP > Base1/1,3 DAP.
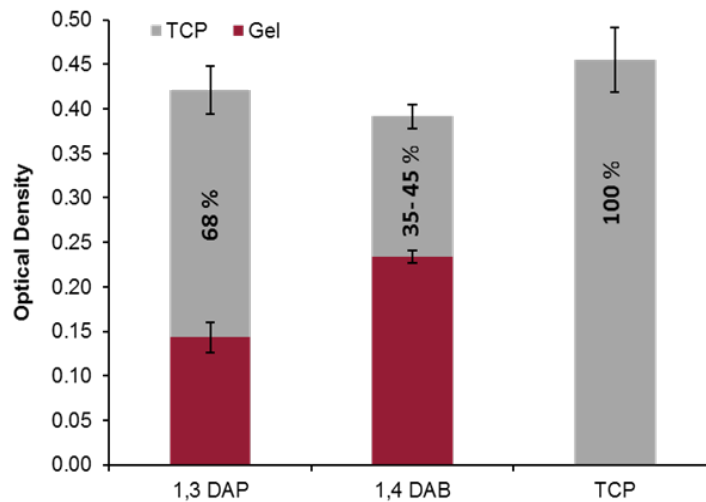
FIGURE 4.7: *The proportion of viable rLECs on Base 1/1,3 DAP or Base 1/1,4 DAB vs TCP, determined by an MTT assay.*
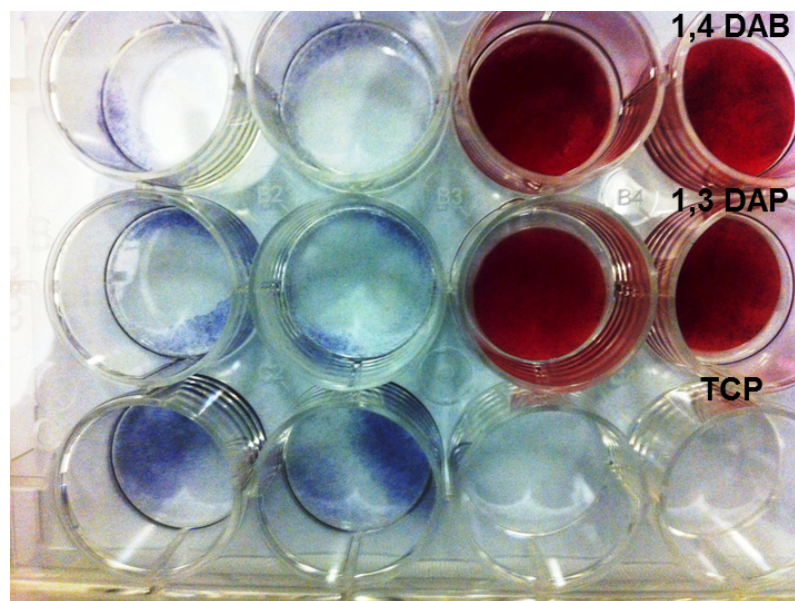
FIGURE 4.8: *Photographs of purple formazan from an MTT assay carried out on TCP and 1,3 DAP and 1,4 DAB functionalised Base 1 gels.*

4.4.6 LIMBAL EPITHELIAL CELL VIABILITY ON INCREASED GME GELS.

So far 1,4 DAB functionalised Base 1 gels possess optimal characteristics for rLEC adhesion and proliferation with 1,3 DAP and 1,6 DAH functionality also showing promise. The question that is now asked is, can increasing surface amine concentration improve adhesion and proliferation, and if so is there a

balance between adhesion and proliferation? The interaction of rLECs with these modified materials may enable further optimisation of these hydrogels for use as a corneal inlay. Gels with increased GME content were made and functionalised according to 2.3.4 and functionalised with 1,3 DAP or 1,4 DAB. Figure 4.9 a) shows that increasing 1,3 DAP content increases initial rLEC adhesion however they appear to fail to proliferate over 4 days in culture, table 4.4 shows larger average decreases in cell viability with decreasing concentrations of 1,3 DAP. A similar trend is seen with 1,4 DAB functionalised gels (figure 4.9 b) however Base 1.30 is the only material that supports proliferation, all other gels support greater cell adhesion in the first 24 hrs, Then cell viability appears to drop and remain the same over 4 days. Images in figure 4.10 show how many cells have remained adhered to 1,4 DAB functionalised gels after 4 days. It can be seen that the most cells are on base 1.20 however they exhibit mixed morphologies some are very small and rounded while some are spread with obvious lamellipodia.
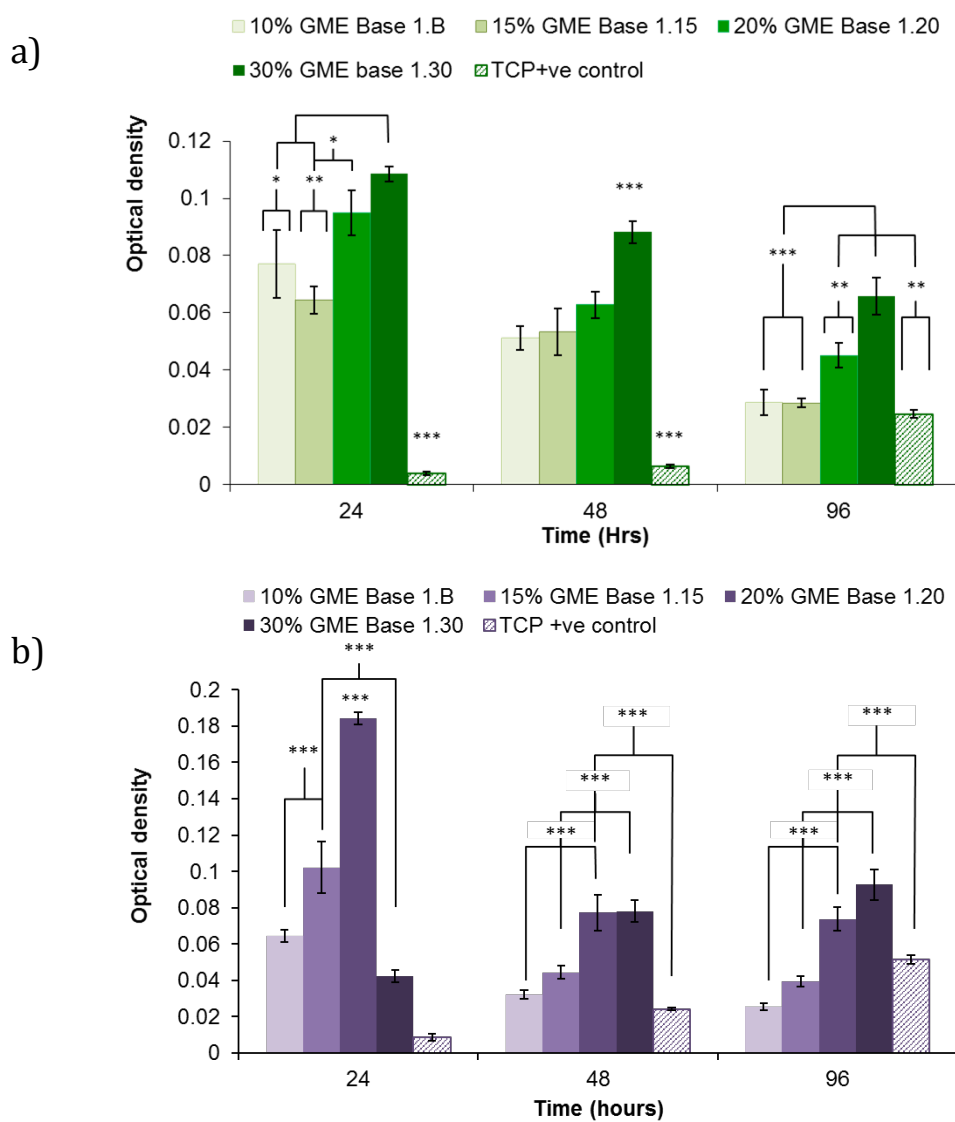
FIGURE 4.9: *Metabolic activity of rLECs cultured on 1,3 DAP (a) and on 1,4 DAB (b) functionalised Base 1.B, 1.15, 1.20 and 1.30 over 4 days. Results shown are means ±SEM of triplicate cultures. Significance is relative to each sample. *p<0.05, **p<0.005, ***p<0.001.*

TABLE 4.4: Average percentage change in viability of rLECs cultured on hydrogels containing increasing concentrations of 1,3 DAP

Hydrogel	Day 1 to Day 3
TCP +ve control	+517%
30% GME base 1.30	-39%
20% GME base 1.20	-52%
15% GME base 1.15	-56%
10% GME base 1.B	-63%
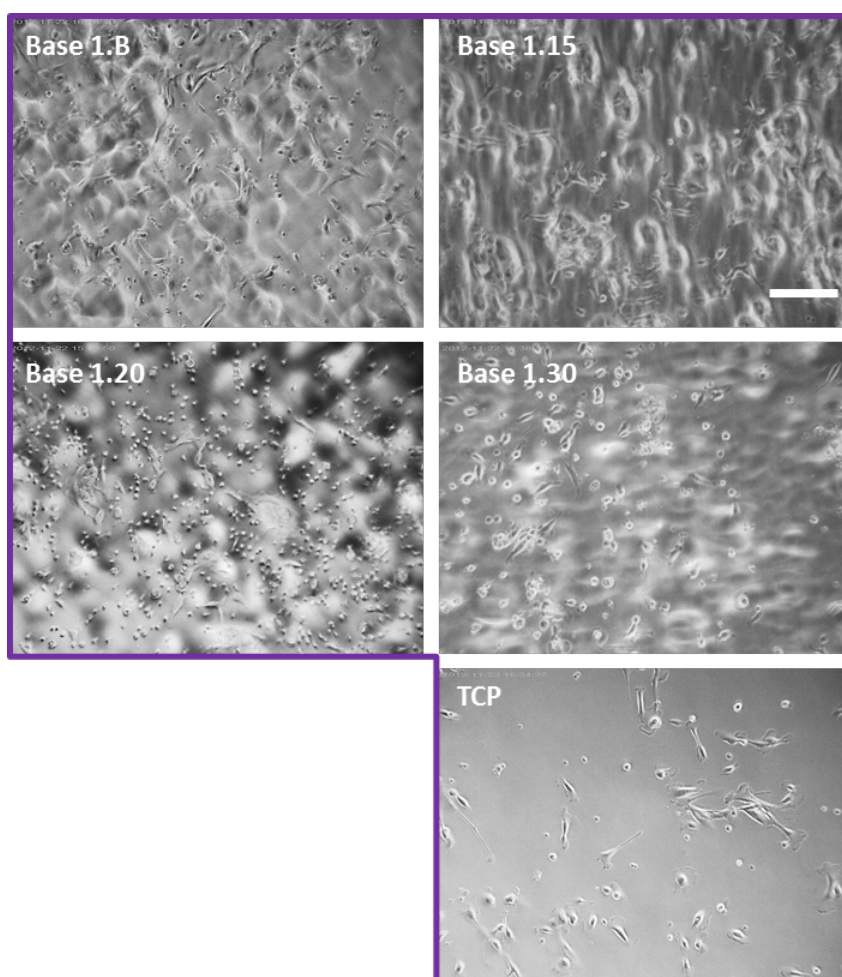
FIGURE 4.10: *Light microscopy images of rLECs on 1,4 DAB functionalised Base 1.B, 1.15, 1.20 and 1.30 after 4 days in culture. Scale bar represents 200 µm.*

4.4.7 CELL OUTGROWTH FROM TISSUE EXPLANTS ON HYDROGELS

Hydrogels that supported good rLEC adhesion and proliferation were selected and used to assess the gels' ability to support epithelial outgrowth from limbal explants. A summary of these explant experiments is given in table 4.5. From this and figure 4.11 it can be seen that Base 1 hydrogels were much more effective than Base 2 hydrogels in supporting cell outgrowth from explants, which reflected the MTT data from cultured cells on these materials. Epithelialisation of the gels from explants were examined with light microscopy after 6 days. Since minimal outgrowth was observed after 7 days on Base 2 gels, they were monitored for a further 7 days. (Figure 4.11)

TABLE 4.5: Summary of explant culture on Base 1 and Base 2 hydrogels functionalized with 1,3 DAP, 1,4 DAB and 1,6 DAH. (Hassan et al., 2014)

Gel formula	Summary of gel performance		Score
	limbal tissue explants	Direct seeding of rLECs	
BASE 1			
1,3 DAP	Good explant adherence but little or no outgrowth from explants	Good cell adhesion and proliferation	−/+
1,4 DAB	Excellent outgrowth and explant adherence	Excellent cell adhesion and proliferation	++/++
1,6 DAH	Little or no adherence some poor outgrowth	Good adhesion and proliferation	− −/+
BASE 2			
1,3 DAP	Good explant adherence, outgrowth ranged from none to good	Moderate adhesion but poor proliferation	+/−
1,4 DAB	Excellent explant adherence very poor to some outgrowth	Good adhesion and very good proliferation	+/+
1,6 DAH	Poor short lived explant adherence some outgrowth	Moderate adhesion and proliferation	−/+

The most favourable hydrogel recipe was Base 1/1,4 DAB, which enabled rapid cell outgrowth in just 6 days, with a large proportion of explants achieving outgrowth. Visually most cells appeared to have normal flattened epithelial cell morphology (figure 4.11) with some small dense clusters of cells close to the explant. In contrast, Base 2 hydrogels were poorer substrates for explant

culture as few explants adhered and any outgrowth was slow, scattered and in some cases cells did not appear to have epithelial cell morphology.
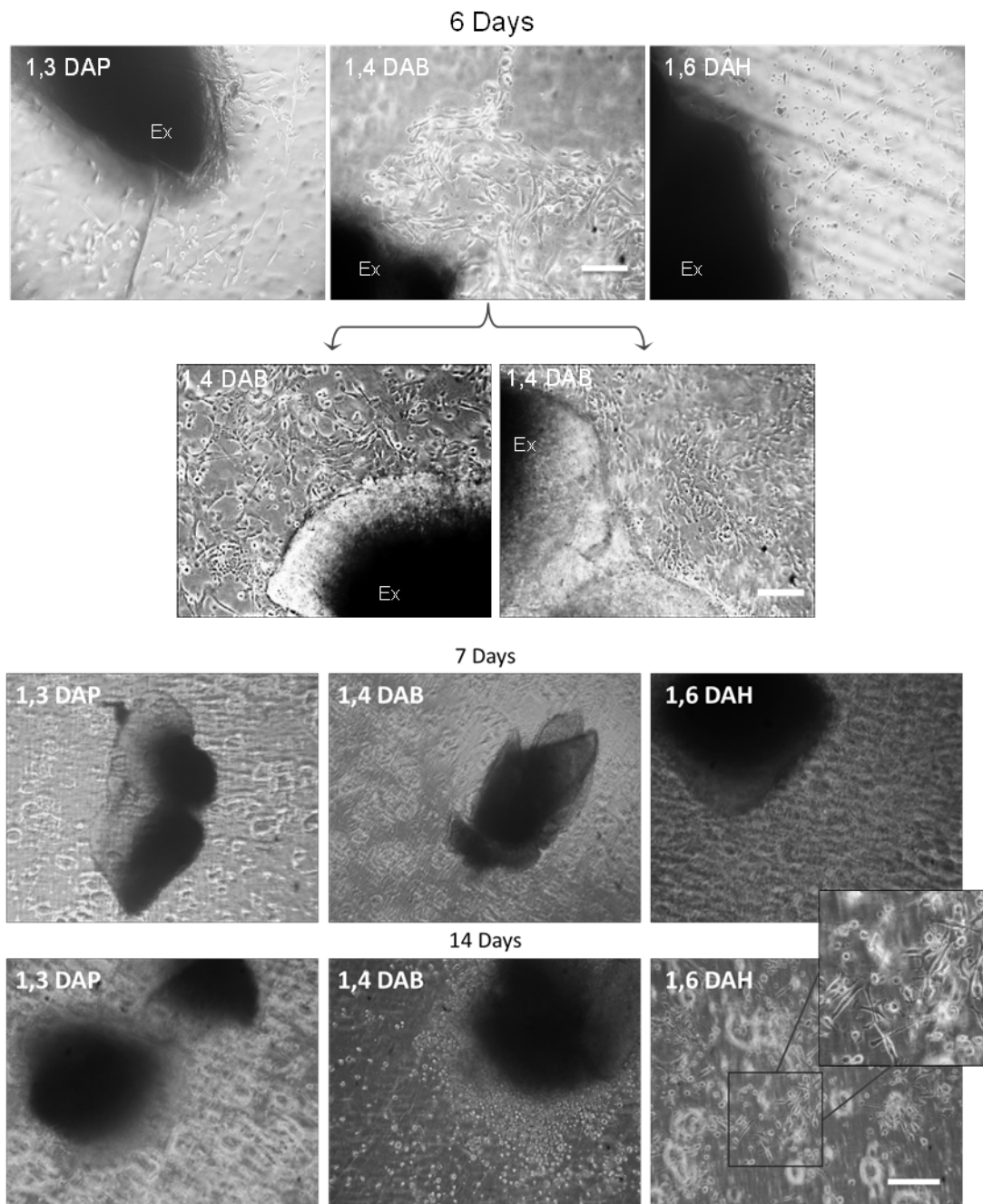
Figure 4.11: *Epithelial outgrowth from limbal explants imaged by light microscopy after 6 days on Base 1 functionalised with 1,3 DAP, 1,4 DAB and 1,6 DAH (a) and after 7 and 14 days on Base 2 functionalised with 1,3 DAP, 1,4 DAB and 1,6 DAH (b). Scale represents 200 μm.*

From the data in figure 4.12 explant adherence efficiency after 5 days on 1,4 DAB functionalised Base 1 and Base 2 were calculated as 84% and 77%, respectively. These gels also achieved the highest outgrowth efficiency in their corresponding groups. However, consistent, reliable results were only seen with Base 1/1,4 DAB. All other materials showed inconsistent and variable results with much less vigorous outgrowth.
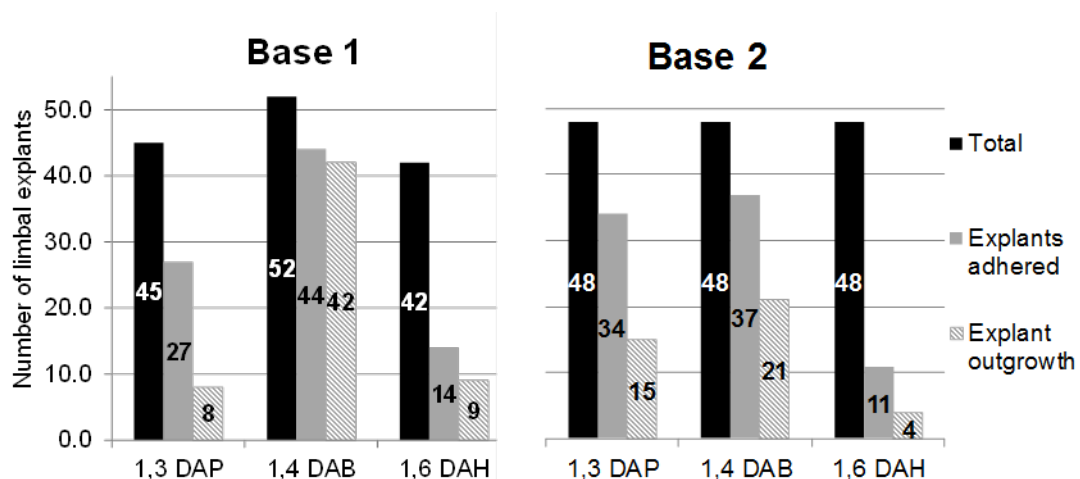
FIGURE 4.12: *The total number of explants across three cultures vs. the number of explants that adhered onto the gels and those that achieved outgrowth after 5 days on Base 1 and Base 2 functionalised with 1,3 DAP, 1,4 DAB and 1,6 DAH.*

4.4.8 CHARACTERISATION OF EXPLANT OUTGROWTH

The cells that migrated and proliferated from explants on Base 1/1,4 DAB were then characterised by staining for the differentiation epithelial maker cytokeratin 3 and the putative stem cell marker p63. Substantial cytokeratin 3-positive staining was observed in all explant outgrowths. The majority of cells were cytokeratin positive with the exception of a narrow band of cells located close to the periphery of the explant. On the contrary, with respect to p63-stained cells, these were comparatively few in number and p63-positive cells were only seen at the edge of the explants (Figure 4.13) (Hassan et al., 2014).
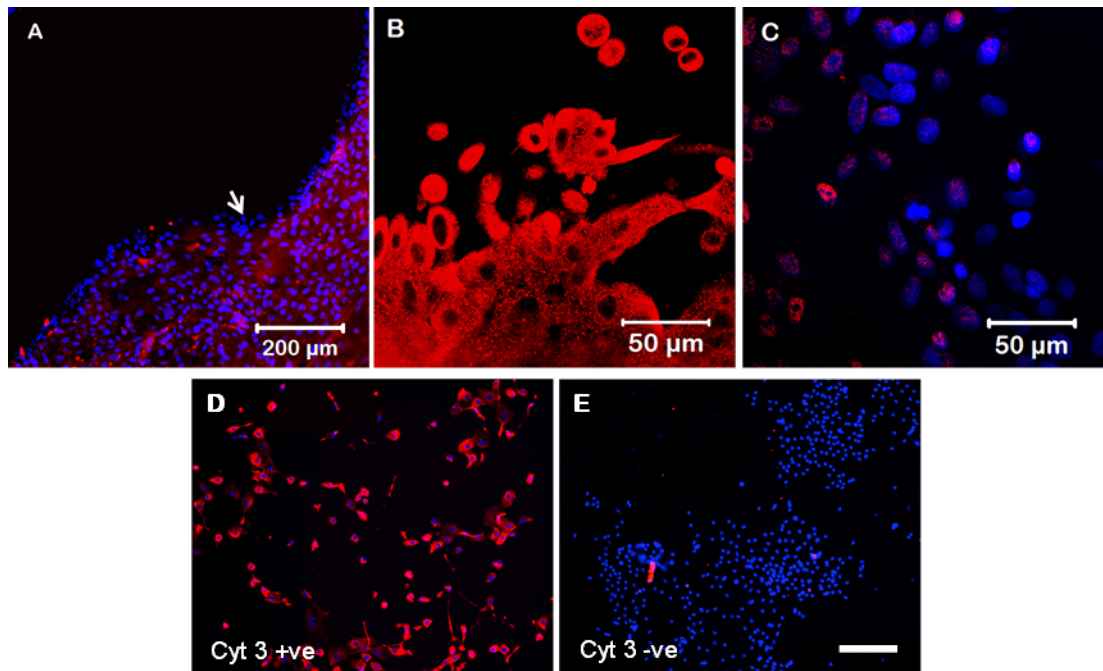
FIGURE 4.13: *Immunohistochemistry of explant outgrowths on the Base 1/1,4 DAB gels. (A,B) Cells stained for cytokeratin 3 (red) at ×10 magnification (A) and at ×40 magnification (B). (C) Cells stained for P63 (red). Cells in (A) and (C) were counterstained with DAPI (blue). (D,E) show positive controls for cytokeratin 3 by staining terminally differentiated rabbit corneal cells cultured on TCP for 6 days (D). Negative cytokeratin 3 control is shown in (E) by staining freshly isolated undifferentiated rLECs cultured for only 48 h. Both controls are counterstained with DAPI. Scale represents 200 μm.*

4.4.9   CO-CULTURE RLECS AND RLFS

A full set of functionalised Base 1 hydrogels were assessed for selective support of epithelial adhesion and proliferation. An equal number of rLECs and rLFs was seeded at day 0 and imaged at days 1, 3 and 6 (figure 4.14). Over the 6 days the poorer substrates with shorter alkyl amine groups stopped supporting cells. Initial adhesion of rLFs and rLECs were seen on all materials at day 1. Over time the rLECS on 1,4 DAB and 1,6 DAH functional gels remained adhered and proliferated gradually, while rLFs detached. In the TCP control rLFs quickly outgrew the rLECS after 6 days (Figure 4.14).
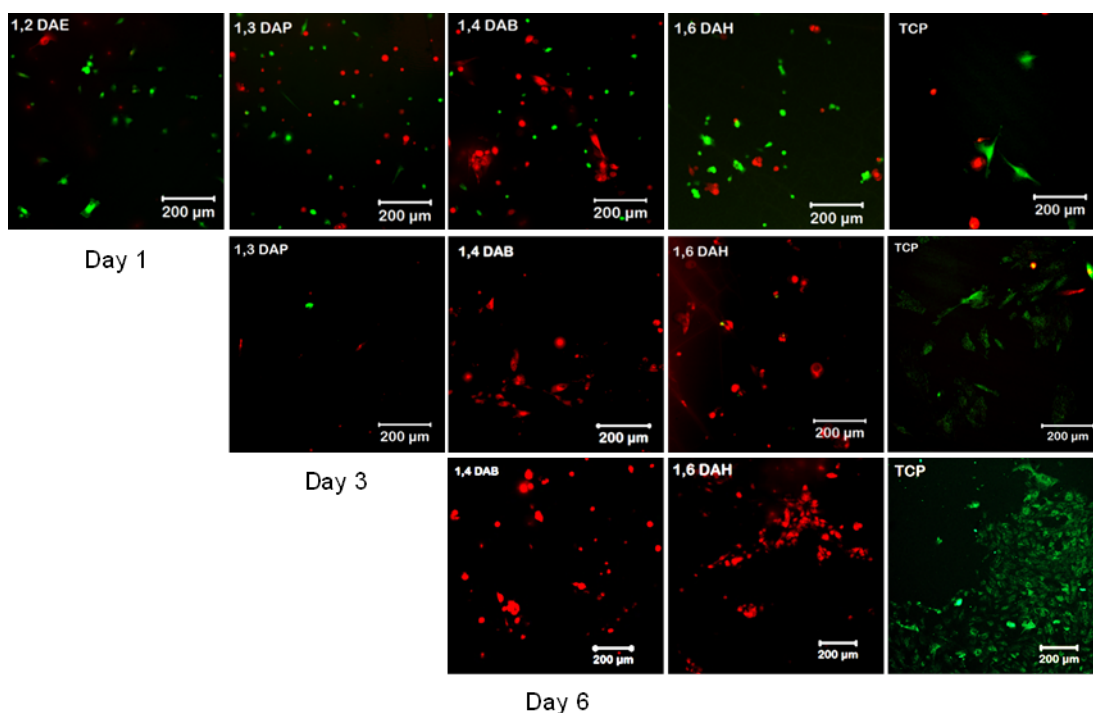
FIGURE 4.14: *Co-culture of cell tracker labelled rLECs (red) and rLFs (green) on amine-functionalised Base 1 hydrogels. Gels and TCP were seeded with 5 × 10³ of each cell type at day 0. Confocal microscopy was used to image cells after culture for 1, 3 and 6 days.*

4.4.10 PHENOL FREE rLEC CULTURE ON BASE 1

Base 1 gels functionalised with 1,3 DAP, 1,4 DAB and 1,6 DAH were used to culture rLECs in the absence of phenol red, this experiment was carried out to assess the effects (if any) of phenol red on the performance of the gels after it was observed that more phenol red from the media was absorbed (or even bound) by gels with longer chain alkyl amines. Figures 4.18-4.19 shows the phenol red absorption with increasing alkyl amine chain length. Overall there is no difference in rLECs culture with or without phenol red on TCP and on 1,3 DAP functionalised gels however over 4 days there is a small but significant difference in metabolic activity for phenol free cultures on 1,4 DAB and 1,6 DAH Base1 gels. These cultures appear to show a marginally lower initial cell adhesion and proliferation of rLECs (figure 4.16). The phenol free cultures do not have an effect on the overall relationship between alkyl amine functionality and cell behaviour and images in figure 4.16 and 4.17 confirm that 1,4 DAB will

still outperform the other functional groups in the same way as in normal cultures.
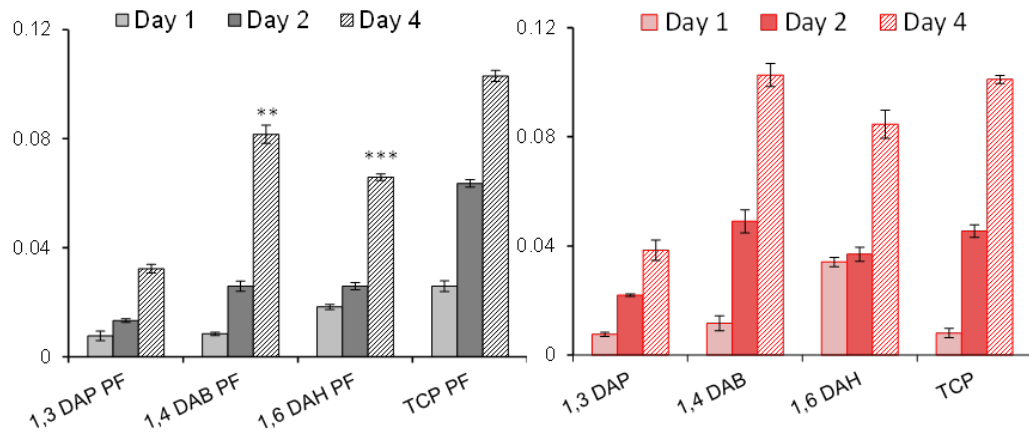
FIGURE 4.15: *Metabolic activity of rLECs cultured on 1,3 DAP, 1,4 DAB and 1,6 DAH functionalised Base 1 with (red) and without phenol red (grey) over 4 days. Results shown are means ±SEM of triplicate cultures. Significance relates to comparison of the same gels in normal and phenol free (PF) culture. *p<0.05, **p<0.005, ***p<0.001.*
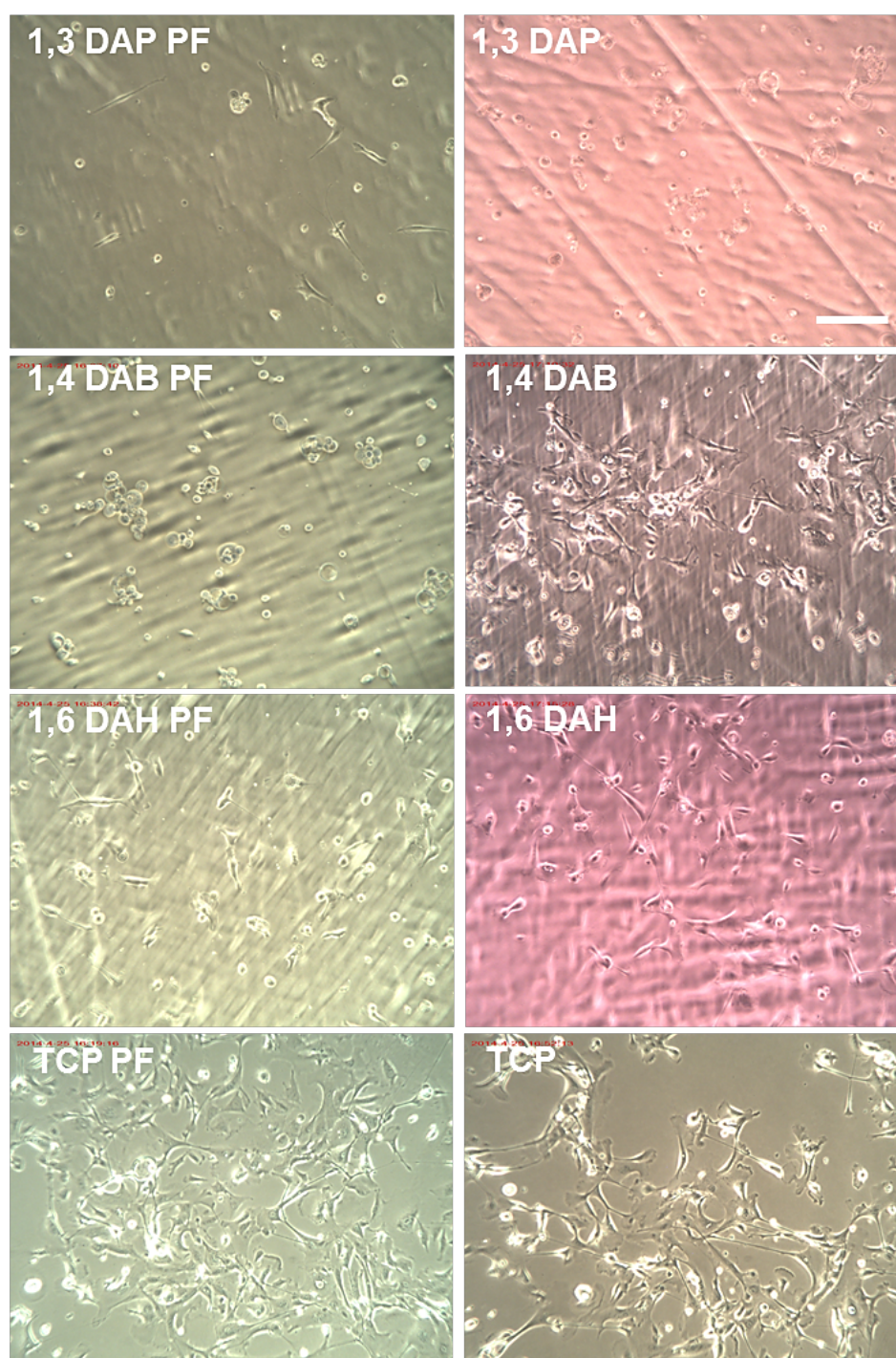
FIGURE 4.16: *Light microscopy images of of rLECs cultured for 24 hrs on 1,3 DAP, 1,4 DAB and 1,6 DAH functionalised Base 1 with (right column) and without phenol red (left column (PF)) Scale represents 200 μm.*
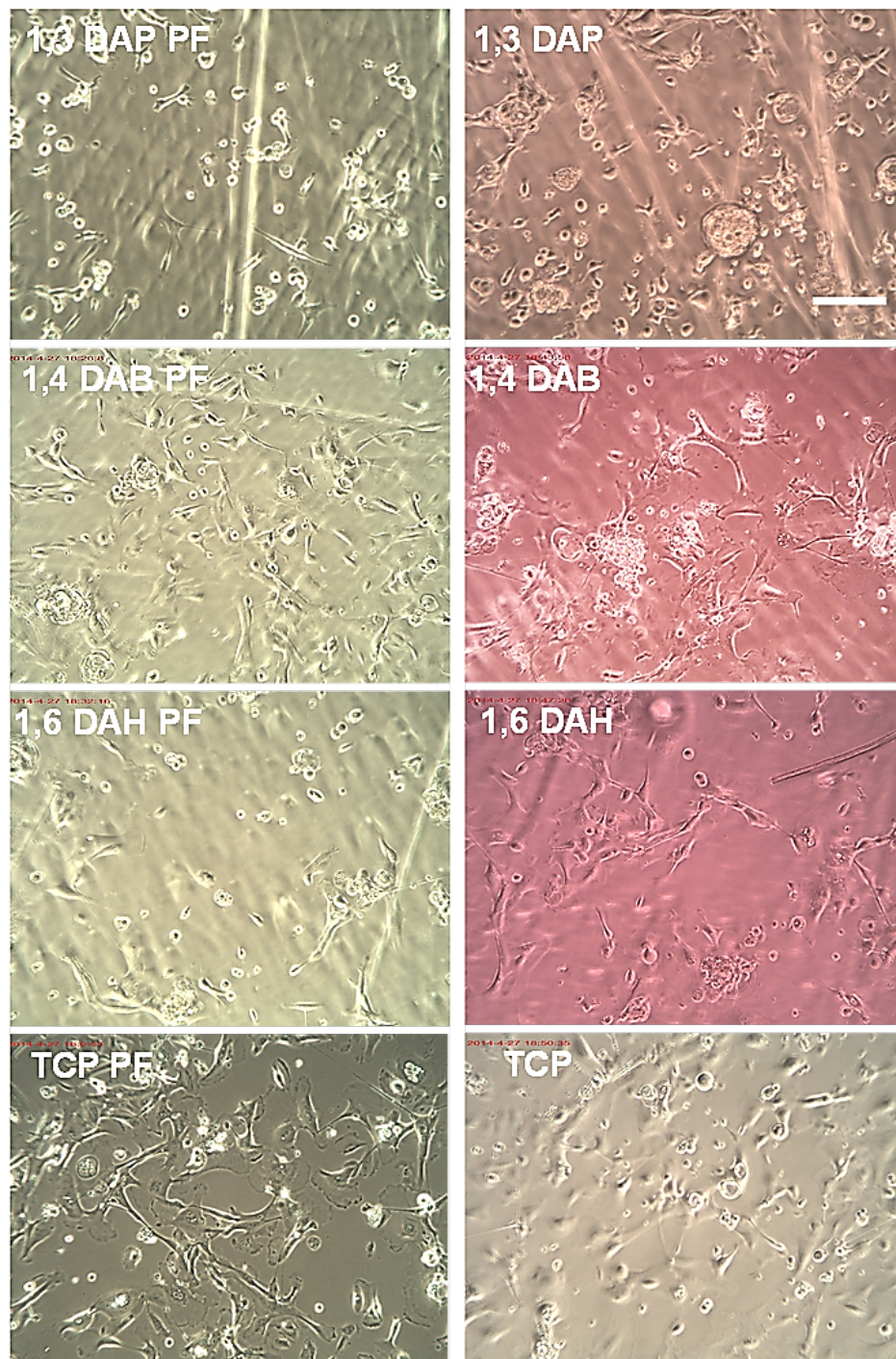
FIGURE 4.17: *Light microscopy images of of rLECs cultured for 96 hrs on 1,3 DAP, 1,4 DAB and 1,6 DAH functionalised Base 1 with (right column) and without phenol red (left column (PF)) Scale represents 200 µm.*
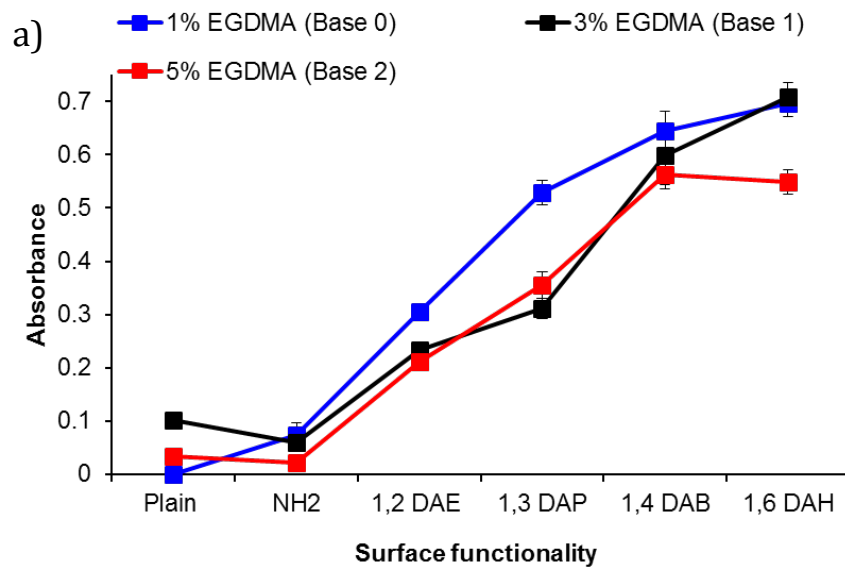
FIGURE 4.18: *Phenol red absorbance readings from each gel after 24 hrs in RLE media containing phenol red showing increases in absorbance with carbon chain length.*

FIGURE 4.19: *Photographs of hydrogel discs immersed in media containing phenol red for 24 hrs then washed in PBS (a) and the change in pH of media over 6 week saturation at 37°C (b).*

149

4.4.11 rLECs on fibronectin coated gels

It has been determined during this thesis that hydrogels with moderate swelling and modification with alkyl amines 1,3 DAP, 1,4 DAB and 1,6 DAH can support rLEC growth and attachment to varying degrees. Base1/1,4 DAB gels gave favourable results comparative to TCP. From chapter 3 it was evident that the same gels were not capable of supporting stromal cells even when coated or bound to fibronectin. In order to gain insights into the mechanism for this selection a final experiment that could indicate protein adsorption is not involved was carried out. RLECs were cultured on Fn coated or bound Base 1 gels functionalised with 1,3 DAP and 1,6 DAH, in the same manner as described in chapter 3, to see if Fn could enhance their performance to the level of TCP.

From figure 4.20 it can be seen that neither binding nor adsorbing Fn to aminated gels significantly improved their performance over 5 days. Plain hydrogels were enhanced by Fn but only marginally and not sufficiently to be considered for use as a biomaterial for corneal regeneration.
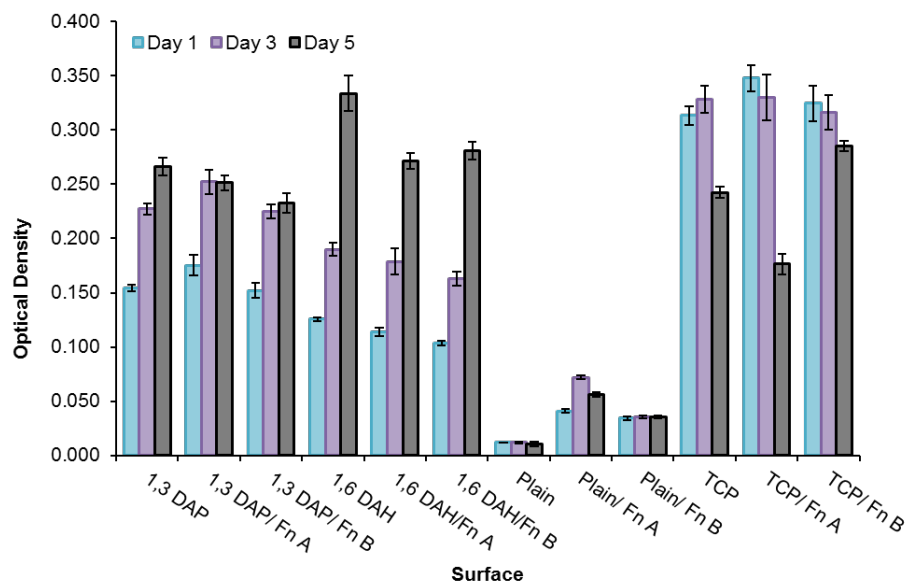
FIGURE 4.20: *Metabolic activity using Alamar Blue assay of rLECs cultured for 5 days on Plain, 1,3 DAP and 1,6 DAH functionalised Base 1, without Fn and with Fn coated and bound with TGase. Results shown are means ±SEM of triplicate cultures.*

150

4.5 DISCUSSION

Previous studies, along with results from this chapter, have indicated a relationship between the alkyl amine carbon chain length and cell adhesion and proliferation. However earlier work had failed to provide adequate epithelialisation without either further protein modification (Evans et al., 2000) or using co-culture of epithelial cells with fibroblasts (Rimmer et al., 2007; Sun et al., 2007). This chapter validates suggestions from previous studies that longer-chain amines were seen as more conducive to cell growth. However, results in this chapter goes beyond this and demonstrates how 1,4 DAB consistently provided a good surface for epithelialisation with the bulk formulation Base 1, but not as much as with Base 0 or Base 2. Interestingly, co-culture with fibroblasts reveals selectivity for rLECs. This phenomenon has also been seen from studies that have utilised soluble putrescine, also known as 1,4 DAB, at concentrations of 10 mM to stimulate human bronchial epithelial cells while totally inhibiting the growth of fibroblasts from bronchial explants (Stoner et al., 1980). Similar selectivity for epithelial cells has also been demonstrated by Jensen et al. also using soluble 1,4 DAB and another polyamine spermine to inhibit fibroblasts in human skin epithelial cultures (Jensen and Therkelsen, 1982). The results in this chapter show similar patterns using covalently bound rather than solubilised 1,4 DAB, which may suggest that polyamines involved in the complex signalling pathways controlling epithelial growth could also be functioning on the cell surface.

One hypothesis for the particular effectiveness of 1,4 DAB as a functional group for promoting epithelialisation, could be related to its structural similarity to the amino acid lysine which is involved in protein crosslinking with glutamine residues. This occurs when transglutaminase forms ϵ-(γ glutamyl) lysine cross-links, but may also include the cross-linking of other polyamines to appropriate proteins (Greenberg et al., 1991). Transglutaminases have been associated with wound healing, coagulation and apoptosis (Greenberg et al., 1991; Inada et al., 2000). Zhang et al. proposed that tissue transglutaminase and extracellular matrix proteins are expressed simultaneously during corneal

wound healing and are possibly involved in maintaining homeostasis of the cornea (Zhang et al., 2004). These studies could provide clues into the mechanism by which the rLECs adhere and proliferate on the higher chain length amines.

By comparing Base1/1,4 DAB with the various ECM proteins, TCP and the i3T3 gold standard for LESC culture, it can be seen that this material appears to promote rapid differentiation seen from the extensive cyt 3 positive staining from explant outgrowths achieved on this gel. This may not be an issue if this material will be used in combination with explant culture as LESCs may be preserved within the explant tissue. However these results suggest that this material may not be ideal for use with ex vivo expanded LESCs as it will not maintain LESC phenotype as well as other substrates such as amniotic membrane (Grueterich et al., 2003, 2002)or even the proteins assessed in figures 4.2 and 4.3.

Interestingly, increasing the concentration of 1,4 DAB on gels appears to increase initial adhesion but not necessarily proliferation. Gels with increased 1,3 DAP concentration saw a similar pattern. Past studies have related high substrate adhesiveness to low motility (Gail and Boone, 1972). Even though it is also acknowledged that low substrate adhesiveness has the same effect due to reduced concentration of ligands and integrins which in turn decreases traction points required for motility (Holly et al., 2000). Many studies suggest cell migration and proliferation are related however there is little evidence suggesting that increased cell-substrate adhesion will effect proliferation in this way.

 It is also worth noting that the addition of proteins to the aminated hydrogels did not significantly alter the performance of the materials in this case which may confirm that these gels are inherently resistant to protein adsorption and may be functioning by specific interactions between alkyl amine groups and epithelial cells.

The culture of rLECs on effective Base 1 gels without out phenol red may have provided new information on how these materials can be exploited for corneal regeneration, since it is possible that these gels bind or interact with phenol red in ways that correspond to alkyl chain length. Phenol red has been shown to be a weak estrogen mimic, which may stimulate proliferation of estrogen responsive cells (Berthois et al., 1986), and some work has suggested that estrogen responsive cells exist in the cornea (Suzuki et al., 2001; Tachibana et al., 2000). Whether or not estrogen responsiveness exists in rLECs and not rLFs is yet to be determined. Nevertheless, it is evident that the majority of the success of Base1/1,4 DAB comes from the 1,4 DAB moiety itself, perhaps altering the bulk composition can improve the effectiveness of the other amines but this thesis has not shown any combination of materials comparable to it. The potential for this material to quickly aid epithelialisation from limbal explants means a barrier to infection can be established faster than on conventional keretoprosthetics. The fact that protein is not required will enhance the selectivity and reduce effects of inflammation, or calcification (Vijayasekaran et al., 2000) that can be caused by utilizing fibronectin (Sandeman et al., 2003) (Jester et al., 1999) or by promoting non-specific protein adsorption.

CHAPTER 5

FINAL DISCUSSION

CHAPTER 5: FINAL DISCUSSION

The aim of this thesis was to produce a set of hydrogels with amine functionality and investigate the potential use of these aminated hydrogels for use as a corneal inlay/onlay device in the treatment of limbal stem cell deficiency. The method employed was to change monomer compositions to create different bulk material properties such as rigidity, swelling and functionality. Bulk hydrogels were functionalised with four alkyl amines of increasing carbon chain length to enhance cell adhesion and proliferation.

Similar polymethacrylate networks have been used for cell culture and biocompatibility studies, (Rimmer et al., 2009) however these systems required further modification with peptides or fibrinogen (Johnson et al., 2010) and for corneal epithelialisation in particular, either co-culture (Rimmer et al., 2007) or further modification with ECM proteins such as collagen and laminin (Ma et al., 2011). These studies reveal little information on the mechanism by which chemical modification with amines directly impacts rLEC adhesion and proliferation. In addition, once the bulk monomer recipe changes the new material must be revalidated as these changes can effect important parameters such as water content, wettability, storage modulus and even transparency. The initial approach was to develop hydrogels with these desirable features and then reassess them for their capacity to support stromal cells; firstly because they grow easily and quickly, and secondly because these cells are traditionally used to support healthy epithelial cultures. That being said, efforts have been made to develop feeder free systems or those that do not rely on co-culture with stromal cells. Accordingly new hydrogel materials were assessed with rLFs in order to determine how the substrates may function. Will they function with or without stromal cell interactions? And if not can they then support epithelialisation adequately without them.

From this thesis it was determined that aminated hydrogels, specifically those with longer alkyl chain length can support the adhesion and proliferation of rLECs while inhibiting the proliferation of rLFs. It was found that bulk and surface properties both contribute to this effect, where it was found Base 1 with

moderate swelling and storage modulus combined with 1,4 DAB functionality gave the best results.

Moreover the addition of fibronectin to hydrogels, either through adsorption or transglutaminase mediated coupling, did not improve or significantly change the performance of the gels for either cell type indicating that the gels are not conducive to protein adsorption. This low affinity for protein could be related to the poor proliferation of fibroblasts. Fibroblasts manufacture ECM proteins and remodel their environment. Results from chapter 3 showed that fibroblasts will initially adhere to the hydrogels (apart from those functionalised with ammonia) but proliferation will be inhibited once these fibroblasts attempt to lay down their own secreted proteins. The proteins fail to adhere and fibroblasts may detach as a result. This in turn impacts the co-culture results, and shows that overall cell adhesion and proliferation on these gels is not improved if cells are co-cultured on these gels.
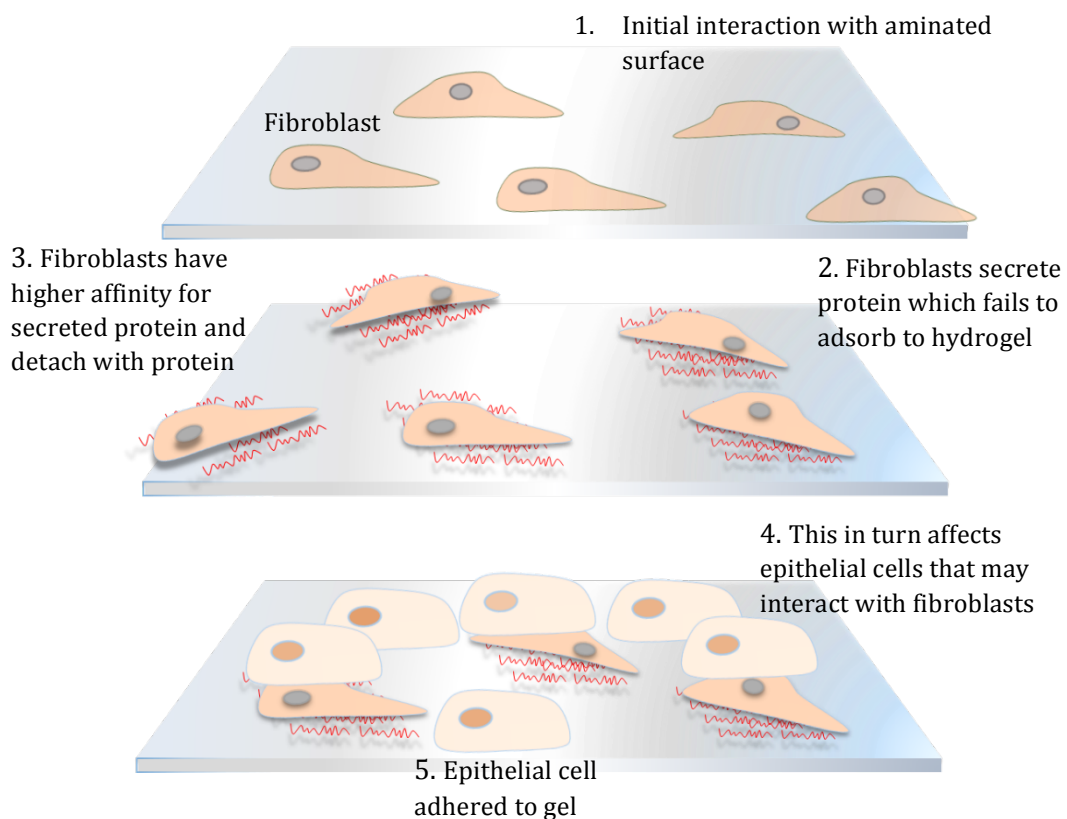
FIGURE 5.1 *Schematic explanation of why fibroblasts do not proliferate.*

During these studies it became apparent that the epithelial cells maybe interacting through specific interactions with the alkyl amines, however observations on the phenol red absorption (see figure 5.2) was also dependent on alkyl chain length as well as amine concentration indicating phenol red may be trapped inside the gels. Since phenol red is an estrogen mimic it was postulated that the mechanism of epithelial cell selectivity may be related to this however from chapter 4 figure 4.15, there appeared to be only a very small change in rLEC proliferation in the absence of phenol red which still suggests 1,4 DAB itself could be a key functional group in the development of a corneal onlay or inlay material. Nevertheless, phenol red may be acting synergistically to amplify the effect.
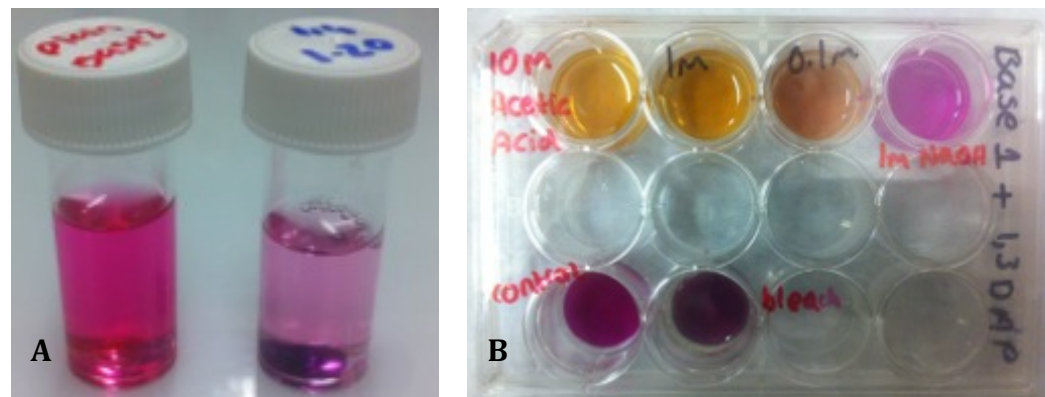
FIGURE 5.2: *Photographs of A) plain Base 2 (left) next to Base 1.20/1,4DAB (right) both soaked in media for 6 weeks, with an apparently higher concentration of phenol red absorbed within the gel, which also turns the solution more alkaline over time. B) Shows Base1/1,3 DAP after immersion in media then immersion in acetic acid 10 M, 1M and 01 M, NaOH, and bleach, phenol red appears to remain in the gel and stays sensitive to pH.*

It is also important to take into account that the proliferative capacity of rLECs on Base1/1,4 DAB comes at a price. The limbal stem cell phenotype is not preserved on these gels and during explant culture showed very rapid outgrowth from the explants with extensive differentiation. If the LESC population within the explants remained present and able to regenerate, the

differentiated outgrowth may not be an issue and in fact positive, as rapid epithelialisation over an inlay device will protect the ocular surface from infection and water loss. No studies were carried out on the explants after sufficient outgrowth was achieved and this maybe a consideration for future work. Nevertheless, a small border of undifferentiated cells at the periphery of the explants was observed. This suggests that despite the high proliferative capacity the regeneration potential from these cells still exists within the explants.

CHAPTER 6

LIMITATIONS AND

FUTURE WORK

CHAPTER 6: LIMITATIONS AND FUTURE WORK

During this thesis, parallel studies from other research projects have worked towards engineering scaffolds to mimic stem cell environments or create artificial stem cell niches within the scaffold. This is so that stem cells with regeneration capacity can survive and continue to renew tissue as they do in vivo. With respect to corneal tissue engineering, issues relating to scaffolds maintaining a stable epithelium have prompted attempts to fabricate specific architectures that can physically protect limbal epithelial stem cells (LESCs) from external stimuli that may trigger abnormal differentiation. Engineering these architectures into the hydrogels produced in this thesis could be an interesting project, however there are limitations. Currently this hydrogel synthesis uses 2-Hydroxy-2-methylpropiophenone (HMPP) as a photo initiator, and the entire radical polymerisation takes place in a sealed mould to prevent oxygen entering the system. This is because the molecular oxygen reacts with radicals generated by the photo initiator rather than the growing polymer chain, inhibiting the polymerisation process. This is important to note, as one method used to incorporate micro architectures is microsteriolithography, which is currently not an oxygen free system. This method cures the monomer solution layer by layer creating a 3D construct incorporating any micro architectures (see figure 6.1). In order to use this method for the polymethacrylate networks produced in this thesis the biocompatibility of any new photo initiator will need to be revalidated. So far no other photo initiators have been optimised for producing these gels. This would be a future pre-requisite should this method be employed for creating cellular microenvironments. A recommendation would be to employ an entirely different method. A laser etching technique was briefly investigated towards the end of this project after attempts at creating sealed systems for steriolithography failed. This method can etch features into dried hydrogels that are proportionally increased when swollen (figure 6.2). The benefit of this could be that small pockets can be incorporated at the periphery of the gels to confine the limbal explants and guide outgrowth

towards the centre. These architectures could also serve as a fixture for the explants so they remain adhered.
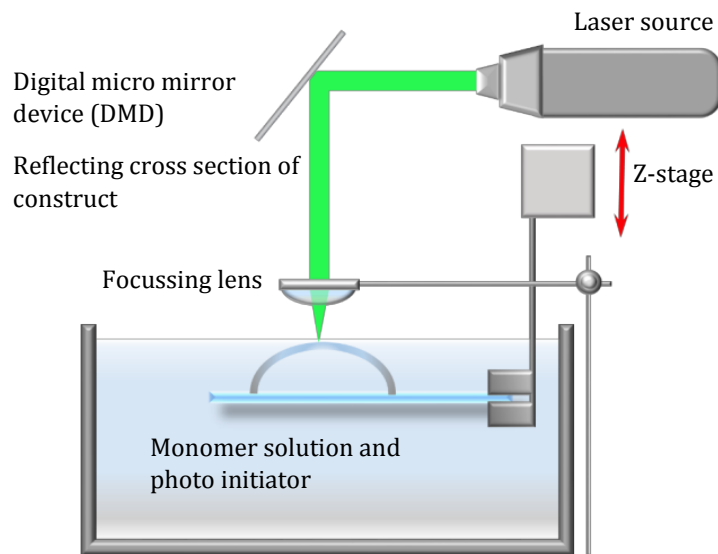
FIGURE 6.1: *Schematic representation of a typical micro steriolithography apparatus, a focused laser polymerises the solution onto a substrate layer by layer.*
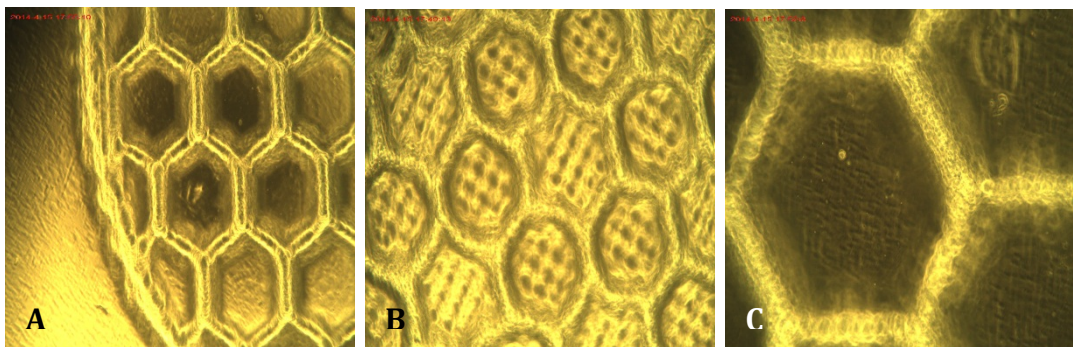
FIGURE 6.2: *light microscopy images at x4 (A and B) and x10 (C) magnification of honeycombed pockets etched into dried Base 1/1,2 DAE and re- swollen in PBS. Each hexagon is 600 µm wide.*

Other limitations for future work that should be considered relate to the GMMA monomer used, which is very expensive. It costs between £780- £1000 per Kg sourced from either BASF or G&K Biomedical Scientific Inc. Sourcing this monomer is also very difficult as most companies to not manufacture it in large quantities. And even during this project sourcing issues were experienced. To

reduce costs of any future work and combat sourcing problems it is recommended that GMMA is replaced by 2-Hydroxyethyl methacrylate (HEMA) and revalidated. This monomer can be sourced from Sigma- Aldrich for £21.20 per kg. The chemical structure of HEMA is very similar to GMMA, however it has one less hydroxyl group which makes it more hydrophobic, If future studies propose to change to HEMA, the recommendation would be to lower the hydrophobic LMA portion of the gel composition. HEMA has been used for ocular materials before and produced promising biocompatibility results (Hicks et al., 1998; Lee et al., 1996; Merrett et al., 2001).

If any proposals are made to conduct effective organ culture studies, consideration must be given to the current curing geometry of these gels. They are currently flat discs, these will not make good contact with a curved cornea. Therefore the gel casting method must be changed to produce gels that curve in the same way as a contact lens. The limitation of changing the geometry would be that explants may not adhere on the edges of a curved gel, or could be more susceptible to dropping off the cornea. Perhaps this limitation may further encourage the use of laser etching to modify the design of a future device.
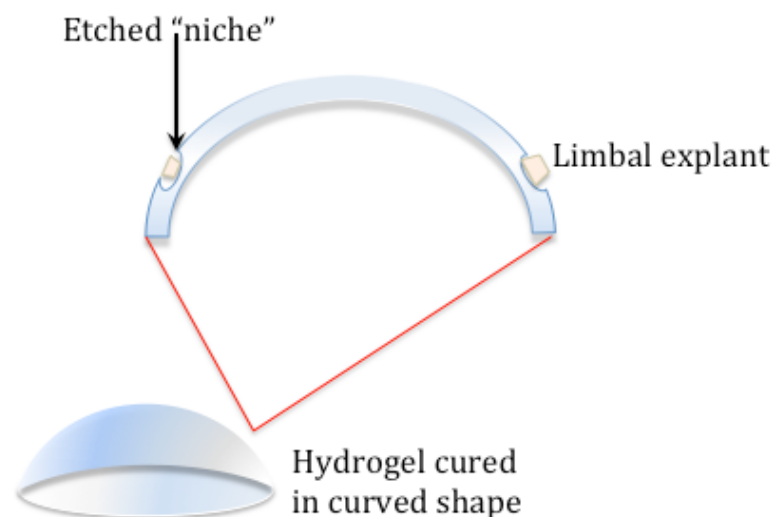
FIGURE 6.3: *Suggestions for conducting organ culture studies with the hydrogels from this thesis*

The recommendations made so far intend to take this project further towards advancing the production of an inlay device. Since this system has established no need for stromal cells or ECM proteins it will be worth investigating also removing serum from cultures to see if these gels can work completely synthetically to produce an epithelium. This may also reveal more about the mechanism by which these gels promote adhesion or even differentiation of rLECs.

Amstein, C.F.; Hartman, P.A., 1975. Adaption of Plastic Surfaces for Tissue Culture by Glow Discharge. J. Clinical Microbiology 2: 46 – 54;

Anderson, D.F., Ellies, P., Pires, R.T.F., Tseng, S.C.G., 2001. Amniotic membrane transplantation for partial limbal stem cell deficiency. Br. J. Ophthalmol. 85, 567–575.

Anderson, R.A., 1977. Actin filaments in normal and migrating corneal epithelial cells. Invest. Ophthalmol. Vis. Sci. 16, 161–166.

Andrade, J.D., Ed., 1985. Surface and lnterfacial Aspects of Biomedical Polymers. Vol. 2, New York, Plenum Press

Arenas, E., Esquenazi, S., Anwar, M., Terry, M., 2012. Lamellar corneal transplantation. Surv. Ophthalmol. 57, 510–29.

Arima, Y., & Iwata, H. 2007. Effect of wettability and surface functional groups on protein adsorption and cell adhesion using well-defined mixed self-assembled monolayers. Biomaterials, 28(20), 3074–3082.

Aydin, H.M., Türk, M., Calimli, A., Pişkin, E., 2006. Attachment and growth of fibroblasts on poly(L-lactide/epsilon-caprolactone) scaffolds prepared in supercritical CO2 and modified by polyethylene imine grafting with ethylene diamine-plasma in a glow-discharge apparatus. Int. J. Artif. Organs 29, 873—880.

Bakhtiari, P., Welder, J., Chan, C., De la Cruz, J., Holland, E.J., Djalilian, A.R., 2012. Surgical and visual outcomes of the type 1 Boston keratoprosthesis for the management of aniridic fibrosis syndrome in congenital aniridia. Am J Ophthalmol.153, 967-971.e2

Baujard-Lamotte, L., Noinville, S., Goubard, F., Marque, P., Pauthe, E., 2008. Kinetics of conformational changes of fibronectin adsorbed onto model surfaces. Colloids Surfaces B Biointerfaces 63, 129–137.

Berthois, Y., Katzenellenbogen, J.A., Katzenellenbogen, B.S., 1986. Phenol red in tissue culture media is a weak estrogen: implications concerning the study of estrogen-responsive cells in culture. Proc. Natl. Acad. Sci. U. S. A. 83, 2496–2500.

Boudreau, N., Sympson, C.J., Werb, Z., Bissell, M.J., 1995. Suppression of ICE and apoptosis in mammary epithelial cells by extracellular matrix. Science (80-.). 267, 891–893.

Bourne, W.M., 2003. Biology of the corneal endothelium in health and disease. Eye 17, 912–918.

Brandl, F., Sommer, F., Goepferich, A., 2007. Rational design of hydrogels for tissue engineering: Impact of physical factors on cell behavior. Biomaterials 28, 134–146.

Briscoe, J., Novitch, B.G., 2008. Regulatory pathways linking progenitor patterning, cell fates and neurogenesis in the ventral neural tube. Philos. Trans. R. Soc. Lond. B. Biol. Sci. 363, 57–70.

Britland, S., Perridge, C., Denyer, M., Morgan, H., Curtis, A., Wilkinson, C., 1997. Morphogenetic guidance cues can interact synergistically and hierarchically in steering nerve cell growth. Exp. Biol. Online 1, 1–15.

Bullock, A.J., Higham, M.C., MacNeil, S., 2006. Use of human fibroblasts in the development of a xenobiotic-free culture and delivery system for human keratinocytes. Tissue Eng. 12, 245–255.

Busuttil, R.A., Rubio, M., Dolle, M.E.T., Campisi, J., Vijg, J., 2003. Oxygen accelerates the accumulation of mutations during the senescence and immortalization of murine cells in culture. Aging Cell 2, 287–294.

Carraher Jr., C., Swift, G., Ramos, M., Huang, S., 2002. Functional hydrophilic-hydrophobic hydrogels derived from condensation of polycaprolactone diol and ppoly(ethylene glycol) with itaconic anhydride, in: Functional Condensation Polymers. Springer US, pp. 185–198.

Chen, J.J., Tseng, S.C., 1991. Abnormal corneal epithelial wound healing in partial-thickness removal of limbal epithelium. Invest. Ophthalmol. Vis. Sci. 32, 2219–2233.

Chen, J.J.Y., Tseng, S.C.G., 1990. Corneal epithelial wound healing in partial limbal deficiency. Investig. Ophthalmol. Vis. Sci. 31, 1301–1314.

Chen, Z., de Paiva, C.S., Luo, L., Kretzer, F.L., Pflugfelder, S.C., Li, D.-Q., 2004. Characterization of Putative Stem Cell Phenotype in Human Limbal Epithelia. Stem Cells 22, 355–366.

Chirila, T. V, 2001. An overview of the development of artificial corneas with porous skirts and the use of PHEMA for such an application. Biomaterials 22, 3311–3317.

Cipolleschi, M.G., Dellosbarba, P., Olivotto, M., 1993. The role of hypoxia in the maintenance of hematopoietic stem cells. Blood 82, 2031–2037.

Clark, E.A., Brugge, J.S., 1995. Integrins and signal transduction pathways: the road taken. Science (80-.). 268, 233–239.

Coates, J., Ed, R.A.M., 2000. Interpretation of Infrared Spectra , A Practical Approach Interpretation of Infrared Spectra , A Practical Approach 10815–10837.

Costa, C., Tortosa, R., Domènech, A., Vidal, E., Pumarola, M., Bassols, A., 2007. Mapping of aggrecan, hyaluronic acid, heparan sulphate proteoglycans and aquaporin 4 in the central nervous system of the mouse. J. Chem. Neuroanat. 33, 111–123.

Crosson, C.E., Klyce, S.D., Beuerman, R.W., 1986. Epithelail wound closure in the rabbit cornea- A biphasic process Invest. Ophthalmol. Vis. Sci. 27, 464–473.

Curtis, A.S.G.; Forrester, J.V.; McInnes, C.; Lawrie, F., 1983. Adhesion of Cells to Polystyrene Surfaces. J. Cell. Biology, Vol. 97: 1500 – 1506.

Curtis, A., Wilkinson, C., 1997. Topographical control of cells. Biomaterials 18, 1573–1583.

Dalby, M.J., Gadegaard, N., Tare, R., Andar, A., Riehle, M.O., Herzyk, P., Wilkinson, C.D.W., Oreffo, R.O.C., 2007. The control of human mesenchymal cell differentiation using nanoscale symmetry and disorder. Nat Mater 6, 997–1003.

Damsky, C.H., Werb, Z., 1992. Signal transduction by integrin receptors for extracellular matrix: Cooperative processing of extracellular information. Curr. Opin. Cell Biol. 4, 772–781.

Dana, M.R., Qian, Y., Hamrah, P., 2000. Twenty-five-year panorama of corneal immunology: emerging concepts in the immunopathogenesis of microbial keratitis, peripheral ulcerative keratitis, and corneal transplant rejection. Cornea 19, 625–643.

Daniels, J.T., Dart, J.K.G., Tuft, S.J., Khaw, P.T., 2001. Corneal stem cells in review. Wound Repair Regen. 9, 483–494.

Davis, K.A., Anseth, K.S., 2002. Controlled release from crosslinked degradable networks. Crit. Rev. Ther. Drug Carrier Syst. 19, 385–423.

Daya, S.M., Ilari, F.A.C.S.L., 2001. Living related conjunctival limbal allograft for the treatment of stem cell deficiency. Ophthalmology 108, 126–134.

Dellatore, S.M., Garcia, A.S., Miller, W.M., 2008. Mimicking stem cell niches to increase stem cell expansion. Curr. Opin. Biotechnol. 19, 534–540.

DeLong, S.A., Moon, J.J., West, J.L., 2005. Covalently immobilized gradients of bFGF on hydrogel scaffolds for directed cell migration. Biomaterials 26, 3227–3234.

Deng, C., Chen, X., Sun, J., Lu, T., Wang, W., Jing, X., 2007. RGD peptide grafted biodegradable amphiphilic triblock copolymer poly(glutamic acid)-b-poly(L-lactide)-b-poly(glutamic acid): Synthesis and self-assembly. J. Polym. Sci. Part a-Polymer Chem. 45, 3218–3230.

Deroanne, C.F., Lapiere, C.M., Nusgens, B. V, 2001. In vitro tubulogenesis of endothelial cells by relaxation of the coupling extracellular matrix-cytoskeleton. Cardiovasc. Res. 49 , 647–658.

Deshpande, P., McKean, R., Blackwood, K.A., Senior, R.A., Ogunbanjo, A., Ryan, A.J., MacNeil, S., 2010. Using poly(lactide-co-glycolide) electrospun scaffolds to deliver cultured epithelial cells to the cornea. Regen. Med. 5, 395–401.

Deshpande, P., Notara, M., Bullett, N., Daniels, J.T., Haddow, D.B., MacNeil, S., 2009. Development of a surface-modified contact lens for the transfer of cultured limbal epithelial cells to the cornea for ocular surface diseases. Tissue Eng. Part A 15, 2889–2902.

Deshpande, P., Ramachandran, C., Sefat, F., Mariappan, I., Johnson, C., McKean, R., Hannah, M., Sangwan, V.S., Claeyssens, F., Ryan, A.J., MacNeil, S., 2013. Simplifying corneal surface regeneration using a biodegradable synthetic membrane and limbal tissue explants. Biomaterials 34, 5088–5106.

Discher, D.E., Janmey, P., Wang, Y.L., 2005. Tissue cells feel and respond to the stiffness of their substrate. Science (80-.). 310, 1139–1143.

Dodson, J.W., Hay, E.D., 1974. Secretion of collagen by corneal epithelium .II. Effect of underlying substratum on secretion and polymerization of epithelial products. J. Exp. Zool. 189, 51–72.

Dohlman, C.H., Refojo, M.F., Rose, J., 1967. Synthetic polymers in corneal surgery. I. Glyceryl methacrylate. Arch. Ophthalmol. 77, 252–257.

Drury, J.L., Mooney, D.J., 2003. Hydrogels for tissue engineering: scaffold design variables and applications. Biomaterials 24, 4337–4351.

Du, L.Q., Chen, H.M., Yan, Y., Wu, X.Y., 2012. In vivo biological stability of chemically pretreated silicone gel inserts intended for use in keratoprostheses. Chin. Med. J. (Engl). 125, 4239–4244.

Dua, H.S., Faraj, L.A., Said, D.G., Gray, T., Lowe, J., 2014. Human corneal anatomy redefined. Ophthalmology 120, 1778–1785.

Dua, H.S., Forrester, J. V, 1990. The corneoscleral limbus in human corneal epithelial wound healing. Am. J. Ophthalmol. 110, 646–656.

Dua, H.S., Gomes, J.A.P., Singh, A., 1994. Corneal epithelial wound healing. Br. J. Ophthalmol. 78, 401–408.

Dua, H.S., Saini, J.S., Azuara-Blanco, A., Gupta, P., 2000. Limbal stem cell deficiency: concept, aetiology, clinical presentation, diagnosis and management. Indian J. Ophthalmol. 48, 83–92.

DuPont-Gillian, Ch. C. Adriaensen, Y. Derclaye, S and. Rouxhet, P. G. 2000.Plasma-oxidized polystyrene: Wetting properties and surface reconstruction. Langmuir Vol. 16: 8194 – 8200.

Ebato, B., Friend, J., Thoft, R.A., 1988. Comparison of limbal and peripheral human corneal epithelium in tissue culture. Investig. Ophthalmol. Vis. Sci. 29 , 1533–1537.

Elbert, D.L., Hubbell, J.A., 2001. Conjugate addition reactions combined with free-radical cross-linking for the design of materials for tissue engineering. Biomacromolecules 2, 430–441.

Elliott, J.H., 1980. Epidermal growth factor: in vivo ocular studies. Trans. Am. Ophthalmol. Soc. 78, 629–656.

Engler, A., Bacakova, L., Newman, C., Hategan, A., Griffin, M., Discher, D., 2004. Substrate compliance versus ligand density in cell on gel responses. Biophys. J. 86, 388A–388A.

Engler, A.J., Sen, S., Sweeney, H.L., Discher, D.E., 2006. Matrix elasticity directs stem cell lineage specification. Cell 126, 677–689.

Evans, M.D.M., Xie, R.Z., Fabbri, M., Bojarski, B., Chaouk, H., Wilkie, J.S., McLean, K.M., Cheng, H.Y., Vannas, A., Sweeney, D.F., 2002. Progress in the development of a synthetic corneal onlay. Invest. Ophthalmol. Vis. Sci. 43, 3196–3201.

Evans, M.D.M., Xie, R.Z., Fabbri, M., Madigan, M.C., Chaouk, H., Beumer, G.J., Meijs, G.F., Griesser, H.J., Steele, J.G., Sweeney, D.F., 2000. Epithelialization of a synthetic polymer in the feline cornea: A preliminary study. Invest. Ophthalmol. Vis. Sci. 41, 1674–1680.

Ezashi, T., Das, P., Roberts, R.M., 2005. Low O-2 tensions and the prevention of differentiation of hES cells. Proc. Natl. Acad. Sci. U. S. A. 102, 4783–4788.

Fini, M.E., 1999. Keratocyte and fibroblast phenotypes in the repairing cornea. Prog. Retin. Eye Res. 18, 529–551.

Fitch, J.M., Birk, D.E., Linsenmayer, C., Linsenmayer, T.F., 1990. The spatial organization of Descemet's membrane-associated type IV collagen in the avian cornea. J. Cell Biol. 110, 1457–1468.

Flanagan, L.A., Ju, Y.-E., Marg, B., Osterfield, M., Janmey, P.A., 2002. Neurite branching on deformable substrates. Neuroreport 13, 2411–2415.

Flemming, R.G., Murphy, C.J., Abrams, G.A., Goodman, S.L., Nealey, P.F., 1999. Effects of synthetic micro- and nano-structured surfaces on cell behavior. Biomaterials 20, 573–588.

Folkman, J., Tucker, R.W., 1980. Cell configuration substratum and growth control. In The Cell Surface Mediator of Developmental Processes (ed. S. Subtelny & N. K. Wessels)., 259-275. New York: Academic Press

Forrester, J. V, Dick, A.D., McMenamin, P.G., Lee, W.R., 2002. The eye: Basic sciences in practice, 2nd ed. Saunders, Edinburgh.

Forsyth, N.R., Musio, A., Vezzoni, P., Simpson, A., Noble, B.S., McWhir, J., 2006. Physiologic oxygen enhances human embryonic stem cell clonal recovery and reduces chromosomal abnormalities. Cloning Stem Cells 8, 16–23.

Freund, D.E., Burlina, P., Banerjee, A., Ieee, 2008. Characterization of spatial ordering of corneal stroma fibrils, in: 2008 Ieee International Symposium on Biomedical Imaging: From Nano to Macro, Vols 1-4. Ieee, New York, pp. 963–966.

Friedenwald, J., Buschke, W., 1944. Some factors concerned in the mitotic and wound-healing activities of the corneal epithelium. Trans. Am. Ophthalmol. Soc. 42, 371–83.

Gail, M.H., Boone, C.W., 1972. Cell-substrate adhesivity: A determinant of cell motility. Exp. Cell Res. 70, 33–40.

Garfias, Y., Nieves-Hernandez, J., Garcia-Mejia, M., Estrada-Reyes, C., Carmen Jimenez-Martinez, M., 2012. Stem cells isolated from the human stromal limbus possess immunosuppressant properties. Mol. Vis. 18, 2087–2095.

Ge, S., Pradhan, D.A., Ming, G. li, Song, H., 2007. GABA sets the tempo for activity-dependent adult neurogenesis. Trends Neurosci.

Gelain, F., Horii, A., Zhang, S., 2007. Designer self-assembling peptide scaffolds for 3-D tissue cell cultures and regenerative medicine. Macromol. Biosci.

Ghiasi, H., Hofman, F.M., Cai, S., Perng, G.C., Nesburn, A.B., Wechsler, S.L., 1999. Vaccination with different HSV-1 glycoproteins induces different patterns of ocular cytokine responses following HSV-1 challenge of vaccinated mice. Vaccine 17, 2576–2582.

Gibbons, J., Hewitt, E., Gardner, D.K., 2006. Effects of oxygen tension on the establishment and lactate dehydrogenase activity of murine embryonic stem cells. Cloning Stem Cells 8, 117–122.

Gillette, T.E., Chandler, J.W., Greiner, J. V, 1982. Langerhans cells of the ocular surface. Ophthalmology 89, 700–711.

Gipson, I.K., Kiorpes, T.C., Brennan, S.J., 1984. Epithelial sheet movement - Effects of Tunicamycin on migration and glycoprotein-synthesis. Dev. Biol. 101, 212–220.

Gomes, J.A.P., dos Santos, M.S., Cunha, M.C., Mascaro, V.L. úci. D., Barros, J. de N., de Sousa, L.B., 2003. Amniotic membrane transplantation for partial and total limbal stem cell deficiency secondary to chemical burn. Ophthalmology 110, 466–473.

Gordon, M.K., Foley, J.W., Birk, D.E., Fitch, J.M., Linsenmayer, T.F., 1994. Type V collagen and Bowman's membrane. Quantitation of mRNA in corneal epithelium and stroma. J. Biol. Chem. 269, 24959–24966.

Gottsch, J.D., Liu, S.H., Stark, W.J., 1992. Mooren's ulcer and evidence of stromal graft rejection after penetrating keratoplasty., American journal of ophthalmology.

Gray, D.S., Tien, J., Chen, C.S., 2003. Repositioning of cells by mechanotaxis on surfaces with micropatterned Young's modulus. J. Biomed. Mater. Res. Part A 66A, 605–614.

Greenberg, C.S., Birckbichler, P.J., Rice, R.H., 1991. Transglutaminases: multifunctional cross-linking enzymes that stabilize tissues. FASEB J. 5, 3071–3077.

Grinnell, F., Feld, M.K., 1982. Fibronectin adsorption on hydrophilic and hydrophobic surfaces detected by antibody binding and analyzed during cell adhesion in serum-containing medium. J. Biol. Chem. 257, 4888–4893.

Grueterich, M., Espana, E.M., Touhami, A., Ti, S.-E., Tseng, S.C.G., 2002. Phenotypic study of a case with successful transplantation of ex vivo expanded human limbal epithelium for unilateral total limbal stem cell deficiency. Ophthalmology 109, 1547–1552.

Grueterich, M., Espana, E.M., Tseng, S.C.G., 2003. Ex vivo expansion of limbal epithelial stem cells: amniotic membrane serving as a stem cell niche. Surv. Ophthalmol. 48, 631–646.

Grushkin-Lerner, L.S., Kewalramani, R., Trinkaus-Randall, V., 1997. Expression of integrin receptors on plasma membranes of primary corneal epithelial cells is matrix specific. Exp. Eye Res. 64, 323–334.

Haddow, D.B., Steele, D.A., Short, R.D., Dawson, R.A., Macneil, S., 2003. Plasma-polymerized surfaces for culture of human keratinocytes and transfer of cells to an in vitro wound-bed model. J. Biomed. Mater. Res. Part A 64A, 80–87.

Haigh, R., Fullwood, N., Rimmer, S., 2002. Synthesis and properties of amphiphilic networks 2: a differential scanning calorimetric study of poly(dodecyl methacrylate-stat-2,3 propandiol-1-methacrylate-stat-ethandiol dimethacrylate) networks and adhesion and spreading of dermal fibroblasts on these materials. Biomaterials 23, 3509–3516.

Haigh, R., Rimmer, S., Fullwood, N.J., 2000. Synthesis and properties of amphiphilic networks. 1: the effect of hydration and polymer composition on the adhesion of immunoglobulin-G to poly(laurylmethacrylate-stat-glycerolmonomethacrylate-stat-ethylene-glycol-dimethacrylate) networks. Biomaterials 21, 735–739.

Hamerli, P., Weigel, T., Groth, T., Paul, D., 2003. Enhanced tissue-compatibility of polyethylenterephtalat membranes by plasma aminofunctionalisation. Surf. Coatings Technol. 174-175, 574–578.

Hanna, C., DS, B., JE, O., 1961. Cell turnover in the adult human eye. Arch. Ophthalmol. 65, 695–698.

Hanna, C., Obrien, J.E., 1960. Cell production and migration in the epithelial layer of the cornea. Arch. Ophthalmol. 64, 536–539.

Hao, Y., Ma, D.H.-K., Hwang, D.G., Kim, W.-S., Zhang, F., 2000. Identification of antiangiogenic and antiinflammatory proteins in human amniotic membrane. Cornea 19, 348–352.

Hassan, E., Deshpande, P., Claeyssens, F., Rimmer, S., MacNeil, S., 2014. Amine functional hydrogels as selective substrates for corneal epithelialization. Acta Biomater. 10, 3029–37.

Heiligenhaus, A., Bauer, D., Zheng, M., Mrzyk, S., Steuhl, K.P., 1999. CD4+ T-cell type 1 and type 2 cytokines in the HSV-1 infected cornea. Graefe's Arch. Clin. Exp. Ophthalmol. 237, 399–406.

Hern, D.L., Hubbell, J.A., 1998. Incorporation of adhesion peptides into nonadhesive hydrogels useful for tissue resurfacing. J. Biomed. Mater. Res. 39, 266–276.

Hicks, C.R., Crawford, G.J., Dart, J.K.G., Grabner, G., Holland, E.J., Stulting, R.D., Tan, D.T., Bulsara, M., 2006. AlphaCor - Clinical outcomes. Cornea 25, 1034–1042.

Hicks, C.R., Crawford, G.J., Lou, X., Tan, D.T., Snibson, G.R., Sutton, G., Downie, N., Werner, L., Chirila, T. V, Constable, I.J., 2003. Corneal replacement using a synthetic hydrogel cornea, AlphaCor (TM) device, preliminary outcomes and complications. Eye 17, 385–392.

Hicks, C.R., Vijayasekaran, S., Chirila, T. V, Platten, S.T., Crawford, G.J., Constable, I.J., 1998. Implantation of PHEMA keratoprostheses after alkali burns in rabbit eyes. Cornea 17, 301–308.

Hodges, R.R., Dartt, D.A., 2003. Regulatory pathways in lacrimal gland epithelium. Int. Rev. Cytol. 231, 129-96

Hoffman, A.S., 2002. Hydrogels for biomedical applications. Adv. Drug Deliv. Rev. 54, 3–12.

Holland, E.J., 1996. Epithelial transplantation for the management of severe ocular surface disease. Trans. Am. Ophthalmol. Soc. 94, 677–743.

Holland, E.J., Schwartz, G.S., 1996. The evolution of epithelial transplantation for severe ocular surface disease and a proposed classification system. Cornea 15, 549–556.

Holly, S.P., Larson, M.K., Parise, L. V, 2000. Multiple roles of integrins in cell motility. Exp. Cell Res. 261, 69–74.

Holmberg, J., Armulik, A., Senti, K.-A., Edoff, K., Spalding, K., Momma, S., Cassidy, R., Flanagan, J.G., Frisén, J., 2005. Ephrin-A2 reverse signaling negatively regulates neural progenitor proliferation and neurogenesis. Genes Dev. 19, 462–471.

Hopp, I., Michelmore, A., Smith, L.E., Robinson, D.E., Bachhuka, A., Mierczynska, A., Vasilev, K., 2013. The influence of substrate stiffness gradients on primary human dermal fibroblasts. Biomaterials 34, 5070–7.

Horbett, T.A., Schway, M.B., 1988. Correlations between mouse 3T3 cell spreading and serum fibronectin adsorption on glass and hydroxyethylmethacrylate-ethylmethacrylate copolymers. J. Biomed. Mater. Res. 22, 763–793.

Horbett, T.A., Waldburger, J.J., Ratner, B.D., Hoffman, A.S., 1988. Cell adhesion to a series of hydrophili–hydrophobic copolymers studies with a spinning disc apparatus. J. Biomed. Mater. Res. 22, 383–404.

Huang, A.J.W., Tseng, S.C.G., 1991. Corneal epithelial wound-healing in the absence of limbal epithelium. Invest. Ophthalmol. Vis. Sci. 32, 96–105.

Huttenlocher, A., Sandborg, R.R., Horwitz, A.F., 1995. Adhesion in cell migration. Curr. Opin. Cell Biol. 7, 697–706.

Imanishi, J., Kamiyama, K., Iguchi, I., Kita, M., Sotozono, C., Kinoshita, S., 2000. Growth factors: importance in wound healing and maintenance of transparency of the cornea. Prog. Retin. Eye Res. 19, 113–129.

Inada, R., Matsuki, M., Yamada, K., Morishima, Y., Shen, S.C., Kuramoto, N., Yasuno, H., Takahashi, K., Miyachi, Y., Yamanishi, K., 2000. Facilitated wound healing by activation of the Transglutaminase 1 gene. Am J Pathol 157, 1875–1882.

Inoue, K., Amano, S., Oshika, T., Tsuru, T., 2001. Risk factors for corneal graft failure and rejection in penetrating keratoplasty. Acta Ophthalmol. Scand. 79, 251–255.

Iuliano, D.J., Saavedra, S.S., Truskey, G.A., 1993. Effect of the conformation and orientation of adsorbed fibronectin on endothelial cell spreading and the strength of adhesion. J. Biomed. Mater. Res. 27, 1103–1113.

Jacob, J.T., Rochefort, J.R., Bi, J., Gebhardt, B.M., 2005. Corneal epithelial cell growth over tethered-protein/peptide surface-modified hydrogels. J Biomed Mater Res B Appl Biomater 72, 198–205.

Javadi, M.A., Motlagh, B.F., Jafarinasab, M.R., Rabbanikhah, Z., Anissian, A., Souri, H., Yazdani, S., 2005. Outcomes of penetrating keratoplasty in keratoconus. Cornea 24, 941–946.

Jenkins, C., Tuft, S., Liu, C., Buckley, R., 1993. Limbal transplantation in the management of chronic contact-lens-associated epitheliopathy. Eye 7, 629–633.

Jensen, P.A., Therkelsen, A., 1982. Selective inhibition of fibroblasts by spermine in primary cultures of normal human skin epithelial cells. Vitr. - Plant 18, 867–871.

Jester, J. V, Petroll, W.M., Cavanagh, H.D., 1999. Corneal stromal wound healing in refractive surgery: the role of myofibroblasts. Prog. Retin. Eye Res. 18, 311–356.

Jhon, M.S., Andrade, J.D., 1973. Water and hydrogels. J. Biomed. Mater. Res. 7, 509–522.

Jirásková, N., Rozsival, P., Burova, M., Kalfertova, M., 2011. AlphaCor artificial cornea: clinical outcome. Eye (Lond). 25, 1138–1146.

Johnson, C., Perlin, L., Wyman, P., Zhao, B., Fullwood, N.J., MacNeil, S., Rimmer, S., 2010. Cell adhesion to polymethacrylate networks prepared by photopolymerization and functionalized with grgds peptide or fibrinogen, in: Patrickios, C.S. (Ed.), Polymer Networks: Synthesis, Properties, Theory and Applications. pp. 314–325.

Jones, R.R., Hamley, I.W., Connon, C.J., 2012. Ex vivo expansion of limbal stem cells is affected by substrate properties. Stem Cell Res. 8, 403–409.

Kai, T., Spradling, A., 2003. An empty Drosophila stem cell niche reactivates the proliferation of ectopic cells. Proc. Natl. Acad. Sci. U. S. A. 100, 4633–4638.

Kandarakis, A.S., Page, C., Kaufman, H.E., 1984. The effect of epidermal growth factor on epithelial healing after penetrating keratoplasty in human eyes. Am. J. Ophthalmol. 98, 411–415.

Karpowicz, P., Willaime-Morawek, S., Balenci, L., DeVeale, B., Inoue, T., van der Kooy, D., 2009. E-Cadherin regulates neural stem cell self-renewal. J. Neurosci. 29, 3885–3896.

Katayama, Y., Battista, M., Kao, W.M., Hidalgo, A., Peired, A.J., Thomas, S.A., Frenette, P.S., 2006. Signals from the sympathetic nervous system regulate hematopoietic stem cell egress from bone marrow. Cell 124, 407–421.

Kawaba, T., Nakayasu, K., Kanai, A., 1984. Effect of human EGF and plasma fibronectin on corneal epithelial regeneration. Nihon. Ganka Gakkai Zasshi 88, 1237–1249.

Kedar, U., Phutane, P., Shidhaye, S., & Kadam, V., 2010. Advances in polymeric micelles for drug delivery and tumor targeting. Nanomed Nanotech Biol Med. 6, 714-729

Kenyon, K.R., 1979. Anatomy and pathology of the ocular surface. Int. Ophthalmol. Clin. 19, 3–35.

Khaireddin, R., Wachtlin, J., Hopfenmüller, W., Hoffmann, F., 2003. HLA-A, HLA-B and HLA-DR matching reduces the rate of corneal allograft rejection. Graefe's Arch. Clin. Exp. Ophthalmol. 241, 1020–1028.

Khan, B., Dudenhoefer, E.J., Dohlman, C.H., 2001. Keratoprosthesis: an update. Curr Opin Ophthalmol 12, 282–287.

Khodadoust, A.A., 2008. The allograft rejection reaction: the leading cause of late failure of clinical corneal grafts, in: Ciba Foundation Symposium 15 - Corneal Graft Failure. John Wiley & Sons, Ltd, pp. 151–167.

Klyce, S.D., 1972. Electrical profiles in the corneal epithelium. J. Physiol. 226, 407–429.

Knowles, W.F., 1961. Effect of intralamellar plastic membranes on corneal physiology. Am. J. Ophthalmol. 51, 1146–1156.

Koay, P.Y., Lee, W.H., Figueiredo, F.C., 2005. Opinions on risk factors and management of corneal graft rejection in the United kingdom. Cornea 24, 292–296.

Korb, D.R., Craig, J., Doughty, M., Guillon, J.-P., Smith, G., Tomlinson, A., 2002. The tear film, The Tear Film. Elsevier.

Krachmer, J.H., Mannis, M.J., Holland, E.J., 2005a. Cornea: Fundamentals, diagnosis and management, 2nd ed. Elsevier Mosby.

Krachmer, J.H., Mannis, M.J., Holland, E.J., 2005b. Cornea, Cornea. Elsevier Mosby.

Lai, K., Kaspar, B.K., Gage, F.H., Schaffer, D. V, 2003. Sonic hedgehog regulates adult neural progenitor proliferation in vitro and in vivo. Nat. Neurosci. 6, 21–27.

Laule, A., Cable, M.K., Hoffman, C.E., Hanna, C., 1978. Endothelial cell-population changes of human cornea during life. Arch. Ophthalmol. 96, 2031–2035.

Lee, J., Lee, S., Khang, G., Lee, H., 2000. The effect of fluid shear stress on endothelial cell adhesiveness to polymer surfaces with wettability gradient. J. Colloid Interface Sci. 230, 84–90.

Lee, J.H., Jung, H.W., Kang, I.-K., Lee, H.B., 1994. Cell behaviour on polymer surfaces with different functional groups. Biomaterials 15, 705–711.

Lee, J.H., Khang, G., Lee, J.W., Lee, H.B., 1998. Interaction of different types of cells on polymer surfaces with wettability gradient. J. Colloid Interface Sci. 205, 323–330.

Lee, S.D., Hsiue, G.H., Kao, C.Y., Chang, P.C., 1996. Artificial cornea: surface modification of silicone rubber membrane by graft polymerization of pHEMA via glow discharge. Biomaterials 17, 587–595.

Lee, S.J., Khang, G., Lee, Y.M., Lee, H.B., 2003. The effect of surface wettability on induction and growth of neurites from the PC-12 cell on a polymer surface. J. Colloid Interface Sci. 259, 228–35.

Legeais, J.-M., Renard, G., 1998. A second generation of artificial cornea (Biokpro II). Biomaterials 19, 1517–1522.

Lestelius, M., Liedberg, B., Tengvall, P., 1997. In vitro plasma protein adsorption on ω-functionalized alkanethiolate self-assembled monolayers. Langmuir 13, 5900–5908.

Levental, I., Georges, P.C., Janmey, P.A., 2007. Soft biological materials and their impact on cell function. Soft Matter 3, 299–306.

Levin, L.A., Nilsson, S.F.E., Ver Hoeve, J., Wu, S.M., 2011. Adler's physiology of the eye, 11th ed. Elsevier Health Sciences, 2011, Edinburgh.

Li, C., Yin, T., Dong, N., Dong, F., Fang, X., Qu, Y.-L., Tan, Y., Wu, H., Liu, Z., Li, W., 2011. Oxygen tension affects terminal differentiation of corneal limbal epithelial cells. J. Cell. Physiol. 226, 2429–2437.

Li, W., Hayashida, Y., Chen, Y.-T., Tseng, S.C.G., 2007. Niche regulation of corneal epithelial stem cells at the limbus. Cell Res 17, 26–36.

Lie, D.-C., Colamarino, S.A., Song, H.-J., Désiré, L., Mira, H., Consiglio, A., Lein, E.S., Jessberger, S., Lansford, H., Dearie, A.R., Gage, F.H., 2005. Wnt signalling regulates adult hippocampal neurogenesis. Nature 437, 1370–1375.

Liu, L., Sheardown, H., 2005. Glucose permeable poly (dimethyl siloxane) poly (N-isopropyl acrylamide) interpenetrating networks as ophthalmic biomaterials. Biomaterials 26, 233–44.

Llobet, A., Gasull, X., Gual, A., 2003. Understanding trabecular meshwork physiology: a key to the control of intraocular pressure? Physiology 18, 205–209.

Lo, C.M., Wang, H.B., Dembo, M., Wang, Y.L., 2000. Cell movement is guided by the rigidity of the substrate. Biophys. J. 79, 144–152.

Lu, L., Reinach, P.S., Kao, W.W.Y., 2001. Corneal epithelial wound healing. Exp. Biol. Med. 226, 653–664.

Lyndon, M.J., 1986. Synthetic hydrogels as substrata for cell-adhesion studies. Br. Polym. J. 18, 22–27.

Ma, A.H., Zhao, B.J., Bentley, A.J., Brahma, A., MacNeil, S., Martin, F.L., Rimmer, S., Fullwood, N.J., 2011. Corneal epithelialisation on surface-modified hydrogel implants Artificial cornea. J. Mater. Sci. Med. 22, 663–670.

Maguen, E., Zorapapel, N.C., Zieske, J.D., Ninomiya, Y., Sado, Y., Kenney, M.C., Ljubimov, A. V, 2002. Extracellular matrix and matrix metalloproteinase changes in human corneas after complicated, laser-assisted in situ keratomileusis (LASIK). Cornea 21, 95–100.

Mamalis, N., CW, A., KR, K., MK, L., RJ, O., 1992. Changing trends in the indications for penetrating keratoplasty. Arch. Ophthalmol. 110, 1409–1411.

Maurice, D.M., 1957. The structure and transparency of the cornea. J. Physiol. 136, 263–286.

McBeath, R., Pirone, D.M., Nelson, C.M., Bhadriraju, K., Chen, C.S., 2004. Cell shape, cytoskeletal tension, and rhoa regulate stem cell lineage commitment. Dev. Cell 6, 483–495.

McCarey, B.E., Schmidt, F.H., 1990. Modeling glucose distribution in the cornea. Curr. Eye Res. 9, 1025–1039.

McMurray, R.J., Gadegaard, N., Tsimbouri, P.M., Burgess, K. V, McNamara, L.E., Tare, R., Murawski, K., Kingham, E., Oreffo, R.O.C., Dalby, M.J., 2011. Nanoscale surfaces for the long-term maintenance of mesenchymal stem cell phenotype and multipotency. Nat Mater 10, 637–644.

Mei, Y., Saha, K., Bogatyrev, S.R., Yang, J., Hook, A.L., Kalcioglu, Z.I., Cho, S.-W., Mitalipova, M., Pyzocha, N., Rojas, F., Van Vliet, K.J., Davies, M.C., Alexander, M.R., Langer, R., Jaenisch, R., Anderson, D.G., 2010. Combinatorial development of biomaterials for clonal growth of human pluripotent stem cells. Nat. Mater. 9, 768–778.

Merindano, M., Costa, J., Canals, M., 2003. A comparative study of Bowman's layer in some mammals: relationships with other constituent corneal structures. Eur. J. … 6, 133–140.

Merrett, K., Griffith, C.M., Deslandes, Y., Pleizier, G., Sheardown, H., 2001. Adhesion of corneal epithelial cells to cell adhesion peptide modified pHEMA surfaces. J. Biomater. Sci. Ed. 12, 647–671.

Miller, J.K., Laycock, K.A., Nash, M.M., Pepose, J.S., 1993. Corneal Langerhans cell dynamics after herpes simplex virus reactivation. Invest. Ophthalmol. Vis. Sci. 34, 2282–2290.

Mirzadeh, Z., Merkle, F.T., Soriano-Navarro, M., Garcia-Verdugo, J.M., Alvarez-Buylla, A., 2008. Neural stem cells confer unique pinwheel architecture to the ventricular surface in neurogenic regions of the adult brain. Cell Stem Cell 3, 265–278.

Miyashita, H., Higa, K., Kato, N., Kawakita, T., Yoshida, S., Tsubota, K., Shimmura, S., 2007. Hypoxia enhances the expansion of human limbal epithelial progenitor cells in vitro. Invest. Ophthalmol. Vis. Sci. 48, 3586–3593.

Miyata, K., Christie, R. J., & Kataoka, K. 2011. Polymeric micelles for nano-scale drug delivery. React. Funct. Polym., 71, 227–234.

Mobley, A.K., Tchaicha, J.H., Shin, J., Hossain, M.G., McCarty, J.H., 2009. Beta8 integrin regulates neurogenesis and neurovascular homeostasis in the adult brain. J. Cell Sci. 122, 1842–1851.

Mohyeldin, A., Garzon-Muvdi, T., Quinones-Hinojosa, A., 2010. Oxygen in stem cell biology: A critical component of the stem cell niche. Cell Stem Cell 7, 150–161.

Moldovan, S.-M., Borderie, V., Baudrimont, M., Laroche, L., 1999. Limbal autograft for reconstruction of the ocular surface in patients with unilateral limbal stem cell deficiency [Traitement du syndrome d'insuffisance en cellules souches limbiques unilateral par autogreffe de limbe]. J. Fr. Ophtalmol. 22, 302–309.

Moon, J.J., Hahn, M.S., Kim, I., Nsiah, B.A., West, J.L., 2009. Micropatterning of poly(ethylene glycol) diacrylate hydrogels with biomolecules to regulate and guide endothelial morphogenesis. TISSUE Eng. PART A 15, 579–585.

Morgan, S., 1996. Limbal autotransplantation in the acute and chronic phases of severe chemical injuries. Eye 10, 349–354.

Myung, D., Duhamel, P.-E., Cochran, J.R., Noolandi, J., Ta, C.N., Frank, C.W., 2008. Development of hydrogel-based keratoprostheses: A materials perspective. Biotechnol. Prog. 24, 735–741.

Myung, D., Farooqui, N., Zheng, L.L., Koh, W., Gupta, S., Bakri, A., Noolandi, J., Cochran, J.R., Frank, C.W., Ta, C.N., 2009. Bioactive interpenetrating polymer network hydrogels that support corneal epithelial wound healing. J. Biomed. Mater. Res. Part A 90A, 70–81.

Myung, D., Koh, W., Bakri, A., Zhang, F., Marshall, A., Ko, J., Noolandi, J., Carrasco, M., Cochran, J.R., Frank, C.W., Ta, C.N., 2007. Design and fabrication of an artificial cornea based on a photolithographically patterned hydrogel construct. Biomed. Microdevices 9, 911–922.

Ngakeng, V., Hauck, M.J., Price, M.O., Price Jr., F.W., 2008. AlphaCor keratoprosthesis - A novel approach to minimize the risks of long-term postoperative complications. Cornea 27, 905–910.

Nguyen, K.T., West, J.L., 2002. Photopolymerizable hydrogels for tissue engineering applications. Biomaterials 23, 4307–4314.

Niederkorn, J.Y., 1995. Effect of cytokine-induced migration of Langerhans cells on corneal allograft survival. Eye (Lond). 9 (Pt 2), 215–218.

Niederkorn, J.Y., 2003. The immune privilege of corneal grafts. J. Leukoc. Biol. 74 , 167–171.

Niederkorn, J.Y., Callanan, D., Ross, J.R., 1990. Prevention of the induction of allospecific cytotoxic T lymphocyte and delayed-type hypersensitivity responses by ultraviolet irradiation of corneal allografts. Transplantation 50, 281–286.

Nilsson, S.K., Johnston, H.M., Occhiodoro, T., Brown, T.J., Simmons, P.J., Haylock, D.N., 2002. Hyaluronan is synthesized by primitive hemopoietic cells, participates in their lodgment at the endosteum following transplantation, and is involved in the regulation of their proliferation and differentiation in vitro. Blood 101, 856–862.

Nitschke, M., Gramm, S., Götze, T., Valtink, M., Drichel, J., Voit, B., Engelmann, K., Werner, C., 2007. Thermo-responsive poly(NiPAAm-co-DEGMA) substrates for gentle harvest of human corneal endothelial cell sheets. J. Biomed. Mater. Res. - Part A 80, 1003–1007.

No Authors, L., 1992. The collaborative corneal transplantation studies (ccts): Effectiveness of histocompatibility matching in high-risk corneal transplantation. Arch. Ophthalmol. 110, 1392–1403.

Noback, C.R., Strominger, N.L., Demarest, R.J., Ruggiero, D.A., 2005. The human nervous system - Structure and function, 6th ed. Humana Press, Totowa, NJ.

Notara, M., Bullett, N.A., Deshpande, P., Haddow, D., MacNeil, S., Daniels, J., 2007. Plasma polymer coated surfaces for serum-free culture of limbal epithelium for ocular surface disease. J. Mater. Sci. Mater. Med. 18, 329–338.

Notara, M., Schrader, S., Daniels, J.T., 2011. The porcine limbal epithelial stem cell niche as a new model for the study of transplanted tissue-engineered human limbal epithelial cells. Tissue Eng. Part A 17, 741–750.

Nur-E-Kamal, A., Ahmed, I., Kamal, J., Schindler, M., Meiners, S., 2006. Three-dimensional nanofibrillar surfaces promote self-renewal in mouse embryonic stem cells. Stem Cells 24, 426–433.

Oelker, A.M., Grinstaff, M.W., 2012. Synthesis, characterization, and in vitro evaluation of a hydrogel-based corneal onlay. IEEE Trans. Nanobioscience 11, 37–45.

Ohlstein, B., Spradling, A., 2006. The adult Drosophila posterior midgut is maintained by pluripotent stem cells. Nature 439, 470–474.

Ohno, K., Mitooka, K., Nelson, L.R., Hodge, D.O., Bourne, W.M., 2002. Keratocyte activation and apoptosis in transplanted human corneas in a xenograft model. Invest. Ophthalmol. Vis. Sci. 43, 1025–1031.

Opas, M., 1989. Expression of the differentiated phenotype by epithelial cells in vitro is regulated by both biochemistry and mechanics of the substratum. Dev. Biol. 131, 281–293.

Otori, T., 1967. Electrolyte content of rabbit corneal stroma. Exp. Eye Res. 6, 356–&.

Palmer, T.D., Willhoite, A.R., Gage, F.H., 2000. Vascular niche for adult hippocampal neurogenesis. J. Comp. Neurol. 425, 479–494.

Panda, A., Vanathi, M., Kumar, A., Dash, Y., Priya, S., 2007. Corneal Graft Rejection. Surv. Ophthalmol.

Park, J., Bansal, T., Pinelis, M., Maharbiz, M.M., 2006. A microsystem for sensing and patterning oxidative microgradients during cell culture. Lab Chip 6, 611–622.

Paszek, M.J., Zahir, N., Johnson, K.R., Lakins, J.N., Rozenberg, G.I., Gefen, A., Reinhart-King, C.A., Margulies, S.S., Dembo, M., Boettiger, D., Hammer, D.A., Weaver, V.M., 2005. Tensional homeostasis and the malignant phenotype. Cancer Cell 8, 241–254.

Peerani, R., Zandstra, P.W., 2010. Enabling stem cell therapies through synthetic stem cell-niche engineering. J. Clin. Invest. 120, 60–70.

Pelham, R.J., Wang, Y., 1997. Cell locomotion and focal adhesions are regulated by substrate flexibility. Proc. Natl. Acad. Sci. 94, 13661–13665.

Pelham, R.J., Wang, Y., 1997. Cell locomotion and focal adhesions are regulated by substrate flexibility. Proc. Natl. Acad. Sci. 94, 13661–13665.

Pellegrini, G., Golisano, O., Paterna, P., Lambiase, A., Bonini, S., Rama, P., De Luca, M., 1999. Location and Clonal Analysis of Stem Cells and Their Differentiated Progeny in the Human Ocular Surface. J. Cell Biol. 145 , 769–782.

Pellegrini, G., Traverso, C.E., Franzi, A.T., Zingirian, M., Cancedda, R., De Luca, M., 1997. Long-term restoration of damaged corneal surfaces with autologous cultivated corneal epithelium. Lancet 349, 990–993.

Peppas, N.A., Bures, P., Leobandung, W., Ichikawa, H., 2000. Hydrogels in pharmaceutical formulations. Eur. J. Pharm. Biopharm. 50, 27–46.

Perlin, L., MacNeil, S., Rimmer, S., 2008. Cell adhesive hydrogels synthesised by copolymerisation of arg-protected Gly-Arg-Gly-Asp-Ser methacrylate monomers and enzymatic deprotection. Chem. Commun. 5951–5953.

Perlin, L., MacNeil, S., Rimmer, S., 2008. Production and performance of biomaterials containing RGD peptides. Soft Matter 4, 2331–2349.

Pu, F.R., Williams, R.L., Markkula, T.K., Hunt, J.A., 2002. Effects of plasma treated PET and PTFE on expression of adhesion molecules by human endothelial cells in vitro. Biomaterials 23, 2411–2428.

Thoft RA, Friend J, Dohlman CH. Corneal glucose flux. II. Its response to anterior chamber blockade and endothelial damage. Arch Ophthalmol. 1971;86(6):685–691.

Ratner, B., 1997. Biomaterials Science: An introduction to materials in medicine. Elsevier.

Ricard, J., Salinas, J., Garcia, L., Liebl, D.J., 2006. EphrinB3 regulates cell proliferation and survival in adult neurogenesis. Mol. Cell. Neurosci. 31, 713–722.

Rider, C.C., 2006. Heparin/heparan sulphate binding in the TGF-beta cytokine superfamily. Biochem. Soc. Trans. 34, 458–460.

Rimmer, S., German, M.J., Maughan, J., Sun, Y., Fullwood, N., Ebdon, J., MacNeil, S., 2005. Synthesis and properties of amphiphilic networks 3: preparation and characterization of block conetworks of poly(butyl methacrylate-block-(2,3 propandiol-1-methacrylate-stat-ethandiol dimethacrylate)). Biomaterials 26, 2219–2230.

Rimmer, S., Johnson, C., Zhao, B., Collier, J., Gilmore, L., Sabnis, S., Wyman, P., Sammon, C., Fullwood, N.J., MacNeil, S., 2007. Epithelialization of hydrogels achieved by amine functionalization and co-culture with stromal cells. Biomaterials 28, 5319–31.

Rimmer, S., Wilshaw, S.-P., Pickavance, P., Ingham, E., 2009. Cytocompatibility of poly(1,2 propandiol methacrylate) copolymer hydrogels and conetworks with or without alkyl amine functionality. Biomaterials 30, 2468–2478.

Romano, A.C., Espana, E.M., Yoo, S.H., Budak, M.T., Wolosin, J.M., Tseng, S.C.G., 2003. Different Cell Sizes in Human Limbal and Central Corneal Basal Epithelia Measured by Confocal Microscopy and Flow Cytometry. Investig. Ophthalmol. Vis. Sci. 44 , 5125–5129.

Rozsa, A.J., Beuerman, R.W., 1982. Density and organization of free nerve endings in the corneal epithelium of the rabbit. Pain 14, 105–120.

Saha, K., Schaffer, D. V, 2006. Signal dynamics in Sonic hedgehog tissue patterning. Development 133, 889–900.

Sandeman, S.R., Lloyd, A.W., Tighe, B.J., Franklin, V., Li, J., Lydon, F., Liu, C.S.C., Mann, D.J., James, S.E., Martin, R., 2003. A model for the preliminary biological screening of potential keratoprosthetic biomaterials. Biomaterials 24, 4729–4739.

Sangwan, V.S., Basu, S., MacNeil, S., Balasubramanian, D., 2012. Simple limbal epithelial transplantation (SLET): a novel surgical technique for the treatment of unilateral limbal stem cell deficiency. Br J Ophthalmol 96, 931–934.

Sangwan, V.S., Basu, S., MacNeil, S., Balasubramanian, D., 2012. Simple limbal epithelial transplantation (SLET): a novel surgical technique for the treatment of unilateral limbal stem cell deficiency. Br J Ophthalmol 96, 931–934.

Sangwan, V.S., Basu, S., Vemuganti, G.K., Sejpal, K., Subramaniam, S. V, Bandyopadhyay, S., Krishnaiah, S., Gaddipati, S., Tiwari, S., Balasubramanian, D., 2011. Clinical outcomes of xeno-free autologous cultivated limbal epithelial transplantation: A 10-year study. Br. J. Ophthalmol. 95, 1525–1529.

Scadden, D.T., 2006. The stem-cell niche as an entity of action. Nature 441, 1075–1079.

Schirmbeck, T., Paula, J., Martin, L., Crósio Filho, H., Romão, E., 2005. Efficacy and low cost in keratoconus treatment with rigid gas-permeable contact lens. Arq. Bras. Oftalmol. 68, 219–222.

Schiro, J.A., Chan, B.M., Roswit, W.T., Kassner, P.D., Pentland, A.P., Hemler, M.E., Eisen, A.Z., Kupper, T.S., 1991. Integrin alpha 2 beta 1 (VLA-2) mediates reorganization and contraction of collagen matrices by human cells. Cell 67, 403–410.

Schlötzer-Schrehardt, U., Dietrich, T., Saito, K., Sorokin, L., Sasaki, T., Paulsson, M., Kruse, F.E., 2007. Characterization of extracellular matrix components in the limbal epithelial stem cell compartment. Exp. Eye Res. 85, 845–860.

Schlötzer-Schrehardt, U., Kruse, F.E., 2005. Identification and characterization of limbal stem cells. Exp. Eye Res. 81, 247–264.

Schrage, N., Cordes, A.K., Storsberg, J., Sel, S., Röthgen, H., Nass, N., Berndt, E., Jockenhövel, S., Meßner, A., Panfil, C., 2014. In-vitro- und In-vivo-Untersuchung einer modifizierten textilen Keratoprothese. Der Ophthalmol. 111, 247–253.

Secker, G.A., Daniels, J.T., 2009. Limbal epithelial stem cells of the cornea, in: Watt, F., Gage, F. (Eds.), StemBook.

Shalaby, S.W.; Hoffman, A.S.; Ratner, B.D. and Horbett, T.A. Ed. 1984. Polymers as Biomaterials. New York, Plenum Press

Sheardown, H., Cheng, Y.L., 1996. Mechanisms of corneal epithelial wound healing. Chem. Eng. Sci. 51, 4517–4529.

Shen, Q., Goderie, S.K., Jin, L., Karanth, N., Sun, Y., Abramova, N., Vincent, P., Pumiglia, K., Temple, S., 2004. Endothelial cells stimulate self-renewal and expand neurogenesis of neural stem cells. Science 304, 1338–1340.

Sherman, L., Sleeman, J., Herrlich, P., Ponta, H., 1994. Hyaluronate receptors: key players in growth, differentiation, migration and tumor progression. Curr. Opin. Cell Biol. 6, 726–733.

Shi, Y.J., Tabesh, M., Sugrue, S.P., 2000. Role of cell adhesion-associated protein, pinin (DRS/memA), in corneal epithelial migration. Invest. Ophthalmol. Vis. Sci. 41, 1337–1345.

Shortt, A.J., Secker, G.A., Munro, P.M., Khaw, P.T., Tuft, S.J., Daniels, J.T., 2007a. Characterization of the limbal epithelial stem cell niche: novel imaging techniques permit in vivo observation and targeted biopsy of limbal epithelial stem cells. Stem Cells 25, 1402–1409.

Shortt, A.J., Secker, G.A., Notara, M.D., Limb, G.A., Khaw, P.T., Tuft, S.J., Daniels, J.T., 2007b. Transplantation of ex vivo cultured limbal epithelial stem cells: A review of techniques and clinical results. Surv. Ophthalmol. 52, 483–502.

Shortt, A.J., Tuft, S.J., Daniels, J.T., 2011. Corneal stem cells in the eye clinic. Br. Med. Bull. 100, 209–225.

Simon, M.C., Keith, B., 2008. The role of oxygen availability in embryonic development and stem cell function. Nat. Rev. Mol. Cell Biol. 9, 285–296.

Sipkins, D.A., Wei, X., Wu, J.W., Runnels, J.M., Côté, D., Means, T.K., Luster, A.D., Scadden, D.T., Lin, C.P., 2005. In vivo imaging of specialized bone marrow endothelial microdomains for tumour engraftment. Nature 435, 969–973.

Snell, R.S., Lemp, M.A., 1998. Clinical anatomy of the eye, 2nd ed. Blackwell Science, Malden.

Solanas, G., Batlle, E., 2011. Control of cell adhesion and compartmentalization in the intestinal epithelium. Exp. Cell Res. 317, 2695–2701.

Song, H., Stevens, C.F., Gage, F.H., 2002. Astroglia induce neurogenesis from adult neural stem cells. Nature 417, 39–44.

Soong, H.K., 1987. Vinculin in focal cell-to-substrate attachments of spreading corneal epithelial-cells. Arch. Ophthalmol. 105, 1129–1132.

Stepp, M.A., Zhu, L., Cranfill, R., 1996. Changes in beta 4 integrin expression and localization in vivo in response to corneal epithelial injury. Invest. Ophthalmol. Vis. Sci. 37, 1593–1601.

Stoner, G.D., Harris, C.C., Myers, G.A., Trump, B.F., Connor, R.D., 1980. Putrescine stimulates growth of human bronchial epithelial cells in primary culture. In Vitro 16, 399–406.

Storsberg, J., Schmidt, C., Rehfeldt, S., Kobuch, K., Messner, A., Röthgen, H., Duncker, G.I.W., Knak, M., Cordes, A., Schrage, N., Nass, N., Sel, S., 2012. Synthetic eye prosthesis. Acta Ophthalmol. 90, 0.

Streilein, J.W., 1995. Immunological non-responsiveness and acquisition of tolerance in relation to immune privilege in the eye. Eye 9, 236–240.

Streilein, J.W., 2003. New thoughts on the immunology of corneal transplantation. Eye 17, 943–948.

Streilein, J.W., Arancibia-Caracamo, C., Osawa, H., 2003. The role of minor histocompatibility alloantigens in penetrating keratoplasty. Dev. Ophthalmol. 36, 74–88.

Stuart, P.M., Griffith, T.S., Usui, N., Pepose, J., Yu, X., Ferguson, T.A., 1997. CD95 ligand (FasL)-induced apoptosis is necessary for corneal allograft survival. J. Clin. Invest. 99, 396–402.

Sun, T., Higham, M., Layton, C., Haycock, J., Short, R., MacNeil, S., 2004. Developments in xenobiotic-free culture of human keratinocytes for clinical use. Wound Repair Regen. 12, 626–634.

Sun, T., Mai, S., Norton, D., Haycock, J.W., Ryan, A.J., MacNeil, S., 2005. Self-organization of skin cells in three-dimensional electrospun polystyrene scaffolds. Tissue Eng. 11, 1023–33.

Sun, Y., Collett, J., Fullwood, N.J., Mac Neil, S., Rimmer, S., 2007a. Culture of dermal fibroblasts and protein adsorption on block conetworks of poly(butyl methacrylate-block-(2,3 propandiol-1-methacrylate-stat-ethandiol dimethacrylate)). Biomaterials 28, 661–670.

Sun, Y., Maughan, J., Haigh, R., Hopkins, S.A., Wyman, P., Johnson, C., Fullwood, N.J., Ebdon, J., MacNeil, S., Rimmer, S., 2007b. Polymethacrylate networks as substrates for cell culture. Macromol. Symp. 256, 137–148.

Suzuki, T., Kinoshita, Y., Tachibana, M., Matsushima, Y., Kobayashi, Y., Adachi, W., Sotozono, C., Kinoshita, S., 2001. Expression of sex steroid hormone receptors in human cornea. Curr. Eye Res. 22, 28–33.

Szycher, M. 1991. High Performance Biomaterials: A Complete Guide to Medical and Pharmacuetical applications. Illustrated Ed., 165–169. CRC Press.

Tachibana, M., Kasukabe, T., Kobayashi, Y., Suzuki, T., Kinoshita, S., Matsushima, Y., 2000. Expression of Estrogen Receptor α and β in the Mouse Cornea. Investig. Ophthalmol. Vis. Sci. 41 , 668–670.

Tan, D.T.H., Ficker, L.A., Buckley, R.J., 1996. Limbal transplantation. Ophthalmology 103, 29–36.

Thoft, R.A., Friend, J., 1983. The x, y, z hypothesis of corneal epithelial maintenance. Invest. Ophthalmol. Vis. Sci. 24, 1442–1443.

Thomasy, S. M., Krishna Raghunathan, V., Winkler, M., Reilly, C. M., Sadeli, A. R., Russell, P., Jester, J.V., Murphy, C. J., 2014. Elastic modulus and collagen organization of the rabbit cornea: epithelium to endothelium. Acta Biomaterialia, 10(2), 785–791.

Torbet, J., Malbouyres, M., Builles, N., Justin, V., Roulet, M., Damour, O., Oldberg, A., Ruggiero, F., Hulmes, D.J.S., 2007. Orthogonal scaffold of magnetically aligned collagen lamellae for corneal stroma reconstruction. Biomaterials 28, 4268–76.

Tsai, R.J.-F., Tseng, S.C.G., 1994. Human allograft limbal transplantation for corneal surface reconstruction. Cornea 13, 389–400.

Tseng, S.C.G., 1996. Regulation and clinical implications of corneal epithelial stem cells. Mol. Biol. Rep. 23, 47–58.

Tsubota, K., Satake, Y., Kaido, M., Shinozaki, N., Shimmura, S., Bissen-Miyajima, H., Shimazaki, J., 1999. Treatment of severe ocular-surface disorders with corneal epithelial stem-cell transplantation. N. Engl. J. Med. 340, 1697–1703.

Tsubota, K., Toda, I., Saito, H., Shinozaki, N., Shimazaki, J., 1995. Reconstruction of the corneal epithelium by limbal allograft transplantation for severe ocular surface disorders. Ophthalmology 102, 1486–1496.

Tuft, S.J., Gartry, D.S., Rawe, I.M., Meek, K.M., 1993. Photorefractive keratectomy - implications of corneal wound-healing. Br. J. Ophthalmol. 77, 243–247.

Tzoneva, R., Faucheux, N., & Groth, T. 2007. Wettability of substrata controls cell-substrate and cell-cell adhesions. Biochimica et Biophysica Acta, 1770(11), 1538–47.

U. Mester, K. Roth, M.U.D., 1972. Versuche mit 2-Hydroxyaethyl-methycrylatlinsen als Kerotophakiematerial. Ber. Ophthalmol. Ges pp. 326–327.

Van der Merwe, E.L., Kidson, S.H., 2010. Advances in imaging the blood and aqueous vessels of the ocular limbus. Exp. Eye Res. 91, 118–126.

Vazin, T., Schaffer, D. V., 2010. Engineering strategies to emulate the stem cell niche. Trends Biotechnol.

Vemuganti, G.K., Kashyap, S., Sangwan, V.S., Singh, S., 2004. Ex-vivo potential of cadaveric and fresh limbal tissues to regenerate cultured epithelium. Indian J. Ophthalmol. 52, 113–120.

Vijayasekaran, S., Chirila, T. V, Robertson, T.A., Lou, X., Fitton, J.H., Hicks, C.R., Constable, I.J., 2000. Calcification of Poly(2-hydroxyethyl methacrylate) hydrogel sponges implanted in the rabbit cornea: a 3-month study. J Biomater Sci Polym Ed 11, 599–615.

Vijayasekaran, S., Hicks, C.R., Chirila, T. V, Fitton, J.H., Clayton, A.B., Lou, X., Platten, S., Crawford, G.J., Constable, I.J., 1997. Histologic evaluation during healing of hydrogel core-and-skirt keratoprostheses in the rabbit eye. Cornea 16, 352–359.

Vogt A., 1921. Atlas of the Slitlamp-Microscopy of the Living Eye. Berlin, Springer. 2-52

Votteler, M., Kluger, P.J., Walles, H., Schenke-Layland, K., 2010. Stem cell microenvironments - unveiling the secret of how stem cell fate is defined. Macromol. Biosci. 10, 1302–1315.

Wagoner, M.D., 1997. Chemical injuries of the eye: Current concepts in pathophysiology and therapy. Surv. Ophthalmol. 41, 275–313.

Walker, M.R., Patel, K.K., Stappenbeck, T.S., 2009. The stem cell niche. J. Pathol. 217, 169–180.

Wang, H.B., Dembo, M., Wang, Y.L., 2000. Substrate flexibility regulates growth and apoptosis of normal but not transformed cells. Am. J. Physiol. Physiol. 279, C1345–C1350.

Watabe, T., Miyazono, K., 2009. Roles of TGF-beta family signaling in stem cell renewal and differentiation. Cell Res. 19, 103–115.

Wei, H., Zhuo, R. X., & Zhang, X. Z. 2013. Design and development of polymeric micelles with cleavable links for intracellular drug delivery. Prog. Polym. Sci., 38, 503–535.

Weingeist, T.A., 1973. The Conjunctiva. Int. Ophthalmol. Clin. 13, 85–91.

Willert, K., Brown, J.D., Danenberg, E., Duncan, A.W., Weissman, I.L., Reya, T., Yates, J.R., Nusse, R., 2003. Wnt proteins are lipid-modified and can act as stem cell growth factors. Nature 423, 448–452.

William M. Hart, J., 1992. Adler's physiology of the eye clinical application, 9th ed, Physiology of the eye. Mosby Year Book in St. Louis.

Williams, K.K., Watsky, M.A., 2002. Gap junctional communication in the human corneal endothelium and epithelium. Curr. Eye Res. 25, 29–36.

Wilson, S.E., Hong, J.W., 2000. Bowman's layer structure and function - Critical or dispensable to corneal function? A hypothesis. Cornea 19, 417–420.

Wójciak-Stothard, B., Curtis, A., Monaghan, W., Macdonald, K., Wilkinson, C., 1996. Guidance and activation of murine macrophages by nanometric scale topography. Exp. Cell Res. 223, 426–435.

Wright, K.K., Spiegel, P.H., 2002. Pediatric opthalmology and strabismus, 2nd ed. Springer Science and Business Media.

Wu, C.Y., Fields, A.J., Kapteijn, B.A.E., McDonald, J.A., 1995. The role of $\alpha 4\beta 1$ integrin in cell motility and fibronectin matrix assembly. J. Cell Sci. 108, 821–829.

Wu, X.Y., Svoboda, K.K.H., Trinkaus-Randall, V., 1995. Distribution of F-actin, vinculin and integrin subunits (alpha6 and beta4) in response to corneal substrata. Exp. Eye Res. 60, 445–458.

Xiong, L.Z., He, Z.Q., 2010. The Biological Evaluation of the PEG/PLA Amphiphilic Diblock Copolymer. Polym. Plast. Technol. Eng. 49, 1201–1206.

Yanagisawa I, Sakuma H, Shimura M, Wakamatsu Y, Yanagisawa S, S.E., 1989. Effects of "wettability" of biomaterials on culture cells. J Oral Implant. 15, 168–77.

Yanez-Soto, B., Liliensiek, S.J., Murphy, C.J., Nealey, P.F., 2012. Biochemically and topographically engineered poly(ethylene glycol) diacrylate hydrogels with biomimetic characteristics as substrates for human corneal epithelial cells. J. Biomed. Mater. Res. A 101, 1184–1194.

Yeung, T., Georges, P.C., Flanagan, L.A., Marg, B., Ortiz, M., Funaki, M., Zahir, N., Ming, W.Y., Weaver, V., Janmey, P.A., 2005. Effects of substrate stiffness on cell morphology, cytoskeletal structure, and adhesion. Cell Motil. Cytoskeleton 60, 24–34.

Zhang, C., Zhang, N., Wen, X., 2007. Synthesis and characterization of biocompatible, degradable, light-curable, polyurethane-based elastic hydrogels. J. Biomed. Mater. Res. Part A 82A, 637–650.

Zhang, W., Shiraishi, A., Suzuki, A., Zheng, X., Kodama, T., Ohashi, Y., 2004. Expression and distribution of tissue transglutaminase in normal and injured rat cornea. Curr. Eye Res. 28, 37–45.

Zhang, Z.H., Morla, A.O., Vuori, K., Bauer, J.S., Juliano, R.L., Ruoslahti, E., 1993. The alpha-v-beta-1-integrin functions as a fibronectin receptor but does not support fibronectin matrix assembly and cell-migration on fibronectin. J. Cell Biol. 122, 235–242.

Zheng, L.L., Shiuey, Y., Waters, D.J., Huie, P., Manivanh, R. V, Cochran, J.R., Frank, C.W., Ta, C.N., 2011. Artificial lamellar cornea based on poly(ethylene glycol) and poly(acrylic acid). ARVO Annu. Meet. Abstr. Search Progr. Plan. 2011, 330.

Zumkeller, W., Orth, U., Gal, A., 2003. Three novel PAX6 mutations in patients with aniridia. Mol. Pathol. 56, 180–183.

LIST OF PUBLICATIONS AND COMMUNICATIONCS

Hassan, E., Deshpande, P., Claeyssens, F., Rimmer, S., & MacNeil, S. (2014). **Amine functional hydrogels as selective substrates for corneal epithelialization**. *Acta Biomaterialia*, *10*(7), 3029–37.

Amine functionalised synthetic hydrogels for corneal regeneration   *2013*

TCES Annual conference July 23rd-25th Cardiff university

Abstract & Oral presentation

Synthetic polymer hydrogels for improved adhesion of limbal epithelial cells   *2012*

BITEG 14th Annual white rose work in progress meeting December 17th The University of York

Oral presentation

Synthetic polymer hydrogels for improved adhesion of limbal epithelial cells   *2012*

5th Limbal Stem Cell Meeting October 4th University College London

Poster presentation

Synthetic polymer hydrogels for improved adhesion of corneal cells   *2012*

TERMIS World Congress 2012 "Tissue Engineering and Regenerative Medicine"

September 5 - 8, Hofburg Congress Centre | Vienna | Austria

Poster presentation

Mimicking the natural regeneration of the cornea by tissue engineering   *2012*

Joint DTC conference July 20th Keele University

Oral presentation

Synthetic polymer hydrogels for improved adhesion of corneal cells *2012*

EPSRC industry day University of Leeds July 13th

Poster presentation *(**Prize for best poster)*

Mimicking the natural regeneration of the cornea by tissue engineering *2012*

TATA steel Engineering materials poster competition May 15th University of Sheffield

Poster presentation *(**TATA steel award for best poster)*

Tissue engineering of the cornea: Chemistry vs. Biology *2011*

Joint DTC conference July 8th University of Leeds

Oral presentation

Mimicking the natural regeneration of the cornea by tissue engineering *2010*

BITEG 12th Annual white rose work in progress meeting December 17th University of Leeds

Oral presentation

Development of electrospun scaffolds for tissue engineering of human cornea *2010*

Joint DTC conference July 1st Loughborough University

Poster presentation